

Perturbing isoradial triangulations

François David and Jeanne Scott

Abstract. We consider an infinite planar Delaunay graph G_ϵ which is obtained by locally deforming the coordinate embedding of a general isoradial graph G_{cr} , with respect to a real deformation parameter ϵ . Using Kenyon’s exact and asymptotic results for the critical Green’s function on an isoradial graph, we calculate the leading asymptotics of the first- and second-order terms in the perturbative expansion of the log-determinant of the Laplace–Beltrami operator $\Delta(\epsilon)$, the David–Eynard Kähler operator $\mathcal{D}(\epsilon)$, and the conformal Laplacian $\underline{\Delta}(\epsilon)$ on the deformed Delaunay graph G_ϵ . We show that the scaling limits of the second-order *bi-local* term for both the Laplace–Beltrami and David–Eynard Kähler operators exist and coincide, with a shared value independent of the choice of the initial isoradial graph G_{cr} . Our results allow us to define a discrete analog of the stress-energy tensor for each of the three operators. Furthermore, we can identify a central charge ($c = -2$) in the case of both the Laplace–Beltrami and David–Eynard Kähler operators. While the scaling limit is consistent with the stress-energy tensor and the value of the central charge for the Gaussian free field (GFF), the discrete central charge value of $c = -2$ for the David–Eynard Kähler operator is, however, at odds with the value of $c = -26$ expected by Polyakov’s theory of 2D quantum gravity; moreover, there are problems with convergence of the scaling limit of the discrete stress-energy tensor for the David–Eynard Kähler operator. The second-order bi-local term for the conformal Laplacian involves anomalous terms corresponding to the creation of discrete *curvature dipoles* in the deformed Delaunay graph G_ϵ ; we examine the difficulties in defining a convergent scaling limit in this case. Connections with some discrete statistical models at criticality are explored.

Contents

1. Introduction	716
2. Planar graphs and rhombic graphs	735
3. Laplacians and their determinants	748
4. The critical Green’s function and its asymptotics	757
5. Deforming Delaunay lattices and operators	765

Mathematics Subject Classification 2020: 05C10 (primary); 52C26, 81T40, 83C27 (secondary).

Keywords: random maps, isoradial graphs, Delaunay graphs, conformal invariance, 2D gravity, discrete holomorphic functions.

6. Variations of log-determinants	778
7. The scaling limit of variations	799
8. Finite ϵ variations, beyond the linear approximation	807
9. Discussion and perspectives	830
A. Reminders: The stress-energy tensor in quantum field theories and the central charge in 2D conformal field theories	842
B. Proof of Lemma 1.9	848
C. Continuum limits of curvature anomalies: An example	851
References	858

1. Introduction

1.1. Purpose and motivation

This paper studies deformations of infinite isoradial planar graphs and triangulations, and the effect of these deformations on three discrete Laplace-like operators defined on these graphs, and on their determinants.

Our initial motivation for this study is to better understand the relation between a model of random Delaunay triangulations (RDT) in the plane, proposed in [7] by Eynard and the first author (FD), and the field theory model of two-dimensional gravity (Liouville gravity) proposed first by Polyakov in [23]. The random triangulation model of [7] is a model where any (finite) distribution of points $\mathbf{z} = \{z_i\}$ in the plane (or the Riemann sphere) is weighted by the determinant $\det[\mathcal{D}]$ of a discrete operator \mathcal{D} defined from the Delaunay triangulation \mathcal{T} associated to \mathbf{z} (hence the terminology random Delaunay triangulation model). This discrete model has very interesting properties. Thanks to [7, 24], it can be viewed as a model of $\mathrm{PSL}(2, \mathbb{C})$ invariant embeddings of random abstract discrete rhombic surfaces into the Riemann sphere, and thus is related to random planar maps models and discrete 2d gravity. As shown in [4], it also provides an alternative description of the moduli space of the punctured sphere $\mathcal{M}_{0,N}$ equipped with the Weil–Petersson metric, since \mathcal{D} defines a Kähler form on the space of Delaunay triangulations.

The authors of [7] pointed out a similarity between the discrete operator \mathcal{D} of the RDT model and the continuous gauge fixing Faddeev–Popov operator \mathbf{J} in Polyakov’s model [23] (see Appendix A.4 and references therein for details), whose determinant gives the famous Liouville action for the conformal factor (the Liouville field, see Appendix A.4). Like the discrete RDT model, Liouville gravity is a conformal field theory (CFT), invariant under $\mathrm{PSL}(2, \mathbb{C})$ transformations on the sphere. We therefore want to probe this analogy further, and find discrete analogs of CFT structures in the RDT model, such as a stress-energy tensor T , some short distance operator product expansion (OPE), and whether such an OPE has a discrete central charge c which can

be compared to the central charge of the ghost sector of Liouville gravity, famously known to be $c_{\text{ghost}} = -26$.

The operator \mathcal{D} on a general Delaunay triangulation is a special case of a discretized Laplace-like operator (elliptic operator) defined on graphs. These operators can be viewed as discretizations of differential operators defined on Riemannian spaces, with respect to some metric, and are related to some quantum field theories (QFT), in particular, some CFT's. They are interesting objects in their own right, both in mathematics (index theorems, Seeley–DeWitt heat kernel expansions, trace formulas) and in physics (conformal field theories, quantum gravity, string theory, statistical mechanics, etc.). The simplest and perhaps most notable example is the scalar Laplace–Beltrami operator Δ acting on functions ϕ over a Riemannian manifold M with metric $\mathbf{g} = (g_{\mu\nu})$ and given by

$$\Delta = -\frac{1}{\sqrt{g}} \partial_\mu \sqrt{g} g^{\mu\nu} \partial_\nu$$

with ∂_μ the standard derivative with respect to the local coordinate x^μ acting on scalar functions. The operator Δ is related to the massless scalar quantum free field theory (i.e., the Gaussian free field, or GFF) on the manifold M , see Appendix A.3 for details. Its functional determinant (properly defined), is related to the GFF partition function Z through

$$\det(\Delta) = Z^{-2} \quad \text{with } Z = \int \mathcal{D}[\phi] e^{-S[\phi]},$$

where ϕ is the free field (a random scalar real function) and $S[\phi]$ is the GFF action (see (A.7)). Both the action $S[\phi]$ and the partition function Z depend explicitly on the metric \mathbf{g} on M , and the effect of varying the metric in the action $S[\phi]$ is encoded in the so-called stress-energy tensor $\mathbf{T} = (T^{\mu\nu})$. For a CFT such as the GFF, one has to consider the holomorphic and antiholomorphic components $T = -2\pi T_{zz}$ and $\bar{T} = -2\pi T_{\bar{z}\bar{z}}$ of \mathbf{T} which encode the effect of changing the metric by an infinitesimal anti-analytic diffeomorphism

$$z \rightarrow z + \epsilon F(\bar{z}) \tag{1.1}$$

with F such that $\partial F/\partial z = 0$ on M (for details, see Appendix A.2). The OPE for T ,

$$T(z)T(z') = \frac{c}{2} \frac{1}{(z - z')^4} + \dots \tag{1.2}$$

with central charge c of the CFT, is of special importance. It implies (Appendix A.2) that the second variation of the logarithm of the partition function of the CFT, $\log Z$, under (1.1) is

$$\frac{c}{4\pi^2} \iint d^2u d^2v \frac{\bar{\partial} F(u) \bar{\partial} F(v)}{(u - v)^4} + \frac{\partial \bar{F}(u) \partial \bar{F}(v)}{(\bar{u} - \bar{v})^4} + \text{contact terms.} \tag{1.3}$$

In the cases we are interested in, the central charge c is real, and this can of course be rewritten as the double integral of the real part of $\frac{\bar{\partial}F(u)\bar{\partial}F(v)}{(u-v)^4}$.

Accordingly, we shall try to define

- (i) a discrete analog of diffeomorphisms (1.3) for Delaunay triangulations,
- (ii) a discrete stress-energy tensor \mathbf{T} associated to the operator \mathcal{D} of the RDT model,
- (iii) an analog for \mathcal{D} of the OPE (1.2) and of formula (1.3).

This requires us to introduce and study an appropriate “scaling limit” (in the QFT sense) of the RDT model.

This program turns out to be very difficult for general random Delaunay triangulations. As a first step, we shall study deformations of a very specific subclass of Delaunay triangulations, namely, *isoradial Delaunay triangulations*. One reason for this restriction is technical. The analysis is much simpler and explicit calculations can be done, thanks to the fact that on isoradial triangulations, the \mathcal{D} operator is proportional to the critical Laplacian Δ_{cr} considered by Kenyon in [17] (to be defined later). Thanks to the methods of discrete analyticity, both the determinant $\det[\Delta_{\text{cr}}]$ and the Green’s function Δ_{cr}^{-1} (the propagator) take simple explicit forms in terms of the geometry of the isoradial triangulation. A second reason is that isoradial triangulations can be viewed as analogs of “discrete flat metric” (see Section 1.2.1). It is therefore natural to study the operator \mathcal{D} and the associated measure for triangulations which are close to but not exactly isoradial, as a means of understanding the relationship between the RDT model and 2d gravity, as suggested in [7].

This work is rather technical, limited in scope, but it represents the first step in this general program. In addition to studying the operator \mathcal{D} , we carry out a similar analysis for two related operators, also defined for Delaunay graphs:

- (i) the discrete Laplace–Beltrami operator Δ ,
- (ii) a conformal Laplacian $\underline{\Delta}$ with $\text{PSL}(2, \mathbb{C})$ invariance properties.

Several issues require a lot of attention:

- (1) Under deformations, the Delaunay constraints (see the precise definition in Section 2.1.1) cause the incidence relations of the graph to change (by edge flips). These flips are a potential source of discontinuities and singularities for the operators and the determinants we are interested in.
- (2) We want uniform estimates for the variation of operators and determinants, independent of the initial isoradial Delaunay graph. This is not always possible.
- (3) We also look for the existence of “scaling limits” (in the usual sense of statistical mechanics and quantum field theory), in particular, for the discrete analogs of the OPE (1.2) and of formula (1.3), in order to recover a continuous QFT interpretation of our results.

Point (1) is treated thoroughly. Whitehead flips are under control for the operators \mathcal{D} and Δ , but are shown to induce discontinuities for $\underline{\Delta}$.

For point (2), uniform estimates are obtained for all three operators, for which we get discrete analogs of the stress-energy tensor \mathbf{T} . For Δ , the OPE (1.2) and (1.3) hold with central charge $c = -2$, as expected. For \mathcal{D} , an OPE holds as well, and unexpectedly we obtain a central charge $c = -2$ too. We do not, however, recover formulas (1.2) and (1.3) (specific to CFT's) for the conformal Laplacian $\underline{\Delta}$.

For point (3), good scaling limit results are obtained for Δ (this was to be expected), and we prove similar results for \mathcal{D} , which are valid under some restrictions. This program fails for $\underline{\Delta}$.

Let us now be more specific, and summarize: (1) the main concepts and tools used in this paper, (2) the main results, and (3) the detailed plan and content of the paper.

1.2. The concepts

1.2.1. Delaunay graphs. Delaunay triangulations in the plane are models of discrete space which has been studied by many authors, in particular, in high energy physics [6] as well as in statistical physics, condensed matter and soft matter physics. Anticipating the precise definitions and details given in Section 2, we highlight some notions which are important.

A *polyhedral graph* G is a planar graph (with finitely or infinitely many vertices) equipped with an embedding $z: V(G) \rightarrow \mathbb{C}$ of its vertex set $V(G)$ such that edges are mapped to straight line segments and faces are mapped to convex, cyclic polygons. Accordingly, we can associate with each face f of G the circumcircle C_f , the circumdisk D_f , and the corresponding circumradius $R(f)$ of its cyclic polygon with respect to the embedding.

A *Delaunay graph* is a polyhedral graph G such that, under the embedding,

- (1) the interior of the circumdisk of each face of G contains no vertices,
- (2) no two faces share the same circumdisk.

Equivalently, the dual of Delaunay graph G is the Voronoi complex \mathbf{V} associated to the set of (embedded) vertices of G .

A *weak Delaunay graph* is a polyhedral graph G such that condition (1) is satisfied.

A (*weak*) *Delaunay triangulation* T is a (weak) Delaunay graph whose faces are all triangles.

Following [7], we associate to an oriented edge $\vec{e} = (u, v)$ “north” and “south” faces f_n and f_s along with angles

$$\theta_n(\vec{e}) = \angle v u o_n \quad \text{and} \quad \theta_s(\vec{e}) = \angle o_s u v,$$

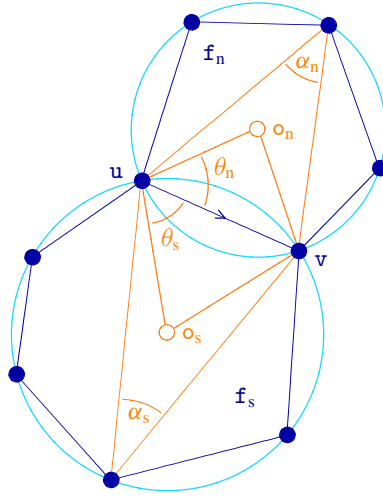


Figure 1. The north and south faces f_n and f_s of an (oriented) edge $\vec{e} = (u, v)$ are drawn in dark blue, while the corresponding circumcircles are outlined in light blue. Their respective circumcenters o_n and o_s , as well the associated north and south angles $\theta_n(\vec{e})$ and $\theta_s(\vec{e})$, are highlighted in orange.

where o_n and o_s are the respective circumcenters of f_n and f_s , as depicted in Figure 1. Reversing the orientation of \vec{e} interchanges the roles of north and south. The *conformal angle* $\theta(e)$ associated to the unoriented edge e is defined as¹

$$\theta(e) = \frac{\theta_n(\vec{e}) + \theta_s(\vec{e})}{2}. \tag{1.4}$$

The clockwise orientability of the north and south triangles enforces

$$-\frac{\pi}{2} < \theta_n(\vec{e}), \theta_s(\vec{e}) < \frac{\pi}{2}.$$

The Delaunay condition ensures that

$$0 < \theta(e) < \frac{\pi}{2},$$

while the weak Delaunay condition ensures that $0 \leq \theta(e) < \frac{\pi}{2}$.

Finally, as explained in [7] and in Section 2, to each plane Delaunay graph \mathcal{G} , we can associate an abstract *rhombic surface* $S_{\mathcal{G}}^{\diamond}$ obtained by gluing rhombi $\diamond(e)$

¹Note that the conformal angle $\theta(e)$ considered in [7] is twice the conformal angle $\theta(e)$ defined here by (1.4) (i.e., $\theta(e) = 2\theta(e)$). We choose definition (1.4) for compatibility with Kenyon’s notations in [17].

associated to the edges e of G according to the incidence relations of G . Each rhombus $\diamond(e)$ has a unit edge length and has a corresponding rhombus angle $2\theta(e)$. We view S_G^\diamond as a discretized Riemann surface with curvature concentrated at the vertices. This rhombic surface S_G^\diamond will be “flat”, i.e., can be isometrically embedded in the plane, *if and only if* for each face f of G , the sum of the conformal angles of the edges e which form the boundary of f equals $\frac{\pi}{2}$

$$\sum_{e \in \partial f} \theta(e) = \frac{\pi}{2}.$$

Equivalently, the Delaunay graph G is *isoradial*, i.e., the circumradii $R(f)$ are all equal. Alternatively, a Delaunay graph G is isoradial if and only if S_G^\diamond coincides with the planar bipartite *kite graph* G^\diamond discussed in Section 2.1. Isoradial Delaunay graphs are also referred to as *flat graphs* or *critical graphs*.

1.2.2. The random Delaunay triangulation model. The David–Eynard model [7] is a theory of random (finite) Delaunay graphs which are sampled (with Lebesgue measure) according to the conformal angle values of the corresponding edges. By the Voronoi construction, a configuration of $N \geq 3$ distinct marked points $\{z_1, \dots, z_N\}$ in the extended plane $\mathbb{C}P^1$ is equivalent to a Delaunay graph G with vertex set $V(G) = \{1, \dots, N\}$ and embedding $k \mapsto z_k$. This correspondence between point configurations and graphs is $PSL(2, \mathbb{C})$ equivariant in the sense that the incidence relations which define the Delaunay graph are invariant under the action of $PSL(2, \mathbb{C})$ by Möbius transformations. In this formulation, the relevant measure on the space of configurations of marked points is, after fixing three points (z_1, z_2, z_3) thanks to $PSL(2, \mathbb{C})$ invariance,

$$\prod_{k=4}^N dz_k^2 \frac{\det' \mathcal{D}}{|z_1 - z_2|^2 |z_2 - z_3|^2 |z_1 - z_3|^2}, \tag{1.5}$$

where \mathcal{D} is the David–Eynard discrete Kähler operator of the graph G as defined in (1.8) below, and $\det' \mathcal{D}$ is the $(N - 3) \times (N - 3)$ principal minor of \mathcal{D} with row and column set $\{4, \dots, N\}$, see [7]. We view $\det' \mathcal{D}$ as a *reduced determinant* which suppresses the effect of the zero modes of \mathcal{D} . As shown in [4], the measure in (1.5) is $PSL(2, \mathbb{C})$ invariant and coincides with the Weil–Petersson measure on $\mathcal{M}_{0,N}$. Points configurations whose corresponding Delaunay graph is a triangulation form a Zariski open subset, and consequently the subspace of non-triangulations has measure zero. For this reason, we speak of the David–Eynard model as a theory of random triangulations.

1.2.3. The operators Δ , $\underline{\Delta}$ and \mathcal{D} . In this paper, we are interested in the three discrete operators defined on generic polyhedral graphs G : the Laplace–Beltrami

operator Δ , the conformal Laplacian $\underline{\Delta}$, and the David–Eynard Kähler operator \mathcal{D} . All three operators act on the space $\mathbb{C}^{V(G)}$ consisting of complex valued functions supported on the vertices $V(G)$ of the graph G .

- The discrete Laplace–Beltrami operator Δ is defined for $\phi \in \mathbb{C}^{V(G)}$ by

$$\begin{aligned} \Delta\phi(u) &= \sum_{\text{edges } \vec{e}=(u,v)} c(\vec{e})(\phi(u) - \phi(v)), \\ c(\vec{e}) &= \frac{1}{2}(\tan \theta_n(\vec{e}) + \tan \theta_s(\vec{e})). \end{aligned} \tag{1.6}$$

This is a standard discretization of the Laplacian in the plane, both in physics (see, e.g., [6]) and in mathematics. It is a symmetric real operator.

- The conformal Laplacian $\underline{\Delta}$, which we introduce here, is defined by

$$\underline{\Delta}\phi(u) = \sum_{\text{edges } \vec{e}=(u,v)} \tan \theta(e)(\phi(u) - \phi(v)). \tag{1.7}$$

It is invariant under global conformal transformations

$$z \xrightarrow{g} \frac{az + b}{cz + d}$$

of the graph embedding $z: V(G) \rightarrow \mathbb{C}$ for $g \in \text{PSL}_2(\mathbb{C})$. It is worth noting that $\underline{\Delta}$ can be viewed as the discrete Laplace–Beltrami operator defined not on the planar graph G , but rather on the image of G inside the rhombic surface S_G^\diamond (i.e., the black vertices of S_G^\diamond where two black vertices are joined by an edge if and only if they lie on a common rhombus). We point the reader to a related construction in [21]. As such, $\underline{\Delta}$ is a discretization of the Laplace–Beltrami operator on a Riemann surface with respect to a non-flat metric. It is also a symmetric real operator.

- The Kähler operator \mathcal{D} , which we are interested in, has been introduced in [7]. It is defined in terms of the geometry of the graph G as

$$\mathcal{D}\phi(u) = \sum_{\text{edges } \vec{e}=(u,v)} \frac{1}{2} \left(\frac{\tan \theta_n(\vec{e}) + i}{R_n^2(\vec{e})} + \frac{\tan \theta_s(\vec{e}) - i}{R_s^2(\vec{e})} \right) (\phi(u) - \phi(v)), \tag{1.8}$$

where $R_n(\vec{e})$ and $R_s(\vec{e})$ are the circumradii of the north and south faces f_n and f_s adjacent to \vec{e} , respectively. It is a Hermitian complex operator. Although it is not obvious from this definition (1.8), the operator \mathcal{D} transforms covariantly under global conformal $\text{PSL}(2, \mathbb{C})$ transformations of the graph embedding, and (even less obviously) it defines a Kähler metric $dz_u \mathcal{D}_{uv} d\bar{z}_v$ on the space of Delaunay graphs in the plane.

These three operators can be defined for any polyhedral graph G . The weak Delaunay condition on G ensures that the three operators are positive semidefinite. If G is isoradial (with common circumradius $R > 0$), then the operators Δ , $\underline{\Delta}$ and $R^2 \mathcal{D}$ all coincide, and agree with the *critical Laplacian* Δ_{cr} considered in [17] and defined by

$$\Delta_{\text{cr}}\phi(u) := \sum_{\text{edges } \vec{e}=(u,v)} \tan \theta(e)(\phi(u) - \phi(v)). \tag{1.9}$$

This coincidence occurs because $\theta_n(\vec{e}) = \theta_s(\vec{e}) = \theta(e)$ for any (oriented) edge \vec{e} in the isoradial case. The Green’s function Δ_{cr}^{-1} of the critical Laplacian Δ_{cr} (see Section 3) turns out to be accessible and can be written explicitly in terms of the graph’s local structure; furthermore, the log-determinant of the critical Laplacian can be computed as a finite sum of local contributions if in addition one assumes the graph is periodic.

1.3. The main results

1.3.1. Asymptotics of the critical Green’s function. The asymptotic behavior of Δ_{cr}^{-1} is essential to us. The leading asymptotics has been worked out by Kenyon in [17]. Our first result is a refinement of Kenyon’s estimate, which entails isolating subleading terms. We shall make use of this series development later in the proof of Theorem 1.6.

Proposition 1.1. *For any vertices u and v in an isoradial Delaunay graph G_{cr} ,*

$$\begin{aligned} [\Delta_{\text{cr}}^{-1}]_{u,v} = & -\frac{1}{2\pi} \left(\log(2|p_1(u, v)|) + \gamma_{\text{Euler}} + \frac{\text{Re}[p_3(u, v)]}{6|p_1(u, v)|^3} \right. \\ & \left. + O\left(\frac{1}{|p_1(u, v)|^4}\right) \right), \end{aligned} \tag{1.10}$$

where γ_{Euler} is the Euler–Mascheroni constant, and

$$p_1(u, v) = z_{\text{cr}}(v) - z_{\text{cr}}(u).$$

The term $p_3(u, v)$ is introduced in Definition 2.23 (and written explicitly in (2.4)) in Section 4.2. It depends on the local geometry of the graph G_{cr} between u and v , but is bounded uniformly and linearly by

$$|p_3(u, v)| \leq 3|p_1(u, v)|.$$

Remark 1.2. Proposition 1.1 sharpens Kenyon’s theorem [17, Theorem 7.3] by identifying and obtaining a uniform bound on the first non-constant subdominant term

$$\frac{1}{6}|p_1(u, v)|^{-3} \text{Re}[p_3(u, v)] \leq \frac{1}{2}|p_1(u, v)|^{-2}.$$

Proposition 4.9 in Section 4 extends these asymptotics to all orders of the large distance asymptotic series expansion of the Green’s function, and gives uniform bounds for those terms. Proposition 1.1 follows from Proposition 4.9.

1.3.2. Deformations of critical graphs. We introduce a scheme for deforming Delaunay graphs (and general polyhedral graphs) and study the response of the corresponding operators supported on the deformed graph.

Definition 1.3. A *Delaunay deformation* G_ϵ of an initial Delaunay graph G_0 is defined as follows. We start by deforming the initial vertex embedding $v \mapsto z_0(v)$ for $v \in V(G_0)$ by

$$z_\epsilon(v) := z_0(v) + \epsilon F(v), \tag{1.11}$$

where $\epsilon \geq 0$ is a real parameter, and where $F: V(G_0) \rightarrow \mathbb{C}$ is a displacement function with finite support $\Omega_F \subset V(G_0)$. Provided the mapping $v \mapsto z_\epsilon(v)$ is one-to-one, the corresponding Delaunay deformation G_ϵ of G_0 is defined to be the unique Delaunay graph with vertex set $V(G_\epsilon) = V(G_0)$ and planar graph embedding $v \mapsto z_\epsilon(v)$. For a generic polyhedral graph G , the *lattice closure* $\bar{\Omega}_F$ of Ω_F is

$$\bar{\Omega}_F = \{v \in V(G) : v \text{ shares a face } f \in F(G) \text{ with a vertex } u \in \Omega_F\}. \tag{1.12}$$

We first need to control the geometry of the deformed graph G_ϵ in terms of the deformation parameter ϵ . This is ensured by Lemmas 5.1, 5.4, 5.7 and Proposition 5.8, which we summarize in the following proposition.

Proposition 1.4. *Let G_0 be an isoradial Delaunay graph, and F a displacement function as above. There is a threshold $\tilde{\epsilon}_F > 0$ such that whenever $0 \leq \epsilon < \tilde{\epsilon}_F$,*

- (1) $z_\epsilon: V(G_0) \rightarrow \mathbb{C}$ is an embedding,
- (2) there is an inclusion of edge sets $E(G_0) \subseteq E(G_\epsilon)$,
- (3) the edge sets are stable, i.e., $E(G_{\epsilon_1}) = E(G_{\epsilon_2})$ whenever $0 < \epsilon_1, \epsilon_2 < \tilde{\epsilon}_F$.

Proposition 1.4 ensures the existence of a right-sided limit graph when $\epsilon \rightarrow 0$, which is weakly Delaunay.

Definition 1.5. The *refinement* G_{0+} of G_0 determined by F is the weak Delaunay graph with vertex set $V(G_{0+}) := V(G_0)$ and embedding $z_{0+} := z_0$, whose edge set is given by

$$E(G_{0+}) := \lim_{\epsilon \rightarrow 0^+} E(G_\epsilon).$$

Note that G_{0+} will be a *weak* Delaunay graph precisely when the inclusion of edge sets is strict, otherwise G_{0+} and G_0 will coincide. It will be convenient to *complete* G_{0+} to a (weak) Delaunay triangulation \hat{G}_{0+} by maximally saturating $E(G_{0+})$

with additional non-crossing edges (see Definition 2.8). The choice of these additional edges (referred to as *chords*, introduced in Definition 2.3) will not affect our calculations because the weights assigned to these edges by the operators Δ , \mathcal{D} , and $\underline{\Delta}$ always vanish. We want to emphasize that

$$\widehat{G}_{0+} = G_{0+} = G_0$$

whenever G_0 is a triangulation.

Our chief interest is when the initial graph G_0 is a *critical graph*, i.e., an isoradial Delaunay graph G_{cr} with isoradius R_{cr} . A Delaunay deformation $G_{cr} \rightarrow G_\epsilon$ (corresponding to some F) supports a Kähler operator $\mathcal{D}(\epsilon)$, as well as a Laplace–Beltrami operator $\Delta(\epsilon)$ and a conformal Laplacian $\underline{\Delta}(\epsilon)$. All three of these operators degenerate on the critical graph when $\epsilon \rightarrow 0$,

$$\begin{aligned} \lim_{\epsilon \rightarrow 0} \mathcal{D}(\epsilon) &= \frac{\Delta_{cr}}{R_{cr}^2}, \\ \lim_{\epsilon \rightarrow 0} \Delta(\epsilon) &= \lim_{\epsilon \rightarrow 0} \underline{\Delta}(\epsilon) = \Delta_{cr}, \end{aligned}$$

where Δ_{cr} is the critical Laplacian of Kenyon on G_{cr} .

Let \mathcal{O} denote either Δ or $\underline{\Delta}$ or \mathcal{D} . Accordingly, $\mathcal{O}(\epsilon)$ will denote the corresponding operator on the perturbed Delaunay graph G_ϵ , while \mathcal{O}_{cr} will denote the operator on the critical graph G_{cr} . We introduce the variation of operators

$$\delta\mathcal{O}(\epsilon) := \mathcal{O}(\epsilon) - \mathcal{O}_{cr} \tag{1.13}$$

and formally expand the log-determinant $\log \det \mathcal{O}(\epsilon)$ using the Green’s function \mathcal{O}_{cr}^{-1} of the critical operator as

$$\begin{aligned} \log \det \mathcal{O}(\epsilon) &= \log \det \mathcal{O}_{cr} + \text{tr}[\delta\mathcal{O}(\epsilon) \cdot \mathcal{O}_{cr}^{-1}] \\ &\quad - \frac{1}{2} \text{tr}[(\delta\mathcal{O}(\epsilon) \cdot \mathcal{O}_{cr}^{-1})^2] + \dots \end{aligned} \tag{1.14}$$

The trace terms occurring on the right-hand side of equation (1.14) are well defined owing to the fact that the support of the perturbation is compact; consequently, the difference $\log \det \mathcal{O}(\epsilon) - \log \det \mathcal{O}_{cr}$ is well defined and takes a finite real value.

Our most significant results concern the second-order term $\text{tr}[(\delta\mathcal{O}(\epsilon) \cdot \mathcal{O}_{cr}^{-1})^2]$ arising from a bi-local version of the deformation given in (1.11), executed simultaneously at two distant sites and controlled by a pair $\underline{\epsilon} = (\epsilon_1, \epsilon_2)$ of independent deformation parameters. These results are mainly given by Proposition 6.10 for Δ , Proposition 6.11 for \mathcal{D} , while the analysis of $\underline{\Delta}$ is handled in Sections 6.3 and 6.4. The following theorem summarizes these results.

Theorem 1.6. Consider two complex functions $F_1(z)$ and $F_2(z)$ whose supports

$$\Omega_1 = \text{supp } F_1 \quad \text{and} \quad \Omega_2 = \text{supp } F_2$$

in the vertex set $V(G_{\text{cr}})$ are finite and disjoint (hence at finite distance), and a bi-local deformation of the embedding $v \mapsto z_{\text{cr}}(v)$ given by

$$z_{\underline{\epsilon}}(v) := z_{\text{cr}}(v) + \epsilon_1 F_1(v) + \epsilon_2 F_2(v),$$

where $\underline{\epsilon} = (\epsilon_1, \epsilon_2)$ is a pair of independent deformation parameters.

As functions of ϵ_1 and ϵ_2 , $\log \det \Delta(\underline{\epsilon})$, $\log \det \underline{\Delta}(\underline{\epsilon})$, $\log \det \mathcal{D}(\underline{\epsilon})$ are analytic within the range $0 \leq \epsilon_1, \epsilon_2 < \min(\tilde{\epsilon}_{F_1}, \tilde{\epsilon}_{F_2})$.

Furthermore, the $\epsilon_1 \epsilon_2$ cross-term in the perturbative expansion of $\log \det \Delta(\underline{\epsilon})$, denoted by $\mathfrak{d}_{\epsilon_1 \epsilon_2} \log \det \Delta$, is obtained from $\text{tr}[(\delta \Delta(\underline{\epsilon}) \cdot \Delta_{\text{cr}}^{-1})^2]$. It takes the asymptotic form

$$\begin{aligned} \mathfrak{d}_{\epsilon_1 \epsilon_2} \log \det \Delta = & -\frac{2}{\pi^2} \sum_{\substack{\text{triangles} \\ x_1, x_2}} A(x_1)A(x_2) \left(\text{Re} \left[\frac{\bar{\nabla} F_1(x_1) \bar{\nabla} F_2(x_2)}{(z_{\text{cr}}(x_1) - z_{\text{cr}}(x_2))^4} \right] \right. \\ & \left. + O(|z_{\text{cr}}(x_1) - z_{\text{cr}}(x_2)|^{-5}) \right), \end{aligned} \tag{1.15}$$

where $x_i \in F(\widehat{G}_{0+})$ is a triangle having at least one vertex in Ω_i , whose center has the coordinate $z_{\text{cr}}(x_i)$, and whose area is $A(x_i)$ with $i = 1, 2$. Formula (1.15) makes use of the discrete derivative operators $\nabla, \bar{\nabla}: \mathbb{C}^{V(T)} \rightarrow \mathbb{C}^{F(T)}$ introduced in [7] for polyhedral triangulations T ; see Definition 3.3.

Likewise, the $\epsilon_1 \epsilon_2$ cross-term $\mathfrak{d}_{\epsilon_1 \epsilon_2} \log \det \mathcal{D}$ in the expansion of $\log \det \mathcal{D}(\underline{\epsilon})$ is obtained from $\text{tr}[(\delta \mathcal{D}(\underline{\epsilon}) \cdot \mathcal{D}_{\text{cr}}^{-1})^2]$ and takes the same asymptotic form as formula (1.15).

For the conformal Laplacian $\underline{\Delta}$, the $\epsilon_1 \epsilon_2$ cross-term $\mathfrak{d}_{\epsilon_1 \epsilon_2} \log \det \underline{\Delta}$ in the expansion of $\log \det \underline{\Delta}(\underline{\epsilon})$ does not, in general, have an asymptotic form given by (1.15). ‘‘Anomalous’’ chord-to-edge and chord-to-chord terms have to be added to formula (1.15) in order to obtain the correct asymptotics. They can be interpreted as ‘‘curvature defects’’ arising from the deformation of the graph.

Remark 1.7. Formula (1.15) is independent of the choice of triangulation \widehat{G}_{0+} used to complete G_{0+} , in light of a discretized version of Green’s theorem, namely Lemma 3.5 and Corollary 3.6 as detailed in Section 3.2.

1.3.3. Smooth deformations and scaling limits. In this paper, we are interested in the existence and the form of the continuum limit of the results in Theorem 1.6. For this purpose, we shall consider *smooth Delaunay deformations* implemented by test functions, defined below. We aim for results independent of the initial critical graph G_{cr} , and which reconstitute the continuous formula (1.3) expected from CFT’s.

Definition 1.8. Let F be a smooth (non-holomorphic) function $F: \mathbb{C} \rightarrow \mathbb{C}$ with compact support $\Omega \subset \mathbb{C}$, and consider its restriction to an initial Delaunay graph G_0 by declaring

$$F(v) := F(z_0(v)), \tag{1.16}$$

where $v \in V(G_0)$ is a vertex.

The *smooth Delaunay deformation* G_ϵ of G_0 corresponding to F is the Delaunay deformation of G_0 given by Definition 1.3 with the function $F(v)$ given by formula (1.16).

We shall incorporate a parameter $\ell > 0$ into our deformation rubric (1.16) by rescaling the displacement function accordingly:

$$F_\ell(v) = F_\ell(z_0(v)) := \ell F\left(\frac{z_0(v)}{\ell}\right).$$

Using the construction above, we obtain a rescaled deformed embedding $z_{\epsilon,\ell}$ and a corresponding Delaunay graph $G_{\epsilon,\ell}$ together with an attending refinement $G_{0^+,\ell}$ and a completion $\widehat{G}_{0^+,\ell}$. We shall denote by $\Delta(\epsilon, \ell)$, $\mathcal{D}(\epsilon, \ell)$, and $\underline{\Delta}(\epsilon, \ell)$ the discrete Beltrami–Laplace operator, Kähler operator, and conformal Laplacian on the graph $G_{\epsilon,\ell}$, respectively.

The following estimate (see Appendix B for the proof) explains why ∇ and $\bar{\nabla}$ should be considered as discrete analogs of the holomorphic and anti-holomorphic derivatives ∂ and $\bar{\partial}$.

Lemma 1.9. *Given a smooth function $\phi: \mathbb{C} \rightarrow \mathbb{C}$ and a triangle \mathfrak{f} with vertices z_1, z_2, z_3 (listed in counter-clockwise order), circumcenter $z(\mathfrak{f})$, and circumradius $R(\mathfrak{f})$, we have the following estimate:*

$$|\nabla\phi(\mathfrak{f}) - \partial\phi(z(\mathfrak{f}))| \leq R(\mathfrak{f}) \left(\frac{3}{2} \sup_{z \in B_{\mathfrak{f}}} |\partial^2\phi| + 2 \sup_{z \in B_{\mathfrak{f}}} |\partial\bar{\partial}\phi| + \frac{1}{2} \sup_{z \in B_{\mathfrak{f}}} |\bar{\partial}^2\phi| \right),$$

where $B_{\mathfrak{f}}$ is the disk bounded by the circumcircle of \mathfrak{f} ,

$$B_{\mathfrak{f}} = \{z : |z - z(\mathfrak{f})| \leq R(\mathfrak{f})\}.$$

Using Lemma 1.9, we are able to obtain a smooth version of Theorem 1.6 involving a scaling parameter $\ell > 0$ whose continuum limit is consistent with formula (1.3).

Theorem 1.10. *Consider two smooth complex functions $F_1(z)$ and $F_2(z)$ whose supports $\Omega_1 = \text{supp } F_1$ and $\Omega_2 = \text{supp } F_2$ in the plane are compact and disjoint (hence at finite distance), and a bi-local deformation of the embedding given by*

$$z_{\epsilon,\ell}(v) := z_{\text{cr}}(v) + \epsilon_1 F_{1;\ell}(v) + \epsilon_2 F_{2;\ell}(v),$$

where $\ell > 0$ is a scaling parameter and $F_{i;\ell}(\mathbf{v}) := \ell F_i(\frac{z_{\text{cr}}(\mathbf{v})}{\ell})$ for $i = 1, 2$. The scaling limit $\ell \rightarrow \infty$ of the $\epsilon_1\epsilon_2$ cross-term in the expansion of $\log \det \Delta(\underline{\epsilon}, \ell)$ and of $\log \det \mathcal{D}(\underline{\epsilon}, \ell)$ (given by Theorem 1.6) exist and are given by

$$\begin{aligned} \lim_{\ell \rightarrow \infty} \mathfrak{d}_{\epsilon_1\epsilon_2} \log \det \Delta(\ell) &= \lim_{\ell \rightarrow \infty} \mathfrak{d}_{\epsilon_1\epsilon_2} \log \det \mathcal{D}(\ell) \\ &= \frac{1}{\pi^2} \iint_{\Omega_1 \times \Omega_2} dx_1^2 dx_2^2 \operatorname{Re} \left[\frac{\bar{\partial} F_1(x_1) \bar{\partial} F_2(x_2)}{(x_1 - x_2)^4} \right]. \end{aligned} \tag{1.17}$$

The limit value in formula (1.17) is independent of the initial isoradial Delaunay graph \mathbf{G}_{cr} .

Remark 1.11. Whenever the refinement $\mathbf{G}_{0+,\ell}$ contains finitely many chords (see Definition 2.3), the scaling limit $\ell \rightarrow \infty$ of the bi-local formula for the $\epsilon_1\epsilon_2$ cross-term in $\operatorname{tr}[\delta \underline{\Delta}(\underline{\epsilon}, \ell) \cdot \Delta_{\text{cr}}^{-1}]^2$ of the conformal Laplacian (as presented in Section 6.3.1) agrees with the limit value in formula (1.17) of Theorem 1.10. In general, this is not the case, and a scaling limit does not exist. If it exists, the effect of the anomalous terms may be present in the scaling limit, which need not be universal. An example is given in Appendix C.

Formula (1.17) in Theorem 1.10 implicitly involves a nested limit where the deformation parameters $\underline{\epsilon} = (\epsilon_1, \epsilon_2)$ are first taken to zero, and subsequently the scaling parameter ℓ is taken to ∞ . An interesting question is whether the limits $\underline{\epsilon} \rightarrow 0$ and $\ell \rightarrow \infty$ can be interchanged.

To study this question, one needs uniform bounds on the variations $\delta \Delta(\epsilon)$ and $\delta \mathcal{D}(\epsilon)$ (see (1.13)) with respect to the space of isoradial Delaunay graphs. Since the bound $\tilde{\epsilon}_F$ in Proposition 1.4 depends on the graph, we cannot hope to make a stable deformation simultaneously for all Delaunay graphs. This requires us to work with Delaunay deformations beyond the $\tilde{\epsilon}_F$ threshold, and take into account the occurrence of Whitehead flips as the graph is deformed. This is addressed in Section 8.

Bounding the variation of the circumradii. In order to bound the operator variations $\delta \Delta(\epsilon)$ and $\delta \mathcal{D}(\epsilon)$, it is necessary to track the circumradius $R(\mathbf{f}_\epsilon)$ of each face \mathbf{f}_ϵ of \mathbf{G}_ϵ as a function of ϵ . In Proposition 8.1, we bound the radius $R(\mathbf{f})$ uniformly for all faces and all initial isoradial Delaunay graphs \mathbf{G}_{cr} with isoradius $R_{\text{cr}} = R_0$. Specifically, we show that there exist $\epsilon_{\text{max}}(R_{\text{cr}})$, as well as two functions $\bar{R}_-(\epsilon, R_{\text{cr}})$ and $\bar{R}_+(\epsilon, R_{\text{cr}})$ such that for $0 \leq \epsilon < \epsilon_{\text{max}}(R_{\text{cr}})$,

$$\begin{aligned} \bar{R}_-(\epsilon, R_{\text{cr}}) &\leq R(\mathbf{f}_\epsilon) \leq \bar{R}_+(\epsilon, R_{\text{cr}}), \\ \lim_{\epsilon \rightarrow 0} \bar{R}_-(\epsilon, R_{\text{cr}}) &= \lim_{\epsilon \rightarrow 0} \bar{R}_+(\epsilon, R_{\text{cr}}) = R_{\text{cr}}. \end{aligned} \tag{1.18}$$

The quantities $\epsilon_{\text{max}}(R_{\text{cr}})$, $\bar{R}_-(\epsilon, R_{\text{cr}})$ and $\bar{R}_+(\epsilon, R_{\text{cr}})$ depend only on R_{cr} and on the smooth displacement function F . They are given explicitly in Proposition 8.1.

Results for interchanging the limits $\epsilon \rightarrow 0$ and $\ell \rightarrow \infty$. The matrix entries of the operators $\Delta(\epsilon)$ and $\mathcal{D}(\epsilon)$ are continuous functions of ϵ , and using the bounds \bar{R}_- and \bar{R}_+ of (1.18), we can show that the derivatives $\Delta'(\epsilon)$ and $\mathcal{D}'(\epsilon)$ with respect to ϵ are piecewise continuous functions of ϵ and obtain uniform bounds on their matrix entries. This leads us to the following conjecture for Δ .

Conjecture 1.12. *Let G_{cr} be an isoradial Delaunay triangulation with embedding $v \mapsto z_{cr}(v)$, let F_1, F_2 be two smooth displacement functions with disjoint compact supports, and let $z_{\underline{\epsilon}, \ell} = z_{cr} + \epsilon_1 F_{1;\ell} + \epsilon_2 F_{2;\ell}$ be the corresponding scaled and deformed embedding with respect to a pair of independent parameters $\underline{\epsilon} = (\epsilon_1, \epsilon_2)$ and $\ell > 0$. Then*

$$\begin{aligned} & \lim_{\underline{\epsilon} \rightarrow 0} \lim_{\ell \rightarrow \infty} \operatorname{tr} \left[\frac{\partial}{\partial \epsilon_1} \Delta(\underline{\epsilon}, \ell) \cdot \Delta_{cr}^{-1} \cdot \frac{\partial}{\partial \epsilon_2} \Delta(\underline{\epsilon}, \ell) \cdot \Delta_{cr}^{-1} \right] \\ &= \lim_{\ell \rightarrow \infty} \lim_{\underline{\epsilon} \rightarrow 0} \operatorname{tr} \left[\frac{\partial}{\partial \epsilon_1} \Delta(\underline{\epsilon}, \ell) \cdot \Delta_{cr}^{-1} \cdot \frac{\partial}{\partial \epsilon_2} \Delta(\underline{\epsilon}, \ell) \cdot \Delta_{cr}^{-1} \right] \\ &= \frac{2}{\pi^2} \int_{\Omega_1} d^2 x_1 \int_{\Omega_2} d^2 x_2 \operatorname{Re} \left[\frac{\bar{\partial} F_1(x_1) \bar{\partial} F_2(x_2)}{(x_1 - x_2)^4} \right]. \end{aligned}$$

Conjecture 1.12 is a special case of Proposition 8.8, which relies on the rigorous estimates obtained in Section 8, and also on Conjecture 8.5, the later of which stipulates a bound on ∇p_3 for critical lattices (where p_3 is defined in Definition 2.23 and appears already in Proposition 1.1).

For \mathcal{D} , we do not get such a strong result, but only the following weaker conjecture, which follows from Propositions 8.10 and 8.11.

Conjecture 1.13. *Let G_{cr} be an isoradial Delaunay triangulation with embedding $v \mapsto z_{cr}(v)$, let F_1, F_2 be two smooth displacement functions with disjoint compact supports, and let $z_{\underline{\epsilon}, \ell} = z_{cr} + \epsilon_1 F_{1;\ell} + \epsilon_2 F_{2;\ell}$ be the corresponding scaled and deformed embedding with respect to a pair of independent parameters $\underline{\epsilon} = (\epsilon_1, \epsilon_2)$ and $\ell > 0$. In general, the limit*

$$\lim_{\ell \rightarrow \infty} \operatorname{tr} \left[\frac{\partial}{\partial \epsilon_1} \mathcal{D}(\underline{\epsilon}, \ell) \cdot \mathcal{D}_{cr}^{-1} \cdot \frac{\partial}{\partial \epsilon_2} \mathcal{D}(\underline{\epsilon}, \ell) \cdot \mathcal{D}_{cr}^{-1} \right]$$

does not exist for non-zero $\underline{\epsilon}$.

The double “simultaneous” limit exists, where $\ell \rightarrow \infty$ and $\underline{\epsilon} \rightarrow 0$ such that $\ell \underline{\epsilon} = \underline{c}$ with $\underline{c} > 0$ staying constant. Its value is

$$\begin{aligned} & \lim_{\substack{\ell \rightarrow \infty \\ \ell \underline{\epsilon} = \underline{c}}} \operatorname{tr} \left[\frac{\partial}{\partial \epsilon_1} \mathcal{D}(\underline{\epsilon}, \ell) \cdot \mathcal{D}_{cr}^{-1} \cdot \frac{\partial}{\partial \epsilon_2} \mathcal{D}(\underline{\epsilon}, \ell) \cdot \mathcal{D}_{cr}^{-1} \right] \\ &= \frac{2}{\pi^2} \int_{\Omega_1} d^2 x_1 \int_{\Omega_2} d^2 x_2 \operatorname{Re} \left[\frac{\bar{\partial} F_1(x_1) \bar{\partial} F_2(x_2)}{(x_1 - x_2)^4} \right]. \end{aligned}$$

1.3.4. Interpretation in terms of discrete stress-energy tensors and discrete central charge. The results presented above can be formulated in the language of CFT in terms of an action, a stress-energy tensor and a central charge. This is done in Section 9.2. For the Laplace–Beltrami operator Δ , the associated discrete action is

$$S[\Phi, \bar{\Phi}] = \Phi \cdot \Delta \bar{\Phi} = \sum_{\substack{\text{vertices} \\ u, v \in \mathcal{G}}} \Phi_u \Delta_{uv} \bar{\Phi}_v,$$

where $(\Phi, \bar{\Phi})$ are Grassmann fields supported on vertices of the Delaunay graph \mathcal{G} . The corresponding functional integral is

$$\det(\hat{\Delta}) = \int \mathfrak{D}[\Phi, \bar{\Phi}] e^{-S[\Phi, \bar{\Phi}]}.$$

A general deformation $z \mapsto z + \epsilon F$ of the coordinate embedding induces a deformed action $S_\epsilon[\Phi, \bar{\Phi}] = \Phi \cdot \Delta(\epsilon) \bar{\Phi}$, which we can develop as $S_\epsilon = S + \epsilon \delta_\epsilon S + O(\epsilon^2)$. Using the variation of $\Delta(\epsilon)$ given by Proposition 5.12, the linear term $\delta_\epsilon S$ reads explicitly as

$$\delta_\epsilon S[\Phi, \bar{\Phi}] = -4 \sum_{\substack{\text{faces} \\ x \in \hat{\mathcal{G}}_{0+}}} A(x) (\bar{\nabla} F(x) \nabla \Phi(x) \nabla \bar{\Phi}(x) + \text{c.c.}).$$

In analogy with the continuous case, the components of the discrete stress-energy tensor \mathbf{T}_Δ can be identified as

$$T_\Delta(x) = -4\pi \nabla \Phi(x) \nabla \bar{\Phi}(x) \quad \text{and} \quad \bar{T}_\Delta(x) = -4\pi \bar{\nabla} \Phi(x) \bar{\nabla} \bar{\Phi}(x) \tag{1.19}$$

while \mathbf{T}_Δ is traceless, namely, $\text{tr } \mathbf{T}_\Delta(x) = 0$. See (9.4) for details. Taking vacuum expectation values of the components of the stress-energy tensor, we recover our results (Proposition 6.1 and Theorem 1.6) for the first and second-order variations of $\log \det(\Delta)$ in the case of a critical lattice $\mathcal{G} = \mathcal{G}_{\text{cr}}$. In the scaling limit, the discrete T_Δ given in (1.19) becomes the continuum stress-energy tensor $T = -4\pi \partial \Phi \partial \bar{\Phi}$ for the CFT of a free Grassmann field (see Appendix A for details).

Theorem 1.10 shows that, when perturbing a critical lattice, the scaling limit for the second-order variation $\delta_{\epsilon_1 \epsilon_2} \log \det \Delta$ of the Laplace–Beltrami operator Δ exists, and can be calculated in terms of the connected vacuum expectation values

$$\langle T_\Delta(x) T_\Delta(y) \rangle \quad \text{and} \quad \langle \bar{T}_\Delta(x) \bar{T}_\Delta(y) \rangle.$$

This implies that in the scaling limit, we recover a short distance operator product expansion for T_Δ ,

$$\langle T_\Delta(u) T_\Delta(v) \rangle = -\frac{1}{(u-v)^4} + \dots, \tag{1.20}$$

which is the OPE for a CFT with central charge $c = -2$ (through (1.2)). This is the expected result for a complex Grassmann field, which is indeed a conformal field theory with central charge $c = -2$ (see Appendix A and, e.g., [10]).

The same analysis is carried out for the Kähler operator \mathcal{D} . From the variation of $\mathcal{D}(\epsilon)$ given by Proposition 5.13, we can isolate the components of the corresponding discrete stress-energy tensor $\mathbf{T}_{\mathcal{D}}$ (see (9.7))

$$\begin{aligned} T_{\mathcal{D}}(\mathbf{x}) &= -4\pi \frac{1}{R(\mathbf{x})^2} (\nabla\Phi(\mathbf{x})\nabla\bar{\Phi}(\mathbf{x}) + C(\mathbf{x})\bar{\nabla}\Phi(\mathbf{x})\nabla\bar{\Phi}(\mathbf{x})), \\ \bar{T}_{\mathcal{D}}(\mathbf{x}) &= -4\pi \frac{1}{R(\mathbf{x})^2} (\bar{\nabla}\Phi(\mathbf{x})\bar{\nabla}\bar{\Phi}(\mathbf{x}) + \bar{C}(\mathbf{x})\bar{\nabla}\Phi(\mathbf{x})\nabla\bar{\Phi}(\mathbf{x})), \\ \text{tr } \mathbf{T}_{\mathcal{D}}(\mathbf{x}) &= 8 \frac{1}{R(\mathbf{x})^2} \bar{\nabla}\Phi(\mathbf{x})\nabla\bar{\Phi}(\mathbf{x}), \end{aligned}$$

where $R(\mathbf{x})$ is the radius of the face \mathbf{x} , and $C(\mathbf{x})$ is a geometrical factor given in formula (5.13), which depends on the shape and orientation of the face \mathbf{x} . Note that $\mathbf{T}_{\mathcal{D}}$ is no longer traceless. The factor $C(\mathbf{x})$ has no obvious scaling limit $\ell \rightarrow \infty$, independent of the details of the Delaunay lattice, so we cannot associate a stress-energy tensor for some continuum QFT to the discrete $\mathbf{T}_{\mathcal{D}}$, as we did for Δ by replacing ∇ by ∂ .

Surprisingly, Theorem 1.10 also shows that, when perturbing a critical lattice, the scaling limit for the second-order variation $\mathfrak{d}_{\epsilon_1\epsilon_2} \log \det \mathcal{D}$ of the Kähler operator \mathcal{D} still exists, and can still be calculated in terms of the connected vacuum expectation values

$$\langle T_{\mathcal{D}}(\mathbf{x})T_{\mathcal{D}}(\mathbf{y}) \rangle \quad \text{and} \quad \langle \bar{T}_{\mathcal{D}}(\mathbf{x})\bar{T}_{\mathcal{D}}(\mathbf{y}) \rangle.$$

Moreover, we recover a short distance OPE for $T_{\mathcal{D}}$ which is identical to the OPE for T_{Δ} given by (1.20)

$$\langle T_{\mathcal{D}}(u)T_{\mathcal{D}}(v) \rangle = -\frac{1}{(u-v)^4} + \dots,$$

and therefore we can associate a “central charge” $c_{\mathcal{D}} = -2$ with the same value as the central charge $c_{\Delta} = -2$ for Δ (see Section 9.2 for a more thorough discussion).

Finally, a similar analysis is taken in Section 9.2.3 for the conformal Laplacian $\underline{\Delta}$, and leads to a discrete stress-energy tensor $\mathbf{T}_{\underline{\Delta}}$. The trace term $\text{tr } \mathbf{T}_{\underline{\Delta}}$ vanishes, and the discretized holomorphic (and anti-holomorphic) component $T_{\underline{\Delta}}$ (and $\bar{T}_{\underline{\Delta}}$) can be written explicitly as

$$\mathfrak{a}(\mathbf{x})\nabla\Phi(\mathbf{x})\nabla\bar{\Phi}(\mathbf{x}) + \mathfrak{b}(\mathbf{x})\nabla\Phi(\mathbf{x})\bar{\nabla}\bar{\Phi}(\mathbf{x}) + \mathfrak{c}(\mathbf{x})\bar{\nabla}\Phi(\mathbf{x})\nabla\bar{\Phi}(\mathbf{x}) + \mathfrak{d}(\mathbf{x})\bar{\nabla}\Phi(\mathbf{x})\bar{\nabla}\bar{\Phi}(\mathbf{x}).$$

The coefficients $\mathfrak{a}(\mathbf{x}), \dots, \mathfrak{d}(\mathbf{x})$ depend in a non-trivial way on the geometry of the face \mathbf{x} and its three neighboring faces in $\hat{\mathbf{G}}_{0+}$, and have no meaningful continuum limit. This is reflected in the fact that the second-order variation $\mathfrak{d}_{\epsilon_1\epsilon_2} \log \det \underline{\Delta}(\ell)$ has no scaling limit in general, as stated in Remark 1.11.

1.4. Plan of the paper

This paper is organized as follows.

The present Section 1 is the introduction.

Section 2 presents basic concepts about the geometry of planar graphs which are relevant to the paper. Most of the material is standard, however we introduce the notion of a *chord* (see Definition 2.3) which allows us to slightly broaden the definition of an isoradial triangulation (given in [17]) to accommodate configurations with four or more cocyclic vertices. Section 2.1 gives definitions and sets notation for polyhedral graphs, edges and chords, (weak) Delaunay graphs, isoradial graphs, etc. and makes precise the notion of the abstract rhombic surface \mathbb{S}_G^\diamond associated to a polyhedral graph G alluded to in Section 1.2.1. Section 2.2 addresses geometrical concepts and properties of rhombic graphs, mainly following the presentations of [17, 18]. In order to help establish the asymptotic formula in Proposition 1.1, we undertake in Proposition 2.27 a careful analysis of the interval of possible angles taken by any path in the rhombic graph of an isoradial Delaunay graph.

In Section 3, we review the ∇ and $\bar{\nabla}$ operators of [7] and show how they are used to obtain “local factorizations” of the Laplace–Beltrami and Kähler operators Δ and \mathcal{D} for a general polyhedral triangulation; see Remarks 3.8 and 3.9. We remark that the conformal Laplacian $\underline{\Delta}$ does not admit a simple local factorization. Following this, we recall two approaches used to define the (normalized) log-determinant of a Laplace-like operator such as Δ , \mathcal{D} , and $\underline{\Delta}$ for infinite polyhedral graphs which are either (1) doubly periodic or (2) obtained as a nested limit of finite graphs, each with Dirichlet boundary conditions. Formulas (3.14) and (3.15) serve respectively as definitions in these two cases. We end the section by discussing Kenyon’s local formula in [17] for the normalized log-determinant of the critical Laplacian for doubly periodic isoradial (weak) Delaunay graphs, as well as its formal extension to the non-periodic case.

In Section 4, we derive the long-range asymptotic formula for the Green’s function of the critical Laplacian (associated to an isoradial Delaunay graph) as stated in Proposition 1.1. We rely on the methods of [17] along with some added improvements, in particular, for non-periodic graphs. Among other things, our analysis provides uniform bounds on the coefficients of the asymptotic expansion (see Lemma 4.3 and (4.4)), thus sharpening the results and approximations in [17].

Section 5 addresses deformations of Delaunay graphs and corresponding operators. In Section 5.3, we introduce the notions of *Delaunay* and *rigid* deformations: In both cases, the coordinate embedding of the graph is perturbed by a local displacement function together with a deformation parameter $\epsilon \geq 0$. Delaunay deformations modify the incidence relations (i.e., the edge and face sets) so that the Delaunay constraints are maintained while rigid deformations always fix the incidence relations of

the initial graph (and so the resulting graph may cease to be Delaunay). In the case of a Delaunay deformation, we explain in Lemma 5.7 how to regulate the parameter $\epsilon \geq 0$ so that the edges of the initial graph are *stable* and do not undergo Lawson “flips”. A generic Delaunay deformation, however, can break the cyclicity of faces having four or more vertices in the initial graph and introduce new edges which subdivide these faces. Nevertheless, these additional edges are shown to be stable for values of $\epsilon > 0$ which are bounded appropriately. This follows from Proposition 5.8 which also proves the existence of a (weak) Delaunay limit graph G_{0+} whose redaction G_{0+}^\bullet coincides with the initial Delaunay graph G_0 . In Section 5.3, we study the first-order variation of the Laplace–Beltrami and Kähler operators, when the underlying polyhedral triangulation is subject to a rigid deformation. Results are given in Propositions 5.12 and 5.13, respectively. The conformal Laplacian $\underline{\Delta}$ does not admit a local factorization of the kind presented in Propositions 5.12 and 5.13, and for this reason there is no analogous formula for its first-order variation. Section 5.4 sets up notation.

The calculations of the first- and second-order variations of the log-determinant for the Laplace–Beltrami operator, the Kähler operator, and the conformal Laplacian are undertaken in Section 6. The first-order variation formulas are entirely local, i.e., expressed as sums of weights of edges. The second-order variations, on the other hand, involve long-range effects of the critical Green’s function Δ_{cr}^{-1} associated to pairs of distant vertices and, in principle, register aspects of the global geometry of the initial isoradial Delaunay graph G_{cr} . In Propositions 6.1 and 6.6 of Section 6.1, we present formulas for the first-order variations of the Laplace–Beltrami and Kähler operators which are valid uniformly for all isoradial Delaunay graphs. The first-order formula for the conformal Laplacian incorporates an additional term which accounts for the effect made by chords in G_{0+} and is given in Proposition 6.4. The second-order formulas for the variation of the log-determinant of the Laplace–Beltrami and Kähler operators are calculated separately in Propositions 6.10 and 6.11 of Section 6.2, respectively; this is the content of Theorem 1.6. In both cases, our approach relies on the asymptotics of the Green’s function in Proposition 1.1 and Lemma 6.9; the latter makes use of the operator factorizations in Propositions 5.12 and 5.13, as well as a novel estimate presented in Lemma 6.8. Formula (1.15) of Theorem 1.6 is not valid for the conformal Laplacian, and it must be modified by defect terms which take into account the effect of chords in G_{0+} . See formulas (6.25) and (6.26). We propose that these defects are indicative of a discrete curvature anomaly arising from the perturbation. This is examined in Section 6.4.

Section 7 handles the proof of Theorem 1.10, which deals with the existence and value of the scaling limit given by formula (1.17) for the Laplace–Beltrami and Kähler operators. Sections 7.1 and 7.2 address some technical points about bi-local deformations, scaling limits, and re-summation. In Section 7.3, we prove the existence of

the scaling limit of (1.15) in the case of a continuous bi-local deformation and settle Theorem 1.10. The basic idea is to interpret (1.15) as a Riemann sum with a mesh controlled by the scaling parameter. The scaling limit considered in Section 7.3 is taken with respect to an isoradial refinement $\widehat{G}_{0^+, \ell}$ associated to a (scaled) deformation of our initial isoradial Delaunay graph G_{cr} . In effect, the result is a calculation of a nested limit: First we take the deformation parameter limit $\epsilon_1, \epsilon_2 \rightarrow 0$ (bringing us to $\widehat{G}_{0^+, \ell}$), and then we subsequently take the scaling limit $\ell \rightarrow \infty$. In Section 7.4, we ask whether these two limits can be interchanged. This question is related to whether the scaling limit in Theorem 1.10 exists for a Delaunay graph (not necessarily isoradial) which is obtained as a small deformation of an isoradial Delaunay graph. We return to this issue in Section 8. Section 7.5 addresses the issue of the uniform convergence in the “flip problem” for smooth scaled deformations. A first attempt is offered in Lemma 7.1, where we introduce a lower bound on the range of conformal angles for an isoradial Delaunay triangulation. This constraint ensures that no flips occur whenever the deformation parameter ϵ is bounded above by a threshold $\check{\epsilon}_F$ which is uniform both with respect to the scaling parameter and this proper subclass of isoradial Delaunay triangulations.

In Section 8, we return to the general case of deformations G_ϵ of Delaunay graphs G_{cr} which may incur edge flips. We look for uniform bounds on the variation of the corresponding operators $\Delta(\epsilon)$ and $\mathcal{D}(\epsilon)$ for small but non-zero values of the deformation parameters. In order to get uniform bounds with respect to the choice of the initial graph G_0 , we obtain in Proposition 8.1 an estimate for the variation of the radius $R(f_\epsilon)$ of an arbitrary triangle f_ϵ of G_ϵ as the deformation parameter ϵ varies. We deduce strong results (summarized in Conjecture 1.12) on the uniform convergence of the scaling limit for Δ (Proposition 8.4) and of the scaling limit of the second-order bi-local term (leading to the OPE) (Proposition 8.7); the later result depends on a conjectural uniform estimate (Conjecture 8.5) on $\nabla p_3(f)$ and $\bar{\nabla} p_3(f)$ in terms of the radius $R(f)$ of a face f and the scaling parameter. We finish the section by showing that there is a qualitative difference between Δ and \mathcal{D} , and we obtain a weaker but interesting “simultaneous convergence” result for the scaling limit of the second-order bi-local term for \mathcal{D} (Proposition 8.11), summarized in Conjecture 1.12.

Section 9 summarizes our results and presents them from a more statistical physics point of view. After reviewing the aims of the paper in Section 9.1, we discuss in Section 9.2 the first-order variation of the log-determinant for the three operators Δ , $\underline{\Delta}$ and \mathcal{D} vis-à-vis the Gaussian free field. We show that formula (6.3) for the Laplace–Beltrami operator Δ can be re-expressed in terms of the vacuum expectation value of a discrete stress-energy tensor T_Δ for a Grassmann free field theory (for convenience, we opt for a fermionic analog of the massless free field (GFF)) supported on G_{cr} and whose scaling limit coincides with the standard continuous free field. This is not a sur-

prise. Our results for \mathcal{D} and $\underline{\Delta}$ are similarly expressed using discrete stress-energy tensors $T_{\mathcal{D}}$ and $T_{\underline{\Delta}}$ however neither formula (6.6) nor formula (6.4) have an obvious continuous limit relating it to the continuous free field. In Section 9.3, we discuss the bi-local second-order variation formula and the universal form of its scaling limit for Δ and \mathcal{D} in terms of their respective discrete stress-energy tensors. Furthermore, we address the (in general) non-existence of a scaling limit for $\underline{\Delta}$. In Section 9.4, we discuss the relation and differences between (i) the model and the questions addressed for Delaunay graphs in our work, and (ii) previous studies made by Chelkak et al. on the $O(n)$ model and by Hongler et al. on the GFF and the Ising model on the hexagonal and square lattices respectively. Finally, in Section 9.5, we briefly list some open questions and some possible extensions of this work.

Some standard material, technical derivations of results and matters not central to this work are relegated to appendices. Appendix A presents some standard notations and reminders about QFT, CFT and the stress-energy tensor, in particular, for the free boson and the b - c ghost theory. Appendix B gives the derivation of Lemma 1.9, which is instrumental for Theorem 1.10 and the derivation of the scaling limit. Appendix C examines the conformal Laplacian $\underline{\Delta}$ on a particular critical Delaunay graph \mathcal{G} , as well as the anomalous terms associated with chords in \mathcal{G}_{0+} which arise in the second-order variation of the log-determinant formula for $\underline{\Delta}$ addressed in Section 6.3.1. The graph \mathcal{G} is sufficiently regular, and \mathcal{G}_{0+} has a sufficient density of chords to ensure that these anomalous terms have a convergent scaling limit, which is computed explicitly in Proposition C.4.

2. Planar graphs and rhombic graphs

2.1. Definitions and properties of the basic objects

Let us first introduce the basic geometrical objects that we shall consider: plane triangulations, plane polyhedral graphs (whose faces are cyclic polygons), Delaunay graphs, rhombic graphs, etc. Most of the notations and properties are standard, and can be found in, for instance, [1, 8, 13]. Some notations and concepts on isoradial graphs come from [17, 18].

2.1.1. Plane graphs and Delaunay graphs.

Definition 2.1. An *embedded planar graph* will be – for the purpose of this article – a graph \mathcal{G} given by a set of vertices $V(\mathcal{G})$ and a set of edges $E(\mathcal{G})$, together with an injective map $z: V(\mathcal{G}) \rightarrow \mathbb{C}$. For a vertex $v \in V(\mathcal{G})$, we shall denote its complex coordinate by $z(v)$; if there is no risk of confusion, we shall sometimes denote the complex coordinate by the vertex label v itself. Each edge $e = \overline{uv}$ is embedded as

a *straight line segment* joining its end-points $z(u)$ and $z(v)$, while the oriented edge $\bar{e} = (u, v)$ corresponds to the displacement vector $z(v) - z(u)$. We require that for any pair of edges the corresponding line segments are non-crossing (i.e., do not share any interior points). The embedding determines an abstract set of faces $F(G)$, and we require that each face $f \in F(G)$ is embedded as a *convex polygon* endowed with a counter-clockwise orientation (so that no face is folded onto an adjacent face). Furthermore, the set of faces must cover the plane and they must not accumulate in any finite region of the plane (i.e., each open disk must contain only finitely many faces). We shall occasionally suppress the distinction between G as an abstract combinatorial entity (i.e., vertices, edges, faces and their incidence relations) and its description as an embedded object in the plane (points, segments, and polygons with the geometrical restrictions described above).

Definition 2.2. A *polyhedral graph* will be an embedded planar graph such that each face is a *cyclic polygon*, i.e., all the vertices of the face lie on a circle (the circumcircle C_f of the face f), in *cyclic order*. Two faces may have the same circumcircle.

Definition 2.3. An edge $e \in E(G)$ of a polyhedral graph G is a *chord* if the two faces f and g of G adjacent to e share the same circumcircle (i.e., the circumcenters of f and g coincide). An edge which is not a chord is said to be a *regular edge* of G . If no ambiguity arises, we shall use the term edge for regular edges only, and chords for the others.

Definition 2.4. A *chordless polyhedral graph* is a polyhedral graph without chords, i.e., no pair of faces share the same circumcircle. Obviously, chordless polyhedral graphs correspond to a special class of circle patterns in the plane. In a general polyhedral graph, a face which does not share its circumcircle with another face will be said to be a *chordless face*.

Definition 2.5 (Redacted graph). Given a polyhedral graph G , let G^\bullet be the graph with the same vertex set $V(G^\bullet) = V(G)$, the same embedding $z^\bullet = z$, and with edge set $E(G^\bullet) = E(G) - \text{chords}(G)$, where $\text{chords}(G)$ is the set of all chords in G . We call G^\bullet the *redaction*, or *redacted graph*, of G .

Definition 2.6. A *weak Delaunay graph* is a polyhedral graph G such that for any face f , the *interior* of the circumdisk D_f (the closed disk whose boundary is the circumcircle C_f) contains no vertex of G . The circumcircle itself contains the vertices of f , and possibly other vertices. A *Delaunay graph* is a chordless weak Delaunay graph.²

²Note that in the literature the term *Delaunay graph* often denotes what we call here a *weak Delaunay graph*.

Definition 2.7. A *triangulation* is an embedded planar graph T such that each face is a triangle. Obviously, a triangulation is a polyhedral graph. A *Delaunay triangulation* is a triangulation which is a Delaunay graph. A *weak Delaunay triangulation* is a triangulation which is a weak Delaunay graph.

Definition 2.8. A triangulation T is called a *completion* of a weak Delaunay graph G if $E(G) \subset E(T)$. Such a triangulation is necessarily weakly Delaunay, and is obtained by saturating G with a maximal collection of non-crossing chords. Clearly, the reductions T^\bullet and G^\bullet coincide. Throughout the paper, \hat{G} will denote a choice of completion of a weakly Delaunay graph G .

Remark 2.9. The concepts of polygonal and Delaunay graphs can be extended to finite graphs embedded in the Riemann sphere. This is done in [7], for instance. Such a graph can be visualized either on the sphere or as an embedded planar Delaunay graph together with edges (represented as infinite rays) joining vertices on the boundary of the convex hull of the graph to a vertex situated at ∞ (if present). Likewise, the Voronoi construction, as well as the Lawson flip algorithm [20], can be adapted to construct a unique embedded Delaunay graph from any finite configuration of points in the Riemann sphere. A similar approach can be undertaken for (finite) graphs embedded in a compact Riemann surface; for example, this is done implicitly in [17] for the torus.

Möbius transformations preserve the Delaunay property for finite graphs embedded in the Riemann sphere, and so one can incorporate the $PSL_2(\mathbb{C})$ symmetry into the model, as done in [7]. Our situation is different: We are chiefly interested in infinite Delaunay graphs in the plane which are locally finite, i.e., having only finitely many vertices in any open ball. Although the application of a $PSL_2(\mathbb{C})$ transformation preserves the Delaunay property, the resulting graph may cease to be locally finite, since a neighborhood of ∞ can be mapped to a finite radius ball containing an infinite number of vertices. This is not a problem for our study, since we shall consider graph deformations which are implemented by bounded functions with compact support.

2.1.2. Isoradial graphs.

Definition 2.10. An *isoradial graph* is a polyhedral graph G such that the *circumradii* $R(\mathfrak{f})$ (the radius of the circumcircle $C_{\mathfrak{f}}$ of \mathfrak{f}) of all the faces \mathfrak{f} of G are equal.

Definition 2.11. Following [17], a face \mathfrak{f} whose circumcenter is inside or on the boundary of \mathfrak{f} (considered as a cyclic polyhedron) is called a *regular face*. A polyhedral graph such that all its faces are regular is called a *regular graph*.

Remark 2.12. Given an oriented edge \vec{e} of a polyhedral graph, we define the corresponding *north* and *south angles* $\theta_n(\vec{e})$ and $\theta_s(\vec{e})$ through Figure 1 in Section 1.2.1. By the inscribed angle theorem, $\theta_n(\vec{e})$ does not depend upon the choice of vertex

$n \in f_n$ in the north face. Likewise, $\theta_s(\vec{e})$ is independent of the vertex $s \in f_s$ in the south face. Note that reversing the orientation of \vec{e} exchanges the roles of north and south, and so the *conformal angle* $\theta(e) := \frac{1}{2}(\theta_n(\vec{e}) + \theta_s(\vec{e}))$ is independent of the choice of edge orientation, hence the notation $\theta(e)$.

Remark 2.13. Given an edge $e = \overline{uv}$ with vertices $u, v \in V(G)$, the value of the conformal angle $\theta(e)$ equals the argument of the following cross-ratio involving the (coordinates of the) vertices u, v, n, s :

$$\theta(e) = \frac{1}{2} \arg(-[z(u), z(v); z(n), z(s)]) \tag{2.1}$$

with the anharmonic cross-ratio

$$[z_1, z_2; z_3, z_4] = \frac{(z_1 - z_3)(z_2 - z_4)}{(z_1 - z_4)(z_2 - z_3)}.$$

Consequently, the conformal angle is $SL_2(\mathbb{C})$ -invariant owing to the fact that the cross-ratio is invariant.

Remark 2.14. We want to reiterate the comments in Section 1.2.1, and stress that the Delaunay condition as stated in Definition 2.6 is equivalent to the condition that for any edge e of a polyhedral graph, its conformal angle $\theta(e)$ is positive and bounded between

$$0 < \theta(e) < \frac{\pi}{2}.$$

The weak Delaunay condition holds for a polyhedral graph if and only if for any edge e of the graph the conformal angle $\theta(e)$ is non-negative and bounded between $0 \leq \theta(e) < \frac{\pi}{2}$.

Remark 2.15. In a weak Delaunay graph, an edge e is a chord if and only if

$$\theta_n(\vec{e}) + \theta_s(\vec{e}) = 2\theta(e) = 0,$$

i.e., if and only if the conformal angle $\theta(e)$ vanishes. However, in this case, the north and south angles $\theta_n(\vec{e})$ and $\theta_s(\vec{e})$ need not to be both zero. The special case

$$\theta_n(\vec{e}) = \theta_s(\vec{e}) = \theta(e) = 0$$

occurs only if the edge e is a diameter of the circumcircle of the cyclic quadrilateral (u, s, v, n) .

Remark 2.16. Note that $\pi - 2\theta(e)$ is the intersection angle between the clockwise oriented north and south circumcircles C_n and C_s . In a polyhedral graph, we have $\theta(e) > 0$ if and only if $z(n)$ lies outside the circumdisk of C_s , or equivalently if and only if $z(s)$ lies outside the circumdisk of C_n .

2.1.3. Some properties. Regular graphs will be useful when discussing rhombic graphs (following Kenyon’s treatment, see [17]) in Section 2.1.4, thanks to the following simple result.

Lemma 2.17. *Let G_{cr} be a planar, isoradial Delaunay graph with common circumradius R_{cr} . Then G_{cr} is regular.*

Proof. Suppose by contradiction there exists an irregular face $f \in F(G_{cr})$. There exists an edge $e \in \partial f$ with an orientation \vec{e} such that $f = f_s$ and such that the face f_s is contained in the intersection of the disks of circles C_s and C , where C is the circle of radius R_{cr} obtained by reflecting C_s about the line determined by the edge e as depicted in Figure 2. In virtue of isoradiality, the vertices $v \in \partial f_n$ with $v \notin \partial e$ must all lie either (1) on the portion of the circle C residing in the interior of the disk of circumcircle C_f or else (2) on the circumcircle C_s . Case (1) is impossible because then any vertex v of this kind would violate the Delaunay property with respect to the face f_s because the edge e would form a chord between faces f_n and f_s . Likewise, case (2) is impossible because the edge e would form a chord between faces f_n and f_s . So G_{cr} must be regular. ■

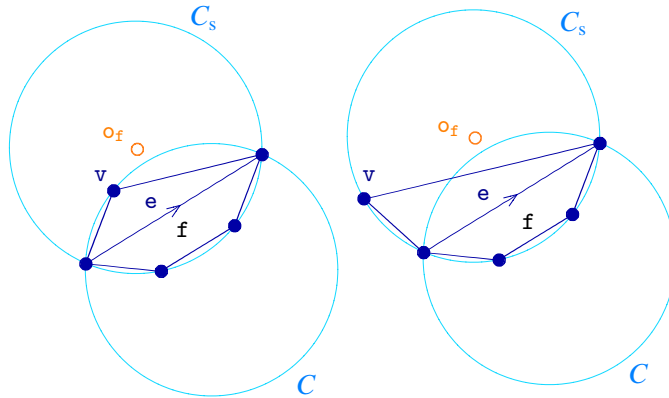


Figure 2. Cases (1) and (2) in the proof of Lemma 2.17.

Corollary 2.18. *By Lemma 2.17, the redacted graph G^\bullet is an isoradial regular Delaunay graph whenever G is isoradial and weakly Delaunay.*

2.1.4. Rhombic graphs and abstract rhombic surfaces. We now consider the bipartite kite graph built from the vertices and the face centers of a Delaunay graph, as well as the associated concept of rhombic surface.

Definition 2.19 (Kite graphs G^\diamond). For a Delaunay graph G , let G^\diamond denote the bipartite graph whose vertex set consists of all vertices v of G (the black vertices \bullet) together

with all circumcenters o_f of faces f of G (the white vertices \circ), and whose edges correspond precisely to those pairs $\{v, o_f\}$ for which $v \in \partial f$. We extend the embedding z of G to G^\diamond by setting $z(o_f) := z(f)$ for each face $f \in F(G)$, where

$$z(f) := \frac{1}{4i} \frac{|z(u)|^2(z(v) - z(w)) + |z(v)|^2(z(w) - z(u)) + |z(w)|^2(z(u) - z(v))}{z(v)\bar{z}(u) - z(u)\bar{z}(v) + z(w)\bar{z}(v) - z(v)\bar{z}(w) + z(u)\bar{z}(w) - z(w)\bar{z}(u)}$$

is the complex coordinate of the circumcenter of the face $f \in F(G)$ with any choice of three vertices $u, v, w \in \partial f$ appearing in counter-clockwise order. As constructed, each face of the graph G^\diamond is quadrilateral (in fact, a kite) $\diamond(\bar{u}\bar{v}) = (u, o_s, v, o_n)$ corresponding to a unique unoriented edge $\bar{u}\bar{v}$ of the graph.

Remark 2.20. For any weak Delaunay graph G , we define $G^\diamond := (G^\bullet)^\diamond$. Clearly, $G_1^\diamond = G_2^\diamond$ if and only if $G_1^\bullet = G_2^\bullet$ for any two weak Delaunay graphs G_1 and G_2 .

Definition 2.21 (Rhombic surface S_G^\diamond). Following [7], a rhombic surface S_G^\diamond can be constructed from a Delaunay graph G in the following way: assign to each unoriented edge $e = \bar{u}\bar{v}$ a rhombus $\diamond(e) = \tilde{u}\tilde{o}_s\tilde{v}\tilde{o}_n$ with unit edge lengths $\ell = 1$ and rhombus angle $\angle\tilde{o}_s\tilde{u}\tilde{o}_n = 2\theta(e)$, as depicted in Figure 3.

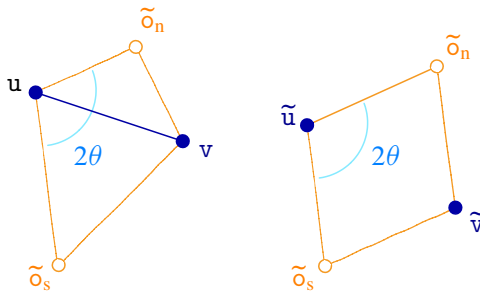


Figure 3. An edge $e = uv$ of G and the associated kite in the plane (left), and the associated rhombus $\diamond(e)$ of S_G^\diamond (right).

If two edges e_1 and e_2 of the graph share a common vertex and simultaneously belong to a common face, then rhombi $\diamond(e_1)$ and $\diamond(e_2)$ are glued together along their common edge. In this way, we obtain an abstract rhombic surface S_G^\diamond .

A simple example is depicted in the Figure 4. In this example, an explicit isometric embedding in \mathbb{R}^3 as a tessellated rhombic surface is possible. Part (a) is a piece of a Delaunay graph G , in blue, with the kites associated to each edge (in orange); (b) is the associated kite graph G^\diamond (in orange); (c) is an isometric embedding in \mathbb{R}^3 of the associated rhombic surface S_G^\diamond . In this particular example, the conformal angles $\theta(e)$ for each edge of G equal $\frac{\pi}{2}$, and so the faces of S_G^\diamond are, in fact, squares, and the embed-

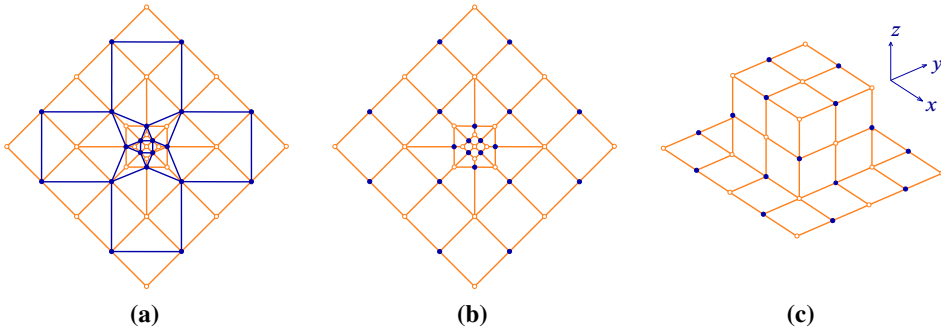


Figure 4. An example (in blue) of a Delaunay graph G (a), of the associated kite graph G^\diamond (b), and of the rhombic surface S_G^\diamond , here represented as consisting of squares embedding in \mathbb{R}^3 (c). The curvature K is localized on the \circ vertices with 3 neighbors \bullet vertices (positive K) or 5 neighbors \bullet vertices (negative K).

ding (c) is a surface in \mathbb{Z}^3 . In general, the rhombic surface S_G^\diamond cannot be embedded isometrically and rigidly into \mathbb{R}^3 .

A rhombic surface is flat at each vertex \tilde{u} associated to a vertex u of G but has a potential curvature defect at each vertex \tilde{o}_f corresponding to a circumcenter o_f of a face f of G , with scalar (Ricci) curvature R_{scal} defined by

$$R_{\text{scal}}(\tilde{o}_f) := 4\pi - 2 \sum_{e \in \partial f} (\pi - 2\theta(e)). \tag{2.2}$$

If $R_{\text{scal}}(\tilde{o}_f) = 0$ for every face f of the graph, G is said to be *flat*. It is easy to see that this is equivalent to saying that the Delaunay graph is *isoradial*, namely that all circumradii are equal to some R . Note that for every oriented edge \vec{e} of an isoradial polyhedral graph either

$$\theta_n(\vec{e}) = \theta_s(\vec{e}) = \theta(e) > 0 \quad \text{or} \quad \theta_n(\vec{e}) = -\theta_s(\vec{e})$$

in which case $\theta(e) = 0$.

When G is isoradial (with common circumradius R), each kite $\diamond(\overline{uv})$ will be a rhombus with side length R ; in this case, we shall refer to G^\diamond as a *rhombic graph*; see Figure 5 for an illustration. Up to a global rescaling $R \rightarrow 1$, we have

$$G^\diamond = S_G^\diamond.$$

This corresponds to the rhombic graphs discussed in [17].

Remark 2.22. Isoradial Delaunay graphs are in bijection with the rhombic graphs of [17].

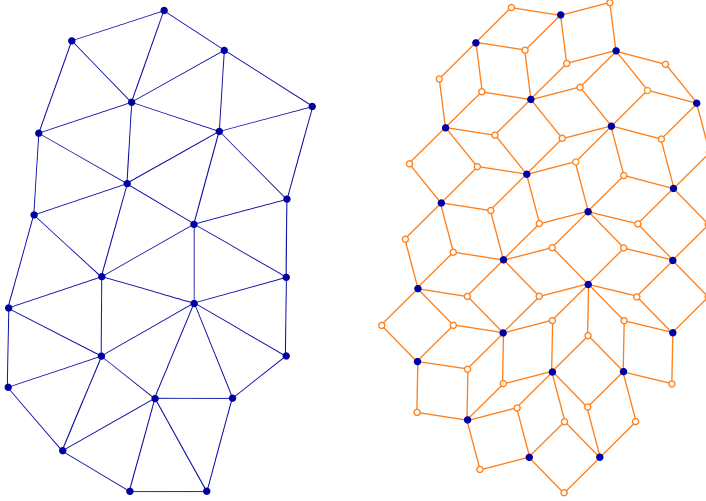


Figure 5. Fragments of an isoradial Delaunay graph G_{cr} (on the left) and its rhombic graph G_{cr}^\diamond (on the right).

2.2. Geometry on rhombic graphs

In the following discussion, G_{cr} will be an isoradial Delaunay graph with embedding $z_{cr}: V(G_{cr}) \rightarrow \mathbb{C}$ and, if not specified otherwise, we shall assume for simplicity that the value of the common circumradius is $R_{cr} = 1$. Let us recall some geometrical concepts of [17, 18], with some more material needed in this paper.

2.2.1. Paths on rhombic graphs. A path in G_{cr}^\diamond is a finite sequence of vertices $\mathfrak{v} = (v_0, \dots, v_k)$ such that for each $1 \leq j \leq k$, the vertices v_{j-1} and v_j are joined by an edge e_j of G_{cr}^\diamond ; in this case, we say \mathfrak{v} is a path of length k from v_0 to v_k ; see Figure 6. Let $\vec{e}_j = (v_{j-1}, v_j)$ be the oriented edge corresponding to e_j , let $\vec{\mathbb{E}}(\mathfrak{v}) = (\vec{e}_1, \dots, \vec{e}_k)$ be the sequence of oriented edges of \mathfrak{v} , and $E(\mathfrak{v}) = \bigcup_j \{e_j\}$ the set of edges of \mathfrak{v} . For each edge \vec{e}_j of \mathfrak{v} , there is a phase $e^{i\theta_j} := z_{cr}(v_j) - z_{cr}(v_{j-1})$ associated to it. We denote by $\underline{\theta}(\mathfrak{v}) = (\theta_1, \dots, \theta_k)$ the sequence of angles of these phases.

We can regard the rhombic graph G_{cr}^\diamond as a cellular decomposition of the plane; accordingly, vertices, oriented edges, and oriented faces of G_{cr}^\diamond can be viewed respectively as 0, 1, and 2-chains of a cellular complex \mathcal{X} with \mathbb{Z} -coefficients. For a path \mathfrak{v} , let $\vec{\mathfrak{v}}$ denote the 1-chain $\vec{e}_1 + \dots + \vec{e}_k$ in $C_1(\mathcal{X}; \mathbb{Z})$. Two paths \mathfrak{v}_1 and \mathfrak{v}_2 are said to differ by an oriented rhombus \diamond^\oslash if $\vec{\mathfrak{v}}_2 = \vec{\mathfrak{v}}_1 + \partial \diamond^\oslash$; see Figure 7 for an example. The vanishing of $H_1(\mathcal{X}; \mathbb{Z})$ is equivalent to the fact that any two paths $\vec{\mathfrak{v}}_1$ and $\vec{\mathfrak{v}}_2$ both from a vertex u to a vertex v must differ by a sum of oriented rhombi.

For an integer n together with an oriented edge \vec{e} joining a vertex u to a vertex v , set $[\vec{e}]_n := e^{in\theta}$, where $e^{i\theta} = z_{cr}(v) - z_{cr}(u)$ is the phase of the difference of the

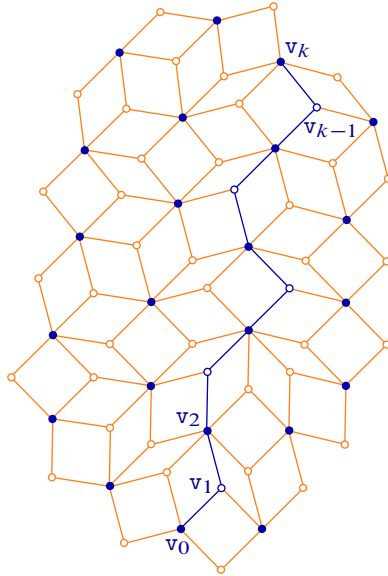


Figure 6. Path $\mathfrak{v} = (v_0, \dots, v_k)$ in the rhombic graph G_{cr}^\diamond .

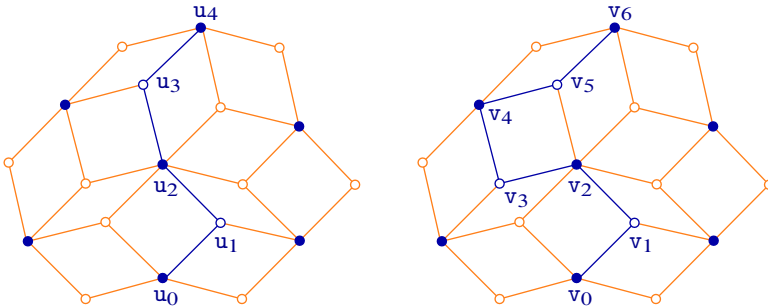


Figure 7. Paths $\mathfrak{u} = (u_0, \dots, u_4)$ and $\mathfrak{v} = (v_0, \dots, v_6)$ are differ by a rhombus.

coordinates of the vertices; extend this by linearity to 1-chains in $C_1(\mathcal{X}; \mathbb{Z})$, and thus define

$$\left[\sum_j a_j \vec{e}_j \right]_n := \sum_j a_j [\vec{e}_j]_n.$$

Notice that $[\diamond^\varnothing]_n = 0$ for any oriented rhombus \diamond^\varnothing whenever n is an odd integer. It follows that for any path \mathfrak{v} , and for any odd integer $n = 2d + 1$, $[\vec{\mathfrak{v}}]_n$ depends only on the two end-points (v_0, v_k) of \mathfrak{v} .

Definition 2.23. For any pair of vertices u and v of G_{cr}^\diamond and for any odd integer $n = 2d + 1$, we define $p_n(u, v) := [\vec{\mathfrak{v}}]_n$, where \mathfrak{v} is any path from u to v .

Note that $p_1(u, v) = z_{\text{cr}}(v) - z_{\text{cr}}(u)$. In addition, $p_n(u, v) = -p_n(v, u)$.

2.2.2. Train-tracks.

Definition 2.24 (train-track). A *train-track* in the rhombic graph G_{cr}^\diamond is an infinite sequence of rhombi $\mathfrak{t} = (\diamond_n : n \in \mathbb{Z})$, whose consecutive rhombi \diamond_n and \diamond_{n+1} are incident along a common edge e_n for each $n \in \mathbb{Z}$, and for which the edges e_n and e_{n+1} are parallel for each $n \in \mathbb{Z}$. We shall denote these parallel edges “train-track tie”, or in short “*tie*”. We consider train-tracks up to shift and inversion, i.e., $\mathfrak{t}^{(1)} = (\diamond_n^{(1)} : n \in \mathbb{Z})$ is equivalent to $\mathfrak{t}^{(2)} = (\diamond_n^{(2)} : n \in \mathbb{Z})$ if $\diamond_n^{(2)} = \diamond_{\pm n+d}^{(1)}$ for some $d \in \mathbb{Z}$. Let $\text{Ties}(\mathfrak{t}) = \{e_n : n \in \mathbb{Z}\}$ denote this set of edges. A train-track \mathfrak{t} has *inclination* $\theta_{\mathfrak{t}} \in [0, \pi)$ if the ties e_n are parallel to the phase $\exp(i\theta_{\mathfrak{t}})$. See Figure 8 for an illustration.

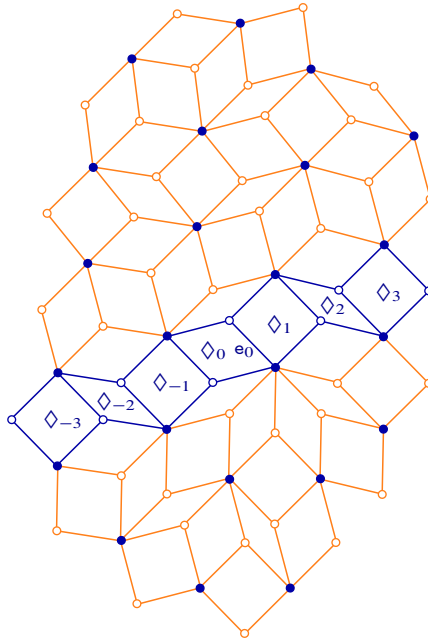


Figure 8. Train-track \mathfrak{t} .

Clearly, any train-track is determined (but not uniquely) by an initial rhombus \diamond_0 together with a choice of one of its edges e_0 . For any choice of initial edge e_0 in \mathfrak{t} , the distance of each edge e_n from the axis determined by e_0 is monotonically increasing with n , i.e., the train-track must move forward in the axis perpendicular to e_0 .

We say two train-tracks $\mathfrak{t}^{(1)} = (\diamond_n^{(1)} : n \in \mathbb{Z})$ and $\mathfrak{t}^{(2)} = (\diamond_n^{(2)} : n \in \mathbb{Z})$ *intersect* if $\diamond_m^{(1)} = \diamond_n^{(2)}$ for some $m, n \in \mathbb{Z}$. Two important features of any rhombic-graph G_{cr}^\diamond are the following facts.

Fact 2.25. No train-track can intersect itself, i.e., if $\mathfrak{t} = (\diamond_n : n \in \mathbb{Z})$, then $\diamond_m \neq \diamond_n$ for all integers $m \neq n$.

Fact 2.26. Any two distinct train-tracks are either disjoint or else intersect once.

The notion of train-track is amenable to any quad-graph (a planar graph consisting entirely of quadrilateral faces) and these two properties characterize rhombic graphs within the broader class of quad-graphs; specifically, any quad-graph satisfying these two properties is a deformation of a rhombic graph (see [18]).

2.2.3. Intersections of train-tracks with paths. A train-track \mathfrak{t} partitions the vertex set $V(G_{\text{cr}}^\diamond)$ into two disjoint subsets V' and V'' . Specifically, the edge set $E(G_{\text{cr}}^\diamond) - \text{Ties}(\mathfrak{t})$ defines a disconnected subgraph of G_{cr}^\diamond with two disjoint components; V' and V'' are the respective vertex sets of these components. Accordingly, we say that two vertices u and v are *separated* by \mathfrak{t} if they lie in different components; furthermore, we say \mathfrak{t} *separates* the path \mathfrak{v} if the end-points of the path v_0 and v_k are separated by \mathfrak{t} .

Given a path $\mathfrak{v} = (v_0, \dots, v_k)$ and a train-track \mathfrak{t} , let $I(\mathfrak{v}; \mathfrak{t}) := \{1 \leq j \leq k : e_j \in \text{Ties}(\mathfrak{t})\}$ be the set of indices of edges common to both \mathfrak{v} and \mathfrak{t} . If \mathfrak{t} separates \mathfrak{v} , then its cardinality $|I(\mathfrak{v}; \mathfrak{t})|$ must be odd due to the fact the path must begin on one side of \mathfrak{t} and end on the other. If, on the other hand, \mathfrak{t} does not separate \mathfrak{v} , then $|I(\mathfrak{v}; \mathfrak{t})|$ is even (and may, in fact, be zero if there is no intersection at all).

The edges e_j for $j \in I(\mathfrak{v}; \mathfrak{t})$ are clearly parallel (since they all inhabit the train-track \mathfrak{t}) but the oriented edges \bar{e}_j for $j \in I(\mathfrak{v}; \mathfrak{t})$ must alternate in direction, and so their phases $e^{i\theta_j}$ for $j \in I(\mathfrak{v}; \mathfrak{t})$ must alternate in sign. Consequently, if $I(\mathfrak{v}; \mathfrak{t}) = \{j_1 < \dots < j_d\}$ and n is odd, then

$$\sum_{s=1}^d e^{in\theta_{j_s}} = \begin{cases} e^{in\theta_{j_1}} & \text{whenever } \mathfrak{t} \text{ separates } \mathfrak{v}, \\ 0 & \text{otherwise.} \end{cases} \tag{2.3}$$

If \mathfrak{t} separates \mathfrak{v} , their *intersection angle* is defined as $\vartheta(\mathfrak{v}, \mathfrak{t}) := \theta_{j_1}$, and $\Theta(\mathfrak{v}) = \{\vartheta(\mathfrak{v}, \mathfrak{t}) : \mathfrak{t} \text{ intersects } \mathfrak{v}\}$ is the set of intersection angles of all train-tracks that separate the path \mathfrak{v} . Define the multiplicity $m_\vartheta := |\{\mathfrak{t} \text{ separates } \mathfrak{v} : \vartheta = \vartheta(\mathfrak{v}, \mathfrak{t})\}|$ for $\vartheta \in \Theta(\mathfrak{v})$. It follows from equation (2.3) that for odd n ,

$$p_n(u, v) = \sum_{j=1}^k e^{in\theta_j} = \sum_{\substack{\text{train-tracks } \mathfrak{t} \\ \text{separating } \mathfrak{v}}} e^{in\vartheta(\mathfrak{v}, \mathfrak{t})} = \sum_{\vartheta \in \Theta(\mathfrak{v})} m_\vartheta e^{in\vartheta}, \tag{2.4}$$

where $v_0 = u$ and $v_k = v$ are the beginning and end points of the path \mathfrak{v} . Given a train-track \mathfrak{t} separating \mathfrak{v} with angle of intersection $\theta = \theta(\mathfrak{v}, \mathfrak{t})$, define $R_\theta^u = z_{\text{cr}}(u) + \mathbb{R}_{>0}e^{i\theta}$ to be the ray (half-line) starting from $z_{\text{cr}}(u)$ in the direction θ , and $R_{\theta+\pi}^v = z_{\text{cr}}(v) + \mathbb{R}_{>0}e^{i(\theta+\pi)}$ be the ray starting from $z_{\text{cr}}(v)$ in the direction $\theta + \pi$. It is

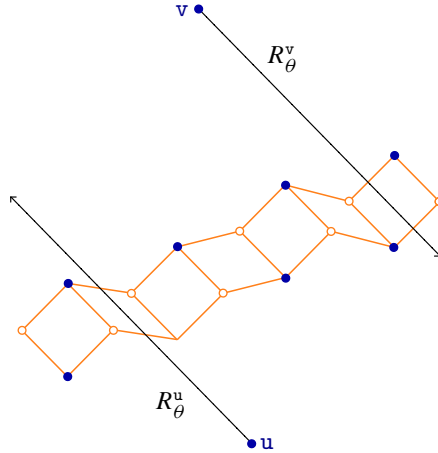


Figure 9. Vertices u and v separated by a train-track \mathfrak{t} .

geometrically clear that \mathfrak{t} must intersect the right-hand sides of rays R_θ^u and $R_{\theta+\pi}^v$, without backtracking in the direction orthogonal to R_θ^u (and without intersecting the opposite rays $R_{\theta+\pi}^u$ and R_θ^v). See Figure 9.

For completeness, one should consider the case where lozenges in \mathfrak{t} become infinitely flat, so that \mathfrak{t} goes to infinity in the θ direction before intersecting R_θ^u (see Figure 10). Then one can consider that \mathfrak{t} crosses R_θ^u at infinity.

Proposition 2.27. *Let $\mathfrak{v} = (v_0, \dots, v_k)$ be a path in $\mathcal{G}_{\text{cr}}^\diamond$, let the direction of the path be $\theta_0 = \arg(z_{\text{cr}}(v_k) - z_{\text{cr}}(v_0))$. Let us fix the determinations of the angles $\vartheta \in \Theta(\mathfrak{v})$ as real numbers in*

$$\vartheta \in (\theta_0 - \pi, \theta_0 + \pi],$$

and let

$$\alpha = \max\{\vartheta \in \Theta(\mathfrak{v})\}, \quad \beta = \min\{\vartheta \in \Theta(\mathfrak{v})\}.$$

Then

$$\alpha - \beta < \pi \quad \text{and} \quad \beta \leq \theta_0 \leq \alpha.$$

In other words, the set $\Theta(\mathfrak{v})$ and the angle θ_0 are contained in the open subinterval $(\theta_{\mathfrak{v}} - \frac{\pi}{2}, \theta_{\mathfrak{v}} + \frac{\pi}{2})$, where $\theta_{\mathfrak{v}} = \frac{1}{2}(\alpha - \beta)$.

Proof. Set $\theta_0 = \arg(z_{\text{cr}}(v_k) - z_{\text{cr}}(v_0)) \in [0, \pi)$. Each $\vartheta \in \Theta(\mathfrak{v})$ is the intersection angle of at least one train-track \mathfrak{t} whose inclination equals ϑ (modulo π) and which separates the vertices v_0 and v_k .

First let us note that the angle $\theta_0 + \pi$ cannot be an element of $\Theta(\mathfrak{v})$. Were this the case, there would be a train-track joining the right-hand sides of the rays $R_{\theta_0+\pi}^u$ and $R_{\theta_0}^v$ without backtracking. This is impossible, as depicted in Figure 11.

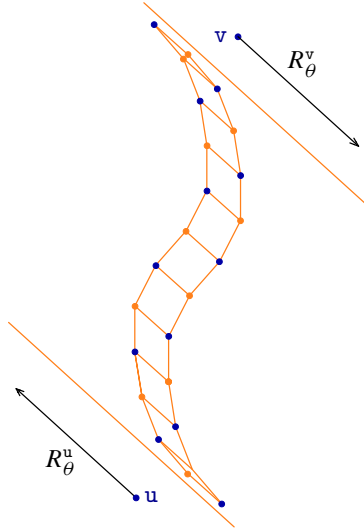


Figure 10. A situation where the vertices u and v are asymptotically separated by a train-track.

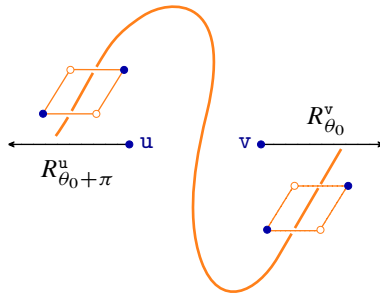


Figure 11. A track separating u and v with orientation $\theta_0 + \pi$ must backtrack.

Consequently, the angles in $\Theta(\mathbb{v})$ are in the interval $(\theta_0 - \pi, \theta_0 + \pi)$. Consider $\alpha = \max \Theta(\mathbb{v})$ and $\beta = \min \Theta(\mathbb{v})$. It is enough to prove that $\alpha - \beta \leq \pi$. Indeed, suppose instead that $\alpha - \beta > \pi$. Both α and β are intersection angles for two respective train-tracks \mathfrak{t}_1 and \mathfrak{t}_2 which separate $u := v_0$ and $v := v_k$. If we attempt to draw \mathfrak{t}_1 and \mathfrak{t}_2 bearing in mind monotonicity and their requisite intersections with the rays $R_\alpha^u, R_\beta^u, R_{\alpha+\pi}^v$, and $R_{\beta+\pi}^v$, we will observe that the two train-tracks are forced to intersect at least three times (as depicted in Figure 12).

Since two distinct train-tracks may intersect at most once, we are forced to conclude that $\alpha - \beta \leq \pi$. Finally, by equation (2.4), the difference $z_{\text{cr}}(v) - z_{\text{cr}}(u)$ can be written as

$$z_{\text{cr}}(v) - z_{\text{cr}}(u) = \sum_{\vartheta \in \Theta(\mathbb{v})} m_\vartheta e^{i\vartheta} \quad \text{with } m_\vartheta \in \mathbb{Z}_{>0}.$$

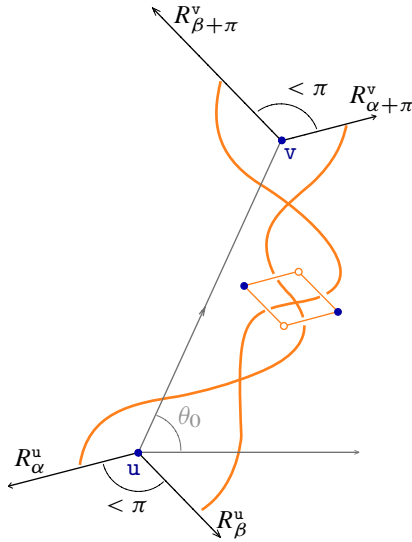


Figure 12. Two train-tracks separating u and v cannot have separating angles differing by more than π .

Any positive combination of phases $e^{i\vartheta}$ for $\vartheta \in \Theta(\mathbb{v})$ must lie in the positive cone $\{ae^{i\alpha} + be^{i\beta} : a, b \in \mathbb{R}_{>0}\}$ because $\alpha - \beta < \pi$. It follows that $\beta < \theta_0 < \alpha$. ■

For obvious topological reasons the set $\{\mathfrak{t} \text{ separates } \mathbb{v} : \vartheta = \vartheta(\mathbb{v}, \mathfrak{t})\}$ only depends on the end-points v_0 and v_k of the path \mathbb{v} . By Proposition 2.27, if $\vartheta \in \Theta(\mathbb{v})$, then $\vartheta + \pi \notin \Theta(\mathbb{v})$, which means that if two distinct train-tracks \mathfrak{t}_1 and \mathfrak{t}_2 share the same inclination and both separate \mathbb{v} , then

$$\vartheta(\mathbb{v}, \mathfrak{t}_1) = \vartheta(\mathbb{v}, \mathfrak{t}_2).$$

Consequently, the set $\Theta(\mathbb{v})$ together with the multiplicities m_ϑ for $\vartheta \in \Theta(\mathbb{v})$ must only depend on the end-points v_0 and v_k of the path \mathbb{v} as well. This observation is consistent with the fact that the value of $[\tilde{\mathbb{v}}]_n$ depends only on the end-points of \mathbb{v} .

3. Laplacians and their determinants

3.1. Laplacians and the critical Laplacian

3.1.1. Laplacians associated to polyhedral graphs and triangulations. Given a polyhedral graph G , we denote by $\mathbb{C}^{V(G)}$, $\mathbb{C}^{E(G)}$, and $\mathbb{C}^{F(G)}$ the vector spaces of complex-valued functions supported on the vertices, edges, and faces of G , respectively. The operators Δ , $\underline{\Delta}$ and \mathcal{D} are associated to a general polyhedral graph G and

were introduced in Section 1.2.3. Each operator is a linear map $\mathbb{C}^{V(\mathcal{G})} \rightarrow \mathbb{C}^{V(\mathcal{G})}$. The Laplace–Beltrami operator Δ is defined as

$$\Delta\phi(u) = \sum_{\text{edge } \vec{e}=(u,v)} c(\vec{e})(\phi(u) - \phi(v)), \quad c(\vec{e}) = \frac{1}{2}(\tan \theta_n(\vec{e}) + \tan \theta_s(\vec{e})). \quad (3.1)$$

The conformal Laplacian $\underline{\Delta}$ is

$$\underline{\Delta}\phi(u) = \sum_{\text{edge } \vec{e}=(u,v)} \tan \theta(e)(\phi(u) - \phi(v)).$$

The Kähler operator \mathcal{D} is

$$\mathcal{D}\phi(u) = \sum_{\text{edge } \vec{e}=(u,v)} \frac{1}{2} \left(\frac{\tan \theta_n(\vec{e}) + i}{R_n^2(\vec{e})} + \frac{\tan \theta_n(\vec{e}) - i}{R_s^2(\vec{e})} \right) (\phi(u) - \phi(v)),$$

where $\theta_n(\vec{e})$, $\theta_s(\vec{e})$ and $\theta(e)$ are the north, south and conformal angles, respectively, associated to the oriented edge $\vec{e} = (u, v)$, while $R_n(\vec{e})$ and $R_s(\vec{e})$ are the circumradii of the respective north f_n and south f_s faces associated to \vec{e} (see Figure 1).

Remark 3.1. The Laplace–Beltrami operator Δ , the conformal Laplacian $\underline{\Delta}$, and the David–Eynard Kähler operator \mathcal{D} on a polygonal graph \mathcal{G} agree with Δ , $\underline{\Delta}$, and \mathcal{D} , respectively, when defined on the associated *redacted* graph \mathcal{G}^\bullet (see Definition 2.5). By definition, the vertex sets of \mathcal{G} and \mathcal{G}^\bullet coincide. So for any pair of vertices u, v , the corresponding matrix entries $\Delta_{u,v}$, $\underline{\Delta}_{u,v}$, and $\mathcal{D}_{u,v}$ are independent of whether we calculate their values with respect to the graph embedding (and incidence relations) of either \mathcal{G} or \mathcal{G}^\bullet . Likewise, Δ , $\underline{\Delta}$, and \mathcal{D} operating on \mathcal{G} agree with their respective counterparts when defined on any *completion* $\widehat{\mathcal{G}}$ of \mathcal{G} (see Definition 2.8).

3.1.2. Areas, angles and circumradii formulas. We recall some basic geometrical formulas for these quantities. Let $f = (v_1, v_2, v_3)$ be a counter-clockwise oriented triangle with vertices labeled v_1, v_2, v_3 and respective coordinates z_1, z_2, z_3 , then the area $A(f)$ of the triangle is

$$A(f) = \frac{1}{4i}(z_2\bar{z}_1 - z_1\bar{z}_2 + z_3\bar{z}_2 - z_2\bar{z}_3 + z_1\bar{z}_3 - z_3\bar{z}_1). \quad (3.2)$$

The circumcenter $z(f)$ of the triangle is given by

$$z(f) = \frac{z_1\bar{z}_1(z_2 - z_3) + z_2\bar{z}_2(z_3 - z_1) + z_3\bar{z}_3(z_1 - z_2)}{4iA(f)},$$

and the circumradius $R(f)$ of the triangle is given by the trigonometric relation

$$R(f) = \frac{|z_1 - z_2||z_2 - z_3||z_3 - z_1|}{4A(f)}, \quad (3.3)$$

while the north angle associated to the oriented edge $\vec{e} = (v_1, v_2)$ is

$$\theta_n(\vec{e}) = \frac{1}{2i} \log\left(-\frac{(\bar{z}_2 - \bar{z}_3)(z_1 - z_3)}{(z_2 - z_3)(\bar{z}_1 - \bar{z}_3)}\right). \tag{3.4}$$

Furthermore, $\tan^2 \theta_n(\vec{e})$ can be written explicitly in coordinates as

$$\begin{aligned} \tan^2 \theta_n(\vec{e}) &= \frac{2 + \frac{z_2 - z_3}{\bar{z}_2 - \bar{z}_3} \frac{\bar{z}_1 - \bar{z}_3}{z_1 - z_3} + \frac{z_1 - z_3}{\bar{z}_1 - \bar{z}_3} \frac{\bar{z}_2 - \bar{z}_3}{z_2 - z_3}}{2 - \frac{z_2 - z_3}{\bar{z}_2 - \bar{z}_3} \frac{\bar{z}_1 - \bar{z}_3}{z_1 - z_3} - \frac{z_1 - z_3}{\bar{z}_1 - \bar{z}_3} \frac{\bar{z}_2 - \bar{z}_3}{z_2 - z_3}} \\ &= 4 \frac{|z(\mathbf{f}) - z_{1\bar{2}}|^2}{|z_2 - z_1|^2} \quad \text{with } z_{1\bar{2}} = \frac{z_2 + z_1}{2}. \end{aligned} \tag{3.5}$$

The derivatives of $A(\mathbf{f})$, $R(\mathbf{f})$ and of the angles $\theta_n(\vec{e})$ under a variation of a vertex coordinate are easy to calculate, using, for instance,

$$\partial_{z_1} A(\mathbf{f}) = \frac{1}{4i} (\bar{z}_3 - \bar{z}_2), \quad \partial_{z_1} |z_1 - z_2| = \frac{1}{2} \frac{\bar{z}_1 - \bar{z}_2}{|z_1 - z_2|} \quad \text{with } \partial_{z_1} = \frac{\partial}{\partial z_1}$$

and will be discussed later.

3.1.3. Laplacians on critical (isoradial) graphs. The critical Laplacian studied by Kenyon in [17] corresponds to the special case of Δ with edge weight $c(\mathbf{e})$ given by (3.1), defined on a *critical graph* (according to the terminology of [17]), i.e., an isoradial, Delaunay graph G_{cr} . Accordingly, we shall use the following terminology for critical Laplacians, given here.

Definition 3.2. Let G_{cr} be an isoradial Delaunay graph. The Laplace–Beltrami operator Δ , the conformal Laplacian $\underline{\Delta}$, and the David–Eynard Kähler operator (normalized by the squared isoradius R_{cr} of the faces of G_{cr}) coincide for G_{cr} . This common operator is called the *critical Laplacian* associated to G_{cr} and is denoted by Δ_{cr} ,

$$\Delta_{cr} = \Delta = \underline{\Delta} = R_{cr}^2 \mathcal{D} \quad \text{on } G_{cr}.$$

An explicit formula for Δ_{cr} is also given in equation (1.9) of Section 1.2.3.

3.2. Factorization of Laplacian using ∇ and $\bar{\nabla}$ operators

In the case of a planar triangulation T , we present an alternative representation of the operators Δ and \mathcal{D} which will be convenient for our calculations. We follow the definition and the notations of [7].

Definition 3.3. The operators ∇ and $\bar{\nabla}$ are linear operators from the space of complex-valued functions over the set of vertices $V(T)$ of T , onto the space of complex-valued functions over the set of triangles (faces) $F(T)$ of T ,

$$\mathbb{C}^{V(T)} \xrightarrow{\nabla} \mathbb{C}^{F(T)}, \quad \mathbb{C}^{V(T)} \xrightarrow{\bar{\nabla}} \mathbb{C}^{F(T)},$$

where ∇ is defined as follows. Given a triangle \mathfrak{f} (a face of the triangulation \mathbb{T}) with vertices v_1, v_2, v_3 (listed in counter-clockwise order) and complex coordinates $z_j := z(v_j)$ for $1 \leq j \leq 3$ together with a function $\phi \in \mathbb{C}^{V(\mathbb{T})}$, define

$$\nabla\phi(\mathfrak{f}) = \frac{\phi(v_1)(\bar{z}_2 - \bar{z}_3) + \phi(v_2)(\bar{z}_3 - \bar{z}_1) + \phi(v_3)(\bar{z}_1 - \bar{z}_2)}{-4iA(\mathfrak{f})}, \tag{3.6}$$

∇ corresponds to a discrete linear derivative with respect to the embedding $v \mapsto z(v)$ because

$$\nabla z = 1, \quad \nabla \bar{z} = 0.$$

Similarly, its conjugate $\bar{\nabla}$ is defined as

$$\bar{\nabla}\phi(\mathfrak{f}) = \frac{\phi(v_1)(z_2 - z_3) + \phi(v_2)(z_3 - z_1) + \phi(v_3)(z_1 - z_2)}{4iA(\mathfrak{f})} \tag{3.7}$$

and satisfies

$$\bar{\nabla} z = 0, \quad \bar{\nabla} \bar{z} = 1.$$

The transposes of these operators are defined accordingly

$$\mathbb{C}^{F(\mathbb{T})} \xrightarrow{\nabla^T} \mathbb{C}^{V(\mathbb{T})}, \quad \mathbb{C}^{F(\mathbb{T})} \xrightarrow{\bar{\nabla}^T} \mathbb{C}^{V(\mathbb{T})}.$$

Remark 3.4. It follows from definitions (3.6) and (3.7) and the area formula (3.2) that for any function $\phi \in \mathbb{C}^{V(\mathbb{T})}$,

$$\phi(v_1) - \phi(v_2) = (z_1 - z_2)\nabla\phi(\mathfrak{f}) + (\bar{z}_1 - \bar{z}_2)\bar{\nabla}\phi(\mathfrak{f}). \tag{3.8}$$

Note that the discrete derivatives ∇ and $\bar{\nabla}$ are defined for general triangulations. Even when the triangulation is isoradial, ∇ and $\bar{\nabla}$ *do not coincide* with the discrete holomorphic and discrete antiholomorphic derivatives ∂ and $\bar{\partial}$ considered in [17] for isoradial bipartite graphs. Indeed, ∇ and $\bar{\nabla}$ do not even act on the same space of functions as ∂ and $\bar{\partial}$.

Nevertheless, we shall need to bound the difference between the $\nabla\phi$ and the ordinary continuous derivative $\partial\phi$ in the case of a smooth complex-valued function $\phi: \mathbb{C} \rightarrow \mathbb{C}$ with compact support and its restriction to $V(\mathbb{T})$ given by

$$\phi(v) := \phi(z(v)),$$

where $z: V(\mathbb{T}) \rightarrow \mathbb{C}$ is the embedding of \mathbb{T} . This estimate is explained in Lemma 1.9 of the introduction and proven in Appendix B.

In addition, the ∇ -operator satisfies a discrete analog of Green’s theorem

$$\iint_{\Omega} \partial\phi(z, \bar{z}) dzd\bar{z} = \oint_{\partial\Omega} \phi(z, \bar{z}) d\bar{z}$$

in complex coordinates, namely, the following lemma.

Lemma 3.5. *Let \mathbb{T} be a polyhedral triangulation with embedding $z: \mathbb{V}(\mathbb{T}) \rightarrow \mathbb{C}$, let $\Omega \subset \mathbb{F}(\mathbb{T})$ be a finite collection of triangular faces (each taken with a counter-clockwise orientation), let $\partial\Omega \subset \mathbb{E}(\mathbb{T})$ be the finite subset of (oriented) edges corresponding to the boundary of Ω , and let $\phi \in \mathbb{C}^{\mathbb{V}(\mathbb{T})}$ be a complex-valued function, then*

$$\sum_{x \in \Omega} A(x) \nabla \phi(x) = \sum_{(u,v) \in \partial\Omega} (\bar{z}(v) - \bar{z}(u)) \frac{\phi(v) + \phi(u)}{-4i}. \tag{3.9}$$

Proof. Use definition (3.6) for ∇ and observe that the area $A(x)$ defined by (3.2) cancels with the area factor in the denominator of $\nabla \phi(x)$, and that for each oriented triangle $x = (u, v, w)$, the term $A(x) \nabla \phi(x)$ can be reorganized as

$$-\frac{1}{4i} \{ (\bar{z}(v) - \bar{z}(u))(\phi(v) + \phi(u)) + (\bar{z}(w) - \bar{z}(v))(\phi(w) + \phi(v)) + (\bar{z}(u) - \bar{z}(w))(\phi(u) + \phi(w)) \}.$$

Now sum over the faces of Ω . Note that all internal edges count twice with opposite orientations and cancel, and so only the oriented edges on the boundary $\partial\Omega$ contribute and give the right-hand side of (3.9). ■

The polyhedral condition can, in fact, be dropped but we assume it to keep the exposition simple. Lemma 3.5 implies the following corollary which is relevant to our results.

Corollary 3.6. *Let \mathbb{T}_1 and \mathbb{T}_2 be two polyhedral triangulations which share a common redacted graph $\mathbb{G} := \mathbb{T}_1^\bullet = \mathbb{T}_2^\bullet$. Given a face $\mathfrak{f} \in \mathbb{F}(\mathbb{G})$ with vertex set $\mathbb{V}(\mathfrak{f})$, let $\Omega_i(\mathfrak{f})$ be the set of triangular faces of \mathbb{T}_i , each of whose vertices are in $\mathbb{V}(\mathfrak{f})$. Then*

$$\sum_{x_1 \in \Omega_1(\mathfrak{f})} A(x_1) \nabla \phi(x_1) = \sum_{x_2 \in \Omega_2(\mathfrak{f})} A(x_2) \nabla \phi(x_2)$$

for any complex-valued function $\phi \in \mathbb{C}^{\mathbb{V}(\mathbb{G})}$.

Definition 3.7. The diagonal operators $A = \text{diag}(\{A(\mathfrak{f}); \mathfrak{f} \in \mathbb{F}(\mathbb{G})\})$ (with $A(\mathfrak{f})$ the area of the face \mathfrak{f} defined by (3.2)), and $R = \text{diag}(\{R(\mathfrak{f}); \mathfrak{f} \in \mathbb{F}(\mathbb{G})\})$ (with $R(\mathfrak{f})$ the circumradius of the face \mathfrak{f} defined by (3.3)) map $\mathbb{C}^{\mathbb{F}(\mathbb{G})} \rightarrow \mathbb{C}^{\mathbb{F}(\mathbb{G})}$ and are defined by their action on all $\psi \in \mathbb{C}^{\mathbb{F}(\mathbb{G})}$ as

$$A\psi(\mathfrak{f}) = A(\mathfrak{f})\psi(\mathfrak{f}), \quad R\psi(\mathfrak{f}) = R(\mathfrak{f})\psi(\mathfrak{f}).$$

Then we shall heavily use the following local decompositions for the \mathcal{D} and Δ operators.

Remark 3.8. The Kähler operator \mathcal{D} can be factored as

$$\mathcal{D} = 4\bar{\nabla}^\top \frac{A}{R^2} \nabla. \tag{3.10}$$

This decomposition is shown in [7, Section 2.6, Proposition 2.2]. Note that A and R commute.

Remark 3.9. The Laplace–Beltrami operator Δ can be factored as

$$\Delta = 2(\bar{\nabla}^\top A \nabla + \nabla^\top A \bar{\nabla}). \tag{3.11}$$

This decomposition can be derived easily using the method of [7]. Alternatively, one can use formula (3.2) for $A(\mathfrak{f})$ and (3.8) to reorganize terms and show that for any $\phi \in \mathbb{C}^{F(G)}$ one has

$$\sum_{u,v} \bar{\phi}(u) \Delta_{uv} \phi(v) = 2 \sum_{\mathfrak{f}} A(\mathfrak{f}) (\bar{\nabla} \bar{\phi}(\mathfrak{f}) \nabla \phi(\mathfrak{f}) + \nabla \bar{\phi}(\mathfrak{f}) \bar{\nabla} \phi(\mathfrak{f}))$$

which amounts to (3.11).

Remark 3.10. No similar decomposition holds for the conformal Laplacian $\underline{\Delta}$, since the weight $\tan \theta(\mathfrak{e})$ associated to an oriented edge $\vec{\mathfrak{e}}$ depends non-additively on the north and south angles $\theta_n(\vec{\mathfrak{e}})$ and $\theta_s(\vec{\mathfrak{e}})$.

3.3. Making sense of the log-determinant for infinite lattices

3.3.1. The problems. As explained in the introduction, we are interested in studying the variation of the log det \mathcal{O} under a variation of the coordinates of the triangulation \mathbb{T} , where \mathcal{O} is any of the Laplace-like operators Δ , $\underline{\Delta}$ and \mathcal{D} . Two potential dangers arise:

- (1) These operators have zero modes and some care is needed in imposing boundary conditions in order to exclude them.
- (2) We consider infinite polygonal graphs – and so by any naive account, the log-determinant will be infinite.

There is a host of standard methods used to handle these issues; below we discuss two situations where problems (1) and (2) can be side-stepped.

3.3.2. Using periodic triangulations. Consider a polyhedral graph \mathbb{G} which is periodic with respect to a lattice $\mathbb{Z} + \tau\mathbb{Z}$ with $\text{Im } \tau > 0$. This means there is an action of the additive group $\Lambda = \mathbb{Z}^2$ on $V(\mathbb{G})$ denoted $v \mapsto v + (a, b)$ such that

- (1) $z(v + (a, b)) = z(v) + a + \tau b$,
- (2) $u + (a, b)$ and $v + (a, b)$ are joined by an edge whenever u and v are joined by an edge (moreover, the weights of these edges agree)

for all $u, v \in V(\mathbb{G})$ and $(a, b) \in \Lambda$. Given a choice of an additive subgroup, $\Lambda_{mn} := m\mathbb{Z} \times n\mathbb{Z}$ of Λ with $m, n \in \mathbb{Z}_{>0}$ form the quotient graph \mathbb{G}/Λ_{mn} , which we can

view as a finite graph embedded in the torus $\mathbb{T}_{mn} := \mathbb{C}/(m\mathbb{Z} + \tau n\mathbb{Z})$. Since the edge weights are periodic, the operator \mathcal{O} descends to an operator \mathcal{O}_{mn} on the quotient graph \mathbb{G}/Λ_{mn} ; moreover, if we identify the vertices of \mathbb{G}/Λ_{mn} with the subset V_{mn} consisting of vertices $v \in V(\mathbb{G})$ for which $z(v) \in \{s + t\tau : (s, t) \in [0, m) \times [0, n)\}$, then \mathcal{O}_{mn} is a finite-dimensional operator acting on a vector space of dimension $|V_{mn}|$.

We define the *reduced log-determinant* $\log \det' \mathcal{O}_{mn}$ as the sum of the logarithms of the non-zero eigenvalues of \mathcal{O} (the non-zero part of the spectrum is real and positive since \mathcal{O} will be a positive operator in the cases we consider). Then the *normalized reduced log-determinant* $\log \det_* \mathcal{O}$ is defined as

$$\log \det_* \mathcal{O}_{mn} = \frac{1}{|V_{mn}|} \log \det' \mathcal{O}_{mn}. \tag{3.12}$$

The *normalized log-determinant* of \mathcal{O} , defined for the entire infinite bi-periodic graph \mathbb{G} , is defined simply as the limit

$$\log \det_* \mathcal{O} = \lim_{m,n \rightarrow \infty} \log \det_* \mathcal{O}_{mn}. \tag{3.13}$$

So $\log \det_* \mathcal{O}$ corresponds to an “effective action” density (free energy density) per vertex on the infinite lattice.

Definition (3.13) agrees with the log-determinant considered by Kenyon in [17] when \mathcal{O} is the critical Laplacian on a bi-periodic infinite isoradial (critical) graph.

In fact, the limit in formula (3.13) exists and coincides with the following description in terms of matrix-valued symbols: Choose complex parameters z and w , and for each pair $(m, n) \in \mathbb{Z}_{>0}^2$ define the space of quasi-periodic functions

$$\mathcal{F}_{mn}(z, w) = \left\{ \phi : V(\mathbb{G}) \rightarrow \mathbb{C} : \phi(v + (am, bn)) = z^a w^b \phi(v) \right. \\ \left. \text{for all } v \in V(\mathbb{G}) \text{ and all } a, b \in \mathbb{Z} \right\}.$$

This is a finite-dimensional vector space of dimension $\dim \mathcal{F}_{mn}(z, w) = |V_{mn}|$. Clearly, $\mathcal{O}\phi \in \mathcal{F}_{mn}$ whenever $\phi \in \mathcal{F}_{mn}$, and consequently the operator \mathcal{O} restricts to a finite-dimensional linear operator $\sigma_{mn}^{\mathcal{O}}$ on $\mathcal{F}_{mn}(z, w)$ which is called the symbol of \mathcal{O} . The entries of the matrix $\sigma_{mn}^{\mathcal{O}}$ are Laurent polynomials in z and w , and for generic values of z and w , this matrix will be invertible; indeed, the work of Kassel and Kenyon [16] implies that its determinant $\det \sigma_{mn}^{\mathcal{O}}$ is non-negative for values of z and w each having unit modulus. One checks that the average value of the log-determinant of this symbol agrees with normalized log-determinant of \mathcal{O} ,

$$\log \det_* \mathcal{O} = \frac{1}{4\pi^2} \frac{1}{|V_{mn}|} \int_0^{2\pi} \int_0^{2\pi} d\zeta d\omega \log \det \sigma_{mn}^{\mathcal{O}}(e^{i\zeta}, e^{i\omega}). \tag{3.14}$$

Remark 3.11. The value of the right-hand side of (3.14) can be evaluated using Jensen’s formula (twice) and is independent of the choice of $m, n \in \mathbb{Z}_{>0}$.

3.3.3. Using Dirichlet boundary conditions. Let us propose the following alternative construction. For an arbitrary polygonal graph G (not necessarily periodic), one can consider a sequence of truncated operators \mathcal{O}_n obtained from a nested sequence of domains $\Omega_1 \subset \dots \subset \Omega_n \subset \Omega_{n+1} \subset \dots$ whose union is \mathbb{C} : for instance, the sequence of $2n \times 2n$ squares $\Omega_n = \{z : |\operatorname{Re}(z)| < n, |\operatorname{Im}(z)| < n\}$, where \mathcal{O}_n is the restriction of the operator \mathcal{O} to the subset of vertices $V_n = \{v \in V(G) : z(v) \in \Omega_n\}$ with Dirichlet boundary conditions imposed on the complement of Ω_n . This amounts to setting the (u, v) matrix entry of \mathcal{O}_n to zero, whenever $z(u), z(v) \notin \Omega_n$. Thus the non-zero part of \mathcal{O}_n is a $|V_n| \times |V_n|$ submatrix. Since we choose Dirichlet boundary conditions on the boundary of Ω_n , \mathcal{O}_n has no zero modes and $\log \det \mathcal{O}_n$ is well defined. Then we expect that the normalized ∞ -volume log-determinant, defined in analogy with (3.12) by

$$\lim_{n \rightarrow \infty} \frac{1}{|\Omega_n|} \log \det \mathcal{O}_n, \tag{3.15}$$

exists, at least in the case of a non-periodic graph G which is sufficiently “regular/homogeneous” (e.g., a quasi-periodic lattice), and agrees with the normalized log-determinant $\log \det_* \mathcal{O}$ defined above by (3.13) when the graph is periodic. This is to be expected on physical grounds by arguments analogous to those leading to the existence of a unique infinite volume thermodynamical limit for simple classical statistical systems, such as a lattice of classical oscillators, or spin systems, in their high temperature phase, independent of the boundary conditions chosen for the system. We shall not elaborate more, nor attempt to present a complete and fully rigorous proof, since this is not needed for the rest of this work.

3.3.4. Local variation of ∞ -volume determinants. The finite variation of ∞ -volume determinants (by themselves infinite) under a local deformation can be defined properly for the two schemes that we have presented above. Let us explain the idea in the Dirichlet boundary scheme. We begin with a polyhedral graph G and make a perturbation $G \rightarrow G'$ by moving some of its vertices inside a finite size compact domain Ω . The operator \mathcal{O} changes accordingly

$$\mathcal{O} \rightarrow \mathcal{O}' = \mathcal{O} + \delta\mathcal{O}.$$

If the incidence relations of G do not change, the variation $\delta\mathcal{O}$ will be an operator supported on the finite set $\bar{\Omega}$ consisting of all vertices in Ω plus their nearest neighboring vertices (any vertex which shares a common face with a vertex in Ω). Considering a nested sequence of domains $\Omega_1 \subset \Omega_2 \subset \dots \subset \Omega_n \subset \dots \rightarrow \mathbb{C}$ such that $\bar{\Omega} \subset \Omega_1$, one can write the variation series expansion for the restriction of \mathcal{O} in each Ω_n

$$\log \det \mathcal{O}'_n = \log \det \mathcal{O}_n + \operatorname{tr}[\delta\mathcal{O}_n \cdot \mathcal{O}_n^{-1}] - \frac{1}{2} \operatorname{tr}[(\delta\mathcal{O}_n \cdot \mathcal{O}_n^{-1})^2] + \dots$$

In the limit $n \rightarrow \infty$, since the $\delta\mathcal{O}_n$ extended to \mathbb{G} are equal to $\delta\mathcal{O}$, every term in the expansion will converge to its ∞ -volume limit, so that we have for any positive integer K

$$\text{tr}[(\delta\mathcal{O}_n \cdot \mathcal{O}_n^{-1})^K] \rightarrow \text{tr}[(\delta\mathcal{O} \cdot \mathcal{O}^{-1})^K], \quad K \in \mathbb{N}_+,$$

so that, although $\log \det \mathcal{O}'$ and $\log \det \mathcal{O}$ are formally infinite, the difference is finite and one can write

$$\log \det \mathcal{O}' = \log \det \mathcal{O} + \text{tr}[\delta\mathcal{O} \cdot \mathcal{O}^{-1}] - \frac{1}{2} \text{tr}[(\delta\mathcal{O} \cdot \mathcal{O}^{-1})^2] + \dots \tag{3.16}$$

We shall study the perturbation around an isoradial, Delaunay graph \mathbb{G}_{cr} , where we have seen that $\mathcal{O}_{\text{cr}}^{-1}$ (the Green’s function) can be expressed in a simple contour integral form. Moreover, we shall consider infinitesimal transformations (1.11), namely,

$$z(\mathbf{v}) \rightarrow z_\epsilon(\mathbf{v}) = z(\mathbf{v}) + \epsilon F(\mathbf{v})$$

and study the general form of the first-order term in (3.16), and some especially interesting terms in the second-order term.

3.4. Kenyon’s local formula for $\log \det \Delta_{\text{cr}}$

3.4.1. Kenyon’s formula for a periodic infinite lattice. In [17], Kenyon derived an explicit formula for the normalized log-determinant of Δ_{cr} for periodic, isoradial, Delaunay triangulations \mathbb{T}_{cr} . The proof of this result relies only on the structure of the corresponding rhombic graph $\mathbb{T}_{\text{cr}}^\diamond$ and indeed works for any rhombic graph. For this reason, Kenyon’s formula implicitly extends to all periodic, isoradial, Delaunay graphs \mathbb{G}_{cr} . The formula reads

$$\log \det_* \Delta_{\text{cr}} = \frac{2}{\pi |\mathbb{V}_{11}|} \sum_{\substack{\text{edges } \mathbf{e} \\ \text{of } \mathbb{G}_{\text{cr}}/\Lambda_{11}}} L(\theta(\mathbf{e})) + L\left(\frac{\pi}{2} - \theta(\mathbf{e})\right) + \theta(\mathbf{e}) \log \tan \theta(\mathbf{e})$$

is the volume (number of vertices) of the elementary domain of the infinite periodic graph (see Section 3.3.2), the sum runs over all edges \mathbf{e} in the quotient toric graph, and L is the Lobachevsky function (related to the Clausen function Cl_2) defined by

$$L(x) = - \int_0^x dy |2 \log(y)| = \frac{\text{Cl}_2(2x)}{2}. \tag{3.17}$$

3.4.2. Extension to general isoradial (weak) Delaunay graphs. Kenyon’s formula can be formally extended to express the (formally infinite) un-normalized log-determinant $\log \det \Delta_{\text{cr}}$ for a general isoradial Delaunay graph \mathbb{G}_{cr} as a sum over all edges

$e \in E(G_{cr})$, namely,

$$\log \det \Delta_{cr} = \frac{2}{\pi} \sum_{e \in E(G_{cr})} \mathcal{L}(\theta(e)) \tag{3.18}$$

with for compactness of the function \mathcal{L} of the conformal angles $\theta(e)$ given by

$$\mathcal{L}(\theta(e)) = L(\theta(e)) + L\left(\frac{\pi}{2} - \theta(e)\right) + \theta(e) \log \tan \theta(e). \tag{3.19}$$

We may further generalize this formula to any isoradial *weak* Delaunay graph G obtained from G_{cr} by adding chords inside the faces of G_{cr} , i.e., any graph such that $G^\bullet = G_{cr}$. Indeed, if e is a chord in G , then

$$\theta_n(\bar{e}) = -\theta_s(\bar{e}) \quad \text{and} \quad \mathcal{L}(\theta_n(\bar{e})) = -\mathcal{L}(\theta_s(\bar{e})),$$

where the function $\mathcal{L}(\theta)$ is analytically extended to an *odd function* of θ over $(-\pi, \pi)$. For any isoradial weak Delaunay graph G of this kind, formula (3.18) becomes

$$\log \det \Delta_{cr} = \frac{1}{\pi} \sum_{e \in E(G)} \mathcal{L}(\theta_n(\bar{e})) + \mathcal{L}(\theta_s(\bar{e})) \tag{3.20}$$

since the contribution of any chord is zero. This is true, in particular, for the isoradial weak Delaunay graphs G_{0+} and \hat{G}_{0+} mentioned in Definition 1.5 of the introduction. Note that the derivative of \mathcal{L} is

$$\mathcal{L}'(\theta) = \frac{d}{d\theta} \mathcal{L}(\theta) = \frac{\theta}{\sin \theta \cos \theta}. \tag{3.21}$$

4. The critical Green’s function and its asymptotics

4.1. Kenyon’s formula for the critical Green’s function

The Green’s function Δ_{cr}^{-1} studied by Kenyon in [17] is a right-inverse of the critical Laplacian Δ_{cr} characterized uniquely by the following three conditions:

- (1) $\Delta_{cr} \Delta_{cr}^{-1} = \mathbb{1}$,
- (2) $[\Delta_{cr}^{-1}]_{u,v} = O(\log |z_{cr}(u) - z_{cr}(v)|)$ for $|z_{cr}(u) - z_{cr}(v)| \gg 0$,
- (3) $[\Delta_{cr}^{-1}]_{u,u} = 0$.

Here G_{cr} is an isoradial Delaunay graph with embedding z_{cr} , and G_{cr}^\diamond is its associated rhombic graph (its embedding is also denoted by z_{cr}). Kenyon showed that this critical Green’s function Δ_{cr}^{-1} on G_{cr} is expressed by the explicit integral

$$[\Delta_{cr}^{-1}]_{u,v} = -\frac{1}{8\pi^2 i} \oint_{\mathcal{E}} \frac{dw}{w} \log(w) E_{\underline{\theta}(v)}(w), \tag{4.1}$$

where $\mathbb{v} = (v_0, \dots, v_k)$ is any choice of path from $v_0 = u$ to $v_k = v$ on G_{cr}^\diamond ; $\underline{\theta}(\mathbb{v}) = (\theta_1, \dots, \theta_k)$ is the associated sequence of angles; $E_{\underline{\theta}}(w)$ is the meromorphic function in w ,

$$E_{\underline{\theta}}(w) := \prod_{j=1}^k \frac{w + e^{i\theta_j}}{w - e^{i\theta_j}}. \tag{4.2}$$

The value of $E_{\underline{\theta}}(w)$ depends only on the end points v_0 and v_k of the path; this follows from an argument similar to the proof in demonstrating that the value of $[\mathbb{v}]_n$ for odd positive integers n also depends only on the end points v_0 and v_k of the path. If we fix v_0 and allow the end point $v = v_k$ of the path to vary, then the mapping $v \mapsto E_{\underline{\theta}}(w)$ is an example of a discrete analytic function on G_{cr}^\diamond as discussed in [17]. By Lemma 4.4, the restriction of this mapping to vertices $v \in V(G_{\text{cr}})$ may be viewed as a lattice approximation of the continuous exponential function

$$z \mapsto \exp\{2w[\bar{z} - \bar{z}_{\text{cr}}(v_0)]\}$$

provided $|w| < 1$. For this reason, $E_{\underline{\theta}}(w)$ is referred to as a *discrete exponential function*. Finally, \mathcal{C} is any closed, counter-clockwise oriented contour enclosing the finite set of phases $\Phi(\mathbb{v}) := \{e^{i\vartheta} : \vartheta \in \Theta(\mathbb{v})\}$. As explained in Proposition 2.27, the set of angles $\Theta(\mathbb{v})$, and thus $\Phi(\mathbb{v})$, are finite and depend only on the end-points u and v of the path \mathbb{v} . The set of poles of the integrand in formula (4.1) is precisely $\Phi(\mathbb{v})$ and $e^{-i\theta_0} \notin \Phi(\mathbb{v})$, so a contour C can be chosen to avoid the branch cut $-\theta_0 = \arg(z_{\text{cr}}(u) - \text{cr}(\mathbb{v}))$ of the logarithm; see Section 4.3 below for details.

Remark 4.1. Formula (4.2) is invariant under both global translation and rotation of the graph G_{cr} .

Remark 4.2. Let us consider an oriented edge $\vec{e} = (uv)$ of an *isoradial weak Delaunay graph* G_{cr} . There are two possible situations.

- (1) Either $\vec{e} = (uv)$ is not a chord (see Figure 13, left), in which case the north and south angles of \vec{e} are equal (and generically non-zero) and both coincide with the conformal angle of the edge e ,

$$\theta_n(\vec{e}) = \theta_s(\vec{e}) = \theta(e).$$

- (2) Or $\vec{e} = (uv)$ is a chord (see Figure 13, right), in which case the north and south angles of \vec{e} are opposite, while the conformal angle of e is zero,

$$\theta_n(\vec{e}) = -\theta_s(\vec{e}) \neq 0, \quad \theta(e) = 0.$$

In both cases, Kenyon’s formula for the Green’s function for this pair of vertices u, v reads

$$[\Delta_{\text{cr}}^{-1}]_{u,v} = -\frac{1}{\pi} \theta_n(\vec{e}) \cot \theta_n(\vec{e}) = -\frac{1}{\pi} \theta_s(\vec{e}) \cot \theta_s(\vec{e}).$$

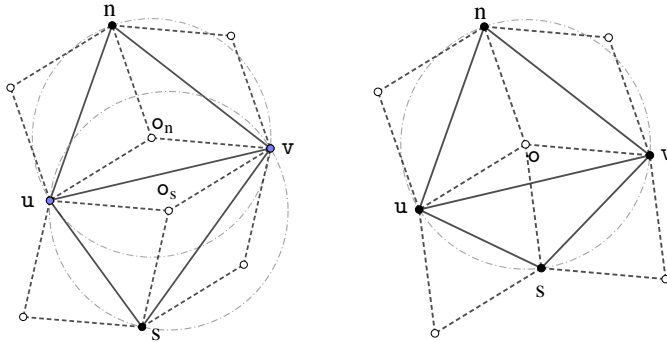


Figure 13. Either the edge $\vec{e} = (uv)$ is not a chord, in which case the respective north and south centers o_n and o_s are different and $\theta_n(\vec{e}) = \theta_s(\vec{e})$ (and generically non-zero). Or else the edge $\vec{e} = (uv)$ is a chord, in which case the centers coincide $o_n = o_s = o$ and $\theta_n(\vec{e}) = -\theta_s(\vec{e})$.

Proof. Select, for instance, the north face f_n and let o_n be its center. Assume that the isoradius of the critical triangulation is $R_{cr} = 1$ for simplicity. Consider the path $\mathbb{V} = (u, o_n, v)$. Set $e^{i\theta_1} = z_{cr}(o_n) - z_{cr}(u)$ and $e^{i\theta_2} = z_{cr}(v) - z_{cr}(o_n)$ and note that $\theta_n(\overline{uv}) = \frac{\theta_1 - \theta_2}{2}$. Then

$$\begin{aligned} [\Delta_{cr}^{-1}]_{u,v} &= -\frac{1}{8\pi^2 i} \oint_{\mathcal{E}} \frac{dw}{w} \log(w) \frac{w + e^{i\theta_1}}{w - e^{i\theta_1}} \frac{w + e^{i\theta_2}}{w - e^{i\theta_2}} \\ &= -\frac{1}{4\pi} \left(2e^{i\theta_1} \frac{e^{i\theta_1} + e^{i\theta_2}}{e^{i\theta_1} - e^{i\theta_2}} \frac{\log(e^{i\theta_1})}{e^{i\theta_1}} + 2e^{i\theta_2} \frac{e^{i\theta_2} + e^{i\theta_1}}{e^{i\theta_2} - e^{i\theta_1}} \frac{\log(e^{i\theta_2})}{e^{i\theta_2}} \right) \\ &= -\frac{1}{4\pi} \left(2i(\theta_1 - \theta_2) \frac{e^{i\theta_1} + e^{i\theta_2}}{e^{i\theta_1} - e^{i\theta_2}} \right) = -\frac{1}{\pi} \frac{\theta_1 - \theta_2}{2} \cot\left(\frac{\theta_1 - \theta_2}{2}\right). \end{aligned}$$

The calculation with the south face f_s gives the same result, regardless of whether $o_s \neq o_n$ or $o_s = o_n$. ■

4.2. Expansion and bounds for the discrete exponential

Lemma 4.3. Consider a finite sequence of angles $(\theta_1, \dots, \theta_k)$ contained in the closed interval of the form $[\vartheta - \frac{\pi}{2}, \vartheta + \frac{\pi}{2}]$ centered about some fixed angle ϑ . Using Definition 2.23, consider

$$p_{2n+1} := \sum_{j=1}^k e^{i(2n+1)\theta_j}.$$

Then we have the uniform bound

$$|p_{2n+1}| \leq (2n + 1)|p_1|.$$

Proof. Clearly, it is enough to verify the lemma in the case of $\vartheta = 0$, otherwise we have $p_{2n+1} = e^{-i\vartheta} \tilde{p}_{2n+1}$, where $\tilde{p}_{2n+1} = \sum_{j=1}^k e^{i(2n+1)\tilde{\theta}_j}$ and where $\tilde{\theta}_j = \theta_j - \vartheta \in [-\frac{\pi}{2}, \frac{\pi}{2}]$.

Begin with the polynomial

$$q_{2n+1}(w) := 2w^2(w^{2n} - (-1)^n)(w^2 + 1)^{-1}$$

and notice that

$$\begin{aligned} q_{2n+1}(iw) &:= 2(iw)^2 \left(\frac{(iw)^{2n} - (-1)^n}{(iw)^2 + 1} \right) = (-1)^n 2w^2 \frac{w^{2n} - 1}{w^2 - 1} \\ &= (-1)^n 2(w^{2n} + w^{2n-2} + \dots + w^2 + 1), \end{aligned}$$

therefore,

$$q_{2n+1}(w) = (-1)^n 2(1 - w^2 + w^4 - w^6 + \dots + (-1)^n w^{2n}).$$

For $w = e^{i\theta}$ with $\theta \in [-\frac{\pi}{2}, \frac{\pi}{2}]$, the function $\theta \mapsto q_{2n+1}(e^{i\theta})$ is clearly continuous and its modulus takes the maximal value $|q_{2n+1}(\pm i)| = 2n$, and so $|q_{2n+1}|_\infty = 2n$. By construction, $e^{i(2n+1)\theta} = \cos(\theta)q_{2n+1}(e^{i\theta}) + (-1)^n e^{i\theta}$, and so

$$p_{2n+1} = \sum_{j=1}^k \cos(\theta_j)q_{2n+1}(e^{i\theta_j}) + (-1)^n p_1.$$

We now proceed with a chain of inequalities:

$$\begin{aligned} |p_{2n+1}| &\leq \left| \sum_{1 \leq j \leq k} \cos(\theta_j)q_{2n+1}(e^{i\theta_j}) \right| + |p_1| \\ &\leq \sum_{1 \leq j \leq k} |\cos(\theta_j)q_{2n+1}(e^{i\theta_j})| + |p_1| \\ &\leq \sum_{1 \leq j \leq k} \cos(\theta_j)|q_{2n+1}(e^{i\theta_j})| + |p_1| \quad \left(\text{note that } \cos(\theta_j) \geq 0 \right. \\ &\quad \left. \text{because } -\frac{\pi}{2} \leq \theta_j \leq \frac{\pi}{2} \right) \\ &\leq \sum_{1 \leq j \leq k} \cos(\theta_j)|q_{2n+1}|_\infty + |p_1| \leq 2n \operatorname{Re}[p_1] + |p_1| \\ &\leq (2n + 1)|p_1| \quad (\text{since } 0 \leq \operatorname{Re}[p_1] \leq |p_1|). \end{aligned}$$

■

Lemma 4.4. *Given a finite sequence of angles $\underline{\theta} = (\theta_1, \dots, \theta_k)$ and $|w| < 1$, the following infinite product expansion of $E_{\underline{\theta}}(w)$ is valid:*

$$E_{\underline{\theta}}(w) = (-1)^k \prod_{n \text{ odd}} \exp\left(\frac{2}{n} w^n \bar{p}_n\right), \quad \text{where } p_n = \sum_{1 \leq j \leq k} e^{in\theta_j}.$$

Proof.

$$\begin{aligned}
 \prod_{j=1}^k \frac{w + e^{i\theta_j}}{w - e^{i\theta_j}} &= (-1)^k \prod_{j=1}^k \frac{1 + we^{-i\theta_j}}{1 - we^{-i\theta_j}} \\
 &= (-1)^k \exp \sum_{j=1}^k \log \left(\frac{1 + we^{-i\theta_j}}{1 - we^{-i\theta_j}} \right) \\
 &= (-1)^k \exp \sum_{j=1}^k 2 \left(we^{-i\theta_j} + \frac{1}{3} w^3 e^{-3i\theta_j} + \frac{1}{5} w^5 e^{-5i\theta_j} + \dots \right) \\
 &= (-1)^k \exp \left(2w \sum_{j=1}^k e^{-i\theta_j} + \frac{2}{3} w^3 \sum_{j=1}^k e^{-3i\theta_j} + \frac{2}{5} w^5 \sum_{j=1}^k e^{-5i\theta_j} + \dots \right) \\
 &= (-1)^k \prod_{n \text{ odd}} \exp \left(\frac{2}{n} w^n \bar{p}_n \right).
 \end{aligned}$$

Note that this can be rewritten as

$$(-1)^k \exp(2w \bar{p}_1) \cdot \left(1 + \sum_{N \geq 3} w^N \bar{c}_N \right)$$

with the coefficients \bar{c}_N of a series. ■

Remark 4.5. Let $\underline{\theta} = (\theta_1, \dots, \theta_n)$ be a finite sequence of angles contained in an interval of the form $[\vartheta - \frac{\pi}{2}, \vartheta + \frac{\pi}{2}]$, where n is a positive odd integer. Define

$$u_n = \frac{1}{n} \frac{p_n}{p_1} \quad \text{and} \quad u(w) = \sum_{\substack{\text{odd} \\ n \geq 3}} u_n w^n. \tag{4.3}$$

By Lemma 4.3, each $|u_n| \leq 1$, and $u(w)$ is analytic in the unit disk and $E_{\underline{\theta}}(w) = (-1)^k \cdot \exp(2\bar{p}_1 w) \cdot \exp(2\bar{p}_1 u(w))$. Furthermore, we have, through the standard combinatorial series expansion,

$$E_{\underline{\theta}}(w) = (-1)^k \cdot \exp(2\bar{p}_1 w) \cdot \left(1 + \sum_{m=1}^{\infty} \sum_{d=1}^m w^{2m+d} (2\bar{p}_1)^d \bar{c}_{m,d} \right)$$

with the coefficients $c_{m,d}$ given by

$$c_{m,d} = \sum_{\substack{\mathbb{r} \vdash m \\ \#(\mathbb{r})=d}} \prod_{s \geq 1} \frac{1}{(r_s)!} (u_{1+2s})^{r_s}, \tag{4.4}$$

and where the sum is taken over infinite tuples $\mathbb{r} = (r_1, r_2, r_3, \dots) \in \mathbb{Z}_{\geq 0}^{\mathbb{N}}$ with $\sum_{s \geq 1} r_s = d$ and such that $\sum_{s \geq 1} s r_s = m$.

Let u and v be distinct vertices of G_{cr} , and let $\nu = (v_0, \dots, v_k)$ be a path from u to v . Translation and rotation invariance of the Green's function allows us to assume without loss of generality that u is situated at the origin and that the phases $e^{i\theta_j} := z_{cr}(v_j) - z_{cr}(v_{j-1})$ of the path lie in the open interval $(-\frac{\pi}{2}, \frac{\pi}{2})$; if not, then the embedding of G_{cr} may be shifted $z \mapsto z - z_{cr}(u)$ and rotated $z \mapsto z \exp(-i\theta_\nu)$ to achieve these features; see Proposition 2.27 for a definition of θ_ν .

4.3. Contour integral for the expansion

In [17], Kenyon handles the asymptotic behavior of the Green's function with respect to the distance $|u - v|$ using a *keyhole* contour C with a corridor of width $\epsilon > 0$ avoiding the cut of the logarithm $\arg(w) = -\pi$. Paraphrasing Kenyon, this contour C_ϵ runs counter-clockwise along the circle of radius R about the origin (connecting $-R \pm i\epsilon$), then travels horizontally above the x -axis from $-R + i\epsilon$ to $-r + i\epsilon$, runs clockwise along the circle of radius r about the origin (connecting $-r \pm i\epsilon$), and finally returns horizontally from $-r - i\epsilon$ to $-R - i\epsilon$ below the x -axis. Here $R \gg |u - v|$ and $r \ll |u - v|^{-1}$ (see Figure 14).

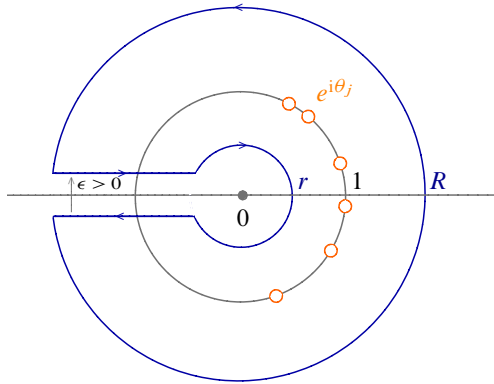


Figure 14. Keyhole contour C .

The following lemma allows us to compute the Green's function by integrating along the cut of the logarithm provided we subtract off the logarithmic divergences.

Lemma 4.6. *Let $F(w)$ be a function which is holomorphic on the extended complex plane $\mathbb{C} \cup \{\infty\}$ outside a subset S contained in the interior of the keyhole contour C for some values of $R, r,$ and $\epsilon,$ and such that $F(0) = F(\infty) = 1$. Then*

$$\oint_C \frac{dw}{w} \log(w)F(w) = -2\pi i \int_0^\infty (F(-t) - 1) \frac{dt}{t}.$$

Proof.

$$\begin{aligned}
 & \oint_C \frac{dw}{w} \log(w)F(w) \\
 &= \lim_{\substack{r \rightarrow 0 \\ R \rightarrow \infty}} \lim_{\epsilon \rightarrow 0} \oint_C \frac{dw}{w} \log(w)F(w) \\
 &= \lim_{\substack{r \rightarrow 0 \\ R \rightarrow \infty}} \left(\underbrace{i \int_{\pi}^{-\pi} \log(re^{i\phi})F(re^{i\phi}) d\phi}_{\text{contribution from the circle of radius } r} + 2\pi i \underbrace{\int_{-R}^{-r} F(t) \frac{dt}{t}}_{\text{contribution along the cut}} \right. \\
 &\quad \left. + i \underbrace{\int_{-\pi}^{\pi} \log(Re^{i\phi})F(Re^{i\phi}) d\phi}_{\text{contribution from the circle of radius } R} \right) \\
 &= \lim_{\substack{r \rightarrow 0 \\ R \rightarrow \infty}} \left(-2\pi i \log(r) - 2\pi i \sum_{N \geq 1} \frac{1}{N} (-r)^N a_N - 2\pi i \int_r^R F(-t) \frac{dt}{t} \right. \\
 &\quad \left. + 2\pi i \log(R) + 2\pi i \sum_{N \geq 1} \frac{1}{N} (-R)^{-N} b_N \right) \\
 &= -2\pi i \int_0^\infty \frac{dt}{t} (F(-t) - 1),
 \end{aligned}$$

where $1 + \sum_{N \geq 1} a_N w^N$ and $1 + \sum_{N \geq 1} b_N w^N$ are the power series expansions of $F(w)$ at 0 and ∞ , respectively. ■

Corollary 4.7. *For vertices u and v in G_{cr} , the value of the Green's function is*

$$[\Delta_{cr}^{-1}]_{u,v} = \frac{1}{2\pi} \operatorname{Re} \int_0^1 (E_{\underline{\theta}(v)}(-t) - 1) \frac{dt}{t}. \tag{4.5}$$

Proof. We begin with the observation that $E_{\underline{\theta}}(w^{-1}) = (-1)^k \bar{E}_{\underline{\theta}}(w)$ for any finite sequence of angles $\underline{\theta} = (\theta_1, \dots, \theta_k)$. Since u and v are vertices in G_{cr} , the length k of any path $\mathfrak{v} = (v_0, \dots, v_k)$ from $v_0 = u$ to $v_k = v$ in G_{cr}^\diamond must be even. Thus $E_{\underline{\theta}}(w^{-1}) = \bar{E}_{\underline{\theta}(v)}(w)$. Then

$$\begin{aligned}
 [\Delta_{cr}^{-1}]_{u,v} &= -\frac{1}{8\pi^2 i} \oint_C \frac{dw}{w} \log(w) E_{\underline{\theta}(v)}(w) = \frac{1}{4\pi} \int_0^\infty (E_{\underline{\theta}(v)}(-t) - 1) \frac{dt}{t} \\
 &= \frac{1}{4\pi} \int_0^1 (E_{\underline{\theta}(v)}(-t) - 1) \frac{dt}{t} + \frac{1}{4\pi} \int_1^\infty (E_{\underline{\theta}(v)}(-t) - 1) \frac{dt}{t} \\
 &= \frac{1}{4\pi} \int_0^1 (E_{\underline{\theta}(v)}(-t) - 1) \frac{dt}{t} + \frac{1}{4\pi} \int_0^1 (\bar{E}_{\underline{\theta}(v)}(-t) - 1) \frac{dt}{t} \\
 &= \frac{1}{2\pi} \operatorname{Re} \left[\int_0^1 (E_{\underline{\theta}(v)}(-t) - 1) \frac{dt}{t} \right].
 \end{aligned}$$

■

Remark 4.8. Since $|t| < 1$, in formula (4.5) we may use the presentation of $E_{\underline{\theta}(\mathfrak{v})}(t)$ given in Remark 4.5 and write

$$[\Delta_{\text{cr}}^{-1}]_{\mathfrak{u},\mathfrak{v}} = \frac{1}{2\pi} \operatorname{Re} \int_0^1 (\exp(-2p_1 t) \cdot \exp(2p_1 u(-t)) - 1) \frac{dt}{t},$$

where $u(t) = \sum_{n>0} u_{2n+1}(t)^{2n+1}$ is the function defined from the momenta p_{2n+1} in equation (4.3).

We may adopt the view that p_1 and \bar{p}_1 are independent variables on the plane and that $[\Delta_{\text{cr}}^{-1}]_{\mathfrak{u},\mathfrak{v}}$ is a smooth function of p_1 and \bar{p}_1 .

4.4. The general asymptotics

Proposition 4.9. *The Green’s function $[\Delta_{\text{cr}}^{-1}]_{\mathfrak{u},\mathfrak{v}}$ has a series expansion at ∞ given by*

$$-\frac{1}{2\pi} \left(\log(2|p_1|) + \gamma_{\text{Euler}} - \sum_{m \geq d \geq 1} (-1)^d (2m + d - 1)! \operatorname{Re}[c_{m,d}(2p_1)^{-2m}] \right),$$

where the coefficients $c_{m,d}$ are defined in equation (4.4) in terms of the u_{1+2s} defined by (4.3), which are themselves bounded in terms of p_1 by Lemma 4.3.

Proof.

$$\begin{aligned} [\Delta_{\text{cr}}^{-1}]_{\mathfrak{u},\mathfrak{v}} &= \frac{1}{2\pi} \operatorname{Re} \left[\int_0^1 (E_{\underline{\theta}(\mathfrak{v})}(-t) - 1) \frac{dt}{t} \right] = \frac{1}{2\pi} \operatorname{Re} \left[\int_0^1 (\exp(-2p_1 t) - 1) \frac{dt}{t} \right] \\ &\quad + \frac{1}{2\pi} \sum_{m \geq d \geq 1} \operatorname{Re} \left[c_{m,d}(2p_1)^d \int_0^1 -(-t)^{2m+d-1} \exp(-2p_1 t) dt \right] \\ &= -\frac{1}{2\pi} \operatorname{Re} \left[\log(2p_1) + \gamma_{\text{Euler}} + \underbrace{\int_{2p_1}^{\infty} \exp(-t) \frac{dt}{t}}_{\substack{\text{null power series} \\ \text{expansion at } \infty}} \right] \\ &\quad - \frac{1}{2\pi} \sum_{m \geq d \geq 1} \operatorname{Re} \left[c_{m,d}(-1)^d (2p_1)^{-2m} \right. \\ &\quad \quad \times \left. \sum_{i=0}^{2m+d-1} \frac{(2m+d-1)!}{i!} \underbrace{(2p_1 t)^i \exp(-2p_1 t)}_{\substack{\text{null power series} \\ \text{expansion at } \infty}} \right] \Big|_0^1 \\ &= -\frac{1}{2\pi} \left(\log(2|p_1|) + \gamma_{\text{Euler}} \right. \\ &\quad \left. - \sum_{m \geq d \geq 1} (-1)^d (2m + d - 1)! \operatorname{Re}[c_{m,d}(2p_1)^{-2m}] \right). \quad \blacksquare \end{aligned}$$

5. Deforming Delaunay lattices and operators

5.1. Setup and problems for deformations of isoradial Delaunay graphs

We start to address the main problem of this work, which is to study geometric deformations of isoradial Delaunay graphs and their associated operators defined in Section 1.2.3.

Begin with an initial (not necessarily isoradial) *Delaunay graph* G_0 as presented in Definition 2.6 with vertex set $V(G_0)$, edge set $E(G_0)$, and face set $F(G_0)$. We deform the initial vertex embedding $v \mapsto z_0(v)$ for $v \in V(G_0)$ by

$$z_\epsilon(v) := z_0(v) + \epsilon F(v), \tag{5.1}$$

where ϵ is a positive real parameter and the displacements $F(v)$ are implemented by a complex-valued function

$$F: V(G_0) \rightarrow \mathbb{C}$$

with *finite support*, i.e., a finite subset $\Omega_F \subset V(G_0)$ such that $v \in \Omega_F \Leftrightarrow F(v) \neq 0$.

If the deformation parameter ϵ is unconstrained, displaced vertices may potentially collide, i.e., the mapping $v \mapsto z_\epsilon(v)$ may fail to be one-to-one. The following simple lemma allows us to avoid this situation.

Lemma 5.1. *For any pair of distinct vertices $u, v \in G_0$, the corresponding perturbed coordinates $z_\epsilon(u)$ and $z_\epsilon(v)$ will always remain distinct provided*

$$0 \leq \epsilon < \epsilon'_F = M_F^{-1},$$

where

$$M_F = \max_{u \neq v} |dF(\overline{u}v)| \quad \text{with } dF(u, v) = \frac{F(u) - F(v)}{z_0(u) - z_0(v)}. \tag{5.2}$$

Proof. The mapping $v \mapsto F(v)$ has finite support, so the set of pairs $u, v \in G_0$ such that $dF(\overline{u}v) \neq 0$ is finite, and M_F is well defined and finite. The coordinates $z_\epsilon(u)$ and $z_\epsilon(v)$ are distinct, so

$$|z_\epsilon(u) - z_\epsilon(v)| > 0$$

provided $1 + \epsilon dF(u, v)$ is non-zero, which is clearly the case whenever $\epsilon \leq M_F^{-1}$. ■

Definition 5.2. Let G_0 be a Delaunay graph with embedding $v \mapsto z_0(v)$, and let $F: V(G_0) \rightarrow \mathbb{C}$ be a displacement function as above. Let $\epsilon \geq 0$ be a value for which the mapping $v \mapsto z_\epsilon(v)$ given by (5.1) is one-to-one. The corresponding *Delaunay deformation* G_ϵ of G_0 is the unique Delaunay graph with vertex set $V(G_\epsilon) = V(G_0)$, for which the map $v \rightarrow z_\epsilon(v)$ is a planar graph embedding.

Generically, the edge set of G_ϵ differs from the edge set of the initial graph G_0 . This is caused by the Delaunay constraints, and this difference can occur spontaneously for $\epsilon > 0$. We offer two (not unrelated) examples. Consider first a cyclic face f of G_0 with $n > 3$ vertices. As soon as $\epsilon > 0$, these vertices may cease to be concyclic. In this case, the Delaunay condition imposed on G_ϵ will force the appearance of new edges which will subdivide the initial face f into new cyclic sub-faces. An example is depicted in Figure 15. In the limit $\epsilon \rightarrow 0_+$, these new edges would become *chords* of the original face f if they were adjoined to the edge set of G_0 (see Definition 2.3 for the concept of chords and edges of a weak Delaunay graph).

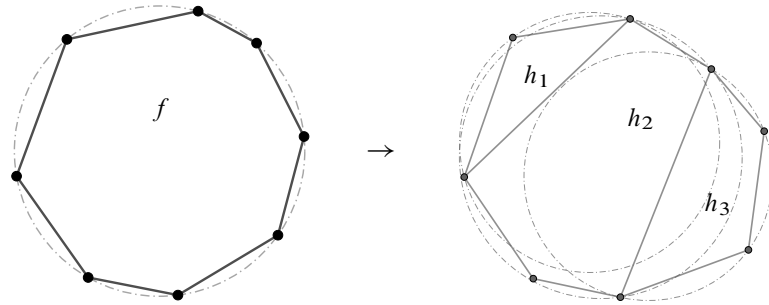


Figure 15. Example of deformation of a general cyclic face of the Delaunay graph G_0 into several cyclic faces; here a cyclic octagon f ($n = 8$) splits into 3 cyclic polygons h_1 , h_2 and h_3 , a triangle ($n_1 = 3$), a pentagon ($n_2 = 5$) and a quadrilateral ($n_3 = 4$).

This phenomenon can also occur around intermediate thresholds $\epsilon_0 > 0$ of the deformation parameter. Two (or more) faces of G_ϵ which are distinct for $\epsilon < \epsilon_0$ may become concyclic and merge into a single face (the boundary edges having vanished) when $\epsilon = \epsilon_0$. For $\epsilon > \epsilon_0$, this larger face may cease to be cyclic and instantaneously split into sub-faces caused by the appearance of new edges, possibly different from those which existed for $\epsilon < \epsilon_0$. The prototypical example is depicted in Figure 16. Two triangular faces for $\epsilon < \epsilon_0$ merge into a cyclic quadrilateral at $\epsilon = \epsilon_0$ and split again along the opposite diagonal of the quadrilateral for $\epsilon > \epsilon_0$. This is, of course, an example of a *Lawson flip* (well known from the flip algorithm used to construct Delaunay triangulations) or, more generally, of a *Pachner move* on a two-dimensional simplicial complex.

In the next section, we shall discuss how to control this phenomenon of face splittings and edge flips. Let us first introduce two other concepts of graph deformations, which shall be used later.

Definition 5.3. Let T_0 be an initial planar triangulation with embedding $v \mapsto z_0(v)$, and let $F: V(T_0) \rightarrow \mathbb{C}$ be a displacement function as above. For $\epsilon \geq 0$, the trian-

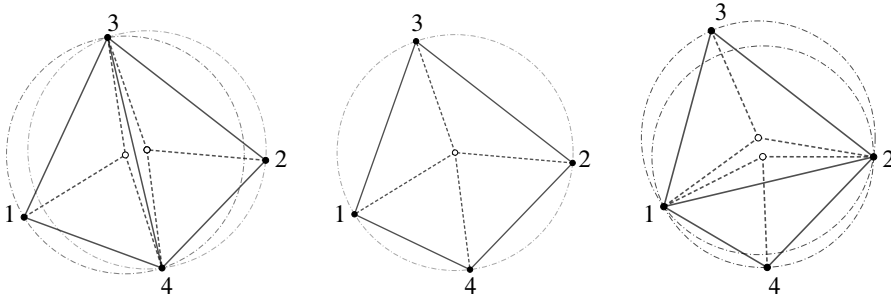


Figure 16. Example of a flip when two triangular faces become concyclic.

gulation $T_{:\epsilon}$ with vertex set $V(T_{:\epsilon}) = V(T_0)$ and edge set $E(T_{:\epsilon}) = E(T_0)$ is called a *rigid deformation* of T_0 if the mapping $v \mapsto z_\epsilon(v)$ given by (5.1) defines a planar embedding of $T_{:\epsilon}$. In particular, this implies that the face set $F(T_{:\epsilon})$ induced by the embedding coincides with the initial face set $F(T_0)$. Stated simply, no flips are allowed during a rigid deformation.

For a Delaunay deformation, the mapping $v \mapsto z_\epsilon(v)$ will be an embedding provided it is one-to-one since, by construction, the edges determined by the Delaunay constraints will never cross in the plane. Injectivity can be achieved, for example, by bounding the deformation parameter $0 \leq \epsilon < \epsilon'_F$ as prescribed in Lemma 5.1. For rigid deformations, the mapping $v \mapsto z_\epsilon(v)$ must be a planar embedding with respect to a predetermined edge set $E(T_0)$. One way to ensure this is to regulate the deformation parameter $\epsilon \geq 0$ so that the area of a triangle $(z_\epsilon(u), z_\epsilon(v), z_\epsilon(w))$ given by formula (3.2) remains positive whenever $\mathfrak{f} = (u, v, w)$ is a triangle of T_0 . This is addressed in the following lemma.

Lemma 5.4. *For an embedded planar triangulation T_0 and a displacement function F as above, let*

$$M'_F = \max_{\mathfrak{f} \in F(T_0)} \max\{|\nabla F(\mathfrak{f})|, |\bar{\nabla} F(\mathfrak{f})|\},$$

where ∇ and $\bar{\nabla}$ are the discrete derivative operators which map $\mathbb{C}^{V(T_0)} \rightarrow \mathbb{C}^{F(T_0)}$ as defined by (3.6) and (3.7) in Section 3.2. Then the rigid deformation $T_{:\epsilon}$ is an embedded planar triangulation if

$$0 \leq \epsilon < \epsilon''_F = \frac{1}{2M'_F}.$$

Proof. Let us consider a face \mathfrak{f}_0 of T_0 with embedding $(z_0(u), z_0(v), z_0(w))$ and the deformed face \mathfrak{f}_ϵ with embedding $(z_\epsilon(u), z_\epsilon(v), z_\epsilon(w))$. Using formula (3.2) for the

area A of a triangle, and result (3.8) of Remark 3.4, it is easy to show that the area of \mathbf{f}_ϵ is related to the area of \mathbf{f}_0 by

$$\begin{aligned} A(\mathbf{f}_\epsilon) &= A(\mathbf{f}_0)(1 + \epsilon(\nabla F(\mathbf{f}_0) + \bar{\nabla} \bar{F}(\mathbf{f}_0)) \\ &\quad + \epsilon^2(\nabla F(\mathbf{f}_0)\bar{\nabla} \bar{F}(\mathbf{f}_0) - \bar{\nabla} F(\mathbf{f}_0)\nabla \bar{F}(\mathbf{f}_0))) \\ &= A(\mathbf{f}_0)((1 + \epsilon\nabla F(\mathbf{f}_0))(1 + \epsilon\bar{\nabla} \bar{F}(\mathbf{f}_0)) - \epsilon^2\bar{\nabla} F(\mathbf{f}_0)\nabla \bar{F}(\mathbf{f}_0)), \end{aligned}$$

where $A(\mathbf{f}_0)$ is positive, and for $0 \leq \epsilon < \frac{1}{M'_F}$, we have the inequality

$$A(\mathbf{f}_\epsilon) \geq A(\mathbf{f}_0)((1 - \epsilon M'_F)^2 - \epsilon^2 M_F'^2) = A(\mathbf{f}_0)(1 - 2\epsilon M'_F).$$

Therefore, $2\epsilon M'_F < 1$ implies that $A(\mathbf{f}_\epsilon) > 0$, so that the face \mathbf{f}_ϵ is clockwise oriented as \mathbf{f}_0 . This bound is valid for all the faces of $\mathbb{T}_{:\epsilon}$. This ends the proof. ■

Note that the concept of rigid deformation can be extended from triangulations to more general embedded planar graphs, but we shall not need it. We shall, however, use the following concept.

Definition 5.5. Let \mathbf{G}_0 be a Delaunay graph, and let F be a displacement function as above. A Delaunay deformation \mathbf{G}_ϵ of \mathbf{G}_0 as defined in Definition 5.2 is said to be *stable* if and only if \mathbf{G}_ϵ is a Delaunay deformation of \mathbf{G}_0 for all $0 \leq \epsilon \leq \epsilon$ and

$$E(\mathbf{G}_0) \subset E(\mathbf{G}_\epsilon) \quad \text{and} \quad E(\mathbf{G}_\epsilon) = E(\mathbf{G}_\epsilon) \quad \text{for all } 0 < \epsilon \leq \epsilon.$$

This means that edges of the initial graph \mathbf{G}_0 remain edges in \mathbf{G}_ϵ and that the deformation creates a common set of new edges in \mathbf{G}_ϵ which persist (i.e., do not flip) within the range $0 < \epsilon \leq \epsilon$.

5.2. Keeping control of stable deformations

The following results allow us to control stable deformations of Delaunay graphs.

Lemma 5.6. *Let \mathbb{T}_0 be an initial planar triangulation with embedding $v \mapsto z_0(v)$, and let $F: \mathbb{V}(\mathbb{T}_0) \rightarrow \mathbb{C}$ be a displacement function with finite support $\Omega_F \subset \mathbb{V}(\mathbf{G}_0)$, as in the previous section. Let $\vec{e} = (u, v)$ be a given oriented edge of \mathbb{T}_0 , and let $\theta_0(\mathbf{e})$ be its conformal angle defined by (2.1). We do not assume \mathbb{T}_0 to be Delaunay, so the conformal angle $\theta_0(\mathbf{e})$ can be positive, zero, or negative. Let $\mathbf{f}_n = (u, v, n)$ and $\mathbf{f}_s = (v, n, s)$ be the adjacent north and south triangular faces of \vec{e} , and let*

$$M_F(\mathbf{e}) = \max\{|dF(v, n)|, |dF(v, s)|, |dF(u, n)|, |dF(u, s)|\} \tag{5.3}$$

with $dF(u_1, u_2) = \frac{F(u_1) - F(u_2)}{z_0(u_1) - z_0(u_2)}$ as in Lemma 5.1. Take ϵ such that

$$0 < \epsilon < \epsilon''_F$$

with ϵ''_F defined as in Lemma 5.4, and let us consider the rigid deformation $T_{:\epsilon}$ of T_0 (which is an embedded planar triangulation by Lemma 5.4). Let $\theta_\epsilon(\mathbf{e})$ be the deformed conformal angle of the edge \mathbf{e} in $T_{:\epsilon}$. Then we have the bound

$$0 < \epsilon M_F(\mathbf{e}) < \mathbf{b} \Rightarrow |\theta_\epsilon(\mathbf{e}) - \theta_0(\mathbf{e})| < \frac{1}{2} \arcsin\left(\frac{\epsilon M_F(\mathbf{e})}{\mathbf{b}}\right) \tag{5.4}$$

with the constant

$$\mathbf{b} = \sqrt{10} - 3 = 0.162278\dots$$

Proof. Consider the triangulation T_0 and an oriented edge $\vec{\mathbf{e}}_0 = (u, v)$ with adjacent north and south faces $\mathbf{f}_n = (u, v, n)$ and $\mathbf{f}_s = (v, n, s)$. Let $T_{:\epsilon}$ be the rigid deformation, and let

$$z_\epsilon(u) = z_0(u) + \epsilon F(u)$$

be the corresponding embedding. By (2.1), the conformal angle of the edge \mathbf{e} in the initial triangulation can be expressed as

$$\theta_0(\mathbf{e}) = \frac{1}{2} \arg\left(-\frac{(z_0(u) - z_0(n))(z_0(v) - z_0(s))}{(z_0(u) - z_0(s))(z_0(v) - z_0(n))}\right),$$

and the deformed conformal angle in $T_{:\epsilon}$ is given by

$$\begin{aligned} \theta_\epsilon(\mathbf{e}) &= \frac{1}{2} \arg\left(-\frac{(z_\epsilon(u) - z_\epsilon(n))(z_\epsilon(v) - z_\epsilon(s))}{(z_\epsilon(u) - z_\epsilon(s))(z_\epsilon(v) - z_\epsilon(n))}\right) \\ &= \theta_0(\mathbf{e}) + \frac{1}{2} \arg\left[\frac{\left(1 + \epsilon \frac{F(u) - F(n)}{z_0(u) - z_0(n)}\right)\left(1 + \epsilon \frac{F(v) - F(s)}{z_0(v) - z_0(s)}\right)}{\left(1 + \epsilon \frac{F(u) - F(s)}{z_0(u) - z_0(s)}\right)\left(1 + \epsilon \frac{F(v) - F(n)}{z_0(v) - z_0(n)}\right)}\right] \\ &= \theta_0(\mathbf{e}) + \frac{1}{2} \arg[1 + X(\mathbf{e})], \end{aligned} \tag{5.5}$$

where

$$X(\mathbf{e}) = \frac{\epsilon X_1(\mathbf{e}) + \epsilon^2 X_2(\mathbf{e})}{\left(1 + \epsilon \frac{F(u) - F(s)}{z_0(u) - z_0(s)}\right)\left(1 + \epsilon \frac{F(v) - F(n)}{z_0(v) - z_0(n)}\right)}$$

with

$$\begin{aligned} X_1(\mathbf{e}) &= \frac{F(u) - F(n)}{z_0(u) - z_0(n)} + \frac{F(v) - F(s)}{z_0(v) - z_0(s)} - \frac{F(u) - F(s)}{z_0(u) - z_0(s)} - \frac{F(v) - F(n)}{z_0(v) - z_0(n)}, \\ X_2(\mathbf{e}) &= \frac{F(u) - F(n)}{z_0(u) - z_0(n)} + \frac{F(v) - F(s)}{z_0(v) - z_0(s)} - \frac{F(u) - F(s)}{z_0(u) - z_0(s)} + \frac{F(v) - F(n)}{z_0(v) - z_0(n)}. \end{aligned}$$

Consider $M_F(\mathbf{e})$ defined by (5.3). Provided that $\epsilon M_F(\mathbf{e}) < 1$, we have

$$|X_1(\mathbf{e})| \leq 4M_F(\mathbf{e}), \quad |X_2(\mathbf{e})| \leq 2M_F(\mathbf{e})^2 \Rightarrow |X(\mathbf{e})| \leq \frac{4\epsilon M_F(\mathbf{e}) + 2\epsilon^2 M_F(\mathbf{e})^2}{(1 - \epsilon M_F(\mathbf{e}))^2}.$$

Define the function $Y(x)$ by

$$Y(x) = \frac{4x + 2x^2}{(1 - x)^2}.$$

It is a monotone convex function on the interval $x \in [0, 1)$ with $Y(0) = 0$ satisfying

$$0 \leq x \leq b = \sqrt{10} - 3 = 0.162278\dots \Rightarrow 0 \leq Y(x) \leq \frac{x}{b}.$$

Now we use the fact that for any complex number $x \in \mathbb{C}$,

$$|x| \leq 1 \Rightarrow |\arg(1 + x)| \leq \arcsin(|x|).$$

Combining these inequalities, we deduce that

$$\epsilon M_F(\mathbf{e}) \leq b \Rightarrow |\arg(1 + X(\mathbf{e}))| \leq \arcsin(Y(\epsilon M_F(\mathbf{e}))) \leq \arcsin\left(\frac{\epsilon M_F(\mathbf{e})}{b}\right).$$

Combining this with (5.5), we get (5.4). ■

We now use this lemma to get our first result for a Delaunay deformation of a Delaunay graph.

Lemma 5.7. *Let G_0 be a Delaunay graph, and let F be a displacement function $F: V(G_0) \rightarrow \mathbb{C}$ with finite support $\Omega_F \subset V(G_0)$, as above. To each edge $\mathbf{e} \in E(G_0)$ of G_0 , we associate its conformal angle $\theta(\mathbf{e})$ defined by (2.1). Define ϑ_F as*

$$\vartheta_F = \min\{\theta(\mathbf{e}) : \mathbf{e} = \overline{uv} \in E(G_0) \text{ such that } u \text{ or } v \in \Omega_F\} \tag{5.6}$$

and M_F as defined by (5.2) in Lemma 5.1. Let G_ϵ be the Delaunay deformation of G_0 as introduced in Definition 5.2. Then the following bound ensures that the edges of G_0 remain edges of G_ϵ , namely,

$$\epsilon < \bar{\epsilon}_F = \sin(2\vartheta_F) \frac{b}{M_F} \Rightarrow E(G_0) \subset E(G_\epsilon).$$

Proof. The proof uses Lemma 5.6 and the Lawson flip algorithm.

Given our initial Delaunay graph G_0 , let us consider a *triangular completion* T_0 of G_0 , as introduced in Definition 2.8. In other words,

$$T_0 \text{ is a triangulation, and } E(G_0) \subset E(T_0).$$

Any completion T_0 is a weak Delaunay graph (see Definition 2.6), and the edges of T_0 which are not edges of G_0 are chords; consequently,

$$\mathbf{e} \notin E(G_0) \Leftrightarrow \theta_0(\mathbf{e}) = 0, \quad \mathbf{e} \in E(G_0) \Leftrightarrow \theta_0(\mathbf{e}) > 0$$

for any edge $\mathbf{e} \in E(T_0)$.

In general, G_0 may have multiple (possibly infinitely many) triangular completions. Let $\mathcal{T}(G_0)$ denote the set of triangular completions of G_0 , and let us extend the bounds M'_F and ϵ''_F of Lemma 5.4 (valid for triangulations) to Delaunay graphs,

$$M'_F = \max_{T_0 \in \mathcal{T}(G_0)} \max_{f \in F(T_0)} \max\{|\nabla F(f)|, |\bar{\nabla} F(f)|\},$$

and then as in Lemma 5.4,

$$\epsilon''_F = \frac{1}{2M'_F}.$$

Now we start the proof. We choose an arbitrary triangular completion T_0 of G_0 and consider the rigid deformation $T_{:\epsilon}$ of T_0 for $\epsilon > 0$ bounded by

$$\epsilon < \sin(2\vartheta_F) \frac{b}{M_F} \quad \text{and} \quad \epsilon < \epsilon''_F. \tag{5.7}$$

For any edge e of T_0 , notice that

$$\epsilon < \sin(2\vartheta_F) \frac{b}{M_F} \Leftrightarrow \epsilon < \frac{b}{M_F(e)},$$

and by Lemma 5.6, we have

$$\theta_\epsilon(e) > \theta_0(e) - \frac{1}{2} \arcsin\left(\frac{\epsilon M_F(e)}{b}\right).$$

If the edge e of $T_{:\epsilon}$ is also an edge of G_0 , then $\theta_0(e) \geq \vartheta_F$. Clearly, $M_F(e) \leq M_F$ and therefore

$$\theta_\epsilon(e) > \vartheta_F - \frac{1}{2} \arcsin\left(\frac{\epsilon M_F}{b}\right) > 0. \tag{5.8}$$

So the initial edges of G_0 still satisfy the Delaunay condition in $T_{:\epsilon}$.

Now we consider whether or not the deformed triangulation $T_{:\epsilon}$ is weakly Delaunay, i.e., whether

$$\theta_\epsilon(e) \geq 0 \quad \text{for all } e \in E(T_{:\epsilon}).$$

If $T_{:\epsilon}$ is weakly Delaunay, it is sufficient to remove all its chords, namely, all edges such that $\theta_\epsilon(e) = 0$. We obtain the redacted graph $T_{:\epsilon}^\bullet$ (see Definition 2.5) which is a Delaunay graph with the same vertex set as G_0 and with embedding $v \rightarrow z_\epsilon(v) = z_0(v) + \epsilon F(v)$. Hence it is the Delaunay deformation G_ϵ of G_0 , and it contains the original edges of G_0 in light of (5.8). In short,

$$G_0 \rightarrow T_0 \rightarrow T_{:\epsilon} \rightarrow T_{:\epsilon}^\bullet = G_\epsilon.$$

If $T_{:\epsilon}$ is not weakly Delaunay, there must exist edges e of $T_{:\epsilon}$ such that

$$\theta_\epsilon(e) < 0.$$

In this case, we recursively apply the Lawson flip algorithm to construct from $T_{:\epsilon}$ a weak Delaunay triangulation $T_{:\epsilon}^D$ which still completes G_0 (see [20] and standard textbooks such as [8, 14]). Let us describe the first iterative step.

- (1) Choose an edge e of $T_{:\epsilon}$ such that $\theta_\epsilon(e) < 0$, and consider the quadrilateral (u, s, v, n) made of its north and south faces.
- (2) Flip the edge e , i.e., perform the replacement

$$e = \overline{uv} \rightarrow e' = \overline{ns},$$

so that one obtains a new triangulation $T'_{:\epsilon}$.

Some conformal angles in $T'_{:\epsilon}$ have changed. Specifically,

$$\theta'_\epsilon(e') = -\theta_\epsilon(e) > 0,$$

and the conformal angles θ'_ϵ of the edges \overline{us} , \overline{vn} , \overline{vs} , and \overline{vn} as measured in $T'_{:\epsilon}$ may differ from their corresponding measures θ_ϵ in $T_{:\epsilon}$. The new triangulation $T'_{:\epsilon}$ is the rigid deformation of *another triangular completion* T'_0 of G_0 , namely, the triangulation with edge set

$$E(T'_0) = E(T_0) \setminus \{e\} \cup \{e'\}.$$

Therefore, $E(G_0) \subset E(T'_{:\epsilon})$ and inequality (5.8) is still valid for the edges of G_0 , i.e.,

$$e \in E(G_0) \Rightarrow \theta'_\epsilon(e) > 0.$$

The Lawson flip algorithm entails iterating of this process: Choose an edge e in $T'_{:\epsilon}$ such that $\theta'_\epsilon(e) < 0$ and perform the edge flip $e \rightarrow e''$ to obtain a new triangulation $T''_{:\epsilon}$ with $\theta''_\epsilon(e'') > 0$. Repeat. This process is known to stop after a finite number of iterations, and the final triangulation $T_{:\epsilon}^D$ will have no edge e with $\theta_{:\epsilon}^D(e) < 0$, and so it will be weakly Delaunay. Clearly, $T_{:\epsilon}^D$ is the rigid deformation of a triangular completion T_0^D of G_0 . Now take the redaction $T_{:\epsilon}^{D\bullet}$ by removing any chords. Schematically,

$$G_0 \rightarrow T_{:\epsilon} \rightarrow T'_{:\epsilon} \rightarrow \dots \rightarrow T_{:\epsilon}^D \rightarrow T_{:\epsilon}^{D\bullet} = G_\epsilon.$$

The redacted graph $T_{:\epsilon}^{D\bullet}$ is a Delaunay deformation of G_0 which coincides with G_ϵ and, to be sure,

$$E(G_0) \subset E(G_\epsilon)$$

as long as the initial bounds (5.7) on ϵ are satisfied. ■

Lemma 5.7 says nothing about the additional edges which can appear and flip within the initial faces of G_0 during the deformation. The following proposition establishes that these additional edges are themselves stable, i.e., undergo no flips, for values of the deformation parameter $\epsilon > 0$ which are sufficiently small.

Proposition 5.8. *Let G_0 be a Delaunay graph and F a displacement function as above. There exists a deformation threshold $\tilde{\epsilon}_F > 0$ such that for any $0 < \epsilon < \tilde{\epsilon}_F$ the deformation G_ϵ is stable (see Definition 5.5). As a consequence, the limit of the Delaunay graph G_ϵ when $\epsilon \rightarrow 0^+$ is unambiguously defined and denoted by*

$$G_{0^+} = \lim_{\epsilon \rightarrow 0^+} G_\epsilon. \tag{5.9}$$

The graph G_{0^+} is a weak-Delaunay graph sharing the same vertex set and embedding as G_0 . Its redacted graph (see Definition 2.5) is the initial Delaunay graph, i.e., $G_{0^+}^\bullet = G_0$.

Proof. Let us consider T_0 be a triangular completion of G_0 (an element of $\mathcal{T}(G_0)$) and an edge $e = \overline{uv}$ of T_0 which is not an edge of G_0 (i.e., a chord such that its conformal angle is $\theta_0(e) = 0$). Now, as in the proof of Lemma 5.7, consider the rigid deformation $T_{;\epsilon}$ of T_0 . The deformed conformal angle of e is given by

$$\begin{aligned} \theta_{;\epsilon}(e) &= \frac{1}{2} \arg(-[z_\epsilon(u), z_\epsilon(v); z_\epsilon(n), z_\epsilon(s)]) \\ &= \frac{1}{2} \arg\left[\frac{(1 + \epsilon dF(u, n)) \cdot (1 + \epsilon dF(v, s))}{(1 + \epsilon dF(u, s)) \cdot (1 + \epsilon dF(v, n))}\right] \end{aligned}$$

with n and s the north and south vertices for the north and south faces f_n and f_s of the edge e in $T_{;\epsilon}$ (remember that for $\epsilon = 0$ this is zero).

Here $\theta_{;\epsilon}$ is a regular function of ϵ (for ϵ small enough). We are interested in the values of ϵ for which $\theta_{;\epsilon}(e)$ vanishes. Clearly, this occurs if (ϵ is taken real)

$$\frac{(1 + \epsilon dF(u, n))(1 + \epsilon dF(v, s))}{(1 + \epsilon dF(u, s))(1 + \epsilon dF(v, n))} \frac{(1 + \epsilon \overline{dF}(u, s))(1 + \epsilon \overline{dF}(v, n))}{(1 + \epsilon \overline{dF}(u, n))(1 + \epsilon \overline{dF}(v, s))} = 1.$$

This amounts to solving a quartic real polynomial equation in ϵ of the form

$$\mathfrak{P}_4(\epsilon) = 0,$$

where \mathfrak{P}_4 is a degree 4 real polynomial,

$$\begin{aligned} \mathfrak{P}_4(\epsilon) &= (1 + \epsilon dF(u, n))(1 + \epsilon dF(v, s))(1 + \epsilon \overline{dF}(u, s))(1 + \epsilon \overline{dF}(v, n)) \\ &\quad - (1 + \epsilon dF(u, s))(1 + \epsilon dF(v, n))(1 + \epsilon \overline{dF}(u, n))(1 + \epsilon \overline{dF}(v, s)). \end{aligned}$$

The polynomial \mathfrak{P}_4 has at least one zero (with multiplicity) at $\epsilon = 0$, and at most three other zeros, unless it is identically zero. Let us define $\epsilon_c(e)$ by

$$\epsilon_c(e) = \begin{cases} +\infty & \text{if } \mathfrak{P}_4 \text{ is identically zero,} \\ \text{the smallest strictly positive root of } \mathfrak{P}_4 & \text{if it exists,} \\ +\infty & \text{if it does not exist.} \end{cases}$$

For the completion T_0 , define

$$\epsilon_c(T_0) = \min_{e \in E(T_0)} \epsilon_c(e).$$

It is strictly positive (possibly infinite) since F has finite support on $V(T_0) = V(G_0)$ and there are only finitely many chords e affected by the deformation. For the initial Delaunay graph G_0 , define

$$\epsilon_c(G_0) = \min_{T_0 \in \mathcal{T}(G_0)} \epsilon_c(T_0).$$

Again, F has finite support on $V(G_0)$ and since the $\epsilon_c(T_0)$'s can only take a finite number of distinct (strictly positive) values, it must be the case that $\epsilon_c(G_0)$ is strictly positive, $\epsilon_c(G_0) > 0$. Now define

$$\tilde{\epsilon}_F = \min\{\epsilon_c(G_0), \epsilon''_F, \bar{\epsilon}_F\}.$$

Take ϵ within the range

$$0 < \epsilon < \tilde{\epsilon}_F$$

and construct T_{ϵ}^D according to the proof of Lemma 5.7. It is weakly Delaunay, hence $\theta_{\epsilon}(e) \geq 0$ for each edge. By the argument above, the conformal angles cannot change sign in the interval $0 \leq \epsilon \leq \epsilon_c(G_0)$. Therefore, for any $\epsilon' \leq \epsilon$, each conformal angle must stay non-negative, and so $T_{\epsilon'}^D$ remains weakly Delaunay. This implies that its redacted graph is the Delaunay deformation $G_{\epsilon'}$ of G_0 and that $E(G_{\epsilon'}) = E(G_{\epsilon})$. In other words, G_{ϵ} is a stable deformation of G_0 .

The graph G_{0+} stipulated in (5.9) exists: it shares the same vertex set and embedding as G_0 , while its edge set coincides with $E(G_{\epsilon})$ for any $0 < \epsilon < \tilde{\epsilon}_F$ by stability. In particular, each edge e of G_0 is an edge of G_{0+} , while the remaining edges of G_{0+} are all chords. ■

Remark 5.9. The bound $\tilde{\epsilon}_F$ (which defines an interval $0 < \epsilon < \tilde{\epsilon}_F$ where no flips occur) may be much smaller than ϵ_F . In fact, even for a fixed initial Delaunay graph G_0 and a generic displacement function F , the threshold $\tilde{\epsilon}_F$ may be arbitrarily small with respect to ϵ_F . This point will become relevant when discussing the scaling limit and the problem of obtaining uniform bounds with respect to the choice of G_0 . We return to this issue in Section 8.

Remark 5.10. As discussed in the proof of Proposition 5.8, the edge sets $E(G_{\epsilon})$ and $E(G_{0+})$ coincide for $0 \leq \epsilon < \tilde{\epsilon}_F$. Consequently, any stable Delaunay deformation G_{ϵ} of G_0 is also a rigid deformation of the corresponding limit graph G_{0+} within the range $0 \leq \epsilon < \tilde{\epsilon}_F$. Accordingly, the notions of stable and rigid deformation agree for the limit graph G_{0+} provided that we work with sufficiently small values of the deformation parameter.

Remark 5.11. Since $E(G_\epsilon) = E(G_{0+})$ for $0 \leq \epsilon < \tilde{\epsilon}_F$, and since the faces of G_{0+} are cyclic polygons, the conformal angle $\theta_\epsilon(e)$ of any edge $e \in E(G_\epsilon)$ is unambiguously defined and strictly positive as ϵ varies in the interval $0 \leq \epsilon < \tilde{\epsilon}_F$.

5.3. Variation of operators under rigid deformations

We now study the variations of the operators $\Delta(\epsilon)$, $\mathcal{D}(\epsilon)$ and $\underline{\Delta}(\epsilon)$ and of the associated local geometrical quantities arising from *rigid* deformations (see Definition 5.3) of triangulations. It will not be necessary to assume that the triangulations are Delaunay at this stage.

Let T be an initial triangulation (possibly Delaunay) with vertex set $V(T)$, edge set $E(T)$ and face set (triangles) $F(T)$. Let $T_{;\epsilon}$ be the rigid deformation of T induced by the deformed embedding

$$z_\epsilon(v) = z(v) + \epsilon F(v),$$

where $F \in \mathbb{C}^{V(T)}$ is a displacement function and where $\epsilon \geq 0$ is bounded by the threshold ϵ''_F defined in Lemma 5.4. Recall that $T_{;\epsilon}$ and T share the same set of vertices, edges and faces. The deformed discrete differential operators are denoted by $\nabla_\epsilon, \bar{\nabla}_\epsilon: \mathbb{C}^{V(T)} \rightarrow \mathbb{C}^{F(T)}$, while the deformed area and radius operators are denoted by $A_\epsilon, R_\epsilon: \mathbb{C}^{F(T)} \rightarrow \mathbb{C}^{F(T)}$. They are obtained by making the substitution $z \mapsto z_\epsilon$ in formulas (3.6), (3.7), (3.2), and (3.3), respectively. This allows us to unambiguously define deformed versions $\Delta(\epsilon)$ and $\mathcal{D}(\epsilon)$ of the Laplace–Beltrami and discrete Kähler operators using factorizations (3.11) and (3.10), namely,

$$\Delta(\epsilon) = 2(\bar{\nabla}_\epsilon^\top A_\epsilon \nabla_\epsilon + \nabla_\epsilon^\top A_\epsilon \bar{\nabla}_\epsilon) \quad \text{and} \quad \mathcal{D}(\epsilon) = 4\bar{\nabla}_\epsilon^\top \frac{A_\epsilon}{R_\epsilon^2} \nabla_\epsilon. \tag{5.10}$$

We may expand all the relevant operators as (formal) series in ϵ (they are, in fact, meromorphic in ϵ). Up to first order in ϵ , the terms in these developments can be compactly expressed using the discrete derivatives ∇F and $\bar{\nabla} F$ with respect to the triangulation T .

Proposition 5.12. *The variation of the Laplace–Beltrami operator is*

$$\Delta(\epsilon) = \Delta - 4\epsilon(\nabla^\top(A\bar{\nabla}F)\nabla + \bar{\nabla}^\top(A\nabla\bar{F})\bar{\nabla}) + O(\epsilon^2). \tag{5.11}$$

Proposition 5.13. *The variation of the Kähler operator is*

$$\begin{aligned} \mathcal{D}(\epsilon) = \mathcal{D} - 4\epsilon \left[\bar{\nabla}^\top \frac{A}{R^2} (\nabla F + \bar{\nabla} \bar{F} + C \bar{\nabla} F + \bar{C} \nabla \bar{F}) \nabla \right. \\ \left. + \nabla^\top \frac{A}{R^2} (\bar{\nabla} F) \nabla + \bar{\nabla}^\top \frac{A}{R^2} (\nabla \bar{F}) \bar{\nabla} \right] + O(\epsilon^2) \end{aligned} \tag{5.12}$$

with the diagonal function $C \in \mathbb{C}^{F(T)}$ and its conjugate \bar{C} which are given for a triangle $\mathbf{f} = (u, v, w)$ by

$$C(\mathbf{f}) = \left(\frac{\bar{z}(u) - \bar{z}(v)}{z(u) - z(v)} + \frac{\bar{z}(v) - \bar{z}(w)}{z(v) - z(w)} + \frac{\bar{z}(w) - \bar{z}(u)}{z(w) - z(u)} \right), \quad \bar{C}(\mathbf{f}) = \overline{C(\mathbf{f})}. \tag{5.13}$$

Before deriving these two equations, let us note that the variation for Δ is rather simple, while the variation for \mathcal{D} is more complicated since we have not found a simple interpretation for the quantities C and \bar{C} in terms of the geometry of the triangle \mathbf{f} .

Proof. From (3.8), for a pair of vertices u and v of a triangle $\mathbf{f} = (u, v, w)$ in $F(T)$,

$$\begin{aligned} z_\epsilon(u) - z_\epsilon(v) &= z(u) - z(v) \\ &\quad + \epsilon((z(u) - z(v))\nabla F(\mathbf{f}) + (\bar{z}(u) - \bar{z}(v))\bar{\nabla} F(\mathbf{f})), \\ \bar{z}_\epsilon(u) - \bar{z}_\epsilon(v) &= \bar{z}(u) - \bar{z}(v) \\ &\quad + \epsilon((z(u) - z(v))\nabla \bar{F}(\mathbf{f}) + (\bar{z}(u) - \bar{z}(v))\bar{\nabla} \bar{F}(\mathbf{f})). \end{aligned} \tag{5.14}$$

Inserting this into (3.2) gives the variation of the area of the triangle \mathbf{f}

$$A_\epsilon(\mathbf{f}) = A(\mathbf{f}) + \epsilon A(\mathbf{f})(\nabla F(\mathbf{f}) + \bar{\nabla} \bar{F}(\mathbf{f})), +O(\epsilon^2),$$

which we can succinctly express as

$$A_\epsilon = A + \epsilon A(\nabla F + \bar{\nabla} \bar{F}) + O(\epsilon^2), \tag{5.15}$$

where we view A , ∇F , and $\bar{\nabla} \bar{F}$ as functions in $\mathbb{C}^{F(T)}$ or, alternatively, as diagonal operators mapping $\mathbb{C}^{F(T)} \rightarrow \mathbb{C}^{F(T)}$.

Using (3.3), we can write the variation of the circumradius $R(\mathbf{f})$ of the face \mathbf{f} . We write only the leading term of order $O(\epsilon)$ with the same compact notation and with C , and \bar{C} defined by (5.13)

$$\frac{A_\epsilon}{R_\epsilon^2} = \frac{A}{R^2} - \epsilon \frac{A}{R^2} (C \bar{\nabla} F + \bar{C} \nabla \bar{F}) + O(\epsilon^2). \tag{5.16}$$

Similarly, we get the variation of the matrix elements of the operator ∇ . At first order,

$$[\nabla_\epsilon]_{\mathbf{f},v} = \nabla_{\mathbf{f},v} - \epsilon(\nabla F(\mathbf{f})\nabla_{\mathbf{f},v} + \nabla \bar{F}(\mathbf{f})\bar{\nabla}_{\mathbf{f},v}) + O(\epsilon^2). \tag{5.17}$$

When read as operators, formula (5.17) for ∇_ϵ and its complex conjugate become

$$\begin{aligned} \nabla_\epsilon &= \nabla - \epsilon(\nabla F \nabla + \nabla \bar{F} \bar{\nabla}) + O(\epsilon^2), \\ \bar{\nabla}_\epsilon &= \bar{\nabla} - \epsilon(\bar{\nabla} \bar{F} \bar{\nabla} + \bar{\nabla} F \nabla) + O(\epsilon^2). \end{aligned} \tag{5.18}$$

Combining this with (5.10) and the Leibnitz product rule, we get (5.11) and (5.12). ■

Remark 5.14. Note that the exact formulas (to all orders in ϵ) for these variations (5.15)–(5.18) are derived in Section 8 (see, in particular, equations (8.5) in Section 8.3).

Remark 5.15. There is no such a compact expression for the variation of the conformal Laplacian $\underline{\Delta}$ in the general case. In particular, the variation of the weight associated to an edge $e = \overline{uv}$ will depend on the discrete derivatives of F both at the north triangle f_n and the south triangle f_s of the oriented edge $\vec{e} = (u, v)$, which are a priori independent (see Figure 1).

We can, of course, make the substitution $z \mapsto z_\epsilon$ into formula (3.4) for the north and south angles (which express the angles as a difference of arguments of edge vectors)

$$\begin{aligned} \theta_n(\vec{e}, \epsilon) &:= \frac{1}{2i} \log \left(-\frac{(\bar{z}_\epsilon(v) - \bar{z}_\epsilon(n))(z_\epsilon(u) - z_\epsilon(n))}{(z_\epsilon(v) - z_\epsilon(n))(\bar{z}_\epsilon(u) - \bar{z}_\epsilon(n))} \right), \\ \theta_s(\vec{e}, \epsilon) &:= \frac{1}{2i} \log \left(-\frac{(\bar{z}_\epsilon(u) - \bar{z}_\epsilon(s))(z_\epsilon(v) - z_\epsilon(s))}{(z_\epsilon(u) - z_\epsilon(s))(\bar{z}_\epsilon(v) - \bar{z}_\epsilon(s))} \right), \end{aligned}$$

where $n \in f_n$ and $s \in f_s$ are the respective north and south vertices of the adjacent triangles f_n and f_s to the edge $\vec{e} = (u, v)$ as depicted in Figure 1. The order zero and order one terms in the formal ϵ series expansion read from (5.14)

$$\begin{aligned} \theta_n(\vec{e}, \epsilon) &= \theta_n(\vec{e}) + \epsilon \frac{i}{2} (\bar{\nabla} F(f_n) \mathcal{E}_n(\vec{e}) - \nabla \bar{F}(f_n) \bar{\mathcal{E}}_n(\vec{e})) + O(\epsilon^2), \\ \theta_s(\vec{e}, \epsilon) &= \theta_s(\vec{e}) + \epsilon \frac{i}{2} (\bar{\nabla} F(f_s) \mathcal{E}_s(\vec{e}) - \nabla \bar{F}(f_s) \bar{\mathcal{E}}_s(\vec{e})) + O(\epsilon^2) \end{aligned} \tag{5.19}$$

with complex coefficients $\mathcal{E}_n(\vec{e})$ and $\mathcal{E}_s(\vec{e})$ given by

$$\begin{aligned} \mathcal{E}_n(\vec{e}) &:= \frac{\bar{z}(v) - \bar{z}(n)}{z(v) - z(n)} - \frac{\bar{z}(u) - \bar{z}(n)}{z(u) - z(n)} = \frac{-4A(f_n)}{(z(v) - z(n))(z(u) - z(n))}, \\ \mathcal{E}_s(\vec{e}) &:= \frac{\bar{z}(u) - \bar{z}(s)}{z(u) - z(s)} - \frac{\bar{z}(v) - \bar{z}(s)}{z(v) - z(s)} = \frac{-4A(f_s)}{(z(v) - z(s))(z(u) - z(s))}. \end{aligned} \tag{5.20}$$

The corresponding first-order variation of the edge weight $\tan \theta(e)$ with $\theta(e) = \frac{1}{2}(\theta_n(\vec{e}) + \theta_s(\vec{e}))$ can be written explicitly in terms of the discrete derivatives $\bar{\nabla} F(f_n)$ and $\bar{\nabla} F(f_s)$, the coefficients $\mathcal{E}_n(\vec{e})$ and $\mathcal{E}_s(\vec{e})$, and their complex conjugates. We shall not write the formula here, since it lacks the simplicity and geometrical interpretation of our results for Δ and \mathcal{D} .

5.4. Generic notation for derivatives under graph deformations

We shall use the following compact notation for derivatives and variations of general objects Obj associated to a rigid deformation $G \rightarrow G_\epsilon$ of a polygonal (Delaunay)

graph induced by a deformed coordinate embedding $z \rightarrow z_\epsilon = z + \epsilon F$ as set up in Definition 5.3. The object Obj can be a local quantity such as the angle θ , θ_n , θ_s associated to oriented edge \vec{e} of G or the area A and circumradius R of a face f . Other objects include the operators Δ , $\underline{\Delta}$ and \mathcal{D} .

If the object Obj is defined on the unperturbed graph G , the corresponding object on the deformed graph G_ϵ is denoted by $\text{Obj}(\epsilon)$ or sometimes Obj_ϵ (for clarity or brevity). This is consistent with the notations of Section 5.3. The variation of Obj for finite ϵ is denoted by

$$\delta \text{Obj}(\epsilon) = \text{Obj}(\epsilon) - \text{Obj}.$$

The initial derivatives with respect to ϵ are denoted by

$$\frac{\partial}{\partial \epsilon} \text{Obj}(\epsilon) = \mathfrak{d}_\epsilon \text{Obj}(\epsilon), \quad \frac{\partial^2}{\partial \epsilon^2} \text{Obj}(\epsilon) = \mathfrak{d}_{\epsilon\epsilon} \text{Obj}(\epsilon), \quad \text{etc.},$$

while their evaluations at zero are denoted by

$$\left. \frac{\partial}{\partial \epsilon} \text{Obj}(\epsilon) \right|_{\epsilon=0} = \mathfrak{d}_\epsilon \text{Obj}, \quad \left. \frac{\partial^2}{\partial \epsilon^2} \text{Obj}(\epsilon) \right|_{\epsilon=0} = \mathfrak{d}_{\epsilon\epsilon} \text{Obj}, \quad \text{etc.}$$

Accordingly, the Taylor expansion of Obj reads

$$\text{Obj}(\epsilon) = \text{Obj} + \epsilon \mathfrak{d}_\epsilon \text{Obj} + \frac{1}{2} \epsilon^2 \mathfrak{d}_{\epsilon\epsilon} \text{Obj} + O(\epsilon^3).$$

The terms of order ϵ obtained in the previous Section 5.3 give the explicit formula of the first derivatives \mathfrak{d}_ϵ for the objects considered there. We do not rewrite them explicitly.

6. Variations of log-determinants

6.1. First-order variations of determinants

6.1.1. The setup. Here we compute the first-order term in the ϵ -expansion of the (formally infinite) logarithm of the determinant of $\mathcal{O}(\epsilon)$, which, in general, has the form

$$\delta \log \det \mathcal{O}(\epsilon) = \text{tr}[\delta \mathcal{O}(\epsilon) \cdot \mathcal{O}_{\text{cr}}^{-1}].$$

Each trace is expressed as a sum of local terms over the weak Delaunay graph G_{0+} arising from the critical graph G_{cr} and the displacement function F . For both the Laplace–Beltrami and Kähler operators, there is a local term associated to each edge of G_{0+} ; there is an additional local term attached to each face of G_{0+} for the Kähler operator. In the case of the conformal Laplacian, the local terms associated to chords of G_{0+} differ from local terms of the regular edges of G_{0+} . For this reason, formula (6.4) is expressed as two sums: one over the regular edges $e \in E(G_{0+}^\bullet) = E(G_{\text{cr}})$ and another over the set of chords $e \in C(G_{0+}) = E(G_{0+}) \setminus E(G_{\text{cr}})$.

6.1.2. The results for first-order variations. We first give the results; their derivations are given in the following sections.

Proposition 6.1 (Laplace–Beltrami). *For the Laplace–Beltrami operator $\Delta(\epsilon)$, the first-order variation of $\log \det \Delta(\epsilon)$ with respect to deformation (5.1) can be expressed simply in terms of the variations of the north and south angles $\theta_n(\vec{e}, \epsilon)$ and $\theta_s(\vec{e}, \epsilon)$ of edges $e \in E(G_{0+})$,*

$$\text{tr}[\delta\Delta(\epsilon) \cdot \Delta_{\text{cr}}^{-1}] = \frac{\epsilon}{\pi} \sum_{\substack{\text{edges} \\ e \in G_{0+}}} \mathfrak{d}_\epsilon \theta_n(\vec{e}) \mathcal{L}'(\theta_n(\vec{e})) + \mathfrak{d}_\epsilon \theta_s(\vec{e}) \mathcal{L}'(\theta_s(\vec{e})) + O(\epsilon^2). \tag{6.1}$$

The function \mathcal{L}' , given by (3.21), is the derivative of the function \mathcal{L} given by (3.19); $\theta_n(\vec{e}, \epsilon)$ and $\theta_s(\vec{e}, \epsilon)$ are given by (5.19).

Remark 6.2. Owing to the extended form (3.20) of Kenyon’s result for $\log \det \Delta_{\text{cr}}$, it is interesting to note that, up to terms of order ϵ^2 , $\log \det \Delta(\epsilon)$ can still be written as a sum of local terms involving the local geometry of the deformed Delaunay graph G_ϵ , similar to Kenyon’s result, although the graph is not isoradial,

$$\log \det \Delta(\epsilon) = \frac{1}{\pi} \sum_{\substack{\text{edges} \\ e \in G_{0+}}} \mathcal{L}(\theta_n(e, \epsilon)) + \mathcal{L}(\theta_s(\vec{e}, \epsilon)) + O(\epsilon^2). \tag{6.2}$$

Remark 6.3. Equivalently, formula (6.1) can be written as a sum over triangles f of any triangular completion \hat{G}_{0+} of G_{0+} , namely

$$\text{tr}[\delta\Delta(\epsilon) \cdot \Delta_{\text{cr}}^{-1}] = -4\epsilon \sum_{\substack{\text{faces} \\ f \in \hat{G}_{0+}}} A(f)(\bar{\nabla} F(f) Q(f) + c.c.) + O(\epsilon^2), \tag{6.3}$$

where $Q(f) = [\nabla \Delta_{\text{cr}}^{-1} \nabla^\top]_{ff}$ is a diagonal matrix entry. This is a direct consequence of the variational formula in Proposition 5.12. Note that the value of (6.3) is independent of the choice of triangular completion.

Proposition 6.4 (Conformal Laplacian). *For the conformal Laplacian $\underline{\Delta}(\epsilon)$, the first-order variation of $\log \det \underline{\Delta}(\epsilon)$ with respect to deformation (5.1) can also be expressed simply in terms of the variations of the north and south angles $\theta_n(\vec{e}, \epsilon)$ and $\theta_s(\vec{e}, \epsilon)$ of edges $e \in E(G_{0+})$. However, we must distinguish between the contributions made by regular edges versus chords in G_{0+} . Keep in mind that the set of regular edges $E(G_{0+}^\bullet)$ coincides with the edge set $E(G_{\text{cr}})$ of the critical graph,*

$$\begin{aligned} \text{tr}[\delta\underline{\Delta}(\epsilon) \cdot \Delta_{\text{cr}}^{-1}] &= \frac{2\epsilon}{\pi} \sum_{\substack{\text{edges} \\ e \in G_{\text{cr}}}} \mathfrak{d}_\epsilon \theta(e) \mathcal{L}'(\theta(e)) + \frac{\epsilon}{\pi} \sum_{\substack{\text{chords} \\ e \in G_{0+}}} \mathfrak{d}_\epsilon \theta_n(\vec{e}) \mathcal{H}'(\theta_n(\vec{e})) \\ &+ \mathfrak{d}_\epsilon \theta_s(\vec{e}) \mathcal{H}'(\theta_s(\vec{e})) + O(\epsilon^2), \end{aligned} \tag{6.4}$$

where $\mathcal{H}'(\theta) = \theta \cot \theta$ is the derivative of the function

$$\mathcal{H}(\theta) = 2\theta \log(2 \sin \theta) + L(\theta),$$

where $L(\theta)$ is the Lobachevsky function defined in (3.17). Remember that $\theta(\mathbf{e}) = \frac{1}{2}(\theta_n(\vec{\mathbf{e}}) + \theta_s(\vec{\mathbf{e}}))$ is the conformal edge angle for general triangulations.

Remark 6.5. Up to order ϵ^2 , $\log \det \underline{\Delta}(\epsilon)$ can still be written as a sum of terms reflecting the local geometry of the weak Delaunay graph \mathcal{G}_{0+} (see Section 5.1),

$$\begin{aligned} \log \det \underline{\Delta}(\epsilon) &= \frac{2}{\pi} \sum_{\substack{\text{edges} \\ \mathbf{e} \in \mathcal{G}_{\text{cr}}}} \mathcal{L}(\theta(\mathbf{e}, \epsilon)) \\ &+ \frac{1}{\pi} \sum_{\substack{\text{chords} \\ \mathbf{e} \in \mathcal{G}_{0+}}} \mathcal{H}(\theta_n(\mathbf{e}, \epsilon)) + \mathcal{H}(\theta_s(\vec{\mathbf{e}}, \epsilon)) + O(\epsilon^2). \end{aligned} \tag{6.5}$$

Proposition 6.6 (Kähler operator). *For the Kähler operator $\mathcal{D}(\epsilon)$, a local formula also holds at order ϵ . It involves the variations of the angles $\theta_n(\vec{\mathbf{e}}, \epsilon)$ and $\theta_s(\vec{\mathbf{e}}, \epsilon)$ for edges $\mathbf{e} \in E(\mathcal{G}_{0+})$, but also the variations of the circumradii $R(\mathbf{f}, \epsilon)$ for faces $\mathbf{f} \in F(\mathcal{G}_{0+})$. We note that*

$$\begin{aligned} R(\mathbf{f}, \epsilon) &= R_{\text{cr}} + \delta R(\mathbf{f}, \epsilon) = R_{\text{cr}} + \epsilon \delta_\epsilon R(\mathbf{f}) + O(\epsilon^2), \\ \text{tr}[\delta \mathcal{D}(\epsilon) \cdot \mathcal{D}_{\text{cr}}^{-1}] &= \frac{\epsilon}{\pi} \sum_{\substack{\text{edges} \\ \mathbf{e} \in \mathcal{G}_{0+}}} \delta_\epsilon \theta_n(\vec{\mathbf{e}}) \mathcal{L}'(\theta_n(\vec{\mathbf{e}})) + \delta_\epsilon \theta_s(\mathbf{e}) \mathcal{L}'(\theta_s(\vec{\mathbf{e}})) \\ &- \epsilon \sum_{\substack{\text{faces} \\ \mathbf{f} \in \mathcal{G}_{0+}}} \frac{\delta_\epsilon R(\mathbf{f})}{R_{\text{cr}}} + O(\epsilon^2). \end{aligned} \tag{6.6}$$

Remark 6.7. Up to order ϵ^2 , $\log \det \mathcal{D}(\epsilon)$ can still be written as a sum of terms reflecting the local geometry of \mathcal{G}_{0+} ,

$$\begin{aligned} \log \det \mathcal{D}(\epsilon) &= \frac{1}{\pi} \sum_{\substack{\text{edges} \\ \mathbf{e} \in \mathcal{G}_{0+}}} \mathcal{L}(\theta_n(\mathbf{e}, \epsilon)) + \mathcal{L}(\theta_s(\mathbf{e}, \epsilon)) \\ &- \sum_{\substack{\text{faces} \\ \mathbf{f} \in \mathcal{G}_{0+}}} \log R(\mathbf{f}, \epsilon) + O(\epsilon^2). \end{aligned} \tag{6.7}$$

Again, we obtain a nice local expression involving the angles $\theta_n(\vec{\mathbf{e}})$ and $\theta_s(\vec{\mathbf{e}})$ and the circumradii $R(\mathbf{f})$. Like the conformal Laplacian, the global conformal invariance properties of the Kähler operator are not evident in the result. However, concyclic configurations and chords do not play any special role.

6.1.3. Proof of Proposition 6.1. We first consider the variation of the Laplace–Beltrami operator Δ under a deformation of form (5.1). One can use (5.11) to compute explicitly the first-order variation of $\log \det \Delta$, but it is simpler to start from its definition in terms of angles (1.6). For an edge $e = \overline{uv}$ of G_ϵ ,

$$[\Delta(\epsilon)]_{uv} = -c(e, \epsilon) = -\frac{\tan \theta_n(\vec{e}, \epsilon) + \tan \theta_s(\vec{e}, \epsilon)}{2}.$$

This implies that the variation is

$$[\delta\Delta(\epsilon)]_{uv} = -\frac{\epsilon}{2}(\delta_\epsilon \theta_n(\vec{e}) \sec^2 \theta_n(\vec{e}) + \delta_\epsilon \theta_s(\vec{e}) \sec^2 \theta_s(\vec{e})) + O(\epsilon^2),$$

where $\delta_\epsilon \theta_n(\vec{e})$ and $\delta_\epsilon \theta_s(\vec{e})$ are of order $O(1)$. The limit graph G_{0+} is weakly Delaunay and isoradial, so either $\theta_n(\vec{e}) = \theta_s(\vec{e})$ or $\theta_n(\vec{e}) = -\theta_s(\vec{e})$. In both cases, $\sec^2 \theta_n(\vec{e}) = \sec^2 \theta_s(\vec{e})$, so that at first order,

$$\begin{aligned} [\delta\Delta(\epsilon)]_{uv} &= -\epsilon \frac{\delta_\epsilon \theta_n(\vec{e}) + \delta_\epsilon \theta_s(\vec{e})}{2} \sec^2 \theta_n(\vec{e}) + O(\epsilon^2) \\ &= -\epsilon \frac{\delta_\epsilon \theta_n(\vec{e}) + \delta_\epsilon \theta_s(\vec{e})}{2} \sec^2 \theta_s(\vec{e}) + O(\epsilon^2). \end{aligned}$$

It remains to combine this with the propagator $[\Delta_{cr}^{-1}]_{vu}$ which for regular edges $e = \overline{uv}$ of $G_{0+}^\bullet = G_{cr}$ is

$$[\Delta_{cr}^{-1}]_{vu} = -\frac{1}{\pi} \theta(e) \cot \theta(e). \tag{6.8}$$

A similar relation is, in fact, valid for chords of G_{0+} ,

$$[\Delta_{cr}^{-1}]_{vu} = -\frac{1}{\pi} \theta_n(\vec{e}) \cot \theta_n(\vec{e}) = -\frac{1}{\pi} \theta_s(\vec{e}) \cot \theta_s(\vec{e}).$$

Thus the first-order variation is

$$\begin{aligned} \text{tr}[\delta_\epsilon \Delta \cdot \Delta_{cr}^{-1}] &= \sum_{\substack{\text{vertices} \\ u, v \in G_{0+}}} \delta_\epsilon \Delta_{uv} [\Delta_{cr}^{-1}]_{vu} = \frac{1}{\pi} \sum_{\substack{\text{edges} \\ e \in G_{0+}}} \delta_\epsilon \theta_n(\vec{e}) \theta_n(\vec{e}) \cot \theta_n(\vec{e}) \sec^2 \theta_n(\vec{e}) \\ &\quad + \delta \theta_s(\vec{e}) \theta_s(\vec{e}) \cot \theta_s(\vec{e}) \sec^2 \theta_s(\vec{e}) \\ &= \frac{1}{\pi} \sum_{\substack{\text{edges} \\ e \in G_{0+}}} \delta_\epsilon \theta_n(\vec{e}) \frac{\theta_n(\vec{e})}{\sin \theta_n(\vec{e}) \cos \theta_n(\vec{e})} + \delta_\epsilon \theta_s(\vec{e}) \frac{\theta_n(\vec{e})}{\sin \theta_s(\vec{e}) \cos \theta_s(\vec{e})} \\ &= \frac{1}{\pi} \sum_{\substack{\text{edges} \\ e \in G_{0+}}} \delta_\epsilon \theta_n(\vec{e}) \mathcal{L}'(\theta_n(\vec{e})) + \delta_\epsilon \theta_s(\vec{e}) \mathcal{L}'(\theta_n(\vec{e})) \\ &= \delta_\epsilon \left[\frac{1}{\pi} \sum_{\substack{\text{edges} \\ e \in G_{0+}}} \mathcal{L}(\theta_n(\vec{e}, \epsilon)) + \mathcal{L}(\theta_s(\vec{e}, \epsilon)) \right]. \end{aligned}$$

This, together with (3.20), leads to (6.2), and this ends the proof of Proposition 6.1.

6.1.4. Proof of Proposition 6.4. For an edge $e = \overline{uv}$ of G_ϵ , the matrix element of the conformal Laplacian $\underline{\Delta}$ is

$$[\underline{\Delta}(\epsilon)]_{uv} = -\tan \theta(e, \epsilon), \quad \theta(e, \epsilon) = \frac{\theta_n(\vec{e}, \epsilon) + \theta_s(\vec{e}, \epsilon)}{2}.$$

This implies that the variation is

$$[\delta \underline{\Delta}(\epsilon)]_{uv} = -\epsilon \frac{\delta_\epsilon \theta_n(\vec{e}) + \delta_\epsilon \theta_s(\vec{e})}{2} \sec^2 \left(\frac{\theta_n(\vec{e}) + \theta_s(\vec{e})}{2} \right) + O(\epsilon^2).$$

Keep in mind that the limit graph G_{0+} is weakly Delaunay and isoradial, and so either $\theta_n(\vec{e}) = \theta_s(\vec{e})$ or $\theta_n(\vec{e}) = -\theta_s(\vec{e})$. The first case corresponds to a regular edge, while the second case corresponds to a chord. Thus, at first order in ϵ , the matrix entry is

$$\begin{aligned} [\delta_\epsilon \underline{\Delta}]_{uv} &= \begin{cases} -\frac{\delta_\epsilon \theta_n(\vec{e}) \sec^2 \theta_n(\vec{e}) + \delta_\epsilon \theta_s(\vec{e}) \sec^2 \theta_s(\vec{e})}{2} & \text{if } \theta_n(\vec{e}) = \theta_s(\vec{e}), \\ -\frac{\delta_\epsilon \theta_n(\vec{e}) + \delta_\epsilon \theta_s(\vec{e})}{2} & \text{if } \theta_n(\vec{e}) = -\theta_s(\vec{e}) \end{cases} \\ &= \begin{cases} [\delta_\epsilon \Delta]_{uv} & \text{if } \theta_n(\vec{e}) = \theta_s(\vec{e}), \\ [\delta_\epsilon \Delta]_{uv} + \frac{\delta_\epsilon \theta_n(\vec{e}) \tan^2 \theta_n(\vec{e}) + \delta_\epsilon \theta_s(\vec{e}) \tan^2 \theta_s(\vec{e})}{2} & \text{if } \theta_n(\vec{e}) = -\theta_s(\vec{e}). \end{cases} \end{aligned} \tag{6.9}$$

The first-order variation of the log-determinant reads as a sum over the edges of G_{0+} , but it is different for the edges in $G_{0+}^\bullet = G_{cr}$ and the chords of G_{0+} . Combining with (6.8), we get at first order

$$\begin{aligned} \text{tr}[\delta_\epsilon \underline{\Delta} \cdot \Delta_{cr}^{-1}] &= \sum_{\substack{\text{vertices} \\ u,v \in G_{0+}}} [\delta_\epsilon \underline{\Delta}]_{uv} [\Delta_{cr}^{-1}]_{vu} = \frac{2}{\pi} \sum_{\substack{\text{edges} \\ e \in G_{cr}}} \delta_\epsilon \theta(e) \mathcal{L}'(\theta(e)) \\ &\quad + \frac{1}{\pi} \sum_{\substack{\text{chords} \\ e \in G_{0+}}} \delta_\epsilon \theta_n(\vec{e}) \mathcal{H}'(\theta_n(\vec{e})) + \delta_\epsilon \theta_s(\vec{e}) \mathcal{H}'(\theta_s(\vec{e})) \end{aligned}$$

with the function $\mathcal{H}(\theta)$ given by

$$\mathcal{H}(\theta) = \int_0^\theta dt t \cot(t) = 2\theta \log(2 \sin \theta) + L(\theta).$$

This leads to (6.5) and the proof of Proposition 6.4.

6.1.5. Proof of Proposition 6.6. The variation of the Kähler operator \mathcal{D} starts from the expression of the matrix elements $\mathcal{D}_{u,v}$ of an edge $\vec{e} = (u, v)$ in terms of the angles $\theta_n(\vec{e}, \epsilon)$ and $\theta_s(\vec{e}, \epsilon)$ and of the circumradii $R_n(\vec{e}, \epsilon)$ and $R_s(\vec{e}, \epsilon)$ given by (1.7), namely,

$$[\mathcal{D}(\epsilon)]_{uv} = -\frac{1}{2} \left(\frac{\tan \theta_n(\vec{e}, \epsilon) + i}{R_n^2(\vec{e}, \epsilon)} + \frac{\tan \theta_s(\vec{e}, \epsilon) - i}{R_s^2(\vec{e}, \epsilon)} \right).$$

Its variation is therefore

$$\begin{aligned}
 [\delta \mathcal{D}(\epsilon)]_{uv} &= \delta_\epsilon \mathcal{D}_{uv}^{(1)} + \delta_\epsilon \mathcal{D}_{uv}^{(2)} + O(\epsilon^2), \\
 \delta_\epsilon \mathcal{D}_{uv}^{(1)} &= -\left(\frac{1}{2R_n^2(\vec{e})} \delta_\epsilon \tan \theta_n(\vec{e}) + \frac{1}{2R_s^2(\vec{e})} \delta_\epsilon \tan \theta_s(\vec{e}) \right), \\
 \delta_\epsilon \mathcal{D}_{uv}^{(2)} &= \left(\frac{\tan \theta_n(\vec{e}) + i}{R_n^3(\vec{e})} \delta_\epsilon R_n(\vec{e}) + \frac{\tan \theta_s(\vec{e}) - i}{R_s^3(\vec{e})} \delta_\epsilon R_s(\vec{e}) \right). \tag{6.10}
 \end{aligned}$$

For an isoradial triangulation (the critical case),

$$R_n(\vec{e}) = R_s(\vec{e}) = R_{cr},$$

therefore one has $\mathcal{D}_{cr} = R_{cr}^{-2} \Delta_{cr}$. Thus in the critical case, the contribution made by the first term in (6.10) to the variation is

$$\delta_\epsilon \mathcal{D}_{uv}^{(1)} = R_{cr}^{-2} \delta_\epsilon \Delta_{uv} \Rightarrow \text{tr}[\delta_\epsilon \mathcal{D}^{(1)} \cdot \mathcal{D}_{cr}^{-1}] = \text{tr}[\delta_\epsilon \Delta \cdot \Delta_{cr}^{-1}].$$

The second term's contribution can be reorganized as a sum over faces of $\widehat{\mathcal{G}}_{0+}$, i.e., counter-clockwise oriented triangles $\mathbf{f} = (u, v, w)$

$$\begin{aligned}
 \text{tr}[\delta_\epsilon \mathcal{D}^{(2)} \cdot \mathcal{D}_{cr}^{-1}] &= \sum_{\substack{\text{vertices} \\ u, v \in \widehat{\mathcal{G}}_{0+}}} \delta_\epsilon \mathcal{D}_{uv}^{(2)} [\mathcal{D}_{cr}^{-1}]_{vu} = \sum_{\substack{\text{triangles} \\ \mathbf{f}=(u,v,w) \text{ in } \widehat{\mathcal{G}}_{0+}}} \frac{\delta_\epsilon R(\mathbf{f})}{R_{cr}^3} \\
 &\quad \times \left((\tan \theta_n(\vec{u}\vec{v}) + i) [\mathcal{D}_{cr}^{-1}]_{vu} + (\tan \theta_s(\vec{v}\vec{u}) - i) [\mathcal{D}_{cr}^{-1}]_{uv} \right. \\
 &\quad \quad + (\tan \theta_n(\vec{v}\vec{w}) + i) [\mathcal{D}_{cr}^{-1}]_{vw} + (\tan \theta_s(\vec{w}\vec{v}) - i) [\mathcal{D}_{cr}^{-1}]_{vw} \\
 &\quad \quad \left. + (\tan \theta_n(\vec{w}\vec{u}) + i) [\mathcal{D}_{cr}^{-1}]_{wu} + (\tan \theta_s(\vec{u}\vec{w}) - i) [\mathcal{D}_{cr}^{-1}]_{wu} \right).
 \end{aligned}$$

Using the fact that $\theta_n(\vec{u}\vec{v}) = \theta_s(\vec{v}\vec{u})$ and that for the critical case

$$[\mathcal{D}_{cr}^{-1}]_{vu} = [\mathcal{D}_{cr}^{-1}]_{uv} = -\frac{1}{\pi} R_{cr}^2 \theta_n(\vec{u}\vec{v}) \cot \theta_n(\vec{u}\vec{v})$$

and the fact that for a triangle $\mathbf{f} = (u, v, w)$, one has

$$\theta_n(\vec{u}\vec{v}) + \theta_n(\vec{v}\vec{w}) + \theta_n(\vec{w}\vec{u}) = \frac{\pi}{2},$$

we obtain

$$\text{tr}[\delta_\epsilon \mathcal{D}^{(2)} \cdot \mathcal{D}_{cr}^{-1}] = - \sum_{\substack{\text{faces} \\ \mathbf{f} \in \widehat{\mathcal{G}}_{0+}}} \frac{\delta_\epsilon R(\mathbf{f})}{R_{cr}} = - \sum_{\substack{\text{faces} \\ \mathbf{f} \in \widehat{\mathcal{G}}_{0+}}} \delta_\epsilon \log R(\mathbf{f}).$$

This leads to (6.7) and to Proposition 6.6.

6.2. Second-order variations

6.2.1. Principle of the calculation. In order to probe the second trace term in the perturbative expansion (1.14), we consider a *bi-local* deformation G_ϵ of the underlying critical graph G_{cr} with an embedding of the form

$$z_\epsilon(v) := z_{cr}(v) + \epsilon_1 F_1(v) + \epsilon_2 F_2(v),$$

where $\epsilon = (\epsilon_1, \epsilon_2)$ is a pair of independent deformation parameters and $F_1, F_2 \in \mathbb{C}^{V(G_{cr})}$ are two functions, with finite supports

$$\Omega_1 := \Omega_{F_1} \quad \text{and} \quad \Omega_2 := \Omega_{F_2}$$

in $V(G_{cr})$ and whose respective *lattice closures* $\bar{\Omega}_1$ and $\bar{\Omega}_2$ are disjoint; see (1.12). To ensure that G_ϵ is a stable Delaunay deformation, we restrict the parameters ϵ_1, ϵ_2 within the range $[0, \tilde{\epsilon}_F]$, where $\tilde{\epsilon}_F := \min(\tilde{\epsilon}_{F_1}, \tilde{\epsilon}_{F_2})$ and $\tilde{\epsilon}_{F_1}, \tilde{\epsilon}_{F_2}$ are the thresholds dictated by Proposition 5.8. Furthermore, we shall assume that the *distance* d between the two supports is large, i.e., $d \gg R_{cr}$, where

$$d = \text{dist}(\bar{\Omega}_1, \bar{\Omega}_2) := \inf\{|z_{cr}(w_1) - z_{cr}(w_2)| : w_1 \in \bar{\Omega}_1, w_2 \in \bar{\Omega}_2\}.$$

We want to isolate and then examine the long-range behavior of the $\epsilon_1 \epsilon_2$ cross-term occurring within the perturbative expansion of the log-determinant, namely, in

$$\log \det \mathcal{O}(\epsilon) = \log \det \mathcal{O}_{cr} + \text{tr}[\delta \mathcal{O}(\epsilon) \cdot \mathcal{O}_{cr}^{-1}] - \frac{1}{2} \text{tr}[(\delta \mathcal{O}(\epsilon) \cdot \mathcal{O}_{cr}^{-1})^2] + \dots$$

The first trace term $\text{tr}[\delta \mathcal{O}(\epsilon) \cdot \mathcal{O}_{cr}^{-1}]$ contributes nothing of order $\epsilon_1 \epsilon_2$ since the lattice closures of the supports $\bar{\Omega}_1$ and $\bar{\Omega}_2$ are disjoint. The only non-vanishing contribution comes from the second trace term

$$-\frac{1}{2} \text{tr}[(\delta \mathcal{O}(\epsilon) \cdot \mathcal{O}_{cr}^{-1})^2]$$

which is bilinear in the total variation $\delta \mathcal{O}(\epsilon)$. Accordingly, the coefficient of $\epsilon_1 \epsilon_2$ can be expressed as

$$-\text{tr}[\mathfrak{d}_{\epsilon_1} \mathcal{O} \cdot \mathcal{O}_{cr}^{-1} \cdot \mathfrak{d}_{\epsilon_2} \mathcal{O} \cdot \mathcal{O}_{cr}^{-1}] = - \sum_{\substack{u, v \in \bar{\Omega}_1 \\ p, q \in \bar{\Omega}_2}} [\mathfrak{d}_{\epsilon_1} \mathcal{O}]_{uv} [\mathcal{O}_{cr}^{-1}]_{vp} [\mathfrak{d}_{\epsilon_2} \mathcal{O}]_{pq} [\mathcal{O}_{cr}^{-1}]_{qu},$$

where $\mathfrak{d}_{\epsilon_1} \mathcal{O}$ and $\mathfrak{d}_{\epsilon_2} \mathcal{O}$ are first-order variations of the Laplace-like operator $\mathcal{O}(\epsilon)$ following the notations set in Section 5.4. The sum on the left-hand side is taken over vertices u, v, p, q such that both matrix entries $[\mathfrak{d}_{\epsilon_1} \mathcal{O}]_{uv}$ and $[\mathfrak{d}_{\epsilon_2} \mathcal{O}]_{pq}$ are non-zero. In particular, this implies that \bar{uv} is an edge in G_{0+} with vertices $u, v \in \bar{\Omega}_1$. Likewise, \bar{pq} must be an edge in G_{0+} with vertices $p, q \in \bar{\Omega}_2$.

Provided the two zones of support Ω_1 and Ω_2 are far enough apart, the matrix entries $[\mathcal{O}_{\text{cr}}^{-1}]_{\text{vp}}$ and $[\mathcal{O}_{\text{cr}}^{-1}]_{\text{qu}}$ of the critical Green’s function will only involve pairs of vertices with $|z_{\text{cr}}(\text{v}) - z_{\text{cr}}(\text{p})| \simeq d$ and $|z_{\text{cr}}(\text{q}) - z_{\text{cr}}(\text{u})| \simeq d$. Under these circumstances, we may estimate the contributions made by these matrix entries using the asymptotic expansion (1.10) for the Green’s function.

It will be convenient to take a triangular completion $\widehat{\mathbb{G}}_\epsilon$ of the deformed Delaunay graph \mathbb{G}_ϵ as defined in Definition 2.8. Likewise, $\widehat{\mathbb{G}}_{0+}$ will be the completion of the limit graph \mathbb{G}_{0+} induced from $\widehat{\mathbb{G}}_\epsilon$. This will allow us to use the variational formulas (5.12) and (5.13) for the Laplace–Beltrami and Kähler operators. In general, such a completion $\widehat{\mathbb{G}}_\epsilon$ will not be unique. Nevertheless, the redactions satisfy $\widehat{\mathbb{G}}_\epsilon^\bullet = \mathbb{G}_\epsilon$ and $\widehat{\mathbb{G}}_{0+}^\bullet = \mathbb{G}_{\text{cr}}$ regardless of the choice of completion. The Laplace–Beltrami operator, Kähler operator, and the conformal Laplacian will not be affected by this choice, since the weights assigned by the operators to any chords, introduced by the completion, must vanish.

6.2.2. The Laplace–Beltrami operator. The simplest case is the Laplace–Beltrami operator Δ . We shall need two intermediate results.

Lemma 6.8. *Let $\mathfrak{f} = (\text{v}_1, \text{v}_2, \text{v}_3)$ be a counter-clockwise oriented triangle with circumcenter $z_{\text{cr}}(\mathfrak{f})$ and circumradius $R = 1$. Define $e^{i\theta_j} := z_{\text{cr}}(\text{v}_j) - z_{\text{cr}}(\mathfrak{f})$ for $j = 1, 2, 3$. Let $\nabla_{\mathfrak{f}\text{v}_j}$ be the matrix elements of the discrete derivative operator ∇ restricted to the triangle \mathfrak{f} . For any integer $m \in \mathbb{Z}$, one has the uniform bounds*

$$\left| \sum_{j=1}^3 \nabla_{\mathfrak{f}\text{v}_j} e^{im\theta_j} \right| \leq \frac{m(m+1)}{2}, \quad m \in \mathbb{Z}, \tag{6.11}$$

and

$$\left| \sum_{j=1}^3 \bar{\nabla}_{\mathfrak{f}\text{v}_j} e^{im\theta_j} \right| \leq \frac{m(m-1)}{2}, \quad m \in \mathbb{Z}. \tag{6.12}$$

Proof. Using definition (3.6) of ∇ , one can rewrite

$$\sum_{j=1}^3 \nabla_{\mathfrak{f}\text{v}_j} e^{im\theta_j} = \det \begin{pmatrix} 1 & e^{-i\theta_1} & e^{im\theta_1} \\ 1 & e^{-i\theta_2} & e^{im\theta_2} \\ 1 & e^{-i\theta_3} & e^{im\theta_3} \end{pmatrix} / \det \begin{pmatrix} 1 & e^{-i\theta_1} & e^{i\theta_1} \\ 1 & e^{-i\theta_2} & e^{i\theta_2} \\ 1 & e^{-i\theta_3} & e^{i\theta_3} \end{pmatrix}. \tag{6.13}$$

For $m > 0$, we can rewrite the numerator as

$$e^{-i(\theta_1+\theta_2+\theta_3)} \det \begin{pmatrix} 1 & e^{i\theta_1} & e^{i(m+1)\theta_1} \\ 1 & e^{i\theta_2} & e^{i(m+1)\theta_2} \\ 1 & e^{i\theta_3} & e^{i(m+1)\theta_3} \end{pmatrix},$$

which involves a special case of the following Vandermonde-like determinant:

$$\det \begin{pmatrix} 1 & z_1 & z_1^{m+1} \\ 1 & z_2 & z_2^{m+1} \\ 1 & z_3 & z_3^{m+1} \end{pmatrix} = (z_1 - z_2)(z_2 - z_3)(z_3 - z_1)S_{m-1}(z_1, z_2, z_3),$$

where S_n is the complete homogeneous symmetric polynomial of degree n (a Schur polynomial),

$$S_n(z_1, z_2, z_3) = \sum_{\substack{p_1, p_2, p_3 \in \mathbb{N} \\ p_1 + p_2 + p_3 = n}} z_1^{p_1} z_2^{p_2} z_3^{p_3},$$

which consists of $\frac{(n+1)(n+2)}{2}$ monomials. The numerator equals the denominator in the right-hand side of (6.13) when $m = 1$, and since $S_0(z_1, z_2, z_3) = 1$, we get

$$\sum_{j=1}^3 \nabla_{\mathbf{f}v_j} e^{im\theta_j} = S_{m-1}(e^{i\theta_1}, e^{i\theta_2}, e^{i\theta_3})$$

when $m > 0$. It is clear that for $m > 0$, we have the bound

$$|S_{m-1}(e^{i\theta_1}, e^{i\theta_2}, e^{i\theta_3})| \leq \frac{(m-1+1)(m-1+2)}{2} = \frac{m(m+1)}{2},$$

which is saturated when $\theta_1 = \theta_2 = \theta_3$. For $m = 0$ or $m = -1$, it is clear that

$$\sum_{j=1}^3 \nabla_{\mathbf{f}v_j} e^{im\theta_j} = 0.$$

When $m \leq -2$, we can rewrite

$$\sum_{j=1}^3 \nabla_{\mathbf{f}v_j} e^{im\theta_j} = e^{-i\theta_1} e^{-i\theta_2} e^{-i\theta_3} S_{-m-2}(e^{-i\theta_1}, e^{-i\theta_2}, e^{-i\theta_3})$$

by a similar trick. Since $-m - 2 \geq 0$, we get the bound

$$\begin{aligned} |S_{-m-2}(e^{-i\theta_1}, e^{-i\theta_2}, e^{-i\theta_3})| &\leq \frac{(-m-2+1)(-m-2+2)}{2} \\ &= \frac{m(m+1)}{2}. \end{aligned}$$

Thus we get (6.11). To obtain (6.12), one uses simply

$$\sum_{j=1}^3 \bar{\nabla}_{\mathbf{f}v_j} e^{im\theta_j} = \overline{\sum_{j=1}^3 \nabla_{\mathbf{f}v_j} e^{-im\theta_j}}$$

and (6.11). ■

Now we can get uniform asymptotic estimates for the discrete derivatives of the Green’s function.

Lemma 6.9. *Let Δ_{cr}^{-1} be the critical Green’s function on an isoradial weak Delaunay triangulation \mathbb{T}_{cr} , let \mathbf{f} and \mathbf{g} be two faces (triangles), and let $z_{\text{cr}}(\mathbf{f})$ and $z_{\text{cr}}(\mathbf{g})$ be the complex coordinates of their respective circumcenters $\circ_{\mathbf{f}}$ and $\circ_{\mathbf{g}}$. Let $d = |z_{\text{cr}}(\mathbf{f}) - z_{\text{cr}}(\mathbf{g})|$ be the distance between the centers. Then the discrete double derivatives of the Green’s function have the following large distance asymptotics:*

$$\begin{aligned} [\nabla \Delta_{\text{cr}}^{-1} \bar{\nabla}^\top]_{\mathbf{f}\mathbf{g}} &= \frac{1}{4\pi} \left(\frac{\prod_{v \in \mathbf{g}} e^{i\theta_v}}{(z_{\text{cr}}(\mathbf{f}) - z_{\text{cr}}(\mathbf{g}))^3} - \frac{\prod_{u \in \mathbf{f}} e^{-i\theta_u}}{(\bar{z}_{\text{cr}}(\mathbf{f}) - \bar{z}_{\text{cr}}(\mathbf{g}))^3} \right) + O(d^{-4}), \\ [\bar{\nabla} \Delta_{\text{cr}}^{-1} \nabla^\top]_{\mathbf{f}\mathbf{g}} &= \frac{1}{4\pi} \left(\frac{\prod_{v \in \mathbf{g}} e^{-i\theta_v}}{(\bar{z}_{\text{cr}}(\mathbf{f}) - \bar{z}_{\text{cr}}(\mathbf{g}))^3} - \frac{\prod_{u \in \mathbf{f}} e^{i\theta_u}}{(z_{\text{cr}}(\mathbf{f}) - z_{\text{cr}}(\mathbf{g}))^3} \right) + O(d^{-4}) \end{aligned} \tag{6.14}$$

and

$$\begin{aligned} [\nabla \Delta_{\text{cr}}^{-1} \nabla^\top]_{\mathbf{f}\mathbf{g}} &= -\frac{1}{4\pi} \frac{1}{(z_{\text{cr}}(\mathbf{f}) - z_{\text{cr}}(\mathbf{g}))^2} + O(d^{-3}), \\ [\bar{\nabla}, \Delta_{\text{cr}}^{-1} \bar{\nabla}^\top]_{\mathbf{f}\mathbf{g}} &= -\frac{1}{4\pi} \frac{1}{(\bar{z}_{\text{cr}}(\mathbf{f}) - \bar{z}_{\text{cr}}(\mathbf{g}))^2} + O(d^{-3}). \end{aligned} \tag{6.15}$$

Proof. Let $\mathbf{f} = (123)$ and $\mathbf{g} = (456)$ be the vertices of \mathbf{f} and \mathbf{g} , respectively. The triangulation \mathbb{T}_{cr} is isoradial, so denote

$$z_{\text{cr}}(\mathbf{u}) - z_{\text{cr}}(\mathbf{f}) = e^{i\theta_u}, \quad \mathbf{u} = 1, 2, 3,$$

and

$$z_{\text{cr}}(\mathbf{v}) - z_{\text{cr}}(\mathbf{g}) = e^{i\theta_v}, \quad \mathbf{v} = 4, 5, 6.$$

Use (1.10) to separate the Green’s function $[\Delta_{\text{cr}}^{-1}]_{\mathbf{u}\mathbf{v}}$ into its leading large distance term (continuous limit term) of order $\log d$, its subleading large distance correction of order d^{-2} , and the rest of its large distance expansion of order d^{-4} ,

$$[\Delta_{\text{cr}}^{-1}]_{\mathbf{u}\mathbf{v}} = G_{\mathbf{u}\mathbf{v}}^{(0)} + G_{\mathbf{u}\mathbf{v}}^{(2)} + G_{\mathbf{u}\mathbf{v}}^{(4)}$$

with

$$\begin{aligned} G_{\mathbf{u}\mathbf{v}}^{(0)} &= -\frac{1}{2\pi} (\log(2|z_{\text{cr}}(\mathbf{u}) - z_{\text{cr}}(\mathbf{v})|) + \gamma_{\text{Euler}}), \\ G_{\mathbf{u}\mathbf{v}}^{(2)} &= -\frac{1}{24\pi} \left(\frac{p_3(\mathbf{u}, \mathbf{v})}{(z_{\text{cr}}(\mathbf{u}) - z_{\text{cr}}(\mathbf{v}))^3} + \frac{\bar{p}_3(\mathbf{u}, \mathbf{v})}{(\bar{z}_{\text{cr}}(\mathbf{u}) - \bar{z}_{\text{cr}}(\mathbf{v}))^3} \right), \\ G_{\mathbf{u}\mathbf{v}}^{(4)} &= O(|z_{\text{cr}}(\mathbf{u}) - z_{\text{cr}}(\mathbf{v})|^{-4}). \end{aligned} \tag{6.16}$$

Begin by writing

$$z_{\text{cr}}(\mathbf{u}) - z_{\text{cr}}(\mathbf{v}) = z_{\text{cr}}(\mathbf{f}) - z_{\text{cr}}(\mathbf{g}) + e^{i\theta_u} - e^{i\theta_v}$$

and expand the logs and powers of $(z_{cr}(u) - z_{cr}(v))$ and $(\bar{z}_{cr}(u) - \bar{z}_{cr}(v))$ in formulas (6.16) as power series in $(z_{cr}(f) - z_{cr}(g))$ and $(\bar{z}_{cr}(f) - \bar{z}_{cr}(g))$, where $d = |z_{cr}(f) - z_{cr}(g)| \gg 1$ is large. For example,

$$G_{uv}^{(0)} = -\frac{1}{2\pi}(\log(2|z_{cr}(f) - z_{cr}(g)|) + \gamma_{\text{Euler}}) + \frac{1}{2\pi} \operatorname{Re} \sum_{r \geq 1} \frac{1}{r} \left(\frac{e^{i\theta_v} - e^{i\theta_u}}{z_{cr}(f) - z_{cr}(g)} \right)^r.$$

The coefficients in these expansions involve the phases $e^{i\theta_u}$ and $e^{i\theta_v}$, and so the matrix entries in formulas (6.14) and (6.15) can be computed using the basic identities

$$\sum_{u \in f} \nabla_{fu} e^{i\theta_u} = 1 \quad \text{and} \quad \sum_{u \in f} \nabla_{fu} e^{-i\theta_u} = \sum_{u \in f} \nabla_{fu} = 0$$

along with values of ∇_{fu} , $\bar{\nabla}_{fu}$ and $\nabla_{vg}^\top = \nabla_{gv}$, $\nabla_{vg}^\dagger = \bar{\nabla}_{gv}$ explicitly given in (3.6) and (3.7). As an illustration,

$$\begin{aligned} [\nabla G^{(0)} \bar{\nabla}^\top]_{fg} &= \sum_{u \in f} \sum_{v \in g} \nabla_{fu} \bar{\nabla}_{gv} G_{uv}^{(0)} \\ &= \frac{1}{4\pi} \left(\frac{\prod_{u \in f} e^{i\theta_u}}{(z_{cr}(f) - z_{cr}(g))^3} - \frac{\prod_{v \in g} e^{-i\theta_v}}{(\bar{z}_{cr}(f) - \bar{z}_{cr}(g))^3} \right) \\ &\quad + \frac{1}{2\pi} \sum_{r \geq 4} \sum_{u \in f} \sum_{v \in g} \nabla_{fu} \bar{\nabla}_{gv} \frac{1}{r} \operatorname{Re} \left(\frac{e^{i\theta_v} - e^{i\theta_u}}{z_{cr}(f) - z_{cr}(g)} \right)^r. \end{aligned}$$

The vanishing of the coefficients of order $r \leq 2$ is straightforward. We present the calculation of the coefficient of $(z_{cr}(f) - z_{cr}(g))^{-3}$ occurring in $[\nabla G^{(0)} \bar{\nabla}^\top]_{fg}$ here,

$$\begin{aligned} &\frac{1}{3} \sum_{u \in f} \sum_{v \in g} \nabla_{fu} \bar{\nabla}_{gv} (e^{i\theta_v} - e^{i\theta_u})^3 \\ &= \frac{1}{3} \left(\underbrace{\left(\sum_{u \in f} \nabla_{fu} \right)}_{\text{vanishes}} \cdot \left(\sum_{v \in g} \bar{\nabla}_{gv} e^{3i\theta_v} \right) - \underbrace{\left(\sum_{u \in f} \nabla_{fu} e^{i\theta_u} \right)}_{\text{equals 1}} \cdot \underbrace{\left(\sum_{v \in g} \bar{\nabla}_{gv} e^{2i\theta_v} \right)}_{-\prod_{v \in g} e^{i\theta_v}} \right) \\ &\quad + \left(\sum_{u \in f} \nabla_{fu} e^{2i\theta_u} \right) \cdot \underbrace{\left(\sum_{v \in g} \bar{\nabla}_{gv} e^{i\theta_v} \right)}_{\text{vanishes}} - \frac{1}{3} \left(\sum_{u \in f} \nabla_{fu} e^{3i\theta_u} \right) \cdot \underbrace{\left(\sum_{v \in g} \bar{\nabla}_{gv} \right)}_{\text{vanishes}}. \end{aligned}$$

Due to Lemma 6.8 (or in this case through a direct estimate), its norm is uniformly bounded by a constant independent of the shape of the faces. For $G^{(0)}$, which is a smooth function of the vertex coordinates, these calculations amount to replacing ∇ and $\bar{\nabla}$ by their corresponding continuous derivatives ∂ and $\bar{\partial}$, up to subdominant terms of order $0(d^{-3})$. This is in agreement with Lemma 1.9. The result is that asymptotics (6.14) and (6.15) are valid for $G^{(0)}$ alone.

To end the proof of the lemma, one must show that the corresponding derivative terms for $G^{(2)}$ and $G^{(4)}$ are $O(d^{-3})$. This is clear for $G^{(4)}$, which is itself $O(d^{-4})$, hence its discrete derivatives are also $O(d^{-4})$. But this is not obvious for $G^{(2)}$ which is only $O(d^{-2})$. We must use the explicit form of $G^{(2)}$. Let us consider the term

$$\sum_{u \in f} \sum_{v \in g} \nabla_{fu} \left(\frac{p_3(u, v)}{(z_{cr}(u) - z_{cr}(v))^3} \right) \nabla_{vg}^\top$$

which appears in $\nabla G^{(2)} \nabla^\top$. One has

$$p_3(u, v) = p_3(o_f, o_g) + e^{-3i\theta_u} - e^{-3i\theta_v}.$$

So we have to consider three terms. The first term is

$$\begin{aligned} & \sum_{u \in f} \sum_{v \in g} \nabla_{fu} \left(\frac{p_3(o_f, o_g)}{(z_{cr}(u) - z_{cr}(v))^3} \right) \nabla_{vg}^\top \\ &= p_3(o_f, o_g) \sum_{u \in f} \sum_{v \in g} \nabla_{fu} \left(\frac{1}{(z_{cr}(u) - z_{cr}(v))^3} \right) \nabla_{vg}^\top \\ &= p_3(o_f, o_g) \left(\frac{-12}{(z_{cr}(f) - z_{cr}(g))^5} + \mathcal{O}(d^{-6}) \right) = O(d^{-4}). \end{aligned}$$

In the last step, we used the uniform bound from Lemma 4.3

$$|p_3(o_f, o_g)| \leq 3|z_{cr}(f) - z_{cr}(g)| = 3d.$$

The second term is

$$\begin{aligned} & \sum_{u \in f} \sum_{v \in g} \nabla_{fu} \left(\frac{e^{-3i\theta_u}}{(z_{cr}(u) - z_{cr}(v))^3} \right) \nabla_{vg}^\top \\ &= \sum_{u \in f} \nabla_{fu} \left(\frac{3e^{-3i\theta_u}}{(z_{cr}(f) - z_{cr}(g))^4} + O(d^{-5}) \right) \\ &= 3 \left(\sum_{u \in f} \nabla_{fu} e^{-3i\theta_u} \right) \frac{1}{(z_{cr}(f) - z_{cr}(g))^4} + O(d^{-5}). \end{aligned}$$

From Lemma 6.8,

$$\left| \sum_{u \in f} \nabla_{fu} e^{-3i\theta_u} \right| \leq 6,$$

hence the second term is of order $O(d^{-4})$. By the same argument, the third term is

$$- \sum_{u \in f} \sum_{v \in g} \nabla_{fu} \left(\frac{e^{-3i\theta_v}}{(z_{cr}(u) - z_{cr}(v))^3} \right) \nabla_{vg}^\top = O(d^{-4}).$$

This ends the derivation of (6.15) (the second equation is the complex conjugate (c.c.)). The derivation of (6.14) proceeds in a similar way. ■

We are now in a position to state the main result.

Proposition 6.10. *The second-order variation for the Laplace–Beltrami operator $\Delta(\epsilon)$ on an isoradial Delaunay graph \mathcal{G}_{cr} is*

$$\begin{aligned} & \text{tr}[\partial_{\epsilon_1} \Delta \cdot \Delta_{\text{cr}}^{-1} \cdot \partial_{\epsilon_2} \Delta \cdot \Delta_{\text{cr}}^{-1}] \\ &= \frac{1}{\pi^2} \sum_{\mathfrak{f} \in \bar{\Omega}_1} \sum_{\mathfrak{g} \in \bar{\Omega}_2} A(\mathfrak{f})A(\mathfrak{g}) \left[\frac{\bar{\nabla} F_1(\mathfrak{f})\bar{\nabla} F_2(\mathfrak{g})}{(z_{\text{cr}}(\mathfrak{f}) - z_{\text{cr}}(\mathfrak{g}))^4} + \frac{\nabla \bar{F}_1(\mathfrak{f})\nabla \bar{F}_2(\mathfrak{g})}{(\bar{z}_{\text{cr}}(\mathfrak{f}) - \bar{z}_{\text{cr}}(\mathfrak{g}))^4} \right] \\ &+ O(d^{-5}), \end{aligned} \tag{6.17}$$

where the double sum is taken over pairs of triangles $\mathfrak{f}, \mathfrak{g} \in F(\hat{\mathcal{G}}_{0+})$ such that all vertices of \mathfrak{f} reside in $\bar{\Omega}_1$ and all vertices of \mathfrak{g} reside in $\bar{\Omega}_2$.

Proof. We start from the local form of the operator $\Delta(\epsilon)$ (3.11), which implies that the first-order variation on $\Delta(\epsilon)$ is

$$\partial_{\epsilon} \Delta = 2(\partial_{\epsilon} \bar{\nabla}^{\top} A \nabla + \bar{\nabla}^{\top} \partial_{\epsilon} A \nabla + \bar{\nabla}^{\top} A \partial_{\epsilon} \nabla + \partial_{\epsilon} \nabla^{\top} A \bar{\nabla} + \nabla^{\top} \partial_{\epsilon} A \bar{\nabla} + \nabla^{\top} A \partial_{\epsilon} \bar{\nabla}).$$

We use the formula for the variation of A ,

$$\partial_{\epsilon} A = A(\nabla F + \bar{\nabla} \bar{F}),$$

as well as the formulas for the variations of the operators ∇ and $\bar{\nabla}$ given by (5.18), which read

$$\begin{aligned} \partial_{\epsilon} \nabla &= -(\nabla F \nabla + \nabla \bar{F} \bar{\nabla}), \\ \partial_{\epsilon} \bar{\nabla} &= -(\bar{\nabla} \bar{F} \bar{\nabla} + \bar{\nabla} F \nabla) \end{aligned}$$

to get

$$\partial_{\epsilon} \Delta = -4(\bar{\nabla}^{\top} (\nabla \bar{F}) A \bar{\nabla} + \nabla^{\top} (\bar{\nabla} F) A \nabla).$$

One uses this and the cyclicity of the trace to rewrite the second-order variation as

$$\begin{aligned} \text{tr}[\partial_{\epsilon_1} \Delta \cdot \Delta_{\text{cr}}^{-1} \cdot \partial_{\epsilon_2} \Delta \cdot \Delta_{\text{cr}}^{-1}] &= 16[\text{tr}(A \nabla \bar{F}_1 \cdot \bar{\nabla} \Delta_{\text{cr}}^{-1} \bar{\nabla}^{\top} \cdot A \nabla \bar{F}_2 \cdot \bar{\nabla} \Delta_{\text{cr}}^{-1} \bar{\nabla}^{\top}) \\ &+ \text{tr}(A \bar{\nabla} F_1 \cdot \nabla \Delta_{\text{cr}}^{-1} \nabla^{\top} \cdot A \nabla \bar{F}_2 \cdot \bar{\nabla} \Delta_{\text{cr}}^{-1} \nabla^{\top}) \\ &+ \text{tr}(A \nabla \bar{F}_1 \cdot \bar{\nabla} \Delta_{\text{cr}}^{-1} \nabla^{\top} \cdot A \bar{\nabla} F_2 \cdot \nabla \Delta_{\text{cr}}^{-1} \bar{\nabla}^{\top}) \\ &+ \text{tr}(A \bar{\nabla} F_1 \cdot \nabla \Delta_{\text{cr}}^{-1} \nabla^{\top} \cdot A \bar{\nabla} F_2 \cdot \nabla \Delta_{\text{cr}}^{-1} \nabla^{\top})]. \end{aligned}$$

Note that the trace on the left-hand side is a sum over vertices, while the trace on the right-hand side is a sum over faces (triangles). Using the large distances asymptotics (6.14) and (6.15), and writing the trace explicitly as a double sum over faces \mathfrak{f} and \mathfrak{g} gives the theorem. ■

We now consider the other operators. The case of the conformal Laplacian is more complicated, so let us first discuss the Kähler operator.

6.2.3. The Kähler operator \mathcal{D} .

Proposition 6.11. *The second-order variation for the Kähler operator $\mathcal{D}(\epsilon)$ on an isoradial, Delaunay graph \mathcal{G}_{cr} has the same form as the second-order variation for the Laplacian $\Delta(\epsilon)$*

$$\begin{aligned} & \text{tr}[\mathfrak{d}_{\epsilon_1} \mathcal{D} \cdot \mathcal{D}_{\text{cr}}^{-1} \cdot \mathfrak{d}_{\epsilon_2} \mathcal{D} \cdot \mathcal{D}_{\text{cr}}^{-1}] \\ &= \frac{1}{\pi^2} \sum_{\mathfrak{f} \in \bar{\Omega}_1} \sum_{\mathfrak{g} \in \bar{\Omega}_2} A(\mathfrak{f})A(\mathfrak{g}) \left[\frac{\bar{\nabla} F_1(\mathfrak{f})\bar{\nabla} F_2(\mathfrak{g})}{(z_{\text{cr}}(\mathfrak{f}) - z_{\text{cr}}(\mathfrak{g}))^4} + \frac{\nabla \bar{F}_1(\mathfrak{f})\nabla \bar{F}_2(\mathfrak{g})}{(\bar{z}_{\text{cr}}(\mathfrak{f}) - \bar{z}_{\text{cr}}(\mathfrak{g}))^4} \right] \\ &+ O(d^{-5}), \end{aligned} \tag{6.18}$$

where the double sum is taken over pairs of triangles $\mathfrak{f}, \mathfrak{g} \in F(\hat{\mathcal{G}}_{0+})$ such that all vertices of \mathfrak{f} reside in $\bar{\Omega}_1$ and all vertices of \mathfrak{g} reside in $\bar{\Omega}_2$.

Proof. The derivation goes along the same line. We start from Proposition 5.13 which gives the explicit form (5.12) of the first-order variation of $\mathcal{D}(\epsilon)$. The graph \mathcal{G}_{cr} is isoradial, so all circumradii are equal $R(\mathfrak{f}) = R_{\text{cr}}$, and thus $\mathcal{D}_{\text{cr}} = R_{\text{cr}}^{-2}\Delta_{\text{cr}}$. This implies that the first-order variation of $\mathcal{D}(\epsilon)$ has the special form

$$\mathfrak{d}_\epsilon \mathcal{D} = R_{\text{cr}}^{-2}\mathfrak{d}_\epsilon \Delta - 4R_{\text{cr}}^{-2}\bar{\nabla}^\top (A(\nabla F + \bar{\nabla} \bar{F}) + C\bar{\nabla} F + \bar{C}\nabla \bar{F})\nabla$$

with C and \bar{C} defined by (5.13). Formula (6.18) follows by repeating the analysis made in the proof of Proposition 6.10, which relies on the asymptotics of Lemma 6.9. One can check that the new terms involving C and \bar{C} do not change asymptotics (6.17) obtained for Δ . ■

6.3. The case of the conformal Laplacian: The anomalous term

6.3.1. Second-order variation for the conformal Laplacian $\underline{\Delta}$. By formula (6.9) in the proof of Proposition 6.4, the contribution made by regular edges $e \in E(\mathcal{G}_{0+}^\bullet)$ to the first-order variation $\mathfrak{d}_\epsilon \underline{\Delta}$ of the conformal Laplacian is identical to the variation $\mathfrak{d}_\epsilon \Delta$ of the Laplace–Beltrami Laplacian. There is, however, an additional term in the first-order variation $\mathfrak{d}_\epsilon \underline{\Delta}$ coming from the chords of \mathcal{G}_{0+} . We call it the “anomalous term” and denote it by $\delta \mathbb{A}$, $\mathfrak{d}_\epsilon \underline{\Delta} = \mathfrak{d}_\epsilon \Delta + \mathfrak{d}_\epsilon \mathbb{A}$.

The non-diagonal elements of $\mathfrak{d}_\epsilon \mathbb{A}$ are non-zero only for chords. From (6.9), for vertices $u \neq v$, they are

$$\begin{aligned} \mathfrak{d}_\epsilon \mathbb{A}(\bar{e}) &= [\mathfrak{d}_\epsilon \mathbb{A}]_{uv} \\ &= \begin{cases} \frac{\mathfrak{d}_\epsilon \theta_n(\bar{e}) \tan^2 \theta_n(\bar{e}) + \mathfrak{d}_\epsilon \theta_s(\bar{e}) \tan^2 \theta_s(\bar{e})}{2} & \text{if } e = \overline{uv} \text{ is a chord} \\ & \text{in } E(\mathcal{G}_{0+}), \\ 0 & \text{otherwise.} \end{cases} \end{aligned} \tag{6.19}$$

Here $e = \overline{uv}$ is an edge of G_{0+} and $\vec{e} = (u, v)$ is an orientation. The graph G_{0+} is isoradial and weakly Delaunay, and so $\theta_n(\vec{e}) = \pm\theta_s(\vec{e})$ for any edge. In particular, $\tan^2 \theta_n(\vec{e}) = \tan^2 \theta_s(\vec{e})$, and so $\mathfrak{d}_\epsilon \mathbb{A}(\vec{e}) = \mathfrak{d}_\epsilon \mathbb{A}(\vec{e}^*)$, where $\vec{e}^* = (v, u)$ is the opposite orientation. As for the diagonal terms, we have

$$[\mathfrak{d}_\epsilon \mathbb{A}]_{uu} = - \sum_{v \neq u} [\mathfrak{d}_\epsilon \mathbb{A}]_{uv}. \tag{6.20}$$

In the case of a chord \vec{e} , we may use (5.19) for the angle variations $\mathfrak{d}_\epsilon \theta_n(\vec{e})$ and $\mathfrak{d}_\epsilon \theta_s(\vec{e})$ and re-express the anomalous term $\mathfrak{d}_\epsilon \mathbb{A}(\vec{e})$ given in formula (6.19) as

$$\mathfrak{d}_\epsilon \mathbb{A}(\vec{e}) = \frac{1}{2} \operatorname{Im}[\overline{\nabla} F(\mathfrak{f}_n) \mathcal{E}_n(\vec{e}) \tan^2 \theta_n(\vec{e}) + \overline{\nabla} F(\mathfrak{f}_s) \mathcal{E}_s(\vec{e}) \tan^2 \theta_s(\vec{e})], \tag{6.21}$$

where the functions $\mathcal{E}_n(\vec{e})$ and $\mathcal{E}_s(\vec{e})$ are defined in (5.20) and where \mathfrak{f}_n and \mathfrak{f}_s are the respective north and south triangles abutting \vec{e} in the triangulation \widehat{G}_{0+} which completes G_{0+} .

The second-order variation

$$\operatorname{tr}[\mathfrak{d}_{\epsilon_1} \underline{\Delta} \cdot \Delta_{\text{cr}}^{-1} \cdot \mathfrak{d}_{\epsilon_2} \underline{\Delta} \cdot \Delta_{\text{cr}}^{-1}]$$

is the sum of the second-order variation made by the Laplace–Beltrami Laplacian, namely

$$\operatorname{tr}[\mathfrak{d}_{\epsilon_1} \Delta \cdot \Delta_{\text{cr}}^{-1} \cdot \mathfrak{d}_{\epsilon_2} \Delta \cdot \Delta_{\text{cr}}^{-1}] \tag{6.22}$$

along with three anomalous trace terms, which we can express (in light of (6.20)) as follows:

$$\begin{aligned} & \underbrace{\operatorname{tr}[\mathfrak{d}_{\epsilon_1} \mathbb{A} \cdot \Delta_{\text{cr}}^{-1} \cdot \mathfrak{d}_{\epsilon_2} \Delta \cdot \Delta_{\text{cr}}^{-1}]}_{\text{chord-edge term}} \\ &= \sum_{\substack{\text{chords } \vec{e}_1 \in G_{0+} \\ \text{edges } \vec{e}_2 \in \widehat{G}_{0+}}} \mathfrak{d}_{\epsilon_1} \mathbb{A}(\vec{e}_1) K(\vec{e}_1, \vec{e}_2) \mathfrak{d}_{\epsilon_2} \Delta(\vec{e}_2) K(\vec{e}_2, \vec{e}_1), \\ & \underbrace{\operatorname{tr}[\mathfrak{d}_{\epsilon_1} \Delta \cdot \Delta_{\text{cr}}^{-1} \cdot \mathfrak{d}_{\epsilon_2} \mathbb{A} \cdot \Delta_{\text{cr}}^{-1}]}_{\text{edge-chord term}} \\ &= \sum_{\substack{\text{edges } \vec{e}_1 \in \widehat{G}_{0+} \\ \text{chords } \vec{e}_2 \in G_{0+}}} \mathfrak{d}_{\epsilon_1} \Delta(\vec{e}_1) K(\vec{e}_1, \vec{e}_2) \mathfrak{d}_{\epsilon_2} \mathbb{A}(\vec{e}_2) K(\vec{e}_2, \vec{e}_1), \\ & \underbrace{\operatorname{tr}[\mathfrak{d}_{\epsilon_1} \mathbb{A} \cdot \Delta_{\text{cr}}^{-1} \cdot \mathfrak{d}_{\epsilon_2} \mathbb{A} \cdot \Delta_{\text{cr}}^{-1}]}_{\text{chord-chord term}} \\ &= \sum_{\substack{\text{chords} \\ \vec{e}_1, \vec{e}_2 \in G_{0+}}} \mathfrak{d}_{\epsilon_1} \mathbb{A}(\vec{e}_1) K(\vec{e}_1, \vec{e}_2) \mathfrak{d}_{\epsilon_2} \mathbb{A}(\vec{e}_2) K(\vec{e}_2, \vec{e}_1), \end{aligned} \tag{6.23}$$

where $\vec{e}_1 = (u_1, v_1)$ and $\vec{e}_2 = (u_2, v_2)$ are oriented edges of the triangulation \widehat{G}_{0+} , whose vertices u_1, v_1 and u_2, v_2 lie in $\overline{\Omega}_1$ and $\overline{\Omega}_2$, respectively, and where

$$K(\vec{e}_1, \vec{e}_2) := [\Delta_{\text{cr}}^{-1}]_{v_1 v_2} - [\Delta_{\text{cr}}^{-1}]_{u_1 v_2} - [\Delta_{\text{cr}}^{-1}]_{v_1 u_2} + [\Delta_{\text{cr}}^{-1}]_{u_1 u_2}.$$

Note that $K(\vec{e}_1, \vec{e}_2) = K(\vec{e}_2, \vec{e}_1) = -K(\vec{e}_1^*, \vec{e}_2)$, where $\vec{e}_1^* = (v_1, u_1)$ has the reverse orientation. Applying two rounds of formula (3.8), we obtain

$$\begin{aligned} K(\vec{e}_1, \vec{e}_2) &= p_1(u_2, v_2)[\Delta_{\text{cr}}^{-1} \nabla^\top]_{u_1 f_2} - p_1(u_2, v_2)[\Delta_{\text{cr}}^{-1} \nabla^\top]_{v_1 f_2} \\ &\quad + \bar{p}_1(u_2, v_2)[\Delta_{\text{cr}}^{-1} \bar{\nabla}^\top]_{u_1 f_2} - \bar{p}_1(u_2, v_2)[\Delta_{\text{cr}}^{-1} \bar{\nabla}^\top]_{v_1 f_2} \\ &= 2 \operatorname{Re} [p_1(u_1, v_1) p_1(u_2, v_2) [\nabla \Delta_{\text{cr}}^{-1} \nabla^\top]_{f_1 f_2} \\ &\quad + p_1(u_1, v_1) \bar{p}_1(u_2, v_2) [\nabla \Delta_{\text{cr}}^{-1} \bar{\nabla}^\top]_{f_1 f_2}], \end{aligned} \tag{6.24}$$

where f_i is a triangle of \widehat{G}_{0+} , north or south, containing the edge \vec{e}_i for $i = 1, 2$. By assumption, $\overline{\Omega}_1$ and $\overline{\Omega}_2$ are separated by a large distance $d \gg R_{\text{cr}}$, and so we can estimate $K(\vec{e}_1, \vec{e}_2)$ as presented in formula (6.24) using asymptotic expansions (6.14) and (6.15) of Lemma 6.9. We end up with

$$K(\vec{e}_1, \vec{e}_2) = \frac{1}{2\pi} \operatorname{Re} \left[\frac{p_1(u_1, v_1) p_1(u_2, v_2)}{(z_{\text{cr}}(f_1) - z_{\text{cr}}(f_2))^2} \right] + O\left(\frac{1}{|z_{\text{cr}}(f_1) - z_{\text{cr}}(f_2)|^3}\right),$$

where $p_1(u, v) = z_{\text{cr}}(v) - z_{\text{cr}}(u)$ as introduced in Definition 2.23.

6.3.2. The chord-chord term. Let us begin by examining the chord-chord term of (6.23). It involves the contribution of two (oriented) chords $\vec{e}_1 = (u_1, v_1)$ and $\vec{e}_2 = (u_2, v_2)$, whose vertices u_1, v_1 and u_2, v_2 are contained in $\overline{\Omega}_1$ and $\overline{\Omega}_2$, respectively. Since $\vec{e}_i = (u_i, v_i)$ is a chord for $i = 1, 2$ in G_{0+} , the corresponding north and south triangles f_{i_n} and f_{i_s} in \widehat{G}_{0+} are concyclic and therefore share a common circumcenter whose complex coordinate we denote by

$$z_{\text{cr}}(\vec{e}_i) = z(f_{i_n}) = z(f_{i_s}).$$

This is depicted in Figure 17.

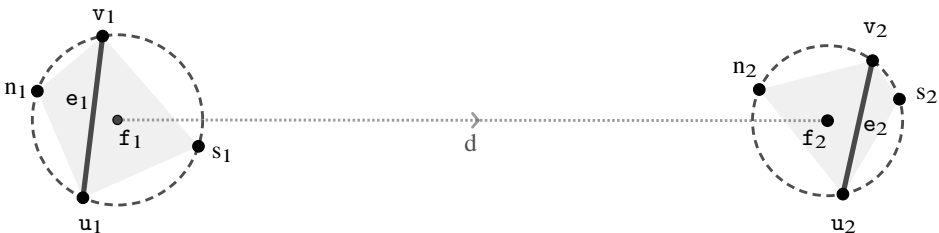


Figure 17. Two far apart chords $\vec{e}_1 = (u_1 v_1)$ and $\vec{e}_2 = (u_2 v_2)$ at distance $d \gg 1$.

Putting things together, we see that the contribution made by a pair of (oriented) chords (\vec{e}_1, \vec{e}_2) to the chord-chord anomalous trace term in (6.23) is

$$\frac{1}{16\pi^2} \mathfrak{d}_{\epsilon_1} \mathbb{A}(\vec{e}_1) \mathfrak{d}_{\epsilon_2} \mathbb{A}(\vec{e}_2) \left(\operatorname{Re} \left[\frac{p_1(u_1, v_1) p_1(u_2, v_2)}{(\mathcal{Z}_{\text{cr}}(\vec{e}_1) - \mathcal{Z}_{\text{cr}}(\vec{e}_2))^2} \right] \right)^2 + O\left(\frac{1}{|\mathcal{Z}_{\text{cr}}(\vec{e}_1) - \mathcal{Z}_{\text{cr}}(\vec{e}_2)|^5}\right) \tag{6.25}$$

with $\mathfrak{d}_{\epsilon_1} \mathbb{A}(\vec{e}_1)$ and $\mathfrak{d}_{\epsilon_2} \mathbb{A}(\vec{e}_2)$ given by (6.21) that we recall for completeness,

$$\mathfrak{d}_{\epsilon} \mathbb{A}(\vec{e}) = \frac{1}{2} \operatorname{Im}[\bar{\nabla} F(\mathbf{f}_n) \mathcal{E}_n^{\epsilon}(\vec{e}) \tan^2 \theta_n(\vec{e}) + \bar{\nabla} F(\mathbf{f}_s) \mathcal{E}_s^{\epsilon}(\vec{e}) \tan^2 \theta_s(\vec{e})]$$

with

$$\mathcal{E}_n(\vec{e}) = \frac{\bar{z}(v) - \bar{z}(n)}{z(v) - z(n)} - \frac{\bar{z}(u) - \bar{z}(n)}{z(u) - z(n)} = \frac{-4A(\mathbf{f}_n)}{(z(v) - z(n))(z(u) - z(n))}$$

and a similar form for $\mathcal{E}_s(\vec{e})$. Any triangulation \hat{G}_{0+} which completes the limit graph G_{0+} is itself isoradial and weakly Delaunay, consequently $\tan^2 \theta_n(\vec{e}) = \tan^2 \theta_s(\vec{e})$ the value of which is given by (3.5).

Result (6.25) for the anomalous chord-chord contribution to the variation of $\log \det \underline{\mathbb{A}}(\epsilon)$ does not have the same form as the “regular” contribution (6.22) which is similar to the variation of the Laplace–Beltrami operator Δ , which is a sum over triangles of terms

$$A(\mathbf{f}_1) A(\mathbf{f}_2) \frac{\bar{\nabla} F_1(\mathbf{f}_1) \cdot \bar{\nabla} F_2(\mathbf{f}_2)}{(z_{\text{cr}}(\mathbf{f}_1) - z_{\text{cr}}(\mathbf{f}_2))^4} + \text{c.c.}$$

First, in addition to harmonic terms in the coordinates of the circumcenters of the form

$$(\mathcal{Z}_{\text{cr}}(\vec{e}_1) - \mathcal{Z}_{\text{cr}}(\vec{e}_2))^{-4} \quad \text{and} \quad (\bar{\mathcal{Z}}_{\text{cr}}(\vec{e}_1) - \bar{\mathcal{Z}}_{\text{cr}}(\vec{e}_2))^{-4},$$

it contains non-harmonic terms of the form

$$|\mathcal{Z}_{\text{cr}}(\vec{e}_1) - \mathcal{Z}_{\text{cr}}(\vec{e}_2)|^{-4}$$

which are problematic with respect to the conformal invariance and an interpretation in terms of CFT, as will be discussed in Section 9.

Second, from the form of $\mathfrak{d}_{\epsilon_1} \mathbb{A}(\vec{e}_1)$ and $\mathfrak{d}_{\epsilon_2} \mathbb{A}(\vec{e}_2)$, it does not contain only terms of the form

$$\bar{\nabla} F_1(\mathbf{f}_1) \cdot \bar{\nabla} F_2(\mathbf{f}_2) \quad \text{and} \quad \nabla \bar{F}_1(\mathbf{f}_2) \cdot \nabla \bar{F}_2(\mathbf{f}_2)$$

but also terms of the form

$$\bar{\nabla} F_1(\mathbf{f}_1) \cdot \nabla \bar{F}_2(\mathbf{f}_2) \quad \text{and} \quad \nabla \bar{F}_1(\mathbf{f}_2) \cdot \bar{\nabla} F_2(\mathbf{f}_2).$$

Third, the geometric terms associated to the faces (the triangles \mathbf{f}_1 and \mathbf{f}_2) are not simply the area terms $A(\mathbf{f}_1)$ and $A(\mathbf{f}_2)$, but they depend on the detailed geometry and orientation of the chords and the triangles through the terms $\mathcal{E}_{n/s}(\vec{e})$ and $\tan^2 \theta_{n/s}(\vec{e})$.

6.3.3. The chord-edge term. We now discuss briefly the chord-edge term present in (6.23), which involves the anomalous variation term $[\mathfrak{d}_{\epsilon_1} \mathbb{A}]_{u_1 v_1}$ of a chord $\vec{e}_1 = (u_1, v_1)$ and the ordinary variation term $[\mathfrak{d}_{\epsilon_2} \Delta]_{u_2 v_2}$ of an edge $\vec{e}_2 = (u_2, v_2)$. It will be simpler to group together the terms made by a single chord

$$\vec{e}_1 = \vec{e} = (u, v)$$

and the edges \vec{e}_2 forming the boundary of a fixed (counter-clockwise oriented) triangle \mathfrak{f} , and then sum the contributions as the chord \vec{e} in \mathcal{G}_{0+} and triangle \mathfrak{f} in $\widehat{\mathcal{G}}_{0+}$ both vary; see the illustration in Figure 18.

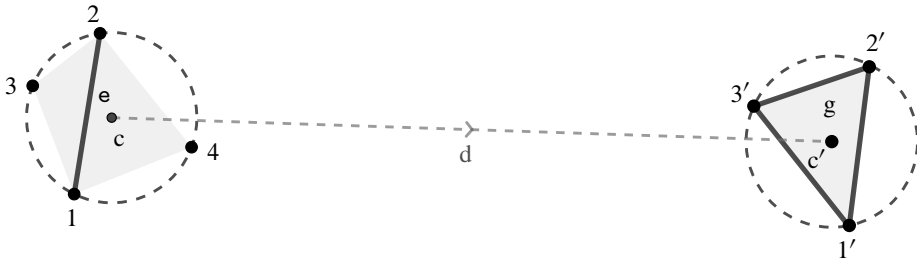


Figure 18. A chord $e = (12)$ and a triangle $g = (1'2'3')$ at distance d .

Accordingly, the contribution made by a chord-triangle pair (\vec{e}, \mathfrak{f}) is found to be

$$\frac{1}{4\pi^2} \mathfrak{d}_{\epsilon_1} \mathbb{A}(\vec{e}) \operatorname{Re} \left[\frac{p_1^2(u, v) A(\mathfrak{f}) \bar{\nabla} F_2(\mathfrak{f})}{(\mathcal{Z}_{\text{cr}}(\vec{e}) - z_{\text{cr}}(\mathfrak{f}))^4} \right] + O\left(\frac{1}{|\mathcal{Z}_{\text{cr}}(\vec{e}) - z_{\text{cr}}(\mathfrak{f})|^5}\right). \quad (6.26)$$

This term is again different from the regular term. Now it is harmonic in the coordinates of the circumcenters, since it does not contain the non-harmonic term

$$|\mathcal{Z}_{\text{cr}}(\vec{e}_1) - \mathcal{Z}_{\text{cr}}(\vec{e}_2)|^{-4}.$$

However, it still contains the terms of the form

$$\bar{\nabla} F_1(\mathfrak{f}_1) \cdot \nabla \bar{F}_2(\mathfrak{f}_2) \quad \text{and} \quad \nabla \bar{F}_1(\mathfrak{f}_2) \cdot \bar{\nabla} F_2(\mathfrak{f}_2),$$

and it depends on the detailed geometry and orientation of the chord, as for the chord-chord term discussed previously.

6.3.4. A simplification for specific deformations. Finally, let us note that the anomalous term $\mathfrak{d}_{\epsilon} \mathbb{A}(\vec{e})$ for a chord \vec{e} from (6.21) takes a simpler form in the special case when the discrete derivatives of F coincide on the north and south triangles $\mathfrak{f}_n(\vec{e})$ and $\mathfrak{f}_s(\vec{e})$ due to the following lemma.

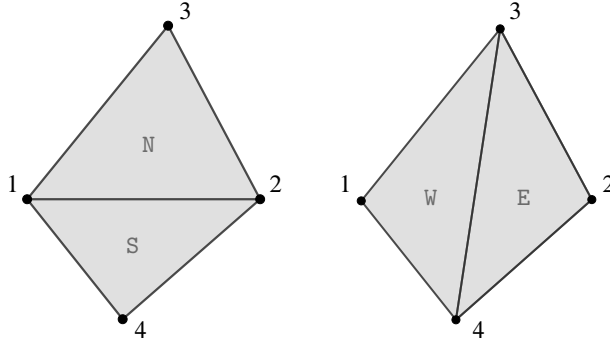


Figure 19. The triangles N, S, E and W.

Lemma 6.12. Consider two triangles $N = (v_1, v_2, v_3)$ and $S = (v_2, v_1, v_4)$ sharing the edge $\overline{v_1 v_2}$ and the flipped triangles $E = (v_3, v_4, v_2)$ and $W = (v_4, v_3, v_1)$ sharing the edge $\overline{v_3 v_4}$ as depicted in Figure 19. Let $v \mapsto F(v)$ be a function defined on the vertices. Then the four following expressions are equivalent:

$$\nabla F(N) = \nabla F(S), \quad \nabla F(E) = \nabla F(W), \quad \bar{\nabla} F(N) = \bar{\nabla} F(S), \quad \bar{\nabla} F(E) = \bar{\nabla} F(W).$$

Note that the four points are not necessarily concyclic.

Proof. The proof follows from definitions (3.6) and (3.7), and it is left to the reader. It has a simple geometric interpretation. Again, note that this is valid for any pair of triangles sharing an edge. ■

In this case, a single pair of discrete derivatives $(\nabla F(c), \bar{\nabla} F(c))$ of F is associated to a cocyclic configuration of points, namely, a simple cyclic polygon

$$P = (z_1, z_2, \dots, z_k), \quad k \geq 4,$$

with circumcenter c . The variation $\mathfrak{d}_{\epsilon_1} \mathbb{A}(\vec{e})$ for a chord \vec{e} is then given by

$$\mathfrak{d}_{\epsilon_1} \mathbb{A}(\vec{e}) = \frac{1}{2} \operatorname{Im}[\bar{\nabla} F(c)(\mathcal{E}_n(\vec{e}) + \mathcal{E}_s(\vec{e}))] \tan^2 \theta_{n/s}(\vec{e}).$$

6.4. Curvature dipoles and the anomalous chord term

Let us discuss a possible explanation of the anomalous terms corresponding to deformations of cocyclic vertex configurations. The adjective “anomalous” indicates that these contributions are not present for either the Laplace–Beltrami operator Δ or the Kähler operator \mathcal{D} , both of which admit a smooth continuum limit consistent with the predictions of conformal invariance.

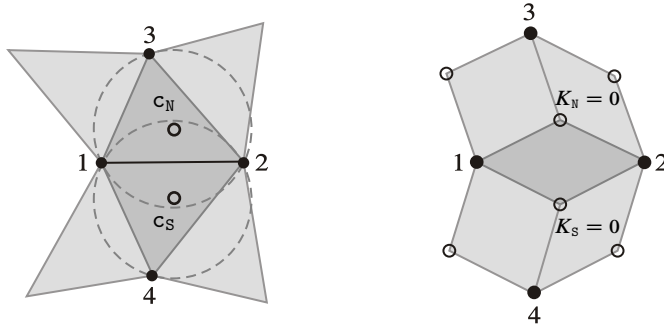


Figure 20. A regular edge $e = (12)$ of a critical triangulation G (left) and its associated rhombic lattice G^\diamond (right), the curvature K associated to each face of G , i.e., its white $\tilde{\circ}$ -vertices of G^\diamond , is zero.

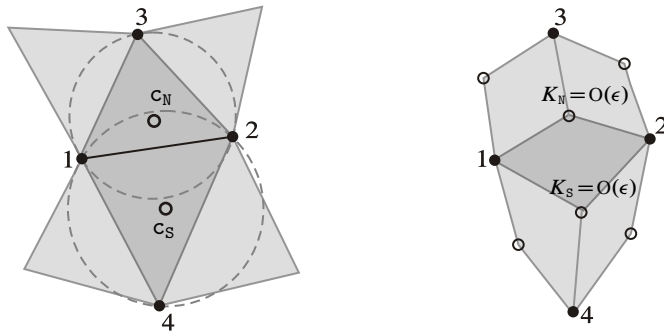


Figure 21. A deformation of G . The Gauss curvatures K of the N and S faces are non-zero, but of order $O(\epsilon)$.

As discussed in definition (1.7), the conformal Laplacian $\underline{\Delta}$ for a Delaunay graph G can be viewed as the discretized *Laplace–Beltrami operator* on the *rhombic surface* S_G^\diamond introduced in Definition 2.21. The construction of S_G^\diamond is illustrated in Figure 20 for an isoradial Delaunay graph G and in Figure 21 for a generic (non-isoradial) Delaunay triangulation G .

It is easy to see that the surface S_G^\diamond is piecewise flat, with curvature defects (i.e., conical singularities) localized at the vertices $\tilde{\circ}_f$ associated to circumcenters of faces f in G . The defect angle $K(f)$ corresponds to a localized curvature defect at $\tilde{\circ}_f$, and its value is given in terms of the conformal angles $\theta(e)$ of the edges forming the boundary of the face f . Recall from Remark 2.2 that the associated scalar curvature $R_{\text{scal}}(\tilde{\circ}_f)$ at a vertex $\tilde{\circ}_f$ is

$$R_{\text{scal}}(\tilde{\circ}_f) = 4\pi - 2 \sum_{e \in \partial f} (\pi - 2\theta(e))$$

or, equivalently, twice the measure of the defect angle around the circumcenter o_f of the face f , i.e., the Gauss curvature

$$K(f) := \underbrace{2\pi - \sum_{e \in f} (\pi - 2\theta(e))}_{\text{discrete Gauss curvature}}.$$

For an isoradial Delaunay graph G , the rhombic surface S_G^\diamond coincides with the planar kite graph G^\diamond whose faces, in this case, are all rhombi. Furthermore, the scalar curvature $R_{\text{scal}}(\tilde{o}_f)$ associated to each face f in G is zero. For a generic Delaunay graph G , the scalar curvature $R_{\text{scal}}(\tilde{o}_f)$ will be non-zero (see Figure 21). Indeed, consider a cyclic quadrilateral face f in an isoradial triangulation G_{cr} depicted in Figure 22 and the effects of a generic deformation $G_{\text{cr}} \rightarrow G_\epsilon$ depicted in Figure 23. In $S_{G_{\text{cr}}}^\diamond$, four lozenges meet at \tilde{o}_f where the scalar curvature $R_{\text{scal}}(\tilde{o}_f)$ vanishes.

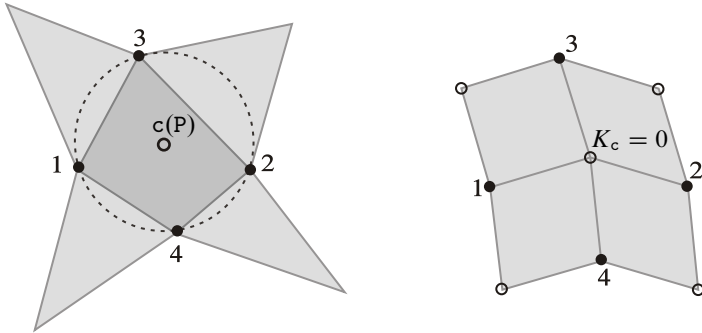


Figure 22. A cocyclic face $P = (1423)$ of a critical triangulation G_{cr} (left) and its associated rhombic lattice G^\diamond (right), the curvature K associated to each face of G , i.e., its white o -vertices of G^\diamond , is zero.

As illustrated in Figure 23, as soon as we deform this cyclic quadrilateral, a diagonal edge e generically emerges in G_ϵ (infinitesimally a chord e in G_{0+}) which subdivides the quadrilateral f into two triangles f_n and f_s , while the circumcenter o_f splits into two circumcenters o_n and o_s . In the deformed rhombic surface $S_{G_\epsilon}^\diamond$ a new lozenge appears between \tilde{o}_n and \tilde{o}_s . However, this new lozenge is “flat”, i.e., to first-order in ϵ its angles are $(0, \pi, 0, \pi)$. Therefore, the Gaussian curvatures $K(f_n)$ and $K(f_s)$ have opposite signs and they are both of order $O(1)$, not of order $O(\epsilon)$. In terms of the north and south angles of the chord \vec{e} , they read

$$K(f_n) = -2\theta_n(\vec{e}) + O(\epsilon), \quad K(f_s) = -2\theta_s(\vec{e}) + O(\epsilon).$$

Thus the deformation produces a *curvature dipole* associated to the chord e , i.e., neighboring curvature defects with non-zero but opposite signs. Said differently, the

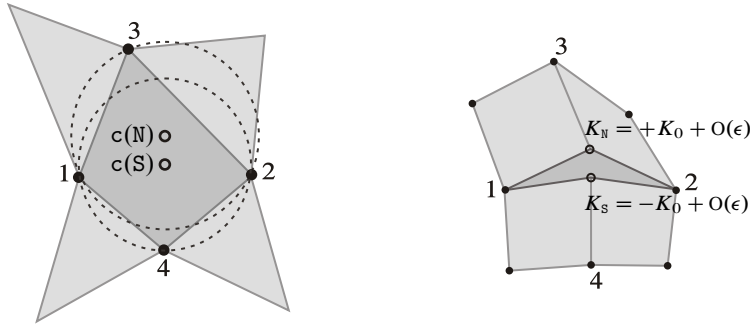


Figure 23. A deformation $O(\epsilon)$ of the cocyclic configuration. The Delaunay condition select a chord $e = (12)$, which splits the face $P = (1423)$ into two triangles $N = (123)$ and $S = (214)$. A flat lozenge $(1S2N)$ appear in the rhombic lattice G^\diamond . The curvatures K of the N and S faces are non-zero, but of order $O(1)$ and opposite. The triangles N and S form a “curvature dipole”.

smooth deformation $G_{cr} \rightarrow G_\epsilon$ manifests a *discontinuity* in the curvature. Generically, when one smoothly deforms a cyclic face f of G_{cr} with four or more vertices, a curvature dipole will emerge for each chord $e \in G_{0+}$ which subdivides the face f .

Finally, let us stress that a curvature dipole appears if the anomalous term $\mathfrak{d}_\epsilon \mathbb{A}(\vec{e})$ discussed above in Section 6.3.1 is non-zero. Indeed, this anomalous term is proportional to $\tan^2 \theta_n(\vec{e})$, while the dipole is proportional to $\theta_n(\vec{e})$. Thus for a chord $e \in G_{0+}$ with $\theta_n(\vec{e}) = \theta_s(\vec{e}) = 0$, no anomalous term is present, and so no curvature dipole appears at first order in the deformation. This occurs if and only if the circumcenter o_f of the face f lies on the edge e . Notice that if f is a quadrilateral (as in Figure 23) where the north and south angles of both $e = (12)$ and the flipped edge $e^* = (34)$ are zero, then the face f is a rectangle. In this case, to first order in ϵ , the deformation is *isoradial* \rightarrow *isoradial*, not *isoradial* \rightarrow *non-isoradial*. These *isoradial* \rightarrow *isoradial* deformations are the ones considered by Kenyon in the seminal paper [17].

7. The scaling limit of variations

7.1. Rescaling smooth deformations

As explained in the introduction, we incorporate a scaling factor $\ell > 0$ into the deformation in order to define and study a continuum limit. We may view the scaling parameter $\ell > 0$ as imparting a *resolution* on the critical graph, i.e., we get a rescaled embedding $z_{cr}^{1/\ell} := \frac{z_{cr}}{\ell}$ of G_{cr} , under which vertices become closer and denser in any compact region of the plane as $\ell > 0$ increases. In particular, the area $A(f)$ of a face

$\mathbf{f} \in \mathbb{F}(\mathbb{G}_{\text{cr}})$ shrinks by a factor of $\frac{1}{\ell^2}$ under the rescaled embedding, while its circum-center coordinate $z_{\text{cr}}(\mathbf{f})$ is rescaled by a factor of $\frac{1}{\ell}$. In this way, the scaling parameter $\ell > 0$ allows us to interpret the critical graph as a planar partition and can be used to define a Riemann sum. More specifically, given any continuous complex-valued function $H: \mathbb{C} \rightarrow \mathbb{C}$ with compact support $\Omega = \text{supp } H$, then

$$\lim_{\ell \rightarrow \infty} \sum_{\mathbf{x} \in \mathbb{F}(\mathbb{G}_{\text{cr}})} \frac{A(\mathbf{x})}{\ell^2} \cdot H\left(\frac{z_{\text{cr}}(\mathbf{x})}{\ell}\right) = \int_{\Omega} d^2x H(x).$$

Given a smooth complex-valued function $F: \mathbb{C} \rightarrow \mathbb{C}$ with compact support, and $\ell > 0$ a scaling real parameter, we set $F_{\ell}(z) := \ell F(\frac{z}{\ell})$. When deforming a critical isoradial Delaunay graph \mathbb{G}_{cr} (with unit circumradius $R_{\text{cr}} = 1$), we shall consider the restriction of F_{ℓ} to (the coordinates of) the vertices of the critical graph. By abuse of notation, we shall write $F_{\ell}(\mathbf{v}) := \ell F(\frac{z_{\text{cr}}(\mathbf{v})}{\ell})$ for each vertex $\mathbf{v} \in \mathbb{V}(\mathbb{G}_{\text{cr}})$. We use F_{ℓ} to displace the coordinates of the critical graph and define a deformed embedding, namely,

$$z_{\epsilon, \ell}(\mathbf{v}) := z_{\text{cr}}(\mathbf{v}) + \epsilon F_{\ell}(\mathbf{v}).$$

7.2. Rescaling bi-local deformations

Our analysis of second-order variations (for the log-determinants which we consider) involve a bi-local deformation implemented by two smooth, complex-valued functions F_1 and $F_2: \mathbb{C} \rightarrow \mathbb{C}$ whose respective supports Ω_1 and Ω_2 are compact and have lattice closures $\bar{\Omega}_1$ and $\bar{\Omega}_2$ which are disjoint. Set

$$d := \text{dist}(\Omega_1, \Omega_2) = \inf\{|w_1 - w_2| : w_i \in \Omega_i\}$$

to be the distance between the supports Ω_1 and Ω_2 . Obviously, $0 < d < \infty$. The corresponding deformed embedding $z_{\epsilon, \ell}: \mathbb{V}(\mathbb{G}_{\text{cr}}) \rightarrow \mathbb{C}$ of the critical lattice is given by

$$z_{\epsilon, \ell}(\mathbf{v}) := z_{\text{cr}}(\mathbf{v}) + \epsilon_1 F_{1; \ell}(\mathbf{v}) + \epsilon_2 F_{2; \ell}(\mathbf{v}),$$

where $\underline{\epsilon} = (\epsilon_1, \epsilon_2)$ is a pair of deformation parameters $\epsilon_1, \epsilon_2 \geq 0$, and where we use the notation $F_{i; \ell}(z) := \ell F_i(\frac{z}{\ell})$ and by abuse of notation $F_{i; \ell}(\mathbf{v}) := F_{i; \ell}(z_{\text{cr}}(\mathbf{v}))$ for a vertex $\mathbf{v} \in \mathbb{V}(\mathbb{G}_{\text{cr}})$ and $i = 1, 2$. The results of Lemma 5.8 still hold for the bi-local deformed embedding $z_{\epsilon, \ell}$; simply apply the lemma to F_1 and F_2 independently and take $\tilde{\epsilon}_F = \min(\tilde{\epsilon}_{F_1}, \tilde{\epsilon}_{F_2})$. Let us denote by $\mathbb{G}_{\underline{\epsilon}, \ell}$ the Delaunay graph uniquely determined by the vertex set $\mathbb{V}(\mathbb{G}_{\underline{\epsilon}, \ell}) := \mathbb{V}(\mathbb{G}_{\text{cr}})$ together with the deformed embedding $z_{\epsilon, \ell}$. As we have seen, the one-sided limit $\epsilon_i \rightarrow 0^+$ for $i = 1, 2$ induces the structure of a weak Delaunay graph $\mathbb{G}_{0^+, \ell}$ on the vertex set $\mathbb{V}(\mathbb{G}_{\text{cr}})$ with respect to the critical embedding z_{cr} . In general, the edge set $\mathbb{E}(\mathbb{G}_{0^+, \ell})$ will vary as the scaling parameter $\ell > 0$ evolves; nevertheless $\mathbb{E}(\mathbb{G}_{\text{cr}}) \subseteq \mathbb{E}(\mathbb{G}_{0^+, \ell})$ for all $0 < \ell \leq \infty$. For each

value of $\ell > 0$, select a weak Delaunay triangulation $\widehat{G}_{0+,\ell}$ which completes $G_{0+,\ell}$. Because $E(G_{\text{cr}}) \subseteq E(G_{0+,\ell}) \subseteq E(\widehat{G}_{0+,\ell})$ for each $0 < \ell \leq \infty$, we may always perform the following resummation:

$$\sum_{x \in F(\widehat{G}_{0+,\ell})} A(x)H(z_{\text{cr}}(x)) = \sum_{y \in F(G_{\text{cr}})} A(y)H(z_{\text{cr}}(y)),$$

where we combine terms on the left-hand side involving triangles of $\widehat{G}_{0+,\ell}$ which share a common circumcenter and where $H(x)$ is any quantity which depends only upon the circumcenter $z_{\text{cr}}(x)$ of $x \in F(\widehat{G}_{0+,\ell})$. Consequently, the choice of triangulation $\widehat{G}_{0+,\ell}$ completing $G_{0+,\ell}$ will not affect our calculations.

7.3. Scaling limit and derivation of Theorem 1.10

We now are in a position to study the scaling limit of the bilocal terms (6.17) (Proposition 6.10) and (6.18) (Proposition 6.11) and to derive Theorem 1.10. For $G = G_{\text{cr}}$ or $G = \widehat{G}_{0+,\ell}$, we denote by $F_{\overline{\Omega}_i(\ell)}(G)$ the subset of faces x of G whose vertices belong to the lattice closure $\overline{\Omega}_i(\ell)$ of the support $\Omega_i(\ell) := \text{supp } F_{i;\ell}$ for $i = 1, 2$.

7.3.1. The initial ℓ finite term. Let $\mathcal{O}(\underline{\epsilon}, \ell)$ denote either the Laplace–Beltrami operator $\Delta(\underline{\epsilon}, \ell)$ or the Kähler operator $\mathcal{D}(\underline{\epsilon}, \ell)$ on the Delaunay graph $G_{\underline{\epsilon},\ell}$. From Propositions 6.10 and 6.11, the $\epsilon_1\epsilon_2$ cross-term of $\log \det \mathcal{O}(\underline{\epsilon}, \ell)$ is given by the trace term

$$-\text{tr}[\mathfrak{d}_{\epsilon_1} \mathcal{O}(\ell) \cdot \Delta_{\text{cr}}^{-1} \cdot \mathfrak{d}_{\epsilon_2} \mathcal{O}(\ell) \cdot \Delta_{\text{cr}}^{-1}],$$

which can be expressed as the following double sum over triangles in $\widehat{G}_{0+,\ell}$:

$$-\frac{2}{\pi^2} \sum_{\substack{x_1 \in F_{\overline{\Omega}_1(\ell)}(\widehat{G}_{0+,\ell}) \\ x_2 \in F_{\overline{\Omega}_2(\ell)}(\widehat{G}_{0+,\ell})}} A(x_1)A(x_2) \times \left(\text{Re} \left[\frac{\overline{\nabla} F_{1;\ell}(x_1) \overline{\nabla} F_{2;\ell}(x_2)}{(z_{\text{cr}}(x_1) - z_{\text{cr}}(x_2))^4} \right] + O(|z_{\text{cr}}(x_1) - z_{\text{cr}}(x_2)|^{-5}) \right), \quad (7.1)$$

where $z_{\text{cr}}(x_i)$ is the circumcenter of x_i for $i = 1, 2$. Both F_1 and F_2 have compact support, so by Lemma 1.9 we have that

$$\overline{\nabla} F_{i;\ell}(x) = \overline{\partial} F_i \left(\frac{z_{\text{cr}}(x)}{\ell} \right) + \frac{R_{\text{cr}}}{\ell} \cdot E_i(x),$$

where $|E_i(x)|$ is bounded by a constant $B_i > 0$ independent of both x and $\ell > 0$. We begin by breaking (7.1) into two pieces and evaluate their large limits ℓ separately.

7.3.2. The subleading term. The large limit ℓ of the second part of (7.1) vanishes as the following computation shows:

$$\begin{aligned} & \left| \sum_{\substack{\mathbf{x}_1 \in F_{\bar{\Omega}_1(\ell)}(\hat{G}_{0+,\ell}) \\ \mathbf{x}_2 \in F_{\bar{\Omega}_2(\ell)}(\hat{G}_{0+,\ell})}} A(\mathbf{x}_1)A(\mathbf{x}_2) \cdot O(|z_{\text{cr}}(\mathbf{x}_1) - z_{\text{cr}}(\mathbf{x}_2)|^{-5}) \right| \\ & \leq \sum_{\substack{\mathbf{x}_1 \in F_{\bar{\Omega}_1(\ell)}(\hat{G}_{0+,\ell}) \\ \mathbf{x}_2 \in F_{\bar{\Omega}_2(\ell)}(\hat{G}_{0+,\ell})}} A(\mathbf{x}_1)A(\mathbf{x}_2) \cdot |O(|z_{\text{cr}}(\mathbf{x}_1) - z_{\text{cr}}(\mathbf{x}_2)|^{-5})| \\ & \leq \sum_{\substack{\mathbf{x}_1 \in F_{\bar{\Omega}_1(\ell)}(\mathcal{G}_{\text{cr}}) \\ \mathbf{x}_2 \in F_{\bar{\Omega}_2(\ell)}(\mathcal{G}_{\text{cr}})}} A(\mathbf{x}_1)A(\mathbf{x}_2) \cdot |O(|z_{\text{cr}}(\mathbf{x}_1) - z_{\text{cr}}(\mathbf{x}_2)|^{-5})| \\ & \leq \frac{1}{d} \frac{1}{\ell} \sum_{\substack{\mathbf{x}_1 \in F_{\bar{\Omega}_1(\ell)}(\mathcal{G}_{\text{cr}}) \\ \mathbf{x}_2 \in F_{\bar{\Omega}_2(\ell)}(\mathcal{G}_{\text{cr}})}} \frac{A(\mathbf{x}_1)}{\ell^2} \frac{A(\mathbf{x}_2)}{\ell^2} \cdot \left| O\left(\left| \frac{z_{\text{cr}}(\mathbf{x}_1)}{\ell} - \frac{z_{\text{cr}}(\mathbf{x}_2)}{\ell} \right|^{-4} \right) \right|. \end{aligned}$$

In the large limit ℓ , the sum over the triangles becomes a standard Riemann integral

$$\begin{aligned} & \leq \lim_{\ell \rightarrow \infty} \sum_{\substack{\mathbf{x}_1 \in F_{\bar{\Omega}_1(\ell)}(\mathcal{G}_{\text{cr}}) \\ \mathbf{x}_2 \in F_{\bar{\Omega}_2(\ell)}(\mathcal{G}_{\text{cr}})}} \frac{A(\mathbf{x}_1)}{\ell^2} \frac{A(\mathbf{x}_2)}{\ell^2} \cdot \left| O\left(\left| \frac{z_{\text{cr}}(\mathbf{x}_1)}{\ell} - \frac{z_{\text{cr}}(\mathbf{x}_2)}{\ell} \right|^{-4} \right) \right| \\ & = \iint_{\Omega_1 \times \Omega_2} d^2x_1 d^2x_2 \cdot |O(|x_1 - x_2|^{-4})| = O(1). \end{aligned}$$

Hence

$$\lim_{\ell \rightarrow \infty} \sum_{\substack{\mathbf{x}_1 \in F_{\bar{\Omega}_1(\ell)}(\mathcal{G}_{\text{cr}}) \\ \mathbf{x}_2 \in F_{\bar{\Omega}_2(\ell)}(\mathcal{G}_{\text{cr}})}} A(\mathbf{x}_1)A(\mathbf{x}_2) \cdot O(|z_{\text{cr}}(\mathbf{x}_1) - z_{\text{cr}}(\mathbf{x}_2)|^{-5}) = 0.$$

7.3.3. The leading term. To evaluate the first part in (7.1), we consider the norm of the difference between the original term with discrete derivative and the corresponding term with continuous derivatives, and use the previous results to get the bounds

$$\begin{aligned} & \left| \sum_{\substack{\mathbf{x}_1 \in F_{\bar{\Omega}_1(\ell)}(\hat{G}_{0+,\ell}) \\ \mathbf{x}_2 \in F_{\bar{\Omega}_2(\ell)}(\hat{G}_{0+,\ell})}} A(\mathbf{x}_1)A(\mathbf{x}_2) \right. \\ & \quad \left. \times \text{Re} \left[\frac{\bar{\nabla} F_{1;\ell}(\mathbf{x}_1) \bar{\nabla} F_{2;\ell}(\mathbf{x}_2) - \bar{\partial} F_1(z_{\text{cr}}(\mathbf{x}_1)/\ell) \bar{\partial} F_2(z_{\text{cr}}(\mathbf{x}_2)/\ell)}{(z_{\text{cr}}(\mathbf{x}_1) - z_{\text{cr}}(\mathbf{x}_2))^4} \right] \right| \end{aligned}$$

$$\begin{aligned}
 &\leq \frac{R_{\text{cr}}}{\ell} \sum_{\substack{\mathbf{x}_1 \in F_{\bar{\Omega}_1(\ell)}(\hat{G}_{0^+, \ell}) \\ \mathbf{x}_2 \in F_{\bar{\Omega}_2(\ell)}(\hat{G}_{0^+, \ell})}} \frac{A(\mathbf{x}_1)}{\ell^2} \frac{A(\mathbf{x}_2)}{\ell^2} \frac{|E_1(\mathbf{x}_1)| \cdot |\bar{\partial}F_2(z_{\text{cr}}(\mathbf{x}_2)/\ell)|}{|z_{\text{cr}}(\mathbf{x}_1)/\ell - z_{\text{cr}}(\mathbf{x}_2)/\ell|^4} \\
 &+ \frac{R_{\text{cr}}}{\ell} \sum_{\substack{\mathbf{x}_1 \in F_{\bar{\Omega}_1(\ell)}(\hat{G}_{0^+, \ell}) \\ \mathbf{x}_2 \in F_{\bar{\Omega}_2(\ell)}(\hat{G}_{0^+, \ell})}} \frac{A(\mathbf{x}_1)}{\ell^2} \frac{A(\mathbf{x}_2)}{\ell^2} \frac{|\bar{\partial}F_1(z_{\text{cr}}(\mathbf{x}_1)/\ell)| \cdot |E_2(\mathbf{x}_2)|}{|z_{\text{cr}}(\mathbf{x}_1)/\ell - z_{\text{cr}}(\mathbf{x}_2)/\ell|^4} \\
 &+ \frac{R_{\text{cr}}^2}{\ell^2} \sum_{\substack{\mathbf{x}_1 \in F_{\bar{\Omega}_1(\ell)}(\hat{G}_{0^+, \ell}) \\ \mathbf{x}_2 \in F_{\bar{\Omega}_2(\ell)}(\hat{G}_{0^+, \ell})}} \frac{A(\mathbf{x}_1)}{\ell^2} \frac{A(\mathbf{x}_2)}{\ell^2} \frac{|E_1(\mathbf{x}_1)| \cdot |E_2(\mathbf{x}_2)|}{|z_{\text{cr}}(\mathbf{x}_1)/\ell - z_{\text{cr}}(\mathbf{x}_2)/\ell|^4} \\
 &\leq \frac{R_{\text{cr}}}{\ell} \sum_{\substack{\mathbf{x}_1 \in F_{\bar{\Omega}_1(\ell)}(\hat{G}_{0^+, \ell}) \\ \mathbf{x}_2 \in F_{\bar{\Omega}_2(\ell)}(\hat{G}_{0^+, \ell})}} \frac{A(\mathbf{x}_1)}{\ell^2} \frac{A(\mathbf{x}_2)}{\ell^2} \frac{B_1 \cdot |\bar{\partial}F_2(z_{\text{cr}}(\mathbf{x}_2)/\ell)|}{|z_{\text{cr}}(\mathbf{x}_1)/\ell - z_{\text{cr}}(\mathbf{x}_2)/\ell|^4} \\
 &+ \frac{R_{\text{cr}}}{\ell} \sum_{\substack{\mathbf{x}_1 \in F_{\bar{\Omega}_1(\ell)}(\hat{G}_{0^+, \ell}) \\ \mathbf{x}_2 \in F_{\bar{\Omega}_2(\ell)}(\hat{G}_{0^+, \ell})}} \frac{A(\mathbf{x}_1)}{\ell^2} \frac{A(\mathbf{x}_2)}{\ell^2} \frac{|\bar{\partial}F_1(z_{\text{cr}}(\mathbf{x}_1)/\ell)| \cdot B_2}{|z_{\text{cr}}(\mathbf{x}_1)/\ell - z_{\text{cr}}(\mathbf{x}_2)/\ell|^4} \\
 &+ \frac{R_{\text{cr}}^2}{\ell^2} \sum_{\substack{\mathbf{x}_1 \in F_{\bar{\Omega}_1(\ell)}(\hat{G}_{0^+, \ell}) \\ \mathbf{x}_2 \in F_{\bar{\Omega}_2(\ell)}(\hat{G}_{0^+, \ell})}} \frac{A(\mathbf{x}_1)}{\ell^2} \frac{A(\mathbf{x}_2)}{\ell^2} \frac{B_1 \cdot B_2}{|z_{\text{cr}}(\mathbf{x}_1)/\ell - z_{\text{cr}}(\mathbf{x}_2)/\ell|^4} \\
 &\leq \frac{R_{\text{cr}}}{\ell} \sum_{\substack{\mathbf{x}_1 \in F_{\bar{\Omega}_1(\ell)}(\mathcal{G}_{\text{cr}}) \\ \mathbf{x}_2 \in F_{\bar{\Omega}_2(\ell)}(\mathcal{G}_{\text{cr}})}} \frac{A(\mathbf{x}_1)}{\ell^2} \frac{A(\mathbf{x}_2)}{\ell^2} \frac{B_1 \cdot |\bar{\partial}F_2(z_{\text{cr}}(\mathbf{x}_2)/\ell)|}{|z_{\text{cr}}(\mathbf{x}_1)/\ell - z_{\text{cr}}(\mathbf{x}_2)/\ell|^4} \\
 &+ \frac{R_{\text{cr}}}{\ell \ell} \sum_{\substack{\mathbf{x}_1 \in F_{\bar{\Omega}_1(\ell)}(\mathcal{G}_{\text{cr}}) \\ \mathbf{x}_2 \in F_{\bar{\Omega}_2(\ell)}(\mathcal{G}_{\text{cr}})}} \frac{A(\mathbf{x}_1)}{\ell^2} \frac{A(\mathbf{x}_2)}{\ell^2} \frac{|\bar{\partial}F_1(z_{\text{cr}}(\mathbf{x}_1)/\ell)| \cdot B_2}{|z_{\text{cr}}(\mathbf{x}_1)/\ell - z_{\text{cr}}(\mathbf{x}_2)/\ell|^4} \\
 &+ \frac{R_{\text{cr}}^2}{\ell^2} \sum_{\substack{\mathbf{x}_1 \in F_{\bar{\Omega}_1(\ell)}(\mathcal{G}_{\text{cr}}) \\ \mathbf{x}_2 \in F_{\bar{\Omega}_2(\ell)}(\mathcal{G}_{\text{cr}})}} \frac{A(\mathbf{x}_1)}{\ell^2} \frac{A(\mathbf{x}_2)}{\ell^2} \frac{B_1 \cdot B_2}{|z_{\text{cr}}(\mathbf{x}_1)/\ell - z_{\text{cr}}(\mathbf{x}_2)/\ell|^4}. \tag{7.2}
 \end{aligned}$$

In the large limit ℓ , each sum over triangles becomes a Riemann integral. Hence the large ℓ limit of the left-hand side of (7.2) is less than or equal to

$$\lim_{\ell \rightarrow \infty} \frac{c}{2\pi^2} \frac{B_1 R_{\text{cr}}}{\ell} \cdot \iint_{\Omega_1 \times \Omega_2} \frac{dx_1 dx_2}{|x_1 - x_2|^4} |\bar{\partial}F_2(x_2)|$$

$$\begin{aligned}
 &+ \lim_{\ell \rightarrow \infty} \frac{c}{2\pi^2} \frac{B_2 R_{\text{cr}}}{\ell} \cdot \iint_{\Omega_1 \times \Omega_2} \frac{dx_1 dx_2}{|x_1 - x_2|^4} |\bar{\partial} F_1(x_1)| \\
 &+ \lim_{\ell \rightarrow \infty} \frac{c}{2\pi^2} \frac{B_1 B_2 R_{\text{cr}}^2}{\ell^2} \cdot \iint_{\Omega_1 \times \Omega_2} \frac{dx_1 dx_2}{|x_1 - x_2|^4} = 0.
 \end{aligned}$$

7.3.4. Summing up. From this it follows that

$$\begin{aligned}
 &\lim_{\ell \rightarrow \infty} \sum_{\substack{x_1 \in F_{\bar{\Omega}_1(\ell)}(\hat{G}_{0^+, \ell}) \\ x_2 \in F_{\bar{\Omega}_2(\ell)}(\hat{G}_{0^+, \ell})}} A(x_1) A(x_2) \operatorname{Re} \left[\frac{\bar{\nabla} F_{1; \ell}(x_1) \bar{\nabla} F_{2; \ell}(x_2)}{(z_{\text{cr}}(x_1) - z_{\text{cr}}(x_2))^4} \right] \\
 &= \lim_{\ell \rightarrow \infty} \sum_{\substack{x_1 \in F(\hat{G}_{0^+, \ell}) \\ x_2 \in F(\hat{G}_{0^+, \ell})}} A(x_1) A(x_2) \operatorname{Re} \left[\frac{\bar{\nabla} F_{1; \ell}(x_1) \bar{\nabla} F_{2; \ell}(x_2)}{(z_{\text{cr}}(x_1) - z_{\text{cr}}(x_2))^4} \right] \\
 &= \lim_{\ell \rightarrow \infty} \sum_{\substack{x_1 \in F(\hat{G}_{0^+, \ell}) \\ x_2 \in F(\hat{G}_{0^+, \ell})}} \frac{A(x_1)}{\ell^2} \frac{A(x_2)}{\ell^2} \operatorname{Re} \left[\frac{\bar{\partial} F_1(z_{\text{cr}}(x_1)/\ell) \bar{\partial} F_2(z_{\text{cr}}(x_2)/\ell)}{(z_{\text{cr}}(x_1)/\ell - z_{\text{cr}}(x_2)/\ell)^4} \right] \\
 &= \lim_{\ell \rightarrow \infty} \sum_{\substack{x_1 \in F(G_{\text{cr}}) \\ x_2 \in F(G_{\text{cr}})}} \frac{A(x_1)}{\ell^2} \frac{A(x_2)}{\ell^2} \operatorname{Re} \left[\frac{\bar{\partial} F_1(z_{\text{cr}}(x_1)/\ell) \bar{\partial} F_2(z_{\text{cr}}(x_2)/\ell)}{(z_{\text{cr}}(x_1)/\ell - z_{\text{cr}}(x_2)/\ell)^4} \right] \\
 &= \iint_{\Omega_1 \times \Omega_2} dx_1 dx_2 \operatorname{Re} \left[\frac{\bar{\partial} F_1(x_1) \bar{\partial} F_2(x_2)}{(x_1 - x_2)^4} \right].
 \end{aligned}$$

Thus we have

$$\begin{aligned}
 &\lim_{\ell \rightarrow \infty} \operatorname{tr} [\mathfrak{d}_{\epsilon_1} \mathcal{O}(\ell) \cdot \Delta_{\text{cr}}^{-1} \cdot \mathfrak{d}_{\epsilon_2} \mathcal{O}(\ell) \cdot \Delta_{\text{cr}}^{-1}] \\
 &= \frac{2}{\pi^2} \iint_{\Omega_1 \times \Omega_2} dx_1 dx_2 \operatorname{Re} \left[\frac{\bar{\partial} F_1(x_1) \bar{\partial} F_2(x_2)}{(x_1 - x_2)^4} \right].
 \end{aligned}$$

This settles the proof of Theorem 1.10 by establishing equation (1.17).

7.4. Controlling the geometry of the lattice for small deformations

7.4.1. The limits we considered. Let us summarize what we did previously, up to Section 7.3. We begin with an infinite critical graph G_{cr} and two displacement functions F_1 and F_2 whose respective supports Ω_1 and Ω_2 are compact and whose lattice closures $\bar{\Omega}_1$ and $\bar{\Omega}_2$ are disjoint. We construct the stable Delaunay deformation $G_{\underline{\epsilon}}$ with embedding $z_{\underline{\epsilon}} = z_{\text{cr}} + \epsilon_1 F_1 + \epsilon_2 F_2$ along with a corresponding deformed operator $\mathcal{O}(\underline{\epsilon})$, where $\underline{\epsilon} = (\epsilon_1, \epsilon_2)$ is a pair of independent parameters. We then proceed

to isolate the coefficient of $\epsilon_1\epsilon_2$ in the Taylor series of $\log \det \mathcal{O}(\underline{\epsilon})$. Since the lattice closures of the supports of F_1 and F_2 are disjoint, the first trace term $\text{tr}[\mathcal{O}(\underline{\epsilon}) \cdot \mathcal{O}_{\text{cr}}^{-1}]$ contributes nothing. The only non-vanishing contribution to $\epsilon_1\epsilon_2$ comes from the second trace and can be expressed as

$$-\text{tr}[\mathfrak{d}_{\epsilon_1} \mathcal{O} \cdot \mathcal{O}_{\text{cr}}^{-1} \cdot \mathfrak{d}_{\epsilon_2} \mathcal{O} \cdot \mathcal{O}_{\text{cr}}^{-1}] \tag{7.3}$$

defined on the weak Delaunay graph \widehat{G}_{0+} (a completion of the isoradial refinement of the initial graph G_{cr} relative to the deformation). We then rescale the deformation by ℓ , consider the family of deformations $z_{\text{cr}} \rightarrow z_{\text{cr}} + \epsilon_1 F_{1;\ell} + \epsilon_2 F_{2;\ell}$ and show that the scaling limit $\ell \rightarrow \infty$ of (7.3) exists and is independent of the choice of initial critical graph G_{cr} . Stated simply, we study the nested limit

$$\lim_{\ell \rightarrow \infty} \lim_{\substack{\epsilon_1 \rightarrow 0 \\ \epsilon_2 \rightarrow 0}} (\text{tr}[\mathfrak{d}_{\epsilon_1} \mathcal{O}(\underline{\epsilon}, \ell) \cdot \mathcal{O}_{\text{cr}}^{-1} \cdot \mathfrak{d}_{\epsilon_2} \mathcal{O}(\underline{\epsilon}, \ell) \cdot \mathcal{O}_{\text{cr}}^{-1}]). \tag{7.4}$$

An interesting question is whether these two limits can be interchanged. A positive answer would be a first step in understanding if one can define a continuum limit of (the total variation of) $\log \det \mathcal{O}(\underline{\epsilon}, \ell)$ starting from an infinite Delaunay graph which is not isoradial, but rather obtained by a small smooth deformation of a Delaunay graph which is isoradial. A simpler question is the following: We know that for a given critical graph G_{cr} , limit (7.4) makes sense when $\epsilon_1, \epsilon_2 \rightarrow 0$. Is the convergence uniform with respect to all critical graphs G_{cr} ? We return to this issue in Section 8.

7.4.2. The problem with flips. The geometrical effects of a finite ϵ -deformation of a Delaunay graph G have already been discussed in Sections 5.1 and 5.2. Lemma 5.6 and Proposition 5.8 ensure that, for a given initial graph G_{cr} and a given displacement function F (with compact support), there exists a strictly positive bound $0 < \tilde{\epsilon}_F$ such that no flip occurs in the interval $0 < \epsilon < \tilde{\epsilon}_F$. However, $\tilde{\epsilon}_F$ depends non-trivially on F and on the geometry of G_{cr} . Furthermore, it is clear that such a bound cannot be made uniform with respect to all critical graphs G_{cr} . This means that given any small value $\epsilon > 0$ of the deformation parameter, flips will occur in G_ϵ for some critical graph G_{cr} within the class of all critical graphs. Consequently, the (matrix entries of the) operators $\mathfrak{d}_\epsilon \mathcal{O}(\epsilon)$ are discontinuous functions of ϵ , and it will be difficult to control them as ϵ varies.

7.5. A simple restriction to control small deformations: Enforcing a global lower bound on the edge angles

A naive but brutal way to manage the “flip problem” is to consider only a subclass of graphs G_{cr} such that the bound $\tilde{\epsilon}_F$ of Proposition 5.8 can be controlled explicitly, so that no flip occurs. Similar constraints (7.5) on the geometry of G_{cr} have been used

in the literature for other problems involving isoradial lattices, see, e.g., the paper by Bücking [3]. Our solution is given by the following lemma.

Lemma 7.1. *Let $F: \mathbb{C} \rightarrow \mathbb{C}$ be a non-zero smooth complex-valued function with compact support Ω_F . We define*

$$\check{M}_F = \max_{z \in \mathbb{C}} |\partial F(z)| + \max_{z \in \mathbb{C}} |\bar{\partial} F(z)|.$$

This is a simple modification of the bound M_F of Lemma 5.1 given by (5.2) which is now independent of the triangulation. For a generic Delaunay triangulation \mathbb{T} , we define, in analogy with ϑ_F given by (5.6) in Lemma 5.7,

$$\check{\vartheta}(\mathbb{T}) = \inf\{\theta(\mathbf{e}) : \mathbf{e} \in E(\mathbb{T})\}.$$

For a fixed, strictly positive $\check{\vartheta} > 0$, define the subset of Delaunay triangulations

$$\mathcal{F}_{\check{\vartheta}} = \{\text{Delaunay triangulation } \mathbb{T} : \check{\vartheta}(\mathbb{T}) \geq \check{\vartheta}\} \tag{7.5}$$

and the strictly positive bound

$$\check{\epsilon}_F = \mathfrak{b} \sin(2\check{\vartheta}) \check{M}_F^{-1}$$

with $\mathfrak{b} = \sqrt{10} - 3$ as in Lemma 5.6.

For any triangulation $\mathbb{T} \in \mathcal{F}_{\check{\vartheta}}$ and any scaling parameter $\ell > 0$, the Delaunay deformation $z \rightarrow z_{\epsilon; \ell} = z + \epsilon F_{\ell}(z)$ of \mathbb{T} preserves all the edges of \mathbb{T} if

$$0 < \epsilon \leq \check{\epsilon}_F, \quad \ell > 0 \quad \text{and} \quad \mathbb{T} \in \mathcal{F}_{\check{\vartheta}} \Rightarrow E(\mathbb{T}_{\epsilon, \ell}) = E(\mathbb{T}).$$

In other words, no flip occurs as long as $0 < \epsilon \leq \check{\epsilon}_F$.

Proof. The mapping $z_{\epsilon, \ell}: V(\mathbb{T}_{\epsilon, \ell}) \rightarrow \mathbb{C}$ is an embedding provided there are no “collisions”, that is, $z_{\epsilon, \ell}(\mathbf{u}) \neq z_{\epsilon, \ell}(\mathbf{v})$ whenever $\mathbf{u} \neq \mathbf{v}$ are distinct vertices in $V(\mathbb{T}_{\text{cr}})$. Equivalently, $1 + \epsilon dF_{\ell}(\mathbf{u}, \mathbf{v})$ must not vanish. Apply the fundamental theorem of calculus using $\gamma_{\mathbf{uv}}(\tau) := \frac{\tau z_{\text{cr}}(\mathbf{u})}{\ell} + \frac{(1-\tau)z_{\text{cr}}(\mathbf{v})}{\ell}$,

$$\begin{aligned} |dF_{\ell}(\mathbf{u}, \mathbf{v})| &= \left| \frac{F(z_{\text{cr}}(\mathbf{u})/\ell) - F(z_{\text{cr}}(\mathbf{v})/\ell)}{z_{\text{cr}}(\mathbf{u})/\ell - z_{\text{cr}}(\mathbf{v})/\ell} \right| \\ &= \frac{1}{|z_{\text{cr}}(\mathbf{u})/\ell - z_{\text{cr}}(\mathbf{v})/\ell|} \cdot \left| \int_0^1 d\tau \frac{d}{d\tau} F(\gamma_{\mathbf{uv}}(\tau)) \right| \\ &= \left| \int_0^1 d\tau \partial F(\gamma_{\mathbf{uv}}(\tau)) + \frac{\bar{z}_{\text{cr}}(\mathbf{u}) - \bar{z}_{\text{cr}}(\mathbf{v})}{z_{\text{cr}}(\mathbf{u}) - z_{\text{cr}}(\mathbf{v})} \int_0^1 d\tau \bar{\partial} F(\gamma_{\mathbf{uv}}(\tau)) \right| \\ &\leq \left| \int_0^1 d\tau \partial F(\gamma_{\mathbf{uv}}(\tau)) \right| + \left| \frac{\bar{z}_{\text{cr}}(\mathbf{u}) - \bar{z}_{\text{cr}}(\mathbf{v})}{z_{\text{cr}}(\mathbf{u}) - z_{\text{cr}}(\mathbf{v})} \right| \cdot \left| \int_0^1 d\tau \bar{\partial} F(\gamma_{\mathbf{uv}}(\tau)) \right| \\ &\leq \max |\partial F| + \max |\bar{\partial} F| = \check{M}_F. \end{aligned}$$

By construction, $\check{\vartheta} \leq \vartheta_{F_\ell}$, and taken it together with the fact that $M_{F_\ell} \leq \check{M}_F$, we can conclude that $\check{\epsilon}_F \leq \bar{\epsilon}_{F_\ell}$. As long as $\epsilon < \check{\epsilon}_F$, we can apply Lemma 5.7 and conclude that the edge set $E(T) \subset E(T_{\epsilon, \ell})$. Since T is a triangulation, no chords appear, and hence $E(T) = E(T_{\epsilon, \ell})$. We stress that this bound on ϵ is valid and independent of all values of the scaling parameter $\ell > 0$, including $\ell = \infty$. ■

8. Finite ϵ variations, beyond the linear approximation

8.1. Outline of the section

In this section, we now consider deformations of an initial critical lattice G_{cr} implemented by a local diffeomorphism of the plane

$$z \rightarrow z + \epsilon F(z, \bar{z})$$

for small values of a deformation parameter ϵ , and a fixed smooth (but non-analytic) displacement function F with compact support. We shall look for uniform bounds for the variation of the operators Δ and \mathcal{D} with respect to ϵ , independent of the particular geometry of the initial critical graph G_{cr} , except for its isoradius R_{cr} .

We therefore need to consider generic Delaunay deformations and take into account the occurrence of edge flips in the deformed Delaunay graph $G_{cr} \rightarrow G_\epsilon$. These flips were avoided in the stable deformation scheme studied in Sections 5, 6 and 7 by imposing tight bounds on the parameter ϵ .

For a fixed smooth displacement function F and a deformation parameter ϵ , it will be necessary to compare the corresponding Delaunay and rigid deformations, as explained in Section 5. We discuss this in Section 8.2, as well as the concept of “backtracking a deformation without flips”.

In Section 8.3, we give explicit variational formulas for the various operators ∇ , $\bar{\nabla}$, Δ and \mathcal{D} , as well as the circumradii R in the case of a rigid deformation of the graph; see Definition 5.3.

In Section 8.4, we derive integral representations of the variations of these objects taking flips into account.

In Sections 8.5 and 8.6, we give variational formulas for the discrete derivatives ∇ and $\bar{\nabla}$, as well as the circumradius of a face. The later result, given in Proposition 8.1, is important and leads to uniform bounds on the variations of ∇ , $\bar{\nabla}$, Δ and \mathcal{D} with respect to ϵ ; see Proposition 8.2.

In Section 8.7, we deduce strong results on the uniform convergence of the scaling limit $\ell \rightarrow \infty$ for Δ (Propositions 8.3 and 8.4) and of the scaling limit of the corresponding second-order bi-local trace term (which leads to the OPE) (Proposition 8.7).

In Section 8.8, we finally address the problem of interchanging the $\underline{\epsilon} \rightarrow 0$ deformation limit and $\ell \rightarrow \infty$ scaling limit when evaluating the bi-local trace term of $\log \det \Delta(\underline{\epsilon}, \ell)$. Specifically, we consider the scaling limit $\ell \rightarrow \infty$ of the bi-local term in the variation of $\log \det \Delta$ for non-zero deformation parameters. The uniformity of this limit depends on a technical bound on the discrete derivatives of the function $p_3(u, v)$ defined for isoradial graphs by (2.4). We explicate this condition and conjecture that the bound is valid for general isoradial graphs in Conjecture 8.5. Provided the bound is satisfied, we prove in Proposition 8.7 that the bi-local trace term has a uniform scaling limit, and that the scaling limit $\ell \rightarrow \infty$ and the $\underline{\epsilon} \rightarrow 0$ deformation parameter limit both exist, are uniform, and commute (see Proposition 8.8).

Finally, in Section 8.9, we address the same questions for deformations of the Kähler operator \mathcal{D} . Proposition 8.9 gives a uniform bound on the variation of \mathcal{D} , but it implies that there is no general scaling limit $\ell \rightarrow \infty$ for \mathcal{D} for non-zero values of the deformation parameters $\underline{\epsilon}$ (Proposition 8.10). This is different from the situation for Δ . We argue that the best uniform convergence result to be expected for the bi-local trace term is a scaling limit where both $\ell \rightarrow \infty$ and $\underline{\epsilon} \rightarrow 0$ simultaneously, keeping the constant $\ell \underline{\epsilon} = \underline{c}$ (Proposition 8.11).

8.2. Deforming triangulations with and without flips

We now define and compare Delaunay deformations of graphs and connectivity-fixed deformations of the same graphs.

8.2.1. Delaunay deformations (with flips). We start from an (isoradial) Delaunay graph $G_0 = G_{cr}$ and then deform its embedding $v \mapsto z_0(v)$ using a smooth function $F: \mathbb{C} \rightarrow \mathbb{C}$ with compact support to obtain a mapping

$$v \mapsto z_\epsilon(v) = z_0(v) + \epsilon F(z_0(v))$$

for vertices v of G_0 . Using the method for proving Lemma 5.1, it is simple to prove that the mapping $v \mapsto z_\epsilon(v)$ defines an embedding of the vertex set $V(G_0)$ as long as ϵ is small enough, namely,

$$|\epsilon| < \dot{\epsilon}_F = (\max(|\partial F|) + \max(|\bar{\partial} F|))^{-1}. \tag{8.1}$$

Indeed, we have

$$\begin{aligned} \left| \frac{z_\epsilon(u) - z_\epsilon(v)}{z_0(u) - z_0(v)} \right| &= \left| 1 - \epsilon \frac{F(z_0(u)) - F(z_0(v))}{z_0(u) - z_0(v)} \right| \\ &\geq |1 - \epsilon(\max |\partial F| + \max |\bar{\partial} F|)|. \end{aligned}$$

This ensures that if $u \neq v$, $|z_\epsilon(u) - z_\epsilon(v)| > 0$ at least as long as (8.1) holds.

As in Definition 5.2, the Delaunay graph G_ϵ is obtained by applying the Delaunay construction to the set of deformed coordinates $z_\epsilon(v)$ for $v \in G_0$. The vertices of G_ϵ and G_0 are identical by definition, however the edges and the faces of G_ϵ may differ from those of G_0 since the Delaunay constraints may force flips to occur during the deformation. Unlike the setup of Lemma 5.7, the inclusion $E(G_0) \subset E(G_\epsilon)$ may now fail. Generically, G_ϵ will be a triangulation regardless of whether the initial graph G_0 is a triangulation.

The operators $\Delta(\epsilon)$, $\mathcal{D}(\epsilon)$ and $\underline{\Delta}(\epsilon)$ act on the same space of functions $\mathbb{C}^{V(G_\epsilon)} = \mathbb{C}^{V(G_0)}$ irrespective of ϵ since, by construction, the vertex sets $V(G_\epsilon) = V(G_0)$ agree. Denote by ∇_ϵ and $\bar{\nabla}_\epsilon$ the discrete derivative operators relative to the faces of G_ϵ , both of which are operators $\mathbb{C}^{V(G_\epsilon)} \rightarrow \mathbb{C}^{F(G_\epsilon)}$. Note that, in general, the set of deformed and critical faces differ, i.e., $F(G_\epsilon) \neq F(G_0)$. Similarly, let A_ϵ and R_ϵ denote the area and circumradius functions for the faces of G_ϵ .

8.2.2. Geometric back-deformation: Deforming without flips. We define the *rigid back-deformation* $G_{\epsilon;0}$ of the Delaunay graph G_ϵ to be the graph whose vertex set and embedding are identical to those of our initial (weak) Delaunay graph G_0 , but whose edge and face sets coincide with those of the Delaunay graph G_ϵ obtained from G_0 by a Delaunay deformation. The construction of $G_{\epsilon;0}$ can be seen in two stages:

- (1) First G_ϵ is the end point of the continuous family of Delaunay deformations

$$G_0 \rightarrow G_\epsilon \rightarrow G_\epsilon: 0 \rightarrow \epsilon \rightarrow \epsilon$$

obtained by continuously deforming the embedding $z_0 \mapsto z_\epsilon = z_0 + \epsilon F(z_0)$ of the initial graph G_0 over the range $0 \leq \epsilon \leq \epsilon$, while maintaining the Delaunay condition (and performing edge flips as required) at each stage of the deformation.

- (2) Then, starting with G_ϵ , reverse the deformation z_ϵ by letting ϵ move from ϵ to 0,

$$G_\epsilon \rightarrow G_{\epsilon;\epsilon} \rightarrow G_{\epsilon;0}: \epsilon \rightarrow \epsilon \rightarrow 0$$

but *without performing any edge flips*. In general, $G_{\epsilon;\epsilon}$ will denote the graph whose vertex, edge, and face sets coincide with G_ϵ but whose embedding is z_ϵ .

More schematically,

$$\begin{array}{ccccc}
 0 & \xrightarrow{\epsilon} & \epsilon & \xrightarrow{\epsilon} & 0 \\
 G_0 & \xrightarrow{\text{Delaunay}} & G_\epsilon & \xrightarrow{\text{rigid}} & G_{\epsilon;0}.
 \end{array} \tag{8.2}$$

It is clear that $G_{\epsilon;0}$ is a graph (and, in general, a triangulation) with the vertex set as the original Delaunay graph G_0 , but is generically *not a Delaunay graph*.

8.2.3. An illustrative example. Let us give a simple but illustrative example of such deformations of a triangulation $T_0 \rightarrow T_\epsilon \rightarrow T_{\epsilon:0}$. The original triangulation T_0 is a biperiodic lattice. Vertices are labeled by $(m, n) \in \mathbb{Z}^2$ with coordinates

$$z_0(m, n) = b\left(m + \frac{n}{2}\right) + in, \quad 0 < b \ll 1 \text{ a small parameter.}$$

Hence the Delaunay triangulation T_0 is made of “thin” up and down triangles such that

$$\text{height} = 1, \quad \text{basis} = b.$$

We choose as a deformation function a simple shear parallel to the real axis, so that the deformed coordinates of vertices are

$$z_\epsilon(m, n) = b\left(m + \frac{n}{2}\right) + in + \epsilon n.$$

The effect of a Delaunay deformation $T_0 \rightarrow T_\epsilon$ is depicted in Figure 24, on the special case of $b = \frac{1}{10}$, and for $0 \leq \epsilon \leq \epsilon_0 = \frac{1}{10}$. Note that a flip occurs for every

$$\epsilon = \frac{2k + 1}{2}b, \quad k \in \mathbb{Z},$$

and that the Delaunay deformation $T_0 \rightarrow T_\epsilon$ is then periodic

$$T_{\epsilon+kb} = T_\epsilon, \quad k \in \mathbb{Z}.$$

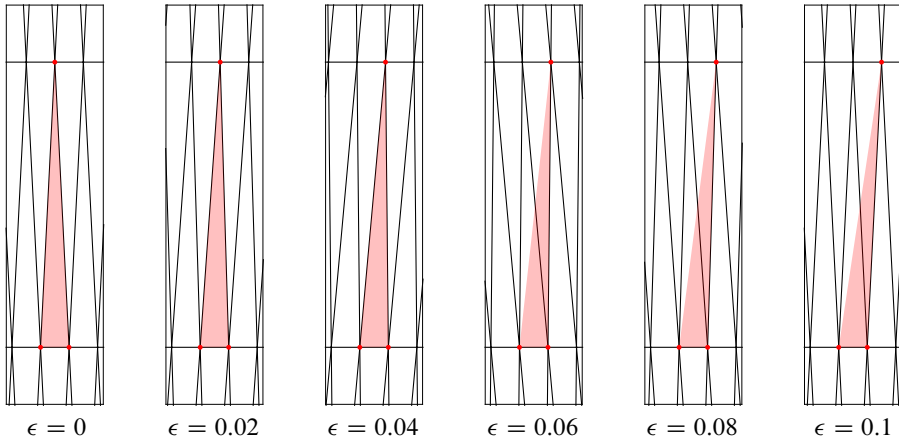


Figure 24. Deformation of a periodic isoradial Delaunay triangulation $T_0 \rightarrow T_\epsilon$ by a global shear $z \rightarrow z + \epsilon \operatorname{Im} z$, keeping it Delaunay. On this example, the base and the height of the triangles are $b = \frac{1}{10}$ and $h = 1$, respectively, so that a flip occur for $\epsilon = \frac{b}{2} = \frac{1}{20}$, and we choose $\epsilon = b = \frac{1}{10}$. Since a flip occurs at $\epsilon_f = \frac{b}{2}$, a triangle such as the one depicted in red, which is an original face of T_0 , stays a face of T_ϵ for $0 < \epsilon < \epsilon_f$, but is not a face after the flip for $\epsilon > \epsilon_f$.

Note also that if

$$0 \ll b \ll \epsilon \ll 1,$$

a large number of flips $N_{\text{flip}}(\epsilon) \simeq \frac{\epsilon}{b}$ occur, even when ϵ is small. The corresponding no-flip back-deformation $\epsilon: \epsilon_0 \rightarrow 0$ which sends back $T_{\epsilon_0} \rightarrow T_{\epsilon;0}$ is depicted in Figure 25. It is clear in this figure that no back-flip occurs at $\epsilon = 0.05$, so that an original face of T_{ϵ_0} stays a face of $T_{\epsilon;0}$. However, $T_{\epsilon;0}$ is a triangulation which is not Delaunay anymore.

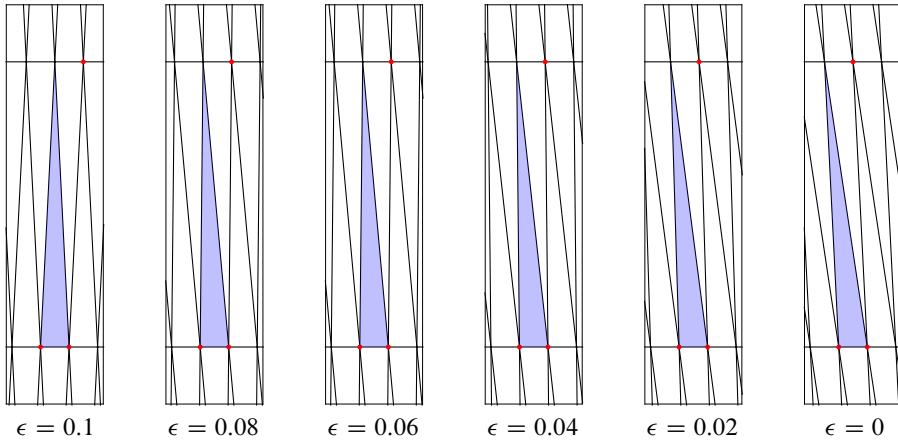


Figure 25. The back-deformation of the triangulation of Figure 24 $T_\epsilon \rightarrow T_{\epsilon;0}$, keeping the edges and faces of the triangulations fixed (no-flips). An original face of T_ϵ (in blue) stays a face of $T_{\epsilon;0}$. However, $T_{\epsilon;0}$ is not Delaunay.

8.3. Full variation of operators without flips

8.3.1. Variation of the area. Consider the variation of the triangulation $T \rightarrow T_\epsilon$ given by deforming the embedding $z(u) \rightarrow z_\epsilon(u) = z(u) + \epsilon F(u)$ without flips (so that, in fact, T_ϵ should be denoted by $T_{0;\epsilon}$ with the notations of the previous section). For a triangle f , the full variation of its area is from (3.2) and (3.8)

$$A \rightarrow A_\epsilon = A(1 + \epsilon(\nabla F + \bar{\nabla} \bar{F}) + \epsilon^2(\nabla F \bar{\nabla} \bar{F} - \bar{\nabla} F \nabla \bar{F})). \tag{8.3}$$

For brevity, $D(\epsilon; F)$ will denote the scaling factor

$$D(\epsilon; F) = 1 + \epsilon(\nabla F + \bar{\nabla} \bar{F}) + \epsilon^2(\nabla F \bar{\nabla} \bar{F} - \bar{\nabla} F \nabla \bar{F}). \tag{8.4}$$

8.3.2. Variation of the discrete derivatives. The vertex sets $V(T)$ and $V(T_\epsilon)$ are, by definition, identical, and the face sets $F(T)$ and $F(T_\epsilon)$ agree so long as no flips occur

in the deformation $T \rightarrow T_\epsilon$. Consequently, the nabla operators ∇ and ∇_ϵ (and their conjugates $\bar{\nabla}$ and $\bar{\nabla}_\epsilon$) share a common range and domain. Accordingly, we have

$$\begin{aligned} \nabla \rightarrow \nabla_\epsilon &= \frac{1 + \epsilon \bar{\nabla} \bar{F}}{D(\epsilon; F)} \nabla - \frac{\epsilon \nabla \bar{F}}{D(\epsilon; F)} \bar{\nabla}, \\ \bar{\nabla} \rightarrow \bar{\nabla}_\epsilon &= \frac{1 + \epsilon \nabla F}{D(\epsilon; F)} \bar{\nabla} - \frac{\epsilon \bar{\nabla} F}{D(\epsilon; F)} \nabla. \end{aligned} \tag{8.5}$$

8.3.3. A word of caution: deformations of functions. Recall that we may *restrict* a smooth, complex-valued function $G: \mathbb{C} \rightarrow \mathbb{C}$ to the vertex set of the triangulation T using its graph embedding $z: V(T) \rightarrow \mathbb{C}$. Bearing some abuse of notation, we define and denote this restriction by $G(v) := G(z(v))$ for vertices $v \in V(T)$. Some care is needed when restricting a smooth function G to the deformed triangulation T_ϵ . The vertex sets of T and T_ϵ are identical but, of course, their respective embeddings z and z_ϵ are not, and consequently the functions $v \mapsto G(z(v))$ and $v \mapsto G(z_\epsilon(v))$ do not agree. In order to side-step this discrepancy, we introduce a deformed smooth function $G_\epsilon: \mathbb{C} \rightarrow \mathbb{C}$ defined implicitly by

$$G_\epsilon(w + \epsilon F(w)) = G(w)$$

for all $w \in \mathbb{C}$, where $\epsilon \geq 0$ is fixed and sufficiently small. By construction,

$$G_\epsilon(z_\epsilon(v)) = G(z(v)) =: G(v).$$

To stress the role of the deformed embedding z_ϵ , we shall define and denote $G_\epsilon(v) := G_\epsilon(z_\epsilon(v))$ for $v \in V(T_\epsilon)$. When $G = F$, this allows us to write

$$z_{\epsilon+\epsilon'}(v) = z(v) + (\epsilon + \epsilon')F(z(v)) = z_\epsilon + \epsilon'F_\epsilon(z_\epsilon(v)). \tag{8.6}$$

8.3.4. Variation of the circumradii. The full variation of the circumradius $R(\mathfrak{f})$ of a face is more complicated. For a face with vertices labeled 1, 2, 3, i.e., $\mathfrak{f} = (123)$ using (3.3), we get

$$R^2 \rightarrow R_\epsilon^2 = R^2 \frac{N_{12}(\epsilon; F)N_{23}(\epsilon; F)N_{31}(\epsilon; F)}{D(\epsilon; F)^2}$$

with

$$\begin{aligned} N_{uv}(\epsilon; F) &= 1 + \epsilon(\nabla F + \bar{\nabla} \bar{F} + \bar{C}_{uv} \nabla \bar{F} + C_{uv} \bar{\nabla} F) \\ &\quad + \epsilon^2(\nabla F \bar{\nabla} \bar{F} + \bar{\nabla} F \nabla \bar{F} + \bar{C}_{uv} \nabla F \nabla \bar{F} + C_{uv} \bar{\nabla} F \bar{\nabla} \bar{F}), \end{aligned}$$

where C_{uv} for an (unoriented) edge $\bar{u}\bar{v}$ denotes

$$C_{uv} = \frac{\bar{z}(u) - \bar{z}(v)}{z(u) - z(v)}. \tag{8.7}$$

8.3.5. Variation of the operators. Thus we get the variation of the Laplacian operators from

$$\begin{aligned} \Delta &\rightarrow \Delta(\epsilon) = 2(\nabla_\epsilon^\top A_\epsilon \nabla_\epsilon + \bar{\nabla}_\epsilon^\top A_\epsilon \bar{\nabla}_\epsilon), \\ \mathcal{D} &\rightarrow \mathcal{D}(\epsilon) = 4\bar{\nabla}_\epsilon^\top \frac{A_\epsilon}{R_\epsilon^2} \nabla_\epsilon \end{aligned}$$

that we do not write explicitly. Note that these expressions are rational functions in ϵ , and the results of Section 5.3 can be recovered by keeping only the first-order terms in the series expansions (in ϵ).

8.4. Full variation of operators under Delaunay deformations (with flips)

Here we address the case of a critical triangulation $T = T_{\text{cr}}$ with isoradius $R_0 > 0$ whose embedding undergoes a deformation

$$z \rightarrow z_\epsilon := z + \epsilon F,$$

where flips are allowed, so that the deformed graph T_ϵ remains Delaunay. As before, the displacement function F is the (restriction) of a smooth complex-valued function on the plane with compact support. We consider the full variation of the operators associated to the deformation $T_{\text{cr}} \rightarrow T_\epsilon$, namely,

$$\delta\Delta(\epsilon) = \Delta(\epsilon) - \Delta_{\text{cr}}, \quad \delta\mathcal{D}(\epsilon) = \mathcal{D}(\epsilon) - \mathcal{D}_{\text{cr}}$$

instead of the instantaneous, first-order terms $\mathfrak{d}_\epsilon\Delta$ and $\mathfrak{d}_\epsilon\mathcal{D}$ in the respective ϵ -expansions, as done in Sections 5.3 and 6. We shall need uniform estimates for the $\epsilon \rightarrow 0$ limit of terms related to the variations $\delta\Delta(\epsilon)$ and $\delta\mathcal{D}(\epsilon)$ which are independent of the initial critical lattice T_{cr} . Furthermore, uniform estimates for the $R_0 \rightarrow 0$ limit will be needed, as this is synonymous with the $\ell \rightarrow \infty$ scaling limit.

Unfortunately, the exact results of the previous Section 8.3 cannot be directly applied, since flips generically occur within the continuous family of Delaunay graphs T_ϵ as the deformation parameter ϵ moves from zero to $\epsilon > 0$. Nevertheless, we may write each variation as the integral of a derivative, and then try to get uniform bounds on the derivatives. This is what we discuss in the remaining part of this section.

Let us first consider the simpler case of the Laplace–Beltrami operator Δ . We can write

$$\delta\Delta(\epsilon) = \int_0^\epsilon d\epsilon \Delta'(\epsilon) \quad \text{with} \quad \Delta'(\epsilon) = \frac{d}{d\epsilon} \Delta(\epsilon) = \mathfrak{d}_\epsilon \Delta(\epsilon). \tag{8.8}$$

Indeed, since F is smooth with compact support, there is a finite (possibly large) number of flips as ϵ increases, and we know that $\Delta(\epsilon)$ is a continuous function of ϵ ,

and its derivative exists and is continuous in the interval between the flips. Therefore, the derivative $\Delta'(\varepsilon)$ is bounded and piecewise continuous, so that integral (8.8) makes sense. For a given value $\varepsilon \geq 0$, the first-order term in formula (5.11) extends to the case of $\Delta(\varepsilon)$ defined on T_ε and with respect to the transported displacement function F_ε in the plane,

$$\Delta'(\varepsilon) = \nabla_\varepsilon^\top \cdot A_\varepsilon \cdot \mathfrak{D}_\varepsilon \cdot \nabla_\varepsilon + \bar{\nabla}_\varepsilon^\top \cdot A_\varepsilon \cdot \bar{\mathfrak{D}}_\varepsilon \cdot \bar{\nabla}_\varepsilon \tag{8.9}$$

with

$$\mathfrak{D}_\varepsilon = -4\bar{\nabla}_\varepsilon F_\varepsilon, \quad \bar{\mathfrak{D}}_\varepsilon = -4\nabla_\varepsilon \bar{F}_\varepsilon. \tag{8.10}$$

Similarly, we can write the variation of the Kähler operator as

$$\delta \mathcal{D}(\varepsilon) = \int_0^\varepsilon d\varepsilon \mathcal{D}'(\varepsilon), \quad \mathcal{D}'(\varepsilon) = \frac{d}{d\varepsilon} \mathcal{D}(\varepsilon) = \mathfrak{d}_\varepsilon \mathcal{D}(\varepsilon).$$

The results of Section 5.3 give for the derivative of \mathcal{D}

$$\mathcal{D}'(\varepsilon) = \bar{\nabla}_\varepsilon^\top A_\varepsilon \mathfrak{K}_\varepsilon \nabla_\varepsilon + \nabla_\varepsilon^\top A_\varepsilon \mathfrak{J}_\varepsilon \nabla_\varepsilon + \bar{\nabla}_\varepsilon^\top A_\varepsilon \bar{\mathfrak{J}}_\varepsilon \bar{\nabla}_\varepsilon \tag{8.11}$$

with

$$\begin{aligned} \mathfrak{K}_\varepsilon &= -\frac{4}{R_\varepsilon^2} (\nabla_\varepsilon F_\varepsilon + \bar{\nabla}_\varepsilon \bar{F}_\varepsilon + C_\varepsilon \bar{\nabla}_\varepsilon F_\varepsilon + \bar{C}_\varepsilon \nabla_\varepsilon \bar{F}_\varepsilon), \\ \mathfrak{J}_\varepsilon &= -\frac{4}{R_\varepsilon^2} \bar{\nabla}_\varepsilon F_\varepsilon, \quad \bar{\mathfrak{J}}_\varepsilon = -\frac{4}{R_\varepsilon^2} \nabla_\varepsilon \bar{F}_\varepsilon \end{aligned} \tag{8.12}$$

and with the C_ε and \bar{C}_ε defined by (5.13) for faces the triangulation T_ε , namely, for a face $\mathfrak{f} = (123)$,

$$C(\mathfrak{f}) = C_{123} = \frac{\bar{z}_1 - \bar{z}_2}{z_1 - z_2} + \frac{\bar{z}_2 - \bar{z}_3}{z_2 - z_3} + \frac{\bar{z}_3 - \bar{z}_1}{z_3 - z_1}. \tag{8.13}$$

Note that we can decompose $C(\mathfrak{f})$ as a sum of the terms C_{uv} defined in (8.7) for edges $\bar{u}\bar{v}$ of \mathfrak{f} . Specifically, $C(123) = C_{12} + C_{23} + C_{31}$, where $\mathfrak{f} = (123)$.

8.5. Uniform bounds under Delaunay deformations (with flips)

8.5.1. Bounds on continuous derivatives. Now we study whether it is possible to give uniform bounds with respect to ε and T_ε on the various coefficients A_ε , R_ε , \mathfrak{D}_ε , \mathfrak{K}_ε and \mathfrak{J}_ε of the previous Section 8.4, and on the operators ∇_ε and $\bar{\nabla}_\varepsilon$. From now on, let $F: \mathbb{C} \rightarrow \mathbb{C}$ be a given smooth deformation function with compact support. Let

$$\begin{aligned} M_1 &= \sup_{z \in \mathbb{C}} \max\{|\partial F(z)|, |\bar{\partial} F(z)|\}, \\ M_2 &= \sup_{z \in \mathbb{C}} \max\{|\partial^2 F(z)|, |\partial \bar{\partial} F(z)|, |\bar{\partial}^2 F(z)|\}. \end{aligned} \tag{8.14}$$

We will consider the transported function F_ϵ defined by (8.6), and the transported version of (8.14)

$$M_1(\epsilon) = \sup_{z \in \mathbb{C}} \max[|\partial F_\epsilon(z)|, |\bar{\partial} F_\epsilon(z)|],$$

$$M_2(\epsilon) = \sup_{z \in \mathbb{C}} \max[|\partial^2 F_\epsilon(z)|, |\partial \bar{\partial} F_\epsilon(z)|, |\bar{\partial}^2 F_\epsilon(z)|].$$

By differentiating the functional relation (8.6) between F and F_ϵ , one gets the general inequalities

$$M_1(\epsilon) \leq \bar{M}_1(\epsilon) = \frac{M_1}{1 - 2\epsilon M_1}, \quad M_2(\epsilon) \leq \bar{M}_2(\epsilon) = \frac{M_2}{(1 - 2\epsilon M_1)^3} \tag{8.15}$$

valid as long as ϵ is small enough, namely,

$$0 \leq \epsilon < \check{\epsilon}_F = \frac{1}{2M_1},$$

which ensures that F_ϵ is not multivalued (and stays smooth with compact support).

8.5.2. Bounds on discrete derivatives. Let T_{cr} be a critical (Delaunay isoradial) triangulation with isoradius R_0 , and let T_ϵ be the Delaunay triangulation T_ϵ obtained by the ϵ -deformation $z \rightarrow z + \epsilon F$. We shall establish bounds on the norm of the discrete derivatives of F_ϵ on the triangulation T_ϵ , as well as inequalities on the radii $R(\mathfrak{f})$ of the faces of T_ϵ .

First we define for a generic triangulation T and a generic smooth function G with compact support

$$B_G(T) = \sup_{\text{faces } \mathfrak{f} \in T} \max(|\nabla G(\mathfrak{f})|, |\bar{\nabla} G(\mathfrak{f})|).$$

We use Lemma 1.9, which gives a bound on the difference between the discrete derivative $\nabla G(\mathfrak{f})$ and the continuous derivative ∂G of G at the circumcenter of \mathfrak{f} . This bound involves the circumradius of \mathfrak{f} and the maximum of the second derivative of G inside the circumcircle. Denote the maximum of the circumradii of the faces \mathfrak{f} of a triangulation T by

$$R_{\max}(T) = \max_{\mathfrak{f} \in T} R(\mathfrak{f}).$$

For the initial critical triangulation T_{cr} , Lemma 1.9 implies

$$B_F(T_{cr}) \leq M_1 + 4M_2 R_0$$

but for T_ϵ , it becomes

$$B_F(T_\epsilon) \leq M_1(\epsilon) + 4M_2(\epsilon) R_{\max}(T_\epsilon),$$

and we need an estimate of $R_{\max}(T_\epsilon)$.

8.6. Inequalities for general variations of circumradii (with or without flips)

8.6.1. The problem. In order to get a bound on $R_{\max}(T_\epsilon)$, we now derive a bound on the variation of the circumradius of the faces, of a triangulation under a deformation $z \rightarrow z + \epsilon F$.

Let us consider the following general deformation scheme. We start with an initial Delaunay triangulation T_0 which need not be isoradial. We deform the embedding $z \rightarrow z + \epsilon F(z)$ of T_0 within the range $0 \leq \epsilon \leq \epsilon$ (with $\epsilon < \epsilon_F$ defined by (8.1)). If at any stage of the deformation the circumradii $R(f_1)$ and $R(f_2)$ of two neighboring faces f_1 and f_2 agree, we may either (1) *perform an edge flip*, so that f_1, f_2 are replaced by two new faces f'_1, f'_2 or (2) *not perform the flip*. Thus we get a family of triangulations $\{T_\epsilon : \epsilon \in [0, \epsilon]\}$, in general, not Delaunay, which share the same vertex set and have vertex embeddings $z_\epsilon = z_0 + \epsilon F(z_0)$.

Now let us consider an initial face (triangle) f_0 of T_0 , with initial circumradius $R(0) = R_0(f_0)$. When deforming T_ϵ from 0 to ϵ , we can continuously follow the face f_0 , and when it sustains a flip, we *choose one of the two faces* created by the flip. In this way we get a ‘‘continuous’’ family of faces $\{f_\epsilon \in T_\epsilon : \epsilon \in [0, \epsilon]\}$, so that $\epsilon \mapsto R(f_\epsilon)$ is a continuous piecewise differentiable function (this is a crucial point for the following argument).

8.6.2. Bounds on the derivative of R and consequences. Now, in between the flips, from (5.15), (5.16) the derivative of the circumradius $R(f_\epsilon)$ of this face f_ϵ is

$$\begin{aligned} R'(f_\epsilon) &= \frac{d}{d\epsilon} R(f_\epsilon) \\ &= \frac{R(f_\epsilon)}{2} (\nabla_\epsilon F_\epsilon(f_\epsilon) + \bar{\nabla}_\epsilon \bar{F}_\epsilon(f_\epsilon) + C_\epsilon(f_\epsilon) \bar{\nabla}_\epsilon F_\epsilon(f_\epsilon) + \bar{C}_\epsilon(f_\epsilon) \nabla_\epsilon \bar{F}_\epsilon(f_\epsilon)). \end{aligned}$$

Using Lemma 1.9 again, for this face f_ϵ of the triangulation T_ϵ , we get the bound

$$|\nabla_\epsilon F_\epsilon(f_\epsilon)| \quad \text{and} \quad |\bar{\nabla}_\epsilon \bar{F}_\epsilon(f_\epsilon)| \leq M_1(\epsilon) + 4R(f_\epsilon)M_2(\epsilon),$$

and from the definition of C (8.13), we have

$$|C_\epsilon(f_\epsilon)| \leq 3.$$

We thus get the bound

$$\left| \frac{d}{d\epsilon} R(f_\epsilon) \right| \leq 4\bar{M}_1(\epsilon)R(f_\epsilon) + 16\bar{M}_2(\epsilon)R(f_\epsilon)^2. \tag{8.16}$$

Remember that the functions $\bar{M}_1(\epsilon)$ and $\bar{M}_2(\epsilon)$ are explicitly known functions of ϵ and the constants M_1 and M_2 associated to the displacement function F ,

$$\bar{M}_1(\epsilon) = \frac{M_1}{1 - 2\epsilon M_1}, \quad \bar{M}_2(\epsilon) = \frac{M_2}{(1 - 2\epsilon M_1)^3}.$$

8.6.3. Bounds on the circumradii $R(\mathbf{f}_\epsilon)$. Using inequality (8.16), we get uniform bounds on the variation of the circumradius of faces $R(\mathbf{f}_\epsilon)$ under deformations $z \rightarrow z_\epsilon = z + \epsilon F(z)$.

Proposition 8.1. *The radius of the face \mathbf{f}_ϵ satisfies the inequalities*

$$\bar{R}_-(\epsilon, R(\mathbf{f}_0)) \leq R(\mathbf{f}_\epsilon) \leq \bar{R}_+(\epsilon, R(\mathbf{f}_0)) \tag{8.17}$$

with the functions of the radius variable R

$$\bar{R}_+(\epsilon, R) = \frac{R}{(1 + M_2 R/M_1)(1 - 2M_1\epsilon)^2 - (M_2 R/M_1)(1 - 2M_1\epsilon)^{-2}} \tag{8.18}$$

and

$$\bar{R}_-(\epsilon, R) = \frac{R(1 - 2M_1\epsilon)^2}{1 + (8M_2 R/M_1) \log(1/(1 - 2M_1\epsilon))}. \tag{8.19}$$

Inequality (8.17) is satisfied at least if

$$0 \leq \epsilon < \epsilon_{\max}(R(\mathbf{f}_0)) \quad \text{with} \quad \epsilon_{\max}(R) := \frac{1}{2M_1} \left(1 - \left(1 + \frac{M_1}{RM_2} \right)^{-1/4} \right) \tag{8.20}$$

the value of ϵ , where $\bar{R}_+(\epsilon, R)$ diverges. Note that $\epsilon_{\max}(R) < \frac{1}{2M_1}$ and that $\bar{R}_-(\epsilon, R)$ is positive and well defined for $\epsilon_{\max}(R) < \frac{1}{2M_1}$.

Proof. Let us perform a change of variable and consider instead of ϵ the variable y

$$y = -\log(1 - 2M_1\epsilon)$$

and the function $V(y)$ defined as

$$V(y) = \frac{(1 - 2M_1\epsilon)^2}{R(\mathbf{f}_\epsilon)}$$

and denote

$$V_0 = V(0) = \frac{1}{R(\mathbf{f}_0)}. \tag{8.21}$$

After some algebra, inequality (8.16) becomes a simple linear inequality

$$-A - 4V(y) \leq \frac{dV(y)}{dy} \leq A, \quad A = \frac{8M_2}{M_1}. \tag{8.22}$$

The rightmost inequality implies obviously

$$V(y) \leq \bar{V}_-(y) = V_0 + Ay.$$

The leftmost inequality gives for the function

$$T(y) = V(y)e^{-4y}$$

which is such that $T(0) = V_0$, the inequality $\frac{dT(y)}{dy} \geq -Ae^{4y}$ which implies

$$T(y) \geq V_0 - \frac{A}{4}(e^{4y} - 1),$$

hence

$$V(y) \geq \bar{V}_+(y) = \left(V_0 + \frac{A}{4}\right)e^{-4y} - \frac{A}{4} = \bar{V}_+(y).$$

Note that the functions $\bar{V}_-(y)$ and $\bar{V}_+(y)$ are the functions which saturate inequalities (8.22) for V with the same initial condition $\bar{V}_-(0) = \bar{V}_+(0) = V(0) = V_0$. Going back from V to $R(\mathfrak{f})$ through (8.21), and defining \bar{R}_+ and \bar{R}_- through

$$V_+(y) = \frac{(1 - 2M_1\epsilon)^2}{\bar{R}_+(\mathfrak{f}_\epsilon)} \quad \text{and} \quad V_-(y) = \frac{(1 - 2M_1\epsilon)^2}{\bar{R}_-(\mathfrak{f}_\epsilon)},$$

we get the results of Proposition 8.1. ■

Proposition 8.1 is the main result of this section. Note that it does not require the initial triangulation to be Delaunay or isoradial. It is also completely independent of whether we perform flips or do not perform flips during the deformation. It depends only on the deformation function F and on the initial radius of the initial face we start from.

Notice that when the initial radius of the initial face becomes very small, (8.17) implies that

$$(1 - 2\epsilon M_1)^2 \leq \lim_{R(\mathfrak{f}_0) \rightarrow 0} \frac{R(\mathfrak{f}_\epsilon)}{R(\mathfrak{f}_0)} \leq (1 - 2\epsilon M_1)^{-2}.$$

8.6.4. Final estimates. With Proposition 8.1, we can complete the estimates of Section 8.5. We start from an initial critical triangulation T_{cr} with initial radius R_0 , and deform it into the Delaunay triangulation T_ϵ . Inequality (8.17) implies that

$$R_{\max}(T_\epsilon) = \max_{\mathfrak{f} \in T_\epsilon} R(\mathfrak{f}) \leq \bar{R}_+(\epsilon, R_0),$$

hence

$$B_F(T_\epsilon) = \max_{\mathfrak{f} \in T_\epsilon} (|\nabla_\epsilon F_\epsilon|, |\bar{\nabla}_\epsilon F_\epsilon|) \leq \bar{M}_1(\epsilon) + 4\bar{M}_2(\epsilon)\bar{R}_+(\epsilon, R_0).$$

We can bound the coefficients in the derivative with respect to ϵ of the Laplace–Beltrami operator $\Delta(\epsilon)$ (in (8.9)), and of the Kähler operator $\mathcal{D}(\epsilon)$ (in (8.11)),

$$\begin{aligned} |\mathfrak{D}_\epsilon| &\leq 4\bar{M}_1(\epsilon) + 16\bar{M}_2(\epsilon)\bar{R}_+(\epsilon, R_0), \\ |\mathfrak{K}_\epsilon| &\leq \frac{16\bar{M}_1(\epsilon) + 64\bar{M}_2(\epsilon)\bar{R}_+(\epsilon, R_0)}{\bar{R}_-(\epsilon, R_0)^2}, \\ |\mathfrak{G}_\epsilon| &\leq \frac{4\bar{M}_1(\epsilon) + 16\bar{M}_2(\epsilon)\bar{R}_+(\epsilon, R_0)}{\bar{R}_-(\epsilon, R_0)^2}. \end{aligned}$$

Using the explicit forms of $\bar{M}_1(\epsilon)$ and $\bar{M}_2(\epsilon)$ given by (8.15), and of $R_+(\epsilon, R_0)$ and $\bar{R}_-(\epsilon, R_0)$ given by (8.18) and (8.19), one deduces that $|\mathfrak{D}_\epsilon|$, $|\mathfrak{K}_\epsilon|$ and $|\mathfrak{S}_\epsilon|$ are uniformly bounded. More precisely, we can summarize the estimates we obtained into the following proposition.

Proposition 8.2. *Let us choose a smooth displacement function F with bounds M_1 and M_2 associated to its first and second derivatives. Let us also choose ϵ_b strictly smaller than $\epsilon_{\max}(R_0 = 1)$ given by*

$$0 < \epsilon_b < \epsilon_{\max}(1) = \frac{1}{2M_1}(1 - (1 + M_1M_2)^{-1/4}), \tag{8.23}$$

for instance, $\epsilon_b = \frac{1}{2}\epsilon_{\max}(R_0 = 1)$; see formula (8.20) for a definition of $\epsilon_{\max}(R_0)$. Then consider an arbitrary initial critical triangulation (isoradial and Delaunay) \mathbb{T}_0 with circumradius R_0 , some $\epsilon > 0$, the deformed Delaunay lattice \mathbb{T}_ϵ obtained from \mathbb{T}_0 by the deformation $z \rightarrow z + \epsilon F(z)$, and an arbitrary face \mathfrak{f} of \mathbb{T}_ϵ .

Then the factors $\mathfrak{D}_\epsilon(\mathfrak{f})$ (given by (8.10)), $\mathfrak{K}_\epsilon(\mathfrak{f})$ and $\mathfrak{S}_\epsilon(\mathfrak{f})$ (given by (8.12)) for the face \mathfrak{f} are uniformly bounded over the sets of

- (i) initial triangulation \mathbb{T}_0 with isoradius R_0 less or equal to one,
- (ii) deformation parameter ϵ smaller or equal to ϵ_b ,
- (iii) faces \mathfrak{f} of \mathbb{T}_ϵ .

Namely, there exist constants D_0 , K_0 and H_0 which depend only on F and on the choice of ϵ_b such that

$$|\mathfrak{D}_\epsilon(\mathfrak{f})| \leq D_0, \quad |\mathfrak{K}_\epsilon(\mathfrak{f})| \leq K_0, \quad |\mathfrak{S}_\epsilon(\mathfrak{f})| \leq H_0.$$

Similarly, there exists a constant P_0 , which depends only on F and on ϵ_b , which uniformly bounds the variation of the radius of the faces

$$\left| \frac{R(\mathfrak{f}_\epsilon) - R_0}{R_0} \right| \leq \epsilon P_0.$$

8.7. Consequence for the control of the scaling limit of Δ

8.7.1. The Laplace–Beltrami operator Δ . To simplify, we use a 2×2 block matrix notation. The Δ operator and its ϵ -derivative Δ' on the deformed lattice \mathbb{T}_ϵ reads

$$\begin{aligned} \Delta(\epsilon) &= 2 \begin{pmatrix} \nabla_\epsilon \\ \bar{\nabla}_\epsilon \end{pmatrix}^\dagger \begin{pmatrix} A_\epsilon & 0 \\ 0 & A_\epsilon \end{pmatrix} \begin{pmatrix} \nabla_\epsilon \\ \bar{\nabla}_\epsilon \end{pmatrix}, \\ \Delta'(\epsilon) &= -4 \begin{pmatrix} \nabla_\epsilon \\ \bar{\nabla}_\epsilon \end{pmatrix}^\dagger \begin{pmatrix} 0 & A_\epsilon \nabla_\epsilon \bar{F}_\epsilon \\ A_\epsilon \bar{\nabla}_\epsilon F_\epsilon & 0 \end{pmatrix} \begin{pmatrix} \nabla_\epsilon \\ \bar{\nabla}_\epsilon \end{pmatrix}. \end{aligned} \tag{8.24}$$

Remember that A_ϵ , $\nabla_\epsilon \bar{F}_\epsilon$ and $\bar{\nabla}_\epsilon F_\epsilon$ are defined for the faces of the deformed triangulation \mathbb{T}_ϵ , whose vertices have positions $z_\epsilon = z + \epsilon F(z)$, while $\Delta(\epsilon)$ and $\Delta'(\epsilon)$ act on the functions defined on the vertices of \mathbb{T}_ϵ . Since \mathbb{T}_ϵ is obtained by deforming an initial critical lattice $\mathbb{T}_0 = \mathbb{T}_{\text{cr}}$, let us rewrite them in terms on objects defined for the “back-deformed” lattice $\mathbb{T}_{\epsilon;0}$ defined by the procedure introduced in Section 8.2 (see (8.2) and the example illustrated in Figures 24 and 25)

$$\mathbb{T}_{\text{cr}} = \mathbb{T}_0 \xrightarrow{\text{Delaunay}} \mathbb{T}_\epsilon \xrightarrow{\text{no flip}} \mathbb{T}_{\epsilon;0}.$$

Again, $\mathbb{T}_{\epsilon;0}$ has the same vertices as \mathbb{T}_0 , but the edges and faces of \mathbb{T}_ϵ . In other words, \mathbb{T}_ϵ is obtained from $\mathbb{T}_{\epsilon;0}$ by the deformation $z \rightarrow z_\epsilon = z + \epsilon F(z)$, but without flips. We can therefore express the objects relative to the faces of \mathbb{T}_ϵ in terms of those relative to the faces of $\mathbb{T}_{\epsilon;0}$. The area A_ϵ of a face f_ϵ of \mathbb{T}_ϵ is related to the area A of the corresponding face $f = f_{\epsilon;0}$ of $\mathbb{T}_{\epsilon;0}$ by (8.3), namely,

$$A_\epsilon = D(\epsilon; F)A,$$

where $D(\epsilon; F)$ is defined by (8.4). Note that the operators ∇ and $\bar{\nabla}$ refer now to faces of $\mathbb{T}_{\epsilon;0}$. In a strict sense, they should be denoted by $\nabla_{\epsilon;0}$ and $\bar{\nabla}_{\epsilon;0}$. We omit the subscript to simplify notation. The discrete derivative operators on \mathbb{T}_ϵ are expressed in terms of those on $\mathbb{T}_{\epsilon;0}$ by (8.5), which can be expressed in the block matrix notation as

$$\begin{pmatrix} \nabla_\epsilon \\ \bar{\nabla}_\epsilon \end{pmatrix} = \frac{1}{D(\epsilon; F)} \begin{pmatrix} 1 + \epsilon \bar{\nabla} \bar{F} & -\epsilon \nabla \bar{F} \\ -\epsilon \bar{\nabla} F & 1 + \epsilon \nabla F \end{pmatrix} \begin{pmatrix} \nabla \\ \bar{\nabla} \end{pmatrix}.$$

In particular,

$$\begin{pmatrix} \nabla_\epsilon F_\epsilon \\ \bar{\nabla}_\epsilon F_\epsilon \end{pmatrix} = \frac{1}{D(\epsilon; F)} \begin{pmatrix} 1 + \epsilon \bar{\nabla} \bar{F} & -\epsilon \nabla \bar{F} \\ -\epsilon \bar{\nabla} F & 1 + \epsilon \nabla F \end{pmatrix} \begin{pmatrix} \nabla F \\ \bar{\nabla} F \end{pmatrix}.$$

Again, the discrete ∇ and $\bar{\nabla}$ refer now to faces of $\mathbb{T}_{\epsilon;0}$. Including this into (8.24), one gets

$$\Delta'(\epsilon) = \begin{pmatrix} \nabla \\ \bar{\nabla} \end{pmatrix}^\dagger A \mathbb{D}(\epsilon; F) \begin{pmatrix} \nabla \\ \bar{\nabla} \end{pmatrix}, \tag{8.25}$$

where \mathbb{D} is the 2×2 block matrix,

$$\begin{aligned} \mathbb{D}(\epsilon; F) &= \frac{(-4)}{D(\epsilon; F)^2} \tag{8.26} \\ &\times \begin{pmatrix} -\epsilon \nabla \bar{F} \bar{\nabla} F (2 + \epsilon(\nabla F + \bar{\nabla} \bar{F})) & \nabla \bar{F} ((1 + \epsilon \nabla F)^2 - \epsilon^2 \bar{\nabla} F \nabla \bar{F}) \\ \bar{\nabla} F ((1 + \epsilon \bar{\nabla} \bar{F})^2 - \epsilon^2 \nabla F \bar{\nabla} F) & -\epsilon \nabla \bar{F} \bar{\nabla} F (2 + \epsilon(\nabla F + \bar{\nabla} \bar{F})) \end{pmatrix}. \end{aligned}$$

8.7.2. Scaling limit for $\Delta(\epsilon)$. We can now study the scaling limit of the deformed operator $\Delta(\epsilon)$. We proceed as follows. As before, we choose a smooth displacement function F with compact support $F: \mathbb{C} \rightarrow \mathbb{C}$. For each $r \in (0, 1]$ (or simply a decreasing sequence of $(r_n)_{n \in \mathbb{N}}$ converging to 0), we associate an arbitrary critical triangulation of the plane $\mathbb{T}_{cr}^r = \mathbb{T}_0^r$ with isoradius r . Finally, we choose a finite bound ϵ'_b such that

$$0 < \epsilon'_b < \frac{1}{2} \epsilon_{\max}(1) \tag{8.27}$$

for the deformation parameter ϵ , where $\epsilon_{\max}(1)$ is given by (8.23) above. The calculations leading to the bounds of Proposition 8.2 for the deformation $\mathbb{T}_0 \rightarrow \mathbb{T}_\epsilon$ can be easily repeated for the double deformations $\mathbb{T}_0^r \rightarrow \mathbb{T}_\epsilon^r \rightarrow \mathbb{T}_{\epsilon,0}^r$. In particular, the circumradius of each face f of $\mathbb{T}_{\epsilon,0}^r$ is bounded uniformly by

$$\epsilon \leq \epsilon_b, \quad r \leq 1 \Rightarrow |R(f) - r| \leq \epsilon r P_0(F; 2\epsilon'_b) \tag{8.28}$$

with P_0 defined in Proposition 8.2. This allows us to uniformly control the $r \rightarrow 0$ limit of the discrete derivatives ∇ and $\bar{\nabla}$ by using Lemma 1.9 combined with the previous ingredients.

Proposition 8.3. *Let F be a smooth displacement function with compact support, fix ϵ , and let $\mathcal{F} = \{\mathbb{T}_0^r\}$ be a family of critical triangulations as above. To each point $z \in \mathbb{C}$ and to each r , we associate the face $f_{\epsilon;0}^r(z)$ of the deformed triangulation $\mathbb{T}_{\epsilon;0}^r$ which contains z . Note that the set of z which are either vertices or else belong to an edge of the triangulation is a set of measure zero and can be ignored. Then in the $r \rightarrow 0$ limit, the discrete derivative operators ∇ and $\bar{\nabla}$ for the face $f_{\epsilon;0}^r(z)$ converge uniformly towards the continuum partial derivative ∂ and $\bar{\partial}$ at the point z . More precisely, let ϕ be a smooth function (or at least of the class C^2) with compact support Ω of the plane. Then*

$$\lim_{r \rightarrow 0} \nabla \phi(f_{\epsilon;0}^r(z)) = \partial \phi(z), \quad \lim_{r \rightarrow 0} \bar{\nabla} \phi(f_{\epsilon;0}^r(z)) = \bar{\partial} \phi(z).$$

Moreover, the limit is uniform: Namely, there is a constant C independent of $z \in \Omega$, the choice of the family \mathcal{F} of triangulations, and the value of $\epsilon \in [0, \epsilon'_b]$ (but still depending on F , on ϵ'_b and on ϕ), such that

$$|\nabla \phi(f_{\epsilon;0}^r(z)) - \partial \phi(z)| \quad \text{and} \quad |\bar{\nabla} \phi(f_{\epsilon;0}^r(z)) - \bar{\partial} \phi(z)| \leq Cr. \tag{8.29}$$

Proof. Let us apply bound (B.5) obtained in Remark B.1 in the proof of Lemma 1.9 in Appendix B to the face $f_{\epsilon;0}^r(z)$, to get

$$|\nabla \phi(f_{\epsilon;0}^r(z)) - \partial \phi(z)| \leq R(f_{\epsilon;0}^r(z)) \left(\frac{5}{2} \sup_{z \in \Omega} |\partial^2 \phi| + 3 \sup_{z \in \Omega} |\partial \bar{\partial} \phi| + \frac{1}{2} \sup_{z \in \Omega} |\bar{\partial}^2 \phi| \right).$$

We then use (8.28) to bound uniformly the circumradius of $f'_{\epsilon;0}(z)$ by

$$R(f'_{\epsilon;0}(z)) \leq r(1 + \epsilon P_0(F; 2\epsilon'_b)).$$

This leads to bound (8.29). The same argument applies to $\bar{\nabla}\phi$. ■

It follows that the full variation of the discrete Laplace–Beltrami operator $\delta\Delta(\epsilon) = \Delta(\epsilon) - \Delta$ converges *uniformly* towards a local Laplace-like operator which depends on ϵ and F , in the following sense.

Proposition 8.4. *Let F , ϵ and $\mathcal{F} = \{\Gamma_0^r\}$ be as in Proposition 8.3, and let ϕ be a smooth function (or at least of the class C^2) with compact support Ω of the plane. Then*

$$\phi \cdot \delta\Delta(\epsilon) \cdot \phi = \sum_{u,v \in \Gamma_0^r} \bar{\phi}(u) [\delta\Delta(\epsilon)]_{uv} \phi(v)$$

converges uniformly when $r \rightarrow 0$ towards the local quadratic form

$$\int_{\Omega} d^2z \left(\frac{\partial\phi}{\partial z} \right)^\dagger \mathbb{E}(\epsilon; F) \left(\frac{\partial\phi}{\partial z} \right), \tag{8.30}$$

where $\mathbb{E}(\epsilon; F)$ is the 2×2 matrix,

$$\mathbb{E}(\epsilon; F) = \int_0^\epsilon d\epsilon \mathbb{E}'(\epsilon; F)$$

with

$$\begin{aligned} \mathbb{E}'(\epsilon; F) &= \frac{-4}{((1 + \epsilon\partial F)(1 + \epsilon\bar{\partial}\bar{F}) - \epsilon^2\bar{\partial}F\partial\bar{F})^2} \\ &\times \begin{pmatrix} -\epsilon\partial\bar{F}\bar{\partial}F(2 + \epsilon(\partial F + \bar{\partial}\bar{F})) & \partial\bar{F}((1 + \epsilon\partial F)^2 - \epsilon^2\bar{\partial}F\partial\bar{F}) \\ \bar{\partial}F((1 + \epsilon\bar{\partial}\bar{F})^2 - \epsilon^2\partial\bar{F}\bar{\partial}F) & -\epsilon\partial\bar{F}\bar{\partial}F(2 + \epsilon(\partial F + \bar{\partial}\bar{F})) \end{pmatrix}. \end{aligned} \tag{8.31}$$

Proof. One just writes $\delta\Delta(\epsilon)$ as

$$\delta\Delta(\epsilon) = \delta\Delta(\epsilon) = \int_0^\epsilon d\epsilon \Delta'(\epsilon)$$

and use the explicit representations (8.25), (8.26) for $\Delta'(\epsilon)$ to write

$$\phi \cdot \Delta'(\epsilon) \cdot \phi = \sum_{\mathfrak{f} \in \Gamma_{\epsilon;0}^r} A(\mathfrak{f}) \left(\frac{\nabla\phi(\mathfrak{f})}{\bar{\nabla}\phi(\mathfrak{f})} \right)^\dagger \cdot [\mathbb{D}(\epsilon; F)](\mathfrak{f}) \cdot \begin{pmatrix} \nabla\phi(\mathfrak{f}) \\ \bar{\nabla}\phi(\mathfrak{f}) \end{pmatrix},$$

which is a Riemann sum. Then (8.28) and Proposition 8.3 ensure that in the $r \rightarrow 0$ limit this converges uniformly towards an ordinary integral involving continuous derivatives of ϕ and F (\mathbb{D} becoming \mathbb{E}). One thus recovers (8.30). ■

8.8. Scaling limit for the bi-local deformation term for Δ

These arguments can be repeated for studying the scaling limit $\ell \rightarrow \infty$ of the bi-local term

$$\text{tr}[\delta_1 \Delta(\epsilon_1) \cdot \Delta_{\text{cr}}^{-1} \cdot \delta_2 \Delta(\epsilon_2) \cdot \Delta_{\text{cr}}^{-1}]$$

for finite deformation parameters ϵ_1 and ϵ_2 . Again, we consider two smooth deformation functions F_1 and F_2 with disjoint compact supports Ω_1 and Ω_2 . Here $\delta_1 \Delta(\epsilon_1) = \Delta(\epsilon_1) - \Delta_{\text{cr}}$ (resp. $\delta_2 \Delta(\epsilon_2) = \Delta(\epsilon_2) - \Delta_{\text{cr}}$) is the variation of the Laplace–Beltrami operator under the deformation $z \rightarrow z + \epsilon_1 F_1(z)$ (resp. $z \rightarrow z + \epsilon_2 F_2(z)$). As above, instead of considering a fixed initial critical lattice T_{cr} with isoradius $R_0 = 1$, and rescaled deformation functions $F_\ell(z) = \ell F(\frac{z}{\ell})$, with rescaling parameter $\ell \rightarrow \infty$, we consider a family $\mathcal{F} = \{T^r\}$ of critical lattices with isoradii r , fixed deformation functions F 's, and study the limit $r \rightarrow 0$. This is equivalent since by a change of variable, $r \sim \frac{1}{\ell}$.

For a finite $0 < r \leq 1$, deforming the initial T_{cr}^r critical lattice, the bi-local deformation term reads as a double sum over the faces of the two non-isoradial lattices $T_{\epsilon_1;0}^r$ and $T_{\epsilon_2;0}^r$, which share the same vertices, but not the same faces, with T_{cr}^r , of the explicit form

$$\begin{aligned} & \text{Tr}[\Delta'(\epsilon_1) \cdot \Delta_{\text{cr}}^{-1} \cdot \Delta'(\epsilon_2) \cdot \Delta_{\text{cr}}^{-1}] \\ &= \sum_{\mathbf{f}_1 \in T_{\epsilon_1;0}^r} \sum_{\mathbf{f}_2 \in T_{\epsilon_2;0}^r} A(\mathbf{f}_1)A(\mathbf{f}_2) \text{tr} \left([\mathbb{D}(\epsilon_1; F_1)](\mathbf{f}_1) \cdot \left[\left(\frac{\nabla}{\nabla} \right) \Delta_{\text{cr}}^{-1} \left(\frac{\nabla}{\nabla} \right)^\dagger \right]_{\mathbf{f}_1 \mathbf{f}_2} \right. \\ & \quad \left. \times [\mathbb{D}(\epsilon_2; F_2)](\mathbf{f}_2) \cdot \left[\left(\frac{\nabla}{\nabla} \right) \Delta_{\text{cr}}^{-1} \left(\frac{\nabla}{\nabla} \right)^\dagger \right]_{\mathbf{f}_2 \mathbf{f}_1} \right). \end{aligned} \tag{8.32}$$

The trace $\text{Tr}[\]$ in the left-hand side of (8.32) is the “big trace” over the infinite set of vertices of the critical lattice. The trace $\text{tr}(\)$ in the right-hand side of (8.32) is a finite trace over a product of 2×2 matrices. This appears again as a double Riemann discrete sum over the faces of the triangulations $T_{\epsilon_1;0}^r$ and $T_{\epsilon_2;0}^r$.

Studying the scaling limit $r \rightarrow 0$ might seem similar to what was done above for Δ . There is, however, a delicate point. The critical propagator Δ_{cr}^{-1} on T_{cr}^r is given by Kenyon’s explicit integral formula, but its matrix elements $[\Delta_{\text{cr}}^{-1}]_{\mathbf{u},\mathbf{v}}$ are not given by the restriction of a smooth function of the vertex positions $G(z(\mathbf{u}), z(\mathbf{v}))$.

Indeed, the large distance asymptotics of Δ_{cr}^{-1} on a critical lattice with isoradius $R_0 = 1$ given by Proposition 4.9 implies that the propagator Δ_{cr}^{-1} on a lattice T_{cr}^r can be separated in a dominant smooth part G_{D} and a subdominant non-smooth part G_{SD} ,

$$[\Delta_{\text{cr}}^{-1}]_{\mathbf{u},\mathbf{v}} = G_{\text{D}}(\mathbf{u}, \mathbf{v}) + G_{\text{SD}}(\mathbf{u}, \mathbf{v}).$$

The dominant smooth part is the continuum propagator (note now the dependence on r)

$$G_D(u, v) = -\frac{1}{2\pi} \left(\log \left(\frac{2|z(u) - z(v)|}{r} \right) + \gamma_{\text{Euler}} \right).$$

The subdominant non-smooth part is

$$G_{SD}(u, v) = \frac{1}{2\pi} \left(\sum_{m \geq d \geq 1} (-1)^d (2m + d - 1)! \times \text{Re} \left(c_{m,d}(u, v) \left(\frac{r/2}{z(v) - z(u)} \right)^{2m} \right) \right) \tag{8.33}$$

with the coefficients $c_{m,d}(u, v)$ defined by (4.4). Note that now $p_1(u, v) = \frac{z(v) - z(u)}{r}$. From Lemma 4.3, the $c_{m,d}$'s are of order $O(1)$ irrespective of (u, v) , so the sum of the terms given by a fixed $m > 0$ is bounded by an $O(r^{2m})$ in the scaling $r \rightarrow 0$ limit, and is indeed subdominant.

In the scaling limit $r \rightarrow 0$, the sum over triangles in equation (8.32) becomes a Riemann integral,

$$\sum_{f_1 \in T_{\epsilon_1;0}^r} \sum_{f_2 \in T_{\epsilon_2;0}^r} A(f_1)A(f_2) \rightarrow \int_{\Omega_1} d^2z_1 \int_{\Omega_2} d^2z_2.$$

The $\mathbb{D}(\epsilon_a; F_a)(f_a)$, $a = 1, 2$, in the right-hand side of equation (8.32) are easy to control since they converge uniformly to $\mathbb{E}'(\epsilon_a; F_a)(z_a)$ given by (8.31). Controlling the scaling limit of the discrete derivatives of the smooth part of the propagator is also easy by means of Lemma 1.9. We get the uniform limit

$$\left[\begin{pmatrix} \nabla \\ \bar{\nabla} \end{pmatrix} G_s \begin{pmatrix} \nabla \\ \bar{\nabla} \end{pmatrix}^\dagger \right]_{f_1 f_2} \xrightarrow{r \rightarrow 0} -\frac{1}{4\pi} \begin{pmatrix} 0 & (z_1 - z_2)^{-2} \\ (\bar{z}_1 - \bar{z}_2)^{-2} & 0 \end{pmatrix}. \tag{8.34}$$

The non-trivial point is to get a uniform bound on the scaling limit of the left + right discrete derivatives of the non-smooth part of the propagator, and to show that it is subdominant. This issue has been discussed in detail in Section 6.2 through Lemmas 6.8 and 6.9. However, Lemma 6.8 relies on the fact that the discrete derivatives ∇ and $\bar{\nabla}$ are relative to the faces f of an isoradial triangulation T_0 . This is not the case anymore here, since the discrete derivatives are relative to the faces of a non-isoradial triangulation $T_{\epsilon;0}^r$ derived from an isoradial one T_0^r by flips of edges, without moving the position of the vertices.

We can repeat the analysis of Section 6.2 for this more general case. The dangerous contribution which could give a term of order $|z_1 - z_2|^{-2}$ is the $m = 1$ term in (8.33), which is explicitly proportional to the real part of

$$\frac{p_3(u, v)r^3}{(z(u) - z(v))^3}.$$

The most dangerous contribution comes from applying left + right discrete derivatives to $p_3(u, v)$. Generically, a naive dimensional analysis shows that each discrete derivative applied on p_3 will bring a term of order r^{-1} , so that we will get for a pair of triangles $f_1 \in T_{\epsilon_1:0}^r \cap \Omega_1, f_2 \in T_{\epsilon_2:0}^r \cap \Omega_2$

$$\sum_{u_1 \in f_1} \sum_{u_2 \in f_2} \left(\frac{\nabla}{\bar{\nabla}} \right)_{f_1, u_1} p_3(u_1, u_2) \left(\frac{\nabla}{\bar{\nabla}} \right)_{u_2, f_1}^\dagger \sim \text{const} \cdot r^{-2}.$$

However, we shall see that this estimate is generically *not uniform*. Namely, the const in this estimate can be arbitrarily large! One should remember that from Lemma 6.8, if f_1 and f_2 are faces of the original isoradial triangulation T_0 , then this const is bounded by $\text{const} \leq 9$.

This is a technical point which comes from the fact that generically, if we start from an isoradial Delaunay triangulation T_0 with isoradius r , and consider an arbitrary triangle $t = (u_1, u_2, u_3)$ which is not a face f of T_0 , this triangle may have a very large circumradius $R(t), R(t) \gg r$, and an arbitrarily small area $A(t), A(t) \ll r^2$. “Experimental mathematics” studies of such singular cases and some analytical estimates lead us to the following conjecture.

Conjecture 8.5. *Let T_0^r be an isoradial Delaunay triangulation of the plane with isoradius r , and let $p_3(u, v)$ be the function defined by*

$$p_3(u, v) = \sum_{j=1}^{2n} e^{3i\theta_j}, \quad \theta_j = \arg(z(v_j) - z(v_{j-1}))$$

for any pair of vertices (u, v) of T_0^r , where $\mathfrak{v} = (v_0, \dots, v_k)$ is a path in the rhombic lattice T_0^{\diamond} going from $v_0 = u$ to $v_k = v$ (see Definition 2.23 and (2.4)).

For any non-degenerate triangle $t = (u_1, u_2, u_3)$ in T_0^r (not necessarily a face, as illustrated in Figure 26), let $\nabla p_3(t)$ and $\bar{\nabla} p_3(t)$ be the discrete derivatives of the function $u \mapsto p_3(u, v)$ evaluated at the triangle t , where the vertex v is fixed, according to definitions (3.6) and (3.7).

Then there is a uniform bound

$$|\nabla p_3(t)| \quad \text{and} \quad |\bar{\nabla} p_3(t)| \leq \text{const} \cdot \frac{R(t)}{r^2},$$

where the circumradius $R(t)$ of the triangle t given by formula (3.3), and const is a number of order $O(1)$ independent of the choice of the critical triangulation T_0^r and of the triangle t . Among the examples we have studied, we found $\text{const} = 6$.

Assuming the validity of the conjecture, it is easy to adapt the arguments of Section 6.2, and to use that fact that the circumradii of the faces f_1 and f_2 of the

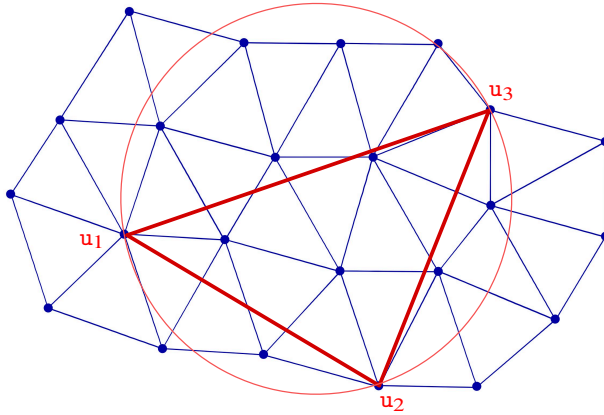


Figure 26. Example of a triangle $t = (u_1, u_2, u_3)$ in an isoradial graph, with its circumcircle, as considered in Conjecture 8.5.

deformed-back-deformed non-isoradial triangulations $T_{\epsilon_1;0}^r$ and $T_{\epsilon_2;0}^r$ are uniformly bounded for ϵ_1 and ϵ_2 small enough by (8.28). This leads to the following assertion.

Lemma 8.6. *Assuming Conjecture 8.5, the left-right discrete derivative of the non-smooth part of the propagator is uniformly bounded in the scaling limit $r \rightarrow 0$ by*

$$\left| \left[\left(\begin{matrix} \nabla \\ \bar{\nabla} \end{matrix} \right) G_{\text{ns}} \left(\begin{matrix} \nabla \\ \bar{\nabla} \end{matrix} \right)^\dagger \right]_{\mathbf{f}_1 \mathbf{f}_2} \right| \leq \text{const} \cdot \frac{r}{|z(\mathbf{f}_1) - z(\mathbf{f}_2)|^3}.$$

It is therefore subdominant when compared to the contribution of the smooth part of the propagator given by (8.34).

Combining the previous results, we can state the following proposition about the existence of the scaling limit of the bi-local term.

Proposition 8.7. *Assuming Conjecture 8.5, $\text{Tr}[\Delta'(\epsilon_1) \cdot \Delta_{\text{cr}}^{-1} \cdot \Delta'(\epsilon_2) \cdot \Delta_{\text{cr}}^{-1}]$, the bi-local term, defined on critical triangulations T_0^r converges uniformly in the scaling limit $r \rightarrow 0$ towards the bi-local term*

$$\int_{\Omega_1} d^2 z_1 \int_{\Omega_2} d^2 z_2 \text{tr} \left[\mathbb{E}'(\epsilon_1; F_1)(z_1) \cdot \begin{pmatrix} 0 & (z_1 - z_2)^{-2} \\ (\bar{z}_1 - \bar{z}_2)^{-2} & 0 \end{pmatrix} \right. \\ \left. \times \mathbb{E}'(\epsilon_2; F_2)(z_2) \cdot \begin{pmatrix} 0 & (z_1 - z_2)^{-2} \\ (\bar{z}_1 - \bar{z}_2)^{-2} & 0 \end{pmatrix} \right].$$

Note that this term depends on the four derivatives $\partial F_1, \bar{\partial} F_1, \partial F_2, \bar{\partial} F_2$ and their c.c., and contains both the analytic term $(z_1 - z_2)^{-4}$, the anti-analytic term $(\bar{z}_1 - \bar{z}_2)^{-4}$, and the mixed term $(z_1 - z_2)^{-2}(\bar{z}_1 - \bar{z}_2)^{-2}$.

Finally, from the explicit expression (8.31), the limit $\epsilon \rightarrow 0$ of $\mathbb{E}'(\epsilon; F)$ exists and is uniform,

$$\lim_{\epsilon \rightarrow 0} \mathbb{E}'(\epsilon; F) = \begin{pmatrix} 0 & -4\partial\bar{F} \\ -4\bar{\partial}F & 0 \end{pmatrix}.$$

Together with Proposition 8.7, this leads to the commutation of limits result for Δ .

Proposition 8.8. *Assuming Conjecture 8.5, the limit $\epsilon \rightarrow 0$ and the scaling limit $r \rightarrow 0$ for the bi-local term exist, are uniform, and commute. One recovers the result obtained previously for the scaling limit of the OPE on the lattice for Δ ,*

$$\begin{aligned} &\lim_{\epsilon \rightarrow 0} \lim_{r \rightarrow 0} \text{Tr}[\Delta'(\epsilon_1) \cdot \Delta_{\text{cr}}^{-1} \cdot \Delta'(\epsilon_2) \cdot \Delta_{\text{cr}}^{-1}] \\ &= \lim_{r \rightarrow 0} \lim_{\epsilon \rightarrow 0} \text{Tr}[\Delta'(\epsilon_1) \cdot \Delta_{\text{cr}}^{-1} \cdot \Delta'(\epsilon_2) \cdot \Delta_{\text{cr}}^{-1}] \\ &= \frac{1}{\pi^2} \int_{\Omega_1} d^2z_1 \int_{\Omega_2} d^2z_2 \frac{\bar{\partial}F_1(z_1)\partial F_2(z_2)}{(z_1 - z_2)^4} + \frac{\partial\bar{F}_1(z_1)\bar{\partial}F_2(z_2)}{(\bar{z}_1 - \bar{z}_2)^4}. \end{aligned}$$

Conjecture 1.12 in the introduction is a special case of Proposition 8.8. We simply repeat the arguments given at the beginning of Section 8.8, which show that one can equivalently define the scaling limit by choosing a given deformation function F , and letting the isoradius R_{cr} of the critical graphs G_{cr} go to zero $R_{\text{cr}} \rightarrow 0$, or fixing the isoradius R_{cr} of the critical graph G_{cr} , but then instead introducing the rescaled displacement function F_ℓ and letting ℓ go to infinity $\ell \rightarrow \infty$.

8.9. About the scaling limit of the Kähler operator \mathcal{D}

We now discuss briefly the deformations of the Kähler operator, without giving details of the calculations. In the block matrix representation, the Kähler operator \mathcal{D} and its ϵ -derivative read

$$\begin{aligned} \mathcal{D}(\epsilon) &= 4 \begin{pmatrix} \nabla_\epsilon \\ \bar{\nabla}_\epsilon \end{pmatrix}^\dagger \begin{pmatrix} \frac{A_\epsilon}{R_\epsilon^2} & 0 \\ 0 & 0 \end{pmatrix} \begin{pmatrix} \nabla_\epsilon \\ \bar{\nabla}_\epsilon \end{pmatrix}, \\ \mathcal{D}'(\epsilon) &= \begin{pmatrix} \nabla_\epsilon \\ \bar{\nabla}_\epsilon \end{pmatrix}^\dagger \begin{pmatrix} A_\epsilon \mathfrak{X}_\epsilon & A_\epsilon \bar{\mathfrak{Z}}_\epsilon \\ A_\epsilon \mathfrak{Z}_\epsilon & 0 \end{pmatrix} \begin{pmatrix} \nabla_\epsilon \\ \bar{\nabla}_\epsilon \end{pmatrix} \end{aligned} \tag{8.35}$$

with A_ϵ and R_ϵ the areas and circumradii of the faces of the deformed lattice T_ϵ , while \mathfrak{X}_ϵ and \mathfrak{Z}_ϵ are given by (8.12) and (8.13). In order to study $\mathcal{D}(\epsilon)$ at a finite epsilon and to compare it to $\mathcal{D}(0) = \mathcal{D}_{\text{cr}}$, and its scaling limit, one can try to repeat the argument for Δ presented in the previous section. It is enough to consider $\mathcal{D}'(\epsilon)$. We start from a critical lattice T'_0 with isoradius r , perform the deformation $z \rightarrow z + \epsilon F(z)$, and reexpress $\mathcal{D}'(\epsilon)$, defined on the deformed Delaunay lattice T'_ϵ , on

the back-deformed lattice $T_{\epsilon;0}^r$. We can thus rewrite $\mathcal{D}'(\epsilon)$ under a block form similar to (8.25)

$$\mathcal{D}'(\epsilon) = \begin{pmatrix} \nabla \\ \bar{\nabla} \end{pmatrix}^\dagger A \cdot \mathbb{F}'(\epsilon; F) \begin{pmatrix} \nabla \\ \bar{\nabla} \end{pmatrix} \tag{8.36}$$

with 2×2 block matrix $\mathbb{F}'(\epsilon; F)$ made of diagonal matrices relative to the faces \mathfrak{f} of $T_{\epsilon;0}^r$, defined implicitly by (8.36). The 2×2 matrix extracted of \mathbb{F}' relative to a face \mathfrak{f} , $[\mathbb{F}'(\epsilon; F)](\mathfrak{f})$ can be computed explicitly out of the $\nabla F(\mathfrak{f})$ and $\bar{\nabla} F(\mathfrak{f})$, and of the geometry of the face \mathfrak{f} , but the result will be quite long and not very illuminating at this stage. The difference with the previous case of Δ is that for a face \mathfrak{f} (let us denote its vertices (123)) \mathbb{F}' will depend explicitly on the circumradius $R(\mathfrak{f})$ of the face, and on the phases C_e associated to the unoriented edges $e = (12), (23)$ and (31) of \mathfrak{f} , defined by (8.7). Indeed, the coefficient $\mathfrak{Z}(\mathfrak{f})$ depends explicitly of $R(\mathfrak{f})$, and the coefficient $\mathfrak{X}(\mathfrak{f})$ depends also on the coefficients $C(\mathfrak{f}) = \sum_{e \in \mathfrak{f}} C_e$. Moreover, the variation of these coefficients under the back-deformation $T_{\epsilon;0} \leftrightarrow T_\epsilon$ depends also on these C_e .

We can now use Proposition 8.2 which bounds the $\mathfrak{Z}(\mathfrak{f})$ and $\mathfrak{X}(\mathfrak{f})$ and $R(\mathfrak{f})$, and the fact that since the C_e are phases so that $|C_e| = 1$, to bound uniformly the coefficients of the matrices $[\mathbb{F}'(\epsilon; F)](\mathfrak{f})$'s with respect to the deformation parameter ϵ (small enough) and the triangulations T_0^r .

Proposition 8.9. *Let F be a displacement function, $\mathcal{F} = \{T_0^r; r \in (0, 1]\}$ a family of critical triangulations labeled by their isoradius r , and $\epsilon \in (0, \epsilon'_b]$ with ϵ'_b defined by (8.27). There is a constant which depends only on F and the choice of ϵ'_b such that there is a uniform bound for the matrix elements of the $[\mathbb{F}'(\epsilon; F)](\mathfrak{f})$ matrices*

$$\|[\mathbb{F}'(\epsilon; F)](\mathfrak{f})\| \leq \text{const} \cdot r^{-2}$$

with the standard operator norm $\|\cdot\|$ on matrices (for instance).

Proof. The proof relies on writing explicitly the matrix \mathbb{F}' . This is lengthy but not difficult. Note that the factor r^{-2} , where r is the isoradius of the initial lattice T_0^r , comes from the $\frac{A}{R_0^2}$ in the initial definition of \mathcal{D} (8.35). ■

If we look now at the limit $r \rightarrow 0$, keeping ϵ fixed, denoting as in Proposition 8.3 the face of $T_{\epsilon;0}^r$ which contains the point z by $\mathfrak{f}_{\epsilon;0}^r(z)$, there is no reason for a generic family $\mathcal{F} = \{T_{\epsilon;0}^r\}$ that the ratio $\bar{R}(\mathfrak{f}_{\epsilon;0}^r(z)) = \frac{R(\mathfrak{f}_{\epsilon;0}^r(z))}{r}$ and the coefficients $C_e(\mathfrak{f}_{\epsilon;0}^r(z))$ and $C(\mathfrak{f}_{\epsilon;0}^r(z))$ converge towards fixed values $\bar{R}(z; \epsilon)$, $C(z; \epsilon)$, $C_e(z; \epsilon)$ in the scaling limit $r \rightarrow 0$. Indeed, these quantities depend explicitly on the detailed local geometrical structure of the lattices T_0^r in the neighborhood of the point z , for each value of r . Only for some *very specific sequences* of T_0^r , for instance, iterative isoradial refinements of the initial lattice for $r = 1$, we can expect strong correlations

leading to the existence of a limit $r \rightarrow 0$ for these quantities. We can therefore state the following.

Proposition 8.10. *Under the hypothesis of Proposition 8.9, the matrix $\frac{\mathbb{F}'(\epsilon; F)}{r^2}$ has generically no local scaling limit for ϵ finite when $r \rightarrow 0$,*

$$\lim_{r \rightarrow 0} \frac{[\mathbb{F}'(\epsilon; F)](\mathfrak{F}_{\epsilon;0}^r(z))}{r^2}$$

does not exist. Of course, one must have

$$z \in \Omega = \text{supp}(F)$$

since otherwise this limit exists and is zero. The same is obviously true for the non-existence of the limit $r \rightarrow 0$ of the bi-local term at finite ϵ_1, ϵ_2 ,

$$\lim_{r \rightarrow 0} \text{Tr}[\mathcal{D}'(\epsilon_1) \cdot \mathcal{D}_{\text{cr}}^{-1} \cdot \mathcal{D}'(\epsilon_2) \cdot \mathcal{D}_{\text{cr}}^{-1}] \tag{8.37}$$

does not exist.

Therefore, the existence of a scaling limit for \mathcal{D} could make sense in a much more limited setting than for Δ . Remember that we want to compare

- (i) the limit $\epsilon \rightarrow 0$, which, for \mathcal{D}' as well as for Δ' , has the effect of keeping only the terms linear in $\nabla F, \bar{\nabla} F$ and their c.c.;
- (ii) the scaling limit $r \rightarrow 0$, which allows replacing the discrete derivatives $\nabla, \bar{\nabla}$ by continuous derivatives ∂ and $\bar{\partial}$, and, in particular, (8.34).

In fact, the best result we obtain so far concerns the “simultaneous limit” when ϵ and r go to zero, and is stated in the following proposition.

Proposition 8.11. *Let F be a displacement function, $\mathcal{F} = \{\mathbb{T}_0^r; r \in (0, 1]\}$ a family of critical triangulations labeled by their isoradius r , and ϵ'_b defined by (8.27). We consider the “simultaneous limit” where*

$$r \rightarrow 0, \quad \epsilon_a = \epsilon(r) = r c_a$$

with $0 \leq c_a \leq \epsilon'_b$ for $a = 1, 2$. Assuming the validity of Conjecture 8.5, the bi-local term of (8.37) converges uniformly towards its continuum limit given in Theorem 1.10,

$$\begin{aligned} & \lim_{\substack{r \rightarrow 0 \\ \epsilon_1/r=c_1 \\ \epsilon_2/r=c_2}} \text{Tr}[\mathcal{D}'(\epsilon_1) \cdot \mathcal{D}_{\text{cr}}^{-1} \cdot \mathcal{D}'(\epsilon_2) \cdot \mathcal{D}_{\text{cr}}^{-1}] \\ &= \frac{1}{\pi^2} \int_{\Omega_1} d^2 z_1 \int_{\Omega_2} d^2 z_2 \left(\frac{\bar{\partial} F_1(z_1) \bar{\partial} F_2(z_2)}{(z_1 - z_2)^4} + \frac{\partial \bar{F}_1(z_1) \partial \bar{F}_2(z_2)}{(\bar{z}_1 - \bar{z}_2)^4} \right). \end{aligned}$$

9. Discussion and perspectives

9.1. The aim of the study

In this work, we study properties of the measure on planar graphs introduced by [7] in order to better understand the relationship between this discrete model and continuum models of random geometries on the plane arising from conformal field theories (CFT), in particular, the quantum Liouville theory. The model is defined as an integral over the space of all Delaunay graphs of the plane. We do not study as a whole the global properties of this integral and its associated measure. Rather, we study the measure in the neighborhood of very specific graphs, namely, isoradial Delaunay graphs. Our motivation is twofold:

- (i) isoradial graphs can be viewed as a discretization of flat geometry, so this should amount to some “semiclassical limit”;
- (ii) deforming the geometry is a way to introduce a stress-energy tensor into the statistical model, whose properties are crucial for conformal theories.

The measure of the model is a Kähler measure (in fact, equivalent to the Weil–Peterson measure), and its density can be written as the determinant of a Laplacian-like Kähler operator \mathcal{D} (defined on the Delaunay graphs), with specific global conformal invariance properties under $\text{PSL}(2, \mathbb{C})$ transformations. In order to compare our result with other cases, we study in parallel the Kähler operator \mathcal{D} , the ordinary discrete Laplace–Beltrami operator Δ (which is not $\text{PSL}(2, \mathbb{C})$ invariant), and the conformal Laplacian $\underline{\Delta}$ which, like \mathcal{D} , also enjoys a global $\text{PSL}(2, \mathbb{C})$ invariance property.

9.2. The first-order variations and discretized conformal field theories

9.2.1. The Laplace–Beltrami operator Δ . The calculation for the first-order variation for the discretized Laplace–Beltrami operator Δ is easy to discuss in the framework of a discretized CFT on the lattice. We refer to Appendix A for a reminder of the definitions and properties of CFT which are needed in this discussion. Our result (6.3) in Proposition 6.1 states that

$$\delta_\epsilon \log \det(\Delta) = - \sum_{\substack{\text{faces} \\ \mathfrak{f} \in \tilde{\mathcal{G}}_0^+}} 4A(\mathfrak{f})(\bar{\nabla} F(\mathfrak{f})Q(\mathfrak{f}) + \nabla \bar{F}(\mathfrak{f})\bar{Q}(\mathfrak{f})) \tag{9.1}$$

with

$$Q(\mathfrak{f}) := [\nabla \Delta^{-1} \nabla^T]_{\mathfrak{f}\mathfrak{f}} = \sum_{u,v} \nabla_{\mathfrak{f}u} \nabla_{\mathfrak{f}v} [\Delta_{\text{cr}}^{-1}]_{uv}, \tag{9.2}$$

where the operators $\nabla, \bar{\nabla}$ are defined in formulas (3.6) and (3.7), respectively. Equation (9.1) can be read as the discretized version of the first-order variation of the partition function under a diffeomorphism for a CFT (see (A.4)) given by

$$\delta_\epsilon \log(Z) = -\frac{1}{\pi} \int d^2x (\bar{\partial}F(x)\langle T(x) \rangle + \partial\bar{F}(x)\langle \bar{T}(x) \rangle),$$

where the sum over faces discretizes the integral over the plane, and the derivatives $\nabla\bar{F}$ and $\bar{\nabla}F$ serve as discrete versions of $\partial\bar{F}$ and $\bar{\partial}F$,

$$\sum_{\mathbf{f}} A(\mathbf{f}) \leftrightarrow \int d^2x, \quad \nabla\bar{F} \leftrightarrow \partial\bar{F}, \quad \bar{\nabla}F \leftrightarrow \bar{\partial}F.$$

The term $Q(\mathbf{f})$ is given by the vacuum expectation value (v.e.v.)

$$4\pi Q(\mathbf{f}) = \langle T_\Delta(\mathbf{f}) \rangle$$

of a discretized stress-energy tensor T_Δ for a theory with Grassmann fields $(\Phi, \bar{\Phi})$ attached to the vertices of the triangulation G_{cr} with discretized action S ,

$$S[\Phi, \bar{\Phi}] = \Phi \cdot \Delta \bar{\Phi} = \sum_{\substack{\text{vertices} \\ u, v \in G_{cr}}} \Phi_u \Delta_{uv} \bar{\Phi}_v, \tag{9.3}$$

where

$$T_\Delta(\mathbf{f}) = -4\pi \nabla\Phi(\mathbf{f})\bar{\nabla}\bar{\Phi}(\mathbf{f}) = -4\pi \sum_{u, v \in \mathbf{f}} \nabla_{fu} \Phi_u \bar{\nabla}_{fv} \bar{\Phi}_v \tag{9.4}$$

for a face (triangle) \mathbf{f} of the triangulation G_{cr} .

Note that this definition (9.4) for the discrete stress-energy tensor follows directly from (9.3) and the variation of the discrete Laplace–Beltrami operator Δ given by Proposition 5.12 and equation (5.11).

The above discussion is valid regardless of whether we consider the variation of the Laplace–Beltrami operator defined on an isoradial Delaunay graph G_{cr} or instead on a general Delaunay graph G . Indeed, (9.4) follows from the general equation (5.11) for the variation of Δ on generic triangulations. Note also that the absence of the term $\nabla F + \bar{\nabla}\bar{F}$ in the variation of Δ means $\text{Tr} \mathbf{T} = T^{z\bar{z}} = \bar{T}^{\bar{z}z}$ is zero, and that the discrete Laplace–Beltrami operator Δ has a discrete conformal invariance property.

The interesting result, relevant for the discussion here, is that for an isoradial Delaunay graph G_{cr} the term $Q(\mathbf{f})$, i.e., the v.e.v. of the discretized stress-energy tensor T , depends only on the local geometry of the graph, i.e., on the shape of the triangle \mathbf{f} , as stated in Proposition 6.1. This is not true when G is not isoradial; in that case, $\langle T(\mathbf{f}) \rangle$ will depend on the full geometry of the lattice.

9.2.2. The Kähler operator \mathcal{D} . The first-order variation for the Kähler operator \mathcal{D} is given by (6.6) in Proposition 6.6. The first term in (6.6) is the same as the first-order variation for Δ in (6.1), which is rewritten in (9.1) as a sum over the triangles of the lattice involving the discrete derivatives of the deformation $\bar{\nabla} F$ and $\nabla \bar{F}$. The second term in (6.6) involves the first-order variation $\mathfrak{d}_\epsilon R(\mathfrak{f})$ of the circumradii $R(\mathfrak{f}, \epsilon)$ of a face, which can be obtained from formulas (5.15) and (5.16). Then the final result is

$$\mathfrak{d}_\epsilon \log \det(\mathcal{D}) = - \sum_{\substack{\text{faces} \\ \mathfrak{f} \in \hat{\mathcal{G}}_{0+}}} \left((4A(\mathfrak{f})Q(\mathfrak{f}) + \frac{1}{2}C(\mathfrak{f}))\bar{\nabla} F(\mathfrak{f}) + \frac{1}{2}\nabla F(\mathfrak{f}) \right) + \text{c.c.} \tag{9.5}$$

with the geometrical factor $C(\mathfrak{f})$ for a triangle \mathfrak{f} given by (5.13), while $Q(\mathfrak{f})$ is given by (9.2), and corresponds to the v.e.v. of the discretized stress energy tensor $T_\Delta(\mathfrak{f})$ defined by (9.4) for the Laplace–Beltrami theory.

Like for the Laplace–Beltrami operator, variation (9.5) can be written in terms of a discretized stress-energy tensor $\mathbf{T}_\mathcal{D}$ for a theory with discretized action

$$S_\mathcal{D}[\Phi, \bar{\Phi}] = \Phi \cdot \mathcal{D}\bar{\Phi}$$

in the following way:

$$\begin{aligned} \mathfrak{d}_\epsilon \log \det(\mathcal{D}) &= \text{tr}[\mathfrak{d}_\epsilon \mathcal{D} \cdot \mathcal{D}^{-1}] \\ &= -\frac{1}{\pi} \sum_{\mathfrak{f}} A(\mathfrak{f})(\bar{\nabla} F(\mathfrak{f})\langle T_\mathcal{D}(\mathfrak{f}) \rangle + \nabla \bar{F}(\mathfrak{f})\langle \bar{T}_\mathcal{D}(\mathfrak{f}) \rangle) \\ &\quad + \frac{1}{2} \sum_{\mathfrak{f}} A(\mathfrak{f})(\nabla F(\mathfrak{f}) + \bar{\nabla} \bar{F}(\mathfrak{f}))\langle \text{tr } \mathbf{T}_\mathcal{D}(\mathfrak{f}) \rangle, \end{aligned} \tag{9.6}$$

where the components of the discretized stress-energy tensor are

$$\begin{aligned} T_\mathcal{D} &= -4\pi \frac{1}{R^2} (\nabla \Phi \nabla \bar{\Phi} + C \bar{\nabla} \Phi \nabla \bar{\Phi}), \\ \bar{T}_\mathcal{D} &= 4\pi \frac{1}{R^2} (\bar{\nabla} \Phi \bar{\nabla} \bar{\Phi} + \bar{C} \bar{\nabla} \Phi \nabla \bar{\Phi}), \\ \text{tr } \mathbf{T}_\mathcal{D} &= 8 \frac{1}{R^2} \bar{\nabla} \Phi \nabla \bar{\Phi}. \end{aligned} \tag{9.7}$$

One should note the non-zero term $\frac{1}{2}(\bar{\nabla} F + \nabla \bar{F})$ in (9.5) and the non-vanishing of the v.e.v. of the trace of a discrete stress-energy tensor $\text{tr } \mathbf{T}_\mathcal{D}$. This follows from the fact that the dimension of the matrix elements of \mathcal{D} is length^{-2} .

Definition (9.7) and the variation formula (9.6) remain valid if we replace the isoradial Delaunay graph \mathcal{G}_{cr} by a generic Delaunay graph \mathcal{G} . The additional term $C(\mathfrak{f})$ in (9.7) depends explicitly on the local geometry of the graph in the neighborhood of

the triangle f . This term cannot be written simply in the continuum limit $\ell \rightarrow \infty$ in terms of continuous derivatives ∂ and $\bar{\partial}$ of a “smooth” complex Grassmann field $\Phi(x)$ in the flat continuum plane \mathbb{R}^2 . This implies that $\mathbf{T}_{\mathcal{D}}$ has no direct interpretation in a continuum field theory setting, in contrast with \mathbf{T}_{Δ} .

Again, the interesting explicit local form given in Proposition 6.6 and in Remark 6.7 are only valid for the variation of an isoradial Delaunay graph G_{cr} .

9.2.3. The conformal Laplacian $\underline{\Delta}$. The result given by Proposition 6.4 for $\underline{\Delta}$ admits a similar interpretation. Again, the absence of a $\nabla F + \bar{\nabla} \bar{F}$ term signals the conformal invariance of $\underline{\Delta}$, which in this case is ensured from the start, before one takes the scaling limit. The first-order variation can still be written as a sum over triangles, of the form

$$\delta_{\epsilon} \log \det(\underline{\Delta}) = - \sum_{\substack{\text{faces} \\ f \in \hat{G}_{0+}}} 4A(f)(\bar{\nabla} F(f) Q_{\text{conf}}(f) + \text{c.c.}) \tag{9.8}$$

but now the local face term $Q_{\text{conf}}(f)$ differs from $Q(f)$ when one or several of the edges of the triangle f are chords, owing to the additional terms in (6.4). More precisely, the contribution for a chord can be separated into equal contributions for its adjacent “north” and “south” triangles, so that one writes

$$A(f) Q_{\text{conf}}(f) = A(f) Q(f) + H_{\text{anom}}(f)$$

with the anomalous term $H_{\text{anom}}(f)$ for a (counter-clockwise oriented) face f expressed as a sum over its (oriented) edges \vec{e} which are chords

$$H_{\text{anom}}(f) := \sum_{\substack{\text{chords} \\ \vec{e} \in \partial f}} H(\vec{e}, f)$$

with

$$H(\vec{e}, f) := \frac{1}{8\pi i} \theta_n(\vec{e}) \cot \theta_n(\vec{e}) \mathcal{E}_n(\vec{e}),$$

where $\mathcal{E}_n(\vec{e})$ is defined in (5.20). These explicit results are valid when deforming an isoradial Delaunay graph G_{cr} .

Again, for a deformation of a generic triangulation G_{cr} , variation (9.8) can be written in terms of a discretized stress-energy tensor $\mathbf{T}_{\underline{\Delta}}$ using a Grassmann field $(\Phi, \bar{\Phi})$ with action $S_{\text{conf}} = \Phi \cdot \underline{\Delta} \bar{\Phi}$,

$$\begin{aligned} \delta_{\epsilon} \log \det(\underline{\Delta}) = & - \frac{1}{\pi} \sum_f A(f) (\bar{\nabla} F(f) \langle T_{\underline{\Delta}}(f) \rangle + \nabla \bar{F}(f) \langle \bar{T}_{\underline{\Delta}}(f) \rangle) \\ & + \frac{1}{2} \sum_f A(f) (\nabla F(f) + \bar{\nabla} \bar{F}(f)) \langle \text{tr } \mathbf{T}_{\underline{\Delta}}(f) \rangle. \end{aligned}$$

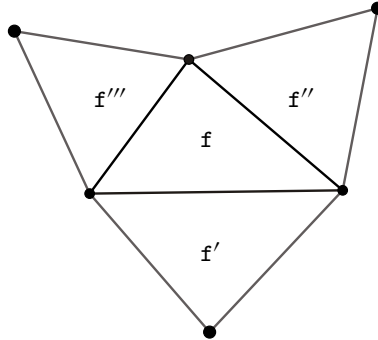


Figure 27. A face f (triangle) and its three neighbors.

One has generically $\text{tr } \mathbf{T}_{\underline{\Delta}} = 0$ (conformal invariance). The discretized analytic and anti-analytic components $T_{\underline{\Delta}}$ and $\bar{T}_{\underline{\Delta}}$ can be written explicitly, using Section 5.3 and, in particular, (5.19) in Remark 5.15. We get a generic form for $T_{\underline{\Delta}}$ involving all possible binomials of discrete derivatives of the fields

$$T_{\underline{\Delta}} = a \nabla \Phi \nabla \bar{\Phi} + b \nabla \Phi \bar{\nabla} \bar{\Phi} + c \bar{\nabla} \Phi \nabla \bar{\Phi} + d \bar{\nabla} \Phi \bar{\nabla} \bar{\Phi}. \tag{9.9}$$

The coefficients $a(f)$, $b(f)$, $c(f)$ and $d(f)$ depend not only on the geometry of the triangle f , but also of its three neighboring triangles f' , f'' and f''' , since they depend explicitly on the conformal angles of the three edges e' , e'' and e''' of f . See Figure 27. Like \mathbf{T}_{Δ} , the discrete stress-energy tensor $\mathbf{T}_{\underline{\Delta}}$ is quadratic in the local derivatives of the fields $(\Phi, \bar{\Phi})$. However, it involves not only the term $\nabla \Phi \nabla \bar{\Phi}$ but three other terms. Furthermore, the coefficient $a(f)$ of the $\nabla \Phi \nabla \bar{\Phi}$ term is non-constant and depends on the geometry of f and its neighbors.

9.3. The second-order variations and discretized conformal field theories

We now discuss along the same lines our result for the second-order variation and its scaling limit.

9.3.1. The Laplace–Beltrami operator Δ . Here we consider the Laplace–Beltrami operator of the Delaunay graph G_{ϵ} obtained through a bi-local deformation

$$z_{\underline{\epsilon}}(\mathbf{v}) := z_{\text{cr}}(\mathbf{v}) + \epsilon_1 F_1(\mathbf{v}) + \epsilon_2 F_2(\mathbf{v})$$

of the critical embedding of an isoradial Delaunay graph G_{cr} . The $\epsilon_1 \epsilon_2$ cross-term of $\log \det \Delta(\underline{\epsilon})$ can be calculated exactly using Proposition 5.12 and expressed using the limit graph G_{0+} and any weak Delaunay triangulation \hat{G}_{0+} which completes it.

This gives

$$\begin{aligned}
 \delta_{\epsilon_1} \delta_{\epsilon_2} \log \det \Delta &= -\operatorname{tr}[\delta_{\epsilon_1} \Delta \cdot \Delta_{\text{cr}}^{-1} \cdot \delta_{\epsilon_2} \Delta \cdot \Delta_{\text{cr}}^{-1}] & (9.10) \\
 &= -64 \operatorname{tr}[\operatorname{Re}[\bar{\nabla}^\top (\nabla \bar{F}_1) A \bar{\nabla}] \cdot \Delta_{\text{cr}}^{-1} \cdot \operatorname{Re}[\bar{\nabla}^\top (\nabla \bar{F}_2) A \bar{\nabla}] \cdot \Delta_{\text{cr}}^{-1}] \\
 &= - \sum_{\substack{\text{triangles} \\ x_1, x_2 \in \hat{\mathcal{G}}_{0+}}} 32A(x_1)A(x_2) \operatorname{Re}[\bar{\nabla} F_1(x_1) \bar{\nabla} F_2(x_2) ([\nabla \Delta_{\text{cr}}^{-1} \nabla^\top]_{x_1 x_2})^2] \\
 &\quad - \sum_{\substack{\text{triangles} \\ x_1, x_2 \in \hat{\mathcal{G}}_{0+}}} 32A(x_1)A(x_2) \operatorname{Re}[\bar{\nabla} F_1(x_1) \nabla \bar{F}_2(x_2) ([\nabla \Delta_{\text{cr}}^{-1} \bar{\nabla}^\top]_{x_1 x_2})^2].
 \end{aligned}$$

Using formula (9.4) for the discrete stress-energy tensor T_Δ and applying Wick’s theorem, we can express the two-point v.e.v.’s

$$\begin{aligned}
 \frac{1}{32\pi^2} \langle T_\Delta(x_1) T_\Delta(x_2) \rangle_{\text{conn.}} &= ([\nabla \Delta_{\text{cr}}^{-1} \nabla^\top]_{x_1 x_2})^2, & (9.11) \\
 \frac{1}{32\pi^2} \langle T_\Delta(x_1) \bar{T}_\Delta(x_2) \rangle_{\text{conn.}} &= ([\nabla \Delta_{\text{cr}}^{-1} \bar{\nabla}^\top]_{x_1 x_2})^2
 \end{aligned}$$

and the c.c. So far we do not require the initial graph to be isoradial: We may, in fact, replace the critical graph \mathcal{G}_{cr} with any Delaunay graph \mathcal{G}_0 equipped with its corresponding Laplace–Beltrami operator Δ_0 and Green’s function Δ_0^{-1} , and the variational formula (9.10) and the double correlator identity (9.11) remain valid. If, however, we incorporate a scaling parameter $\ell > 0$ and consider the bi-local smoothly deformed embedding $z_{\underline{\epsilon}, \ell}(\mathbf{v}) := z_{\text{cr}}(\mathbf{v}) + \epsilon_1 \ell F_{1; \ell}(\mathbf{v}) + \epsilon_2 \ell F_{2; \ell}(\mathbf{v})$, then the isoradial property (responsible for the asymptotic expansion (1.10) for the critical Green’s function Δ_{cr}^{-1}) is sufficient to establish the convergence of the scaling limit of formula (9.10), which is consistent with the OPE of a CFT with the expected central charge $c = -2$, namely,

$$\lim_{\ell \rightarrow \infty} \delta_{\epsilon_1} \delta_{\epsilon_2} \log \det \Delta(\ell) = \frac{c}{\pi^2} \iint_{\Omega_1 \times \Omega_2} dx_1^2 dx_2^2 \operatorname{Re} \left[\frac{\bar{\partial} F_1(x_1) \bar{\partial} F_2(x_2)}{(x_1 - x_2)^4} \right]. \quad (9.12)$$

As we have seen, $\nabla \Delta_0^{-1} \nabla^\top$ and $\nabla \Delta_0^{-1} \bar{\nabla}^\top$ (and their complex conjugates) must decay in accordance with Lemma 6.9 in order for (9.12) to hold. Our result is, of course, not surprising, and should be viewed as a check of the validity of our approach.

9.3.2. The Kähler operator \mathcal{D} . Proposition 6.11 and its scaling limit given in Section 7.3 are the novel results of the paper. They state that the scaling limit of the bi-local second-order variation for $\log \det \mathcal{D}(\underline{\epsilon}, \ell)$ and $\log \det \Delta(\underline{\epsilon}, \ell)$ are identical,

$$-\frac{1}{\pi^2} \iint_{\Omega_1 \times \Omega_2} dx_1 dx_2 \left(\frac{\bar{\partial} F_1(x_1) \bar{\partial} F_2(x_2)}{(x_1 - x_2)^4} + \frac{\partial \bar{F}_1(x_1) \partial \bar{F}_2(x_2)}{(\bar{x}_1 - \bar{x}_2)^4} \right).$$

This result is interesting for two reasons.

The operator \mathcal{D} has a different form and even a different scaling dimension than Δ . Its variation (5.12) and the associated stress-energy tensor (9.7) are different. However, the second-order variation has exactly the same OPE as the second-order variation for Δ , and it corresponds to a CFT with the same central charge

$$c = -2.$$

This value for the central charge is in our opinion somehow unexpected, and this is interesting per se. Indeed, it was suggested by the first author in the original paper [7] that the measure over triangulations given by $\det(\mathcal{D})$ (later shown in [4] to coincide with the Weil–Petersson metric over a marked complex curve), had a direct relation with the gauge fixing Faddeev–Popov determinant in two-dimensional quantum gravity. If true, it should be related to the so-called b – c ghosts system in Polyakov’s formulation as Liouville theory of 2D gravity and non-critical strings (see [12]). Then one could have expected a different value for the central charge, since the central charge for the b – c system is $c = -26$, and the central charge for the corresponding Liouville quantum gravity (at $Q = \frac{5}{\sqrt{6}}$, i.e., $\gamma = \sqrt{\frac{8}{3}}$) is $c = 26$.

9.3.3. The conformal Laplacian $\underline{\Delta}$. For the conformal Laplacian operator $\underline{\Delta}$, we do not have such a simple result, and the corresponding OPE cannot be interpreted as coming from a CFT. There are additional contributions that come from the chords, which have been studied in Section 6.3, namely the chord–chord term given by expression (6.25) and the chord–edge term given by (6.26). The latter chord–edge term has the expected harmonic form (depending only on $(x - x')^{-4}$ and its c.c.), but with a local geometry dependent coefficient involving both $\bar{\nabla} F_1 \bar{\nabla} F_2$ and $\nabla \bar{F}_1 \bar{\nabla} F_2$ terms. The chord–chord term is even more involved and contains a non-harmonic term, proportional to $|x - x'|^{-4}$, with a more complicated geometrical dependence in the geometry of the faces and the chords. In Appendix C, we give an explicit example of a critical lattice with a finite density of chords where these additional “anomalous” terms give a macroscopic anomalous contribution to the second-order variation, which precludes an interpretation in terms of conformal field theory in the scaling limit. Of course, this comes from the anomalous terms in the expression of the discretized stress-energy tensor T_{conf} (of general schematic form given in (9.9)), which does not have a simple universal field theoretical interpretation in the scaling limit. This is also a new, although somehow negative, result.

9.4. Relations and differences with other discrete models

The operators that we study here are defined on planar isoradial Delaunay graphs. Isoradial graph embeddings play a very important role in the study of two-dimensional models of statistical mechanics in theoretical physics and in mathematics. In partic-

ular, they are an essential tool in the proof of the conformal invariance of the Ising model at its critical point, and in the study of the conformal invariance of other critical models. They are very important in our study too, since they allow control of the large distance properties of the respective Green’s functions.

However, we stress that there is an important difference in terms of perspective. In studies of critical statistical models on such graphs, the underlying graph is fixed, and the proofs of the existence of a scaling limit and of its conformal invariance are undertaken for a fixed lattice. The random triangulation model of [7] is a statistical model *of* planar graphs, rather than a statistical model *on a* planar graph. The planar isoradial graphs that we consider here are just some special “semiclassical” configurations, which minimize a “local curvature functional”, as discussed in the Section 2.1.4, formula (2.2).

There are nevertheless relations between our work and some recent works, especially in regard to defining a notion of a discrete stress-energy tensor. Let us briefly discuss two of them.

9.4.1. Discrete stress-energy tensor in the loop model of Chelkak et al. In [5], Chelkak, Glazman and Smirnov study the famous critical $O(n)$ loop model [11, 19, 22] on abstract discrete surfaces with boundaries (denoted by G_δ) made by gluing together equilateral triangles Δ and rhombi $\diamond(\theta)$ of unit length δ , where each rhombus has an independent acute angle θ selected in the range $0 < \theta \leq \frac{\pi}{2}$, as depicted in Figure 28. The surface has, in general, conical singularities at all of its vertices. A discrete surface may admit more than one tessellation into triangles and rhombi if some vertices are flat (no conical defect). Two tessellations are equivalent (i.e., they describe the same surface) if one can be transformed into the other by applying a sequence of the following three kinds of local operations:

- (i) *Yang–Baxter transformations* which flip a flat hexagon made up of three rhombi sharing a common vertex,
- (ii) *pentagonal transformations* which interchange a triangle and a rhombus which form a flat pentagon with a triangle and two rhombi,
- (iii) *split transformations* which dissect a rhombus $\diamond(\frac{\pi}{3})$ into a pair of equilateral triangles sharing a common edge; this is depicted in Figure 29.

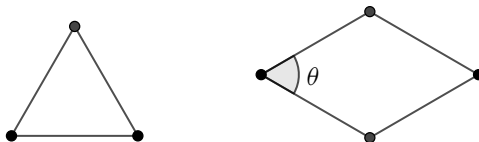


Figure 28. The triangles and rhombi of [5].

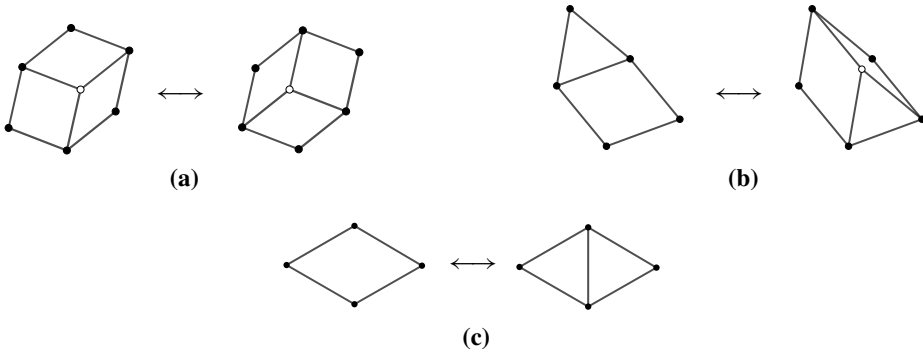


Figure 29. Yang–Baxter (a), pentagonal (b) and split (c) moves of [5]; white vertices \circ have to be flat (no conical singularity).

The states of the $O(n)$ loop model for a tessellated surface G_δ are configurations γ consisting of non-crossing loops and strands (joining boundary components, if present) drawn on the surface G_δ which can be obtained by concatenating local arrangements of arcs, one for each triangle and rhombus in G_δ . A local weight $w_\gamma(\mathbf{f})$ is associated to each face \mathbf{f} of G_δ which depends on the configuration of the loops on \mathbf{f} , the geometry of the face (hence of angle θ if $\mathbf{f} = \diamond(\theta)$ is a rhombus), and on a parameter s (related to the temperature). A factor n (loop fugacity) is associated to each closed loop. The local weights $w_\gamma(\mathbf{f})$ (that we do not discuss here) are taken to have a very specific form in order to satisfy the Yang–Baxter and pentagonal relations, ensuring that the model is the same for equivalent tessellations of the surface.

The partition function $Z^{\mathbf{b}}(G_\delta)$ for the $O(n)$ loop model on a fixed surface G_δ equipped with a boundary condition \mathbf{b} (specifying which boundary edges are joined by arcs), is given by the sum over states (loops+arcs configurations γ) by

$$Z^{\mathbf{b}}(G_\delta) := \sum_{\mathbf{b}\text{-configurations } \gamma} n^{\#\text{loops}(\gamma)} \prod_{\substack{\text{faces} \\ \mathbf{f} \in G_\delta}} w_\gamma(\mathbf{f}).$$

In addition, when the specific relation between n (the loop fugacity) and s (the temperature parameter)

$$n = -\cos\left(\frac{4\pi s}{3}\right)$$

holds, then the loop model is critical.

In [5], Chelkak et al. consider a *planar version* without conical defects where all rhombi have angle $\theta = \frac{\pi}{3}$, and such that the discrete surface G_δ is a compact, connected domain Ω of the triangular lattice. In this planar case, they define a *discrete stress-energy tensor* as the response of the model to an infinitesimal ϵ -deformation

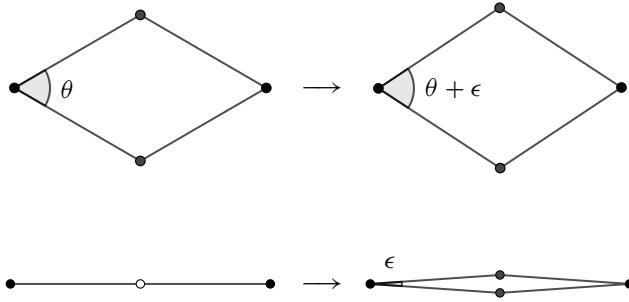


Figure 30. The ϵ -deformations of rhombi in [5].

of the original planar surface into a non-planar surface with conical defects. More precisely, two deformations are considered:

- (i) replacing two adjacent equilateral triangles (forming a rhombus $\diamond(\frac{\pi}{3})$) by a rhombus $\diamond(\theta)$ with angle $\theta = \frac{\pi}{3} + \epsilon$,
- (ii) replacing two aligned edges by an “almost flat” rhombus $\diamond(\epsilon)$ (see Figure 30).

The variation of the logarithm of the partition function under such ϵ -deformations defines the v.e.v. of a discrete stress-energy tensor $\mathcal{T}_{e|m}$ associated to edges e or to midlines m (of the honeycomb lattice built from the original triangular lattice), and out of these related real objects, a discrete complex stress-energy tensor \mathcal{T} can be associated to the vertices and the faces of the lattice (with relations). In [5], it is conjectured that this object is approximately discrete-holomorphic and converges to the stress-energy tensor of the corresponding CFT in the scaling limit.

9.4.2. Similarities and differences. There are similarities but also important differences with the approach and results of our study. The discrete conformal Laplacian $\underline{\Delta}$ defined in (1.7) is also defined with respect to a rhombic tessellated surface S_G^\diamond naturally associated to a Delaunay graph G in the plane (see Section 2.1 and especially Definition 2.21). However, S_G^\diamond is constructed only out of rhombi $\diamond(e)$ associated to edges e of G , and contains no equilateral triangles. Moreover, the rhombic surface S_G^\diamond is bipartite, with black and white vertices corresponding to vertices and faces of G respectively. Finally, and most importantly, the black vertices of S_G^\diamond must be flat (they do not carry a conical singularity), while the white vertices may carry a conical singularity (corresponding to a non-zero Ricci curvature given by (2.2)), see Figure 31. Thus our model considers only a subspace of the space of tessellated surfaces of [5].

Like [5], the stress-energy tensor in our study is defined in terms of deformations. However, an important difference is that we consider deformations of S_G^\diamond which are induced from deformations of the underlying Delaunay graph G in the plane. This space of deformations differs from those considered in [5] in two respects.

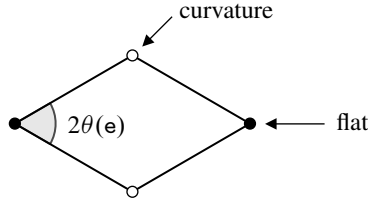


Figure 31. The rhombi which build the tessellated surface S_G^\diamond in this paper.

First, our deformations preserve the flatness of the black vertices of S_G^\diamond . Second, and this is essential, our discrete stress-energy tensor has a specific invariance properties under *global continuous analytic transformations* of the plane, i.e., Möbius transformations. This holds a priori, independent of the specific geometry of the Delaunay graph G .

In [5], as well as in other studies, the framework is different. One looks for a discrete stress-energy tensor on an isoradial critical graph G which has some specific invariance properties under the *discrete analytic and anti-analytic transformations* of G . Discrete analyticity is a very special and powerful property, but it depends explicitly on the critical graph considered. It is only in the scaling limit that discrete analyticity can be shown to “converge” (this is a crude presentation of beautiful and precise results) towards the usual analyticity in the continuum (i.e., in the complex plane \mathbb{C}).

Another difference is that our setting includes deformations of “flat rhombi” (corresponding to chords) which are not deformations of aligned edges, as considered in [5] and depicted in Figure 30. These deformations induce the appearance of the “curvature dipoles” discussed in Section 6.4, which complicate the analysis of $\underline{\Delta}$.

The overlap between our work and the results of [5] is restricted to the case of the operator $\underline{\Delta}$, which is related to the GFF. Strictly speaking, the authors of [5] consider the critical $O(n)$ loop model for $n \in [-2, 2]$, but it is known that the GFF can be related to the $n = 2$ model, and that there is some relation between the Laplace–Beltrami operator on a graph and the $n = -2$ model.

On the other hand, the Laplace–Beltrami operator Δ and the Kähler operator \mathcal{D} , which we would like to study on a general Delaunay graph G , are not defined in terms of the abstract rhombic surface S_G^\diamond . We do not know how to relate precisely, and, in general, their corresponding discrete stress-energy tensors to the construction of the stress-energy tensor given by [5].

9.4.3. Stress-energy tensor constructions through lattice representations of the Virasoro algebra. In an approach taken by Hongler et al. in [15], a stress-energy tensor for some lattice models is defined implicitly by identifying its modes through an action of the Virasoro algebra on an appropriately defined vector space $\mathfrak{F} :=$

$\mathfrak{F}^{\text{loc}}/\mathfrak{F}^{\text{null}}$ of *lattice local fields* (modulo *null fields*) supported on the graph. This construction avoids interpreting the stress-energy tensor as a response to a deformation of the graph embedding. Instead, an intermediate action of the Heisenberg algebra is introduced using a discrete holomorphic current along with a technique of discrete contour integration and a notion of discrete half-integer power functions. Only the special cases of the discrete GFF and of the Ising model on the square lattice $G = \mathbb{Z}_\delta^2$ with mesh size δ are handled in [15]. However, we expect that most of their technology (e.g., the notions of medial and corner graphs, discrete power functions, and discrete contour integration) is readily adaptable to arbitrary isoradial graphs (and their rhombic graphs where the theory of discrete holomorphicity is well behaved). The space of lattice local fields $\mathfrak{F}^{\text{loc}}$ of [15] depends on the translation properties of $G = \mathbb{Z}_\delta^2$. Specifically, $\mathfrak{F}^{\text{loc}}$ consists of fields which can be constructed as polynomial expressions of elementary fields $\phi_\delta(z)$ together with their translates $\phi_\delta(z + x\delta)$ for x in some fixed finite set $V \subset \mathbb{Z}^2$ of admissible displacements. For a general isoradial graph, one would need to specify an adequate vector space of lattice local fields $\mathfrak{F}^{\text{loc}}$ on which a representation of the Virasoro algebra could be supported. Bearing this, it would be natural to examine whether the stress-energy tensor(s) for the operator(s) considered in our paper can be realized by such putative Virasoro algebra action(s). For older references of representations of Virasoro algebra in lattice models, see the references in [15].

9.5. Open questions and possible extensions

Problem 1. *We would like to reiterate the problem of settling Conjecture 8.5 of Section 8.8, or in lieu of that, finding another adequate bound on $R(\mathfrak{f})^{-1}\nabla p_3(\mathfrak{f})$ uniform in the faces \mathfrak{f} of $T_0^{(r)}$ and the scaling parameter ℓ (or $r = \frac{1}{\ell}$), in order to complete the proof of Propositions 8.7 and 8.8 as well as 8.11.*

Problem 2. *Instead of using an isoradial Delaunay graph, we could begin with a Delaunay graph which is “smoothly non-isoradial”, in the sense that the circumradii of the faces $R(\mathfrak{f})$ vary slowly with the position of the faces in the plane. Studying the Laplace-like operators Δ , $\underline{\Delta}$ and \mathcal{D} and their deformations on such a graph is an interesting problem which might entail finding asymptotic expansions of the corresponding Green’s functions.*

Problem 3. *The properties that make a general isoradial graph G so useful as a starting point in our analysis are a reflection of the underlying notion of discrete analyticity supported on the lozenge graph G^\diamond . Chelkak et al. [5] have introduced the concept of s -holomorphicity and s -embeddings of graphs, and one can try to develop a theory of deformations for such graphs and their associated operators.*

Problem 4. *In the scaling limit, random planar graphs are known to be related to the Liouville conformal field theory. Finding a notion of discrete Liouville local field, with good properties in the scaling limit, for the model of random Delaunay triangulations is still an open problem. A solution could lead to an alternative discrete stress-energy tensor on a Delaunay graph, different from the one considered here, and with different properties under geometrical deformations of the graphs; in particular, having a discrete central charge different from $c = -2$ (possibly $c = -26$).*

Problem 5. *It should also be interesting to study the existence and description of a stress-energy tensor for other discrete models on Delaunay graphs, such as Dirac fermions, the Ising model, the $O(N)$ model, etc. using the approach of our work. It would be fruitful to compare the results with the approaches taken in [5, 15] (see Section 9.4).*

A. Reminders: The stress-energy tensor in quantum field theories and the central charge in 2D conformal field theories

A.1. The stress-energy tensor

For completeness, we recall some textbook material of quantum field theories (QFT) and (CFT), which can be found, for instance, in [10]. A central concept in field theory is the *stress-energy tensor* $\mathbf{T} = (T^{\mu\nu})$ (also denoted the *energy-momentum tensor* in the literature). Firstly, \mathbf{T} can be viewed (in flat space) as the conserved current $\mathbf{J}^\nu = (T_\mu^\nu)$ associated to space-time translation invariance, and is defined through Noether’s theorem by the action of an infinitesimal local change of coordinates

$$x^\nu \rightarrow x^\nu + \xi^\nu(x) \tag{A.1}$$

on the action \mathcal{S} (classical or quantum) of the theory. Secondly, \mathbf{T} can be viewed (in a general curved space) as the “response of the theory” to an infinitesimal variation of the classical “background metric” $\mathbf{g} = (g_{\mu\nu})$

$$g_{\mu\nu} \rightarrow g_{\mu\nu} + \delta g_{\mu\nu}$$

of the space-time M where the theory “lives”. More precisely, \mathbf{T} is defined classically by the functional derivative of the action \mathcal{S}

$$T^{\mu\nu}(x) = -\frac{2}{\sqrt{g(x)}} \frac{\delta \mathcal{S}}{\delta g_{\mu\nu}(x)}.$$

For a quantum theory (i.e., a local QFT), \mathbf{T} is now a quantum operator. Its vacuum expectation value (the vacuum-vacuum matrix element) is given by the *first-order*

variation of the logarithm of the partition function Z of the QFT under an infinitesimal variation of the metric $\delta g_{\mu\nu}$

$$\delta \log Z = \frac{1}{2} \int_M dx \sqrt{g(x)} \delta g_{\mu\nu}(x) \langle T^{\mu\nu}(x) \rangle + \dots \tag{A.2}$$

Similarly, the first-order variation of the vacuum expectation of an observable \mathcal{O} , for instance, a product of local operators $\mathcal{O}_1(x_1) \cdots \mathcal{O}_n(x_n)$, gives by the connected correlator of \mathbf{T} times \mathcal{O}

$$\delta \langle \mathcal{O} \rangle = \frac{1}{2} \int_M dx \sqrt{g(x)} \delta g_{\mu\nu} (\langle T^{\mu\nu}(x) \mathcal{O} \rangle_{\text{conn.}} + \text{contact terms}) + \dots, \tag{A.3}$$

where the so-called ‘‘contact terms’’ are present in (A.3) when the position x of \mathbf{T} coincides with that of some local operators in \mathcal{O} .

These two definitions of the stress-energy tensor \mathbf{T} are closely related, and, in fact, equivalent (with the proper definitions of \mathbf{T}), since diffeomorphism (A.1) induces a change of metric

$$\delta g_{\mu\nu} = D_\mu \xi_\nu + D_\nu \xi_\mu$$

with the covariant derivative D_μ and $\xi_\nu = g_{\nu\rho} \xi^\rho$.

These definitions extend to the higher-order terms in $\delta g_{\mu\nu}$ and give expectation values of products of \mathbf{T} (correlators). For instance, the second-order term in the variation of $\log Z$ gives the two-point connected correlator

$$\frac{1}{8} \int_M dx \sqrt{g(x)} \delta g_{\mu\nu}(x) \int_M dy \sqrt{g(y)} \delta g_{\rho\sigma}(y) \langle T^{\mu\nu}(x) T^{\rho\sigma}(y) \rangle_{\text{conn.}} + \text{contact terms}$$

and so on.

A.2. The stress-energy tensor in two-dimensional conformal field theories

In two dimensions, it is standard to work in complex coordinates $z = x^1 + ix^2$, $\bar{z} = x^1 - ix^2$, so that the flat metric is

$$g_{zz} = g_{\bar{z}\bar{z}} = 0, \quad g_{z\bar{z}} = g_{\bar{z}z} = \frac{1}{2}.$$

An infinitesimal diffeomorphism $z \mapsto z + \epsilon F(z, \bar{z})$ thus amounts to a variation of the metric

$$\delta g_{zz} = \epsilon \partial \bar{F}, \quad \delta g_{\bar{z}\bar{z}} = \epsilon \bar{\partial} F, \quad \delta g_{z\bar{z}} = \delta g_{\bar{z}z} = \frac{\epsilon(\partial F + \bar{\partial} \bar{F})}{2}.$$

For QFT’s in two dimensions (in particular, for CFT’s), especially important are the holomorphic and antiholomorphic components of the stress-energy tensor \mathbf{T} ,

which are denoted by T and \bar{T} in the literature (see, e.g., [10]). In the flat metric, they are

$$T = -\frac{\pi}{2}T^{\bar{z}\bar{z}} = -2\pi T_{zz}, \quad \bar{T} = -\frac{\pi}{2}T^{zz} = -2\pi T_{\bar{z}\bar{z}}.$$

The variation of $\log Z$ (A.2) reads

$$\begin{aligned} \delta \log(Z) = & -\frac{\epsilon}{\pi} \int d^2x (\partial\bar{F}(x)\langle\bar{T}(x)\rangle + \bar{\partial}F(x)\langle T(x)\rangle) \\ & + \frac{\epsilon}{2} \int d^2x (\partial F(x) + \bar{\partial}\bar{F}(x))\langle\text{tr}\mathbf{T}(x)\rangle + \dots, \end{aligned} \tag{A.4}$$

where $\text{tr}\mathbf{T} = T^\mu_\mu = T^{\mu\nu}g_{\nu\mu} = T^{z\bar{z}} = T^{\bar{z}z}$.

Conformal invariance in 2D implies that $T^{z\bar{z}} = T^{\bar{z}z} = \text{tr}\mathbf{T} = 0$ identically vanishes. For a quantum theory, this requires a proper definition of the renormalized stress-energy tensor, and this identity is valid up to very specific contact terms. The conservation law for the current $\partial_\mu T^{\mu\nu} = 0$ reduces to $\bar{\partial}T = 0, \partial\bar{T} = 0$, hence the terminology holomorphic and anti-holomorphic components. This is valid for a CFT in a flat metric.

For a 2D CFT defined on a general surface with a non-flat metric \mathbf{g} , one can still use (local) conformal coordinates where the metric reads $ds^2 = \rho(z, \bar{z}) dzd\bar{z}$, so that the analyticity property of T and \bar{T} are preserved. Here ρ is the conformal factor of the metric. A most important property is that the trace of the stress-energy tensor does not vanish anymore. Its expectation value is given by the *trace anomaly*

$$\langle\text{tr}\mathbf{T}(x)\rangle = g_{\mu\nu}(x)\langle T^{\mu\nu}(x)\rangle = \frac{c}{24\pi}R_{\text{scal}}(x) \tag{A.5}$$

with the *central charge* c of the theory, and $R_{\text{scal}}(x)$ the scalar curvature of the metric \mathbf{g} . The trace anomaly is a quantum anomaly, caused by short distance quantum fluctuations and renormalization effects. See, e.g., [12] for details. It can be derived from the *short distance operator product expansion* (OPE) for the stress-energy tensor, which takes the form (for the holomorphic component T)

$$T(z)T(z') \underset{z \rightarrow z'}{=} \frac{c}{2} \frac{1}{(z - z')^4} + \text{subdominant terms.} \tag{A.6}$$

Formula (A.5) can be obtained from (A.6), e.g., by writing $\langle T(z)T(z')\rangle$ as the functional derivative $\frac{\delta\langle T(z)\rangle}{\delta g_{\bar{z}\bar{z}}(z')}$ and comparing with the classical $\frac{\delta R_{\text{scal}}(z)}{\delta g_{\bar{z}\bar{z}}(z')}$ (see, e.g., [12] or [10]).

For a discrete statistical model, corresponding to a lattice regularized QFT, conformal invariance is expected to hold only at a critical point and in the large distance scaling limit (a famous example is the Ising model). The scaling limit of the model corresponds to a CFT. The discretized stress-energy tensor \mathbf{T}_{reg} can be defined, but it contains, in general, short distance UV divergent terms, proportional to negative

powers and logarithms of the short distance regulator a (the lattice mesh) or powers of the high momentum/energy cut-off $\Lambda \sim \frac{1}{a}$. By dimensional analysis,

$$\mathbf{T}_{\text{reg}} \propto \Lambda^2 \sim a^{-2}.$$

The definition of the continuum limit $a \rightarrow 0$ ($\Lambda \rightarrow \infty$) requires a renormalization prescription in order to define a renormalized stress-energy tensor \mathbf{T} with the correct properties for conformal invariance (OPE, trace anomaly).

A.3. The two-dimensional boson and the Δ theory

Finally, we recall that our results for the Laplace–Beltrami operator Δ can be interpreted in the framework of the standard free boson CFT (which has the central charge $c = 1$). Indeed, for the classical free boson, the action S_{boson} and the stress-energy tensor are (on a closed Riemannian manifold \mathcal{M})

$$S_{\text{boson}}[\phi] = \frac{1}{2} \int_{\mathcal{M}} d^2x \sqrt{g} \partial_{\mu} \phi g^{\mu\nu} \partial_{\nu} \phi = \frac{1}{2} \int_{\mathcal{M}} d^2x \sqrt{g} \phi(x) \Delta_g \phi(x) \quad (\text{A.7})$$

with stress-energy tensor

$$T^{\mu\nu} = \left(-\frac{1}{2} g^{\mu\nu} g^{\rho\sigma} \partial_{\rho} \phi \partial_{\sigma} \phi + g^{\rho\mu} g^{\sigma\nu} \partial_{\rho} \phi \partial_{\sigma} \phi \right).$$

In two-dimensional flat space, using complex coordinates, $\Delta_g = -4\partial\bar{\partial}$. The action and the components of the stress-energy tensor are

$$S_{\text{boson}}[\phi] = 2 \int d^2x \partial\phi\bar{\partial}\phi$$

and

$$T = -2\pi(\partial\phi)^2, \quad \bar{T} = -2\pi(\bar{\partial}\phi)^2, \quad \text{tr } \mathbf{T} = T^{z\bar{z}} = T^{\bar{z}z} = 0.$$

The last identity shows that the two-dimensional free boson is indeed conformally invariant. The partition function for the boson is related to the determinant of Δ_g by the functional integral

$$Z_{\text{boson}} = \int \mathfrak{D}[\phi] e^{-S[\phi]} = \det(\Delta_g)^{-1/2}$$

with the properly defined functional determinant $\det(\Delta)$ of Δ , taking into account renormalization and the zero mode.

Formally, $\det(\Delta_g) = Z_{\text{boson}}^{-2}$ is the partition function of the “ $n = -2$ components” free boson CFT, with $c = -2$. Equivalently, a standard trick is to write $\det(\Delta_g)$

as the partition function of a theory for a *scalar complex Grassmann field*: A spin zero field obeying Fermi–Dirac statistics, described by a pair of conjugate Grassmann (anti-commuting) fields $(\Phi, \bar{\Phi})$, where the $\Phi(x)$ ’s and $\bar{\Phi}(x)$ ’s are the generators of an infinite-dimensional Grassmann (or exterior) algebra. The partition function Z_Δ is given by a Berezin functional integral (see, e.g., [9, 10] and the original reference [2]). It reads, using the Berezin integration notation

$$Z_\Delta = \det \Delta_g = \int \mathfrak{D}[\Phi, \bar{\Phi}] e^{-S[\Phi, \bar{\Phi}]}, \quad \mathfrak{D}[\Phi, \bar{\Phi}] = \prod_x d\Phi(x) d\bar{\Phi}(x)$$

with the action S_Δ (here a degree 2 element of the Grassmann algebra) which is simply the Grassmann version of the action for a complex bosonic scalar field

$$S_\Delta[\Phi, \bar{\Phi}] = 4 \int d^2x \partial\Phi\bar{\partial}\bar{\Phi} = \int d^2x \Phi \cdot \Delta_g \bar{\Phi}.$$

Of course, unlike the bosonic case, the Berezin functional integral cannot be considered in terms of probabilistic averages over random real or complex fields “living” on a space-time manifold, but as an algebraic construction. In the fermionic theory, the two-point functions (the propagator) are (note the anticommutativity)

$$\begin{aligned} \langle \bar{\Phi}(x)\Phi(y) \rangle &= -\langle \Phi(x)\bar{\Phi}(y) \rangle = [\Delta_g^{-1}]_{xy}, \\ \langle \Phi(x)\Phi(y) \rangle &= \langle \bar{\Phi}(x)\bar{\Phi}(y) \rangle = 0. \end{aligned}$$

The stress-energy tensor components are

$$T_\Delta = -4\pi \partial\Phi\bar{\partial}\bar{\Phi}, \quad \bar{T}_\Delta = -4\pi \bar{\partial}\Phi\partial\bar{\Phi}, \quad \text{tr } \mathbf{T}_\Delta = 0.$$

As explained in the discussion in Section 9, our results for the variations of the discretized Laplacians $\Delta, \underline{\Delta}$ and the Kähler operator \mathcal{D} (defined on a triangulation \mathbb{T}) can be easily formulated in terms of discretized stress-energy tensors attached to the faces of \mathbb{T} . However, only for the Laplace–Beltrami operator Δ can the discretized stress energy tensor be given a simple continuum limit formulation as the stress-energy tensor of a continuum QFT.

A.4. The conformal ghost-antighost theory

For completeness, we recall what is the ghost-antighost CFT theory for two-dimensional gravity. The two-dimensional gravity is a quantum theory for the Riemannian 2d metric tensor $\mathbf{g} = (g_{\mu\nu})$ on a Riemann surface (e.g., the sphere). It must be invariant under local diffeomorphisms

$$x^\mu \rightarrow x'^\mu = x^\mu + \epsilon \xi^\mu, \quad g_{\mu\nu} \rightarrow g_{\mu\nu} - \epsilon (D_\mu \xi_\nu + D_\nu \xi_\mu) \tag{A.8}$$

with vector field $\xi = (\xi^\mu)$ and covariant derivative $\mathbf{D} = (D_\mu)$ in the metric \mathbf{g} . In Polyakov's formulation (see the original article by Polyakov on the bosonic string [23], and the Les Houches lecture notes by Friedan [12] for details), the diffeomorphism local invariance is fixed by the conformal gauge. A background classical metric $\bar{\mathbf{g}} = (\bar{g}_{\mu\nu})$ is chosen, and the metric is fixed to be conformal with respect to $\bar{\mathbf{g}}$, i.e., of the form

$$g_{\mu\nu}(x) = \Lambda(x)\bar{g}_{\mu\nu}(x), \quad (\text{A.9})$$

where $\Lambda(x)$ is the conformal factor. This amounts to enforcing the local gauge fixing condition

$$\bar{K}^{\mu\nu} = \bar{g}^{\mu\rho}g_{\rho\sigma}\bar{g}^{\sigma\nu} - \frac{1}{2}\bar{g}^{\rho\sigma}g_{\sigma\rho}\bar{g}^{\mu\nu} = 0.$$

The variation of the gauge fixing term \bar{K} under a general diffeomorphism (A.8) is, when deforming a conformal metric of form (A.9),

$$\bar{K}^{\mu\nu} = 0 \rightarrow \bar{K}^{\mu\nu} = -\epsilon\Lambda(\bar{D}^\mu\xi^\nu + \bar{D}^\nu\xi^\mu - \bar{g}^{\mu\nu}\bar{D}_\tau\xi^\tau)$$

with $\bar{\mathbf{D}} = (\bar{D}_\mu)$ the covariant derivative with respect to the background metric \mathbf{g} . It can be written as

$$-\epsilon(\mathbf{J} \cdot \xi)^{\mu\nu},$$

where \mathbf{J} is a differential operator which maps a vector field ξ onto a symmetric traceless tensor (with respect to the background metric $\bar{\mathbf{g}}$). Quantizing the metric \mathbf{g} in the conformal gauge gives in the functional integral a Faddeev–Popov determinant, which can be written as a Grassmann functional integral in terms of two anticommuting ghost fields, \mathbf{c} and \mathbf{b} , where

$$\mathbf{c} = (c^\mu) \quad \text{is a type } (1, 0) \text{ tensor}$$

and

$$\mathbf{b} = (b_{\mu\nu}) \quad \text{is a type } (0, 2) \text{ symmetric traceless tensor}$$

such that $b_{\mu\nu} = b_{\nu\mu}$ and $\bar{g}^{\nu\mu}b_{\mu\nu} = 0$. The Faddeev–Popov determinant reads

$$\det[\mathbf{J}] = \int \mathfrak{D}[\mathbf{b}, \mathbf{c}] e^{\mathbf{b} \cdot \mathbf{J} \cdot \mathbf{c}}.$$

The action for the \mathbf{b} – \mathbf{c} system is (here in the background metric $\bar{\mathbf{g}}$)

$$S_{\text{ghost}}[\mathbf{b}, \mathbf{c}] = \mathbf{b} \cdot \mathbf{J} \cdot \mathbf{c} = \int d^2x \sqrt{\bar{g}} b_{\mu\nu} (\bar{D}^\mu c^\nu + \bar{D}^\nu c^\mu - \bar{g}^{\mu\nu} \bar{D}_\tau c^\tau).$$

The symmetric stress-energy tensor for this ghost action is

$$T_{\text{ghost}}^{\mu\nu} = b^{\mu\tau} \bar{D}^\nu c_\tau + b^{\nu\tau} \bar{D}^\mu c_\tau + \bar{D}_\tau b^{\mu\nu} c^\tau - \bar{g}^{\mu\nu} b^{\tau\rho} \bar{D}_\tau c_\rho.$$

As shown by Polyakov in [23], this b - c system is a conformal theory (CFT) with central charge $c = -26$. As a consequence, when fixing the conformal gauge (A.9) in the functional integral for 2D gravity, which is

$$Z = \int \mathfrak{D}[g] e^{-\int_M d^2x \mu_0 \sqrt{g}},$$

the resulting effective action for the remaining conformal factor

$$\Lambda(x) = \exp(\varphi(x))$$

with the Liouville field $\varphi(x)$ is the Liouville action, which defines the Liouville 2D gravity model.

B. Proof of Lemma 1.9

Proof. For $j = 2, 3$, introduce interpolations $z_j(t) := tz_j + (1 - t)z_1$ between z_j and z_1 . In addition, set

$$z(s, t) := sz_3(t) + (1 - s)z_2(t).$$

We start from the definition of ∇

$$\nabla\phi(\mathfrak{f}) = \frac{[\phi(z_2) - \phi(z_1)][\bar{z}_3 - \bar{z}_1] - [\phi(z_3) - \phi(z_1)][\bar{z}_2 - \bar{z}_1]}{-4iA(\mathfrak{f})},$$

where by formula (3.3), we have for the area of the triangle \mathfrak{f}

$$4A(\mathfrak{f}) = \frac{|z_1 - z_2||z_2 - z_3||z_3 - z_1|}{R(\mathfrak{f})}.$$

The numerator can be expressed by

$$\begin{aligned} & [\phi(z_2) - \phi(z_1)][\bar{z}_3 - \bar{z}_1] - [\phi(z_3) - \phi(z_1)][\bar{z}_2 - \bar{z}_1] \\ &= \int_0^1 dt \frac{d}{dt} [\phi(z_2(t))[\bar{z}_3 - \bar{z}_1] - \phi(z_3(t))[\bar{z}_2 - \bar{z}_2]] \\ &= \underbrace{\int_0^1 dt \left[[z_2 - z_1][\bar{z}_3 - \bar{z}_1] \partial\phi(z_2(t)) - [z_3 - z_1][\bar{z}_2 - \bar{z}_1] \partial\phi(z_3(t)) \right]}_{*\text{-integral}} \\ &+ \underbrace{\int_0^1 dt \left[[\bar{z}_2 - \bar{z}_1][\bar{z}_3 - \bar{z}_1] [\partial\phi(z_2(t)) - \partial\phi(z_3(t))] \right]}_{**\text{-integral}}. \end{aligned} \tag{B.1}$$

Apply the fundamental theorem of calculus once again, the $*$ -integral in (B.1) can be expressed as a double integral

$$\begin{aligned}
 & - \int_0^1 \int_0^1 dt ds \frac{d}{ds} [\partial\phi(z(s,t))(s[z_3 - z_1][\bar{z}_2 - \bar{z}_1] + (1-s)[z_2 - z_1][\bar{z}_3 - \bar{z}_1])] \\
 &= \int_0^1 \int_0^1 dt ds \partial\phi(z(s,t)) \underbrace{([z_2 - z_1][\bar{z}_3 - \bar{z}_1] - [z_3 - z_1][\bar{z}_2 - \bar{z}_1])}_{=-4iA(\mathfrak{f})} \\
 &+ \int_0^1 \int_0^1 t dt ds \partial\partial\phi(z(s,t))[z_2 - z_3] \\
 &\quad \times (s[z_3 - z_1][\bar{z}_2 - \bar{z}_1] + (1-s)[z_2 - z_1][\bar{z}_3 - \bar{z}_1]) \\
 &+ \int_0^1 \int_0^1 t dt ds \partial\bar{\partial}\phi(z(s,t))[\bar{z}_2 - \bar{z}_3] \\
 &\quad \times (s[z_3 - z_1][\bar{z}_2 - \bar{z}_1] + (1-s)[z_2 - z_1][\bar{z}_3 - \bar{z}_1]).
 \end{aligned}$$

Dividing the $*$ -integral in (B.1) by $(-4 \operatorname{Im} A(\mathfrak{f}))$, we obtain a first contribution to $\nabla\phi(\mathfrak{f})$, namely,

$$\begin{aligned}
 & \int_0^1 \int_0^1 dt ds \partial\phi(z(s,t)) \\
 &+ iR(\mathfrak{f}) \int_0^1 \int_0^1 t dt ds \partial\partial\phi(z(s,t)) \frac{z_2 - z_3}{|z_2 - z_3|} \\
 &\quad \times \left(s \frac{z_3 - z_1}{|z_3 - z_1|} \frac{\bar{z}_2 - \bar{z}_1}{|z_2 - z_1|} + (1-s) \frac{z_2 - z_1}{|z_2 - z_1|} \frac{\bar{z}_3 - \bar{z}_1}{|z_3 - z_1|} \right) \\
 &+ iR(\mathfrak{f}) \int_0^1 \int_0^1 t dt ds \partial\bar{\partial}\phi(z(s,t)) \frac{\bar{z}_2 - \bar{z}_3}{|z_2 - z_3|} \\
 &\quad \times \left(s \frac{z_3 - z_1}{|z_3 - z_1|} \frac{\bar{z}_2 - \bar{z}_1}{|z_2 - z_1|} + (1-s) \frac{z_2 - z_1}{|z_2 - z_1|} \frac{\bar{z}_3 - \bar{z}_1}{|z_3 - z_1|} \right).
 \end{aligned}$$

Again, by the fundamental theorem of calculus, we can transform the $**$ -integral in (B.1) and obtain

$$\begin{aligned}
 & \int_0^1 dt ([\bar{z}_2 - \bar{z}_1][\bar{z}_3 - \bar{z}_1][\partial\phi(z_2(t)) - \partial\phi(z_3(t))]) \\
 &= -[\bar{z}_2 - \bar{z}_1][\bar{z}_3 - \bar{z}_1] \int_0^1 \int_0^1 dt ds \frac{d}{ds} (\partial\phi(z(s,t))) \\
 &= [\bar{z}_2 - \bar{z}_1][\bar{z}_3 - \bar{z}_1] \int_0^1 \int_0^1 t dt ds \\
 &\quad \times ([z_2 - z_3]\partial\bar{\partial}\phi(z(s,t)) + [\bar{z}_2 - \bar{z}_3]\overline{\partial\partial}\phi(z(s,t))).
 \end{aligned}$$

Dividing the $**$ -integral in (B.1) by $(-4 \operatorname{Im} A(\mathbf{f}))$, we obtain a second contribution to $\nabla\phi(\mathbf{f})$, namely,

$$iR(\mathbf{f}) \frac{\bar{z}_2 - \bar{z}_1}{|z_2 - z_1|} \frac{\bar{z}_3 - \bar{z}_1}{|z_3 - z_1|} \times \int_0^1 \int_0^1 t \, dt \, ds \left(\frac{z_2 - z_3}{|z_2 - z_3|} \partial\bar{\partial}\phi(z(s, t)) + \frac{\bar{z}_2 - \bar{z}_3}{|z_2 - z_3|} \bar{\partial}\partial\phi(z(s, t)) \right).$$

So we end up with

$$\begin{aligned} \nabla\phi(\mathbf{f}) &- \int_0^1 \int_0^1 dt \, ds \, \partial\phi(z(s, t)) \\ &= iR(\mathbf{f}) \int_0^1 \int_0^1 t \, dt \, ds \, \partial\partial\phi(z(s, t)) \frac{z_2 - z_3}{|z_2 - z_3|} \\ &\quad \times \left(s \frac{z_3 - z_1}{|z_3 - z_1|} \frac{\bar{z}_2 - \bar{z}_1}{|z_2 - z_1|} + (1 - s) \frac{z_2 - z_1}{|z_2 - z_1|} \frac{\bar{z}_3 - \bar{z}_1}{|z_3 - z_1|} \right) \\ &+ iR(\mathbf{f}) \int_0^1 \int_0^1 t \, dt \, ds \, \partial\bar{\partial}\phi(z(s, t)) \frac{\bar{z}_2 - \bar{z}_3}{|z_2 - z_3|} \\ &\quad \times \left(s \frac{z_3 - z_1}{|z_3 - z_1|} \frac{\bar{z}_2 - \bar{z}_1}{|z_2 - z_1|} + (1 - s) \frac{z_2 - z_1}{|z_2 - z_1|} \frac{\bar{z}_3 - \bar{z}_1}{|z_3 - z_1|} \right) \\ &+ iR(\mathbf{f}) \frac{\bar{z}_2 - \bar{z}_1}{|z_2 - z_1|} \frac{\bar{z}_3 - \bar{z}_1}{|z_3 - z_1|} \int_0^1 \int_0^1 t \, dt \, ds \\ &\quad \times \left(\frac{z_2 - z_3}{|z_2 - z_3|} \partial\bar{\partial}\phi(z(s, t)) + \frac{\bar{z}_2 - \bar{z}_3}{|z_2 - z_3|} \bar{\partial}\partial\phi(z(s, t)) \right). \end{aligned} \tag{B.2}$$

Thus we can bound the norm of the right-hand side of (B.2) by

$$R(\mathbf{f}) \int_0^1 \int_0^1 t \, dt \, ds \left(|\partial\partial\phi(z(s, t))| + 2|\partial\bar{\partial}\phi(z(s, t))| + |\bar{\partial}\partial\phi(z(s, t))| \right).$$

Thus we have

$$\begin{aligned} &\left| \nabla\phi(\mathbf{f}) - \int_0^1 \int_0^1 dt \, ds \, \partial\phi(z(s, t)) \right| \\ &\leq R(\mathbf{f}) \left(\frac{1}{2} \sup_{z \in \mathbf{f}} |\partial\partial\phi(z)| + \sup_{z \in \mathbf{f}} |\partial\bar{\partial}\phi(z)| + \frac{1}{2} \sup_{z \in \mathbf{f}} |\bar{\partial}\partial\phi(z)| \right). \end{aligned} \tag{B.3}$$

Finally, we come to bound the difference between $\partial\phi(z(s, t))$ and $\partial\phi(z_{\mathbf{f}})$, where $z_{\mathbf{f}}$ is the circumcenter of \mathbf{f} . Again, by the fundamental theorem of calculus, defining

$$z(p, s, t) = pz(s, t) + (1 - p)z_{\mathbf{f}},$$

we write

$$\begin{aligned} \partial\phi(z(s, t)) - \partial\phi(z_{\mathfrak{f}}) &= \int_0^1 dp \frac{d}{dp} \partial\phi(z(p, s, t)) \\ &= \int_0^1 dp ((z(s, t) - z_{\mathfrak{f}})\partial\partial\phi(z(p, s, t)) \\ &\quad + (\bar{z}(s, t) - \bar{z}_{\mathfrak{f}})\partial\bar{\partial}\phi(z(p, s, t))). \end{aligned}$$

Since $z(s, t)$ is inside the triangle \mathfrak{f} , it is also in the disk $B_{\mathfrak{f}}$ of radius $R(\mathfrak{f})$ with center $z_{\mathfrak{f}}$, hence $|z(s, t) - z_{\mathfrak{f}}| \leq R(\mathfrak{f})$, and we get the bound

$$|\partial\phi(z(s, t)) - \partial\phi(z_{\mathfrak{f}})| \leq R(\mathfrak{f})\left(\sup_{z \in B_{\mathfrak{f}}} |\partial\partial\phi(z)| + \sup_{z \in B_{\mathfrak{f}}} |\partial\bar{\partial}\phi(z)|\right),$$

which when averaged becomes

$$\begin{aligned} \left| \int_0^1 \int_0^1 dt ds \partial\phi(z(s, t)) - \partial\phi(z_{\mathfrak{f}}) \right| \\ \leq R(\mathfrak{f})\left(\sup_{z \in B_{\mathfrak{f}}} |\partial\partial\phi(z)| + \sup_{z \in B_{\mathfrak{f}}} |\partial\bar{\partial}\phi(z)|\right). \end{aligned} \tag{B.4}$$

Combining bounds (B.3) and (B.4), we get the final result of Lemma 1.9,

$$|\nabla\phi(\mathfrak{f}) - \partial\phi(z_{\mathfrak{f}})| \leq R(\mathfrak{f})\left(\frac{3}{2} \sup_{z \in B_{\mathfrak{f}}} |\partial^2\phi| + 2 \sup_{z \in B_{\mathfrak{f}}} |\partial\bar{\partial}\phi| + \frac{1}{2} \sup_{z \in B_{\mathfrak{f}}} |\bar{\partial}^2\phi|\right). \quad \blacksquare$$

Remark B.1. For a general point $w \in B_{\mathfrak{f}}$, we have $|z(s, t) - w| \leq 2R(\mathfrak{f})$ and after modifying our estimates by a factor of 2, we obtain

$$|\nabla\phi(\mathfrak{f}) - \partial\phi(w)| \leq R(\mathfrak{f})\left(\frac{5}{2} \sup_{z \in B_{\mathfrak{f}}} |\partial^2\phi| + 3 \sup_{z \in B_{\mathfrak{f}}} |\partial\bar{\partial}\phi| + \frac{1}{2} \sup_{z \in B_{\mathfrak{f}}} |\bar{\partial}^2\phi|\right). \tag{B.5}$$

C. Continuum limits of curvature anomalies: An example

In this appendix, we present an example of an isoradial Delaunay graph G_{cr} for which the anomalous terms of the associated conformal Laplacian $\underline{\Delta}$ (as defined in formulas (6.23) and examined in equations (6.25) and (6.26) of Section 6) have well-defined non-trivial scaling limits $\ell \rightarrow \infty$. Unlike the continuum limits addressed in Theorem 1.10, the limit values of the anomalous edge-to-chord, chord-to-edge, and chord-to-chord terms computed in Proposition C.4 of this section reflect features of the underlying geometry of the initial critical graph G_{cr} , specifically the choice of fundamental quadrilateral \mathcal{Q} used to construct G_{cr} . See Figure 33. We emphasize that this is a very specific example; for “generic” isoradial Delaunay graph G_{cr} , no such continuum limit exist.

Begin with four angles $\alpha_1 < \alpha_2 < \alpha_3 < \alpha_4$ in the interval $[0, 2\pi)$ and construct the cyclic quadrilateral \mathcal{Q} , whose vertices are the unit complex numbers $\zeta_k := \exp(i\alpha_k)$ with $k \in \{1, 2, 3, 4\}$. We will require that the origin is contained in the interior of \mathcal{Q} , which is achieved whenever $\alpha_3 - \alpha_1 > \pi$ or $\alpha_4 - \alpha_2 > \pi$. This constraint ensures that the tiling we are about to construct is Delaunay. Let \mathcal{Q}^{op} denote the quadrilateral obtained by rotating \mathcal{Q} by 180 degrees. A cyclic quadrilateral with associated angles $\alpha_1 = \frac{\pi}{3}$, $\alpha_2 = \frac{5\pi}{7}$, $\alpha_3 = \frac{13\pi}{9}$, and $\alpha_4 = \frac{21\pi}{11}$ is illustrated in Figure 32.

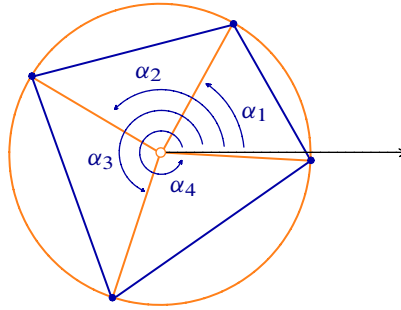


Figure 32. The fundamental quadrilateral \mathcal{Q} considered in the example.

Construct a doubly periodic quadrilateral tiling \mathcal{G}_{cr} of the plane using translations of \mathcal{Q} and \mathcal{Q}^{op} . Clearly, \mathcal{G}_{cr} will be isoradial and Delaunay in the sense of Section 2.1.1; by construction, each face of \mathcal{G}_{cr} is a cyclic quadrilateral. Figure 33 depicts such a tiling.

For each quadrilateral face q of \mathcal{G}_{cr} , let z_q denote the complex coordinate of its center; with respect to this center, the four vertices $v_q(k)$ of q , with $k \in \{1, 2, 3, 4\}$, have complex coordinates $z(v_q(k)) = z_q \pm \zeta_k$, where the sign is $+$ if q is a translation of \mathcal{Q} and $-$ if q is a translation of \mathcal{Q}^{op} . Let e_q^+ denote the chord of the quadrilateral q joining vertices $v_q(2)$ and $v_q(4)$, while e_q^- will denote the chord joining $v_q(1)$ and $v_q(3)$. Up to a sign, the corresponding north angles are given by $\vartheta_+ := \alpha_2 - \alpha_4$ and $\vartheta_- := \alpha_1 - \alpha_3$, respectively. Define $z_+ := \zeta_2 - \zeta_4$ and $z_- := \zeta_1 - \zeta_3$. Let $A_{\mathcal{Q}}$ denote the area of \mathcal{Q} .

Let $F(z)$ be a smooth complex-valued function with compact support together with deformation and scaling parameter values $\epsilon > 0$ and $\ell > 0$. Let $\mathcal{G}_{\epsilon, \ell}$ denote the graph obtained by deforming the embedding of \mathcal{G}_{cr} by $z \mapsto z + \epsilon \ell F(\frac{z}{\ell})$ and then adjoining edges e_q^+ or e_q^- to those quadrilateral faces q of \mathcal{G}_{cr} according to whether $\theta_{\epsilon, \ell}(e_q^+) > 0$ or $\theta_{\epsilon, \ell}(e_q^-) > 0$, respectively; these conditions are mutually exclusive, as the signs of $\theta_{\epsilon, \ell}(e_q^+)$ and $\theta_{\epsilon, \ell}(e_q^-)$ are opposite. Neither edge is selected if both conformal angles are zero. As long as $\epsilon > 0$ lies within the range $0 < \epsilon < \tilde{\epsilon}_{F, \ell}$ prescribed by Proposition 5.8, the graph $\mathcal{G}_{\epsilon, \ell}$ will remain Delaunay.

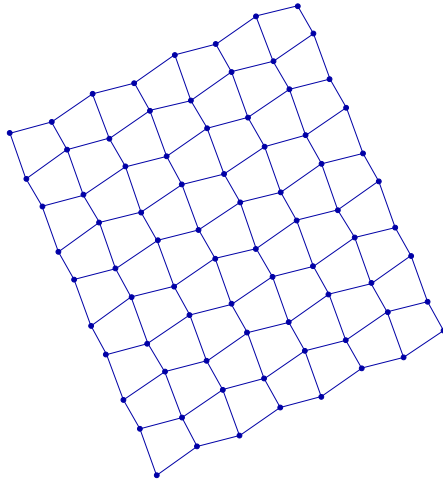


Figure 33. Fragment of a tiling G_{cr} by a cyclic quadrilateral q .

As an example, consider the following “mollified” shear of G_{cr} . For simplicity, we consider the case where the support of F has *one* connected component (in particular, it is a disk \mathbb{D} with unit radius):

$$F(z) := \begin{cases} \exp\left(i\phi + \frac{|z|^2}{|z|^2-1}\right) \operatorname{Im}[z] & \text{if } |z| \leq 1, \\ 0 & \text{otherwise.} \end{cases}$$

Figure 34 depicts the effect of the corresponding deformation $z \mapsto z + \epsilon \ell F(\frac{z}{\ell})$. The reader will notice that the support of $F_\ell: z \mapsto \ell F(\frac{z}{\ell})$ is partitioned roughly into three “unidirectional” zones consisting of deformed quadrilaterals whose diagonals share the same alignment. In general, for any smooth compactly supported perturbation $z \mapsto z + \epsilon \ell F(\frac{z}{\ell})$, the support of F_ℓ will be partitioned into such zones of constant alignment. If we ignore the quadrilaterals q for which $\theta'_{0,\ell}(e_q^+)$ vanishes, then the remaining set of quadrilaterals can be partitioned into zones over which the sign of $\theta'_{0,\ell}(e_q^+)$ is constant. For $\ell \gg 0$ large, the interfaces between these zones approximate the level curves of $\operatorname{Im}[\bar{\partial} F_\ell \mathcal{E}] = 0$ within the disk \mathbb{D}_ℓ of radius ℓ , where

$$\mathcal{E} := e_{12} - e_{23} + e_{34} - e_{14} \quad \text{and} \quad e_{mn} := \frac{\bar{\partial}_m - \bar{\partial}_n}{\partial_m - \partial_n} \quad \text{for } m, n \in \{1, 2, 3, 4\}.$$

The appearance of continuous interfaces is a prodigy (of the existence) of the scaling limit for the anomaly, as formalized in Lemma C.1 and Proposition C.4. In the case of the mollified-shear example, the corresponding level curves are depicted in red in Figure 34.

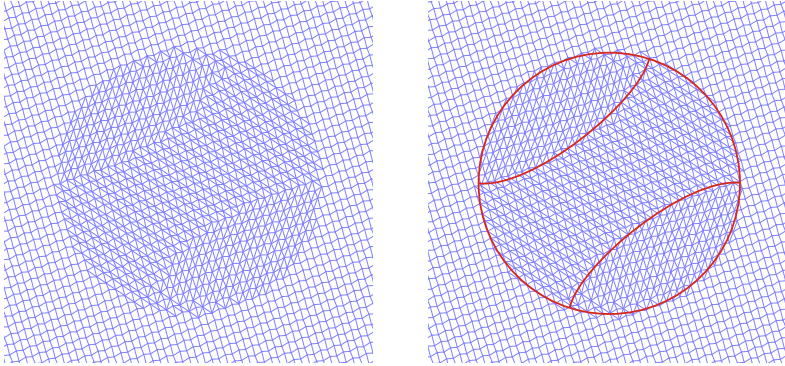


Figure 34. Mollified-shear with angle value $\phi = -\frac{\pi}{5}$, deformation parameter value $\epsilon = 0.1$, and scaling parameter value $\ell = 22$.

In order to analyze the anomalous terms arising in the second-order variation of the conformal Laplacian, we return to using a scaled, bi-local perturbation as prescribed in Section 7. As before, $F_1(z)$ and $F_2(z)$ are complex-valued functions whose supports Ω_1 and Ω_2 are compact and whose lattice closures $\bar{\Omega}_1$ and $\bar{\Omega}_2$ are disjoint. In addition, $\underline{\epsilon} = (\epsilon_1, \epsilon_2)$ is a pair of independent deformation parameters, and $\ell > 0$ is a scaling parameter. Let $G_{\underline{\epsilon}, \ell}$ denote the Delaunay graph associated to the deformed embedding $z_{\underline{\epsilon}, \ell}(v) := z(v) + \epsilon_1 F_{1; \ell}(z(v)) + \epsilon_2 F_{2; \ell}(z(v))$, where the deformation parameters are constrained within the range $0 \leq \epsilon_1, \epsilon_2 < \min(\tilde{\epsilon}_{F_1}, \tilde{\epsilon}_{F_2})$, whose bounds $\tilde{\epsilon}_{F_1}, \tilde{\epsilon}_{F_2}$ are specified in Proposition 5.8.

Given $p \in \mathbb{C}$ and a value of the scaling parameter $\ell > 0$, center a copy of the fundamental quadrilateral \mathcal{Q} about the dilated point $\ell p \in \mathbb{C}$. The coordinates of its vertices are $q_\ell(p; k) = \ell p + \mathfrak{z}_k$ for $k \in \{1, 2, 3, 4\}$. The perturbation will displace these vertices by $q_\ell(p; k) \mapsto q_{\underline{\epsilon}, \ell}(p; k)$, where

$$q_{\underline{\epsilon}, \ell}(p; k) := q_\ell(p; k) + \epsilon_1 F_{1; \ell}(q_\ell(p; k)) + \epsilon_2 F_{2; \ell}(q_\ell(p; k)).$$

The conformal angle $\kappa_{\underline{\epsilon}, \ell}(p)$ and its ϵ_i -derivatives $\mathfrak{d}_{\epsilon_i} \kappa_{\underline{\epsilon}, \ell}(p)$ are accordingly defined by

$$\begin{aligned} \kappa_{\underline{\epsilon}, \ell}(p) &= \text{Im} \log \left[\frac{(q_{\underline{\epsilon}, \ell}(p; 4) - q_{\underline{\epsilon}, \ell}(p; 3))(q_{\underline{\epsilon}, \ell}(p; 2) - q_{\underline{\epsilon}, \ell}(p; 1))}{(q_{\underline{\epsilon}, \ell}(p; 4) - q_{\underline{\epsilon}, \ell}(p; 1))(q_{\underline{\epsilon}, \ell}(p; 2) - q_{\underline{\epsilon}, \ell}(p; 3))} \right], \\ \mathfrak{d}_{\epsilon_i} \kappa_{\underline{\epsilon}, \ell}(p) &= \frac{\partial}{\partial \epsilon_i} \Big|_{\epsilon_i=0} \kappa_{\underline{\epsilon}, \ell}(p) \\ &= \text{Im} \left[\bar{\nabla} F_i \left(p + \frac{\mathfrak{z}_1}{\ell}, p + \frac{\mathfrak{z}_2}{\ell}, p + \frac{\mathfrak{z}_4}{\ell} \right) (e_{12} - e_{14}) \right] \\ &\quad + \text{Im} \left[\bar{\nabla} F_i \left(p + \frac{\mathfrak{z}_2}{\ell}, p + \frac{\mathfrak{z}_3}{\ell}, p + \frac{\mathfrak{z}_4}{\ell} \right) (e_{34} - e_{23}) \right] \\ &= \text{Im} [\bar{\partial} F_i(p) \mathcal{E}] + \mathcal{O}\left(\frac{1}{\ell}\right). \end{aligned} \tag{C.1}$$

Lemma C.1. Fix a value of the scaling parameter $\ell > 0$, then for any pair of points $p, z \in \text{supp} F_i$ with $|z - p| < \frac{1}{\ell}$,

$$|\mathfrak{d}_{\epsilon_i} \kappa_\ell(z) - \text{Im}[\bar{\partial} F_i(p) \mathcal{E}]| \leq \frac{4}{\ell} M_i(z, \ell),$$

where

$$M_i(z, \ell) := \max_{|w-z| < \frac{1}{\ell}} |\partial^2 F_i(w)| + 2 \max_{|w-z| < \frac{1}{\ell}} |\partial \bar{\partial} F_i(w)| + \max_{|w-z| < \frac{1}{\ell}} |\bar{\partial}^2 F_i(w)|.$$

Proof. For brevity, we will simply write F instead of either F_1 or F_2 and $\mathfrak{d}_{\epsilon} \kappa_\ell(z)$ instead of $\mathfrak{d}_{\epsilon_1} \kappa_\ell(z)$ or $\mathfrak{d}_{\epsilon_2} \kappa_\ell(z)$. For indices $i, j, k \in \{1, 2, 3, 4\}$, we will use the provisional notation

$$A_{ijk} := \bar{\nabla} F\left(z + \frac{\mathfrak{z}_i}{\ell}, z + \frac{\mathfrak{z}_j}{\ell}, z + \frac{\mathfrak{z}_k}{\ell}\right) - \bar{\partial} F(p).$$

By Remark B.1, if $|z - p| < \frac{1}{\ell}$, we have

$$|A_{ijk}| \leq R \left(\frac{5}{2} \max_{z \in B} |\partial^2 F| + 3 \max_{z \in B} |\partial \bar{\partial} F| + \frac{1}{2} \max_{z \in B} |\bar{\partial}^2 F| \right),$$

where B is the disk of radius $R = \frac{1}{\ell}$ centered at z . By formula (C.1), we have

$$\begin{aligned} |\mathfrak{d}_{\epsilon} \kappa_\ell(z) - \text{Im}[\bar{\partial} F(p) \mathcal{E}]| &= |\text{Im}[A_{124}(e_{12} - e_{14}) + A_{234}(e_{34} - e_{23})]| \\ &\leq |A_{124}| \cdot |e_{12} - e_{14}| + |A_{234}| \cdot |e_{34} - e_{23}| \\ &\leq 2(|A_{124}| + |A_{234}|). \end{aligned}$$

Accordingly, we have

$$|\mathfrak{d}_{\epsilon} \kappa_\ell(z) - \text{Im}[\bar{\partial} F(p) \mathcal{E}]| \leq \frac{4}{\ell} \left(\frac{5}{2} \max_{z \in B} |\partial^2 F| + 3 \max_{z \in B} |\partial \bar{\partial} F| + \frac{1}{2} \max_{z \in B} |\bar{\partial}^2 F| \right). \quad \blacksquare$$

Definition C.2. For a fixed value of the scaling parameter $\ell > 0$ and any (continuous) function $\phi: \mathbb{C} \rightarrow \mathbb{C}$, let us introduce the following piecewise abridgment:

$$\langle \phi \rangle_\ell(p) := \begin{cases} \phi\left(\frac{z_q}{\ell}\right) & \text{whenever } \ell p \in \text{int}(q) \text{ for a quadrilateral } q, \\ \frac{1}{2} \sum_{k=1}^2 \phi\left(\frac{z_{q_k}}{\ell}\right) & \text{whenever } \ell p \in \text{int}(\partial q_1 \cap \partial q_2) \text{ for} \\ & \text{a pair of quadrilaterals } q_1 \text{ and } q_2, \\ \frac{1}{4} \sum_{k=1}^4 \phi\left(\frac{z_{q_k}}{\ell}\right) & \text{whenever } \ell p \in \partial q_1 \cap \partial q_2 \cap \partial q_3 \cap \partial q_4 \\ & \text{for quadrilaterals } q_1, q_2, q_3, \text{ and } q_4. \end{cases}$$

Remark C.3. Let $\chi_{i;\ell} := \langle \mathfrak{d}_{\epsilon_i} \kappa_\ell \rangle_\ell$, then $\chi_{i;\ell} \rightarrow \text{Im}[\bar{\partial} F_i \mathcal{E}]$ uniformly in the limit $\ell \rightarrow \infty$. Furthermore, $\chi_{i;\ell}^\pm \rightarrow \text{Im}^\pm[\bar{\partial} F_i \mathcal{E}]$ uniformly as $\ell \rightarrow \infty$, where

$$g^+(p) := \max(g(p), 0) \quad \text{and} \quad g^-(p) := -\min(g(p), 0)$$

for any real-valued function $g: \mathbb{C} \rightarrow \mathbb{R}$.

Proposition C.4. For signs $\sigma, \tau \in \{+, -\}$, define

$$\begin{aligned} J^{(\sigma,\tau)} &:= \frac{\tan^2 \vartheta_\sigma \tan^2 \vartheta_\tau}{16\pi^2 A_\mathcal{Q}^2} \iint_{\Omega_1 \times \Omega_2} d^2 x d^2 y \text{Im}^\sigma[\bar{\partial} F_1(x) \mathcal{E}] \\ &\quad \times \left[\text{Re} \frac{z_\sigma z_\tau}{(x-y)^2} \right]^2 \text{Im}^\tau[\bar{\partial} F_2(y) \mathcal{E}], \\ J_\sigma^{(1)} &:= \frac{\tan^2 \vartheta_\sigma}{8\pi^2 A_\mathcal{Q}} \iint_{\Omega_1 \times \Omega_2} d^2 x d^2 y \text{Im}^\sigma[\bar{\partial} F_1(x) \mathcal{E}] \text{Re} \left[\frac{z_\sigma^2 \bar{\partial} F_2(y)}{(x-y)^4} \right], \\ J_\sigma^{(2)} &:= \frac{\tan^2 \vartheta_\sigma}{8\pi^2 A_\mathcal{Q}} \iint_{\Omega_1 \times \Omega_2} d^2 x d^2 y \text{Re} \left[\frac{\bar{\partial} F_1(x) z_\sigma^2}{(x-y)^4} \right] \text{Im}^\sigma[\bar{\partial} F_2(y) \mathcal{E}]. \end{aligned}$$

The continuum limits of the edge-to-chord $\mathbb{A}_\ell^{\text{ed} \times \text{ch}}$, chord-to-edge $\mathbb{A}_\ell^{\text{ch} \times \text{ed}}$, and chord-to-chord $\mathbb{A}_\ell^{\text{ch} \times \text{ch}}$ anomalies exist and their values are

$$\begin{aligned} \lim_{\ell \rightarrow \infty} \mathbb{A}_\ell^{\text{ed} \times \text{ch}} &= J_+^{(2)} + J_-^{(2)}, \\ \lim_{\ell \rightarrow \infty} \mathbb{A}_\ell^{\text{ch} \times \text{ed}} &= J_+^{(1)} + J_-^{(1)}, \\ \lim_{\ell \rightarrow \infty} \mathbb{A}_\ell^{\text{ch} \times \text{ch}} &= J^{(+,+)} + J^{(+,-)} + J^{(-,+)} + J^{(-,-)}. \end{aligned}$$

Proof. We will verify the claim in the case of the chord-to-chord anomaly $\mathbb{A}_\ell^{\text{ch} \times \text{ch}}$ and leave the remaining cases to the reader. Begin with a pair of signs $\sigma, \tau \in \{\pm\}$. For $(x, y) \in \Omega_1 \times \Omega_2$, let us introduce the following step-function

$$\Phi_\ell^{\sigma,\tau}(x, y) := \begin{cases} [\mathfrak{d}_{\epsilon_1} \kappa_\ell(\frac{z_x}{\ell})]^\sigma \cdot \left[\text{Re} \frac{z_\sigma z_\tau}{(z_x - z_y)^2} \right]^2 \cdot [\mathfrak{d}_{\epsilon_2} \kappa_\ell(\frac{z_y}{\ell})]^\tau, & \ell x \in \text{int}(x), \ell y \in \text{int}(y), \\ & x, y \in F(\mathbb{G}_{\text{cr}}), \\ \text{bounded noise} & \text{otherwise.} \end{cases}$$

Note that $\mathbb{A}_\ell^{\text{ch} \times \text{cr}} = \mathbb{J}_\ell^{(+,+)} + \mathbb{J}_\ell^{(+,-)} + \mathbb{J}_\ell^{(-,+)} + \mathbb{J}_\ell^{(-,-)}$, where

$$\mathbb{J}_\ell^{(\sigma,\tau)} = \frac{\tan^2 \vartheta_\sigma \tan^2 \vartheta_\tau}{16\pi^2} \sum_{\substack{x \in F(\mathbb{G}_{\text{cr}}) \\ x \cap \Omega_1(\ell) \neq \emptyset}} \sum_{\substack{y \in F(\mathbb{G}_{\text{cr}}) \\ y \cap \Omega_2(\ell) \neq \emptyset}} \Phi_\ell^{\sigma,\tau} \left(\frac{z_x}{\ell}, \frac{z_y}{\ell} \right).$$

It follows from Lemma C.1 that $\Phi_\ell^{\sigma,\tau}(x, y) \rightarrow \Phi^{\sigma,\tau}(x, y)$ converges uniformly on $\Omega_1 \times \Omega_2$ as $\ell \rightarrow \infty$, where

$$\begin{aligned} \Phi^{\sigma,\tau}(x, y) &:= \operatorname{Im}^\sigma[\bar{\partial}F_1(x)\mathcal{E}] \cdot \left[\operatorname{Re} \frac{z_\sigma z_\tau}{(x-y)^2} \right]^2 \cdot \operatorname{Im}^\tau[\bar{\partial}F_2(y)\mathcal{E}], \\ J^{(\sigma,\tau)} &= \frac{\tan^2 \vartheta_\sigma \tan^2 \vartheta_\tau}{16\pi^2 A_\mathcal{Q}^2} \iint_{\Omega_1 \times \Omega_2} d^2x d^2y \Phi^{\sigma,\tau}(x, y) \\ &= \frac{\tan^2 \vartheta_\sigma \tan^2 \vartheta_\tau}{16\pi^2 A_\mathcal{Q}^2} \lim_{\ell \rightarrow \infty} \iint_{\Omega_1 \times \Omega_2} d^2x d^2y \Phi_\ell^{\sigma,\tau}(x, y) \\ &= \frac{\tan^2 \vartheta_\sigma \tan^2 \vartheta_\tau}{16\pi^2} \lim_{\ell \rightarrow \infty} \sum_{\substack{x \in F(\mathcal{G}_{\text{cr}}) \\ x \cap \Omega_1(\ell) \neq \emptyset}} \sum_{\substack{y \in F(\mathcal{G}_{\text{cr}}) \\ y \cap \Omega_2(\ell) \neq \emptyset}} \Phi_\ell^{\sigma,\tau}\left(\frac{z_x}{\ell}, \frac{z_y}{\ell}\right) \\ &= \lim_{\ell \rightarrow \infty} \mathbb{J}_\ell^{(\sigma,\tau)}. \quad \blacksquare \end{aligned}$$

Acknowledgements. The authors thank for hospitality Universidad de los Andes, Bogotá, Colombia, where this work was started, as well as the Chebyshev Laboratory at St. Petersburg State University, Russia, the Perimeter Institute, Waterloo, Canada, and the Institute of the Mathematical Sciences of the Americas, University of Miami, USA, where part of this work was done. In addition to these institutions, J. S. also thanks Institut Henri Poincaré in Paris, Institut des Hautes Études Scientifiques in Bures-sur-Yvette, and Institut de Physique Théorique of Saclay for their hospitality; the later for several visits during the course of this project.

The authors thank Dmitry Chelkak for discussions at IHES hosted by Hugo Dumitnil-Copin. F. D. thanks Bertrand Eynard and Philippe di Francesco for discussions. J. S. would also like to thank Peter Zograf and Gaëtan Borot: Peter Zograf for the opportunity to present a short lecture course addressing preliminary results of this paper at the Chebyshev Laboratory, and Gaëtan Borot for inviting and hosting J. S. at the 2017 IHP trimester program “Combinatorics and interactions” and later at the Max-Planck-Institut, Bonn for a short visit to discuss aspects of the project. We are very grateful to the reviewer of this paper, for their perceptive remarks and questions, which led to many improvements.

Funding. This paper is partly a result of the ERC-SyG project, Recursive and Exact New Quantum Theory (ReNewQuantum) which received funding from the European Research Council (ERC) under the European Union’s Horizon 2020 research and innovation programme under grant agreement No 810573.

References

- [1] F. Aurenhammer, R. Klein, and D.-T. Lee, *Voronoi diagrams and Delaunay triangulations*. World Scientific Publishing, Hackensack, NJ, 2013 Zbl [1295.52001](#) MR [3186045](#)
- [2] F. A. Berezin, *The method of second quantization*. Pure Appl. Phys. 24, Academic Press, New York, 1966 Zbl [0151.44001](#) MR [208930](#)
- [3] U. Bücking, [Approximation of conformal mappings by circle patterns](#). *Geom. Dedicata* **137** (2008), 163–197 Zbl [1151.52018](#) MR [2449151](#)
- [4] S. Charbonnier, F. David, and B. Eynard, [Local properties of the random Delaunay triangulation model and topological models of 2D gravity](#). *Ann. Inst. Henri Poincaré D* **6** (2019), no. 3, 313–355 Zbl [1426.52010](#) MR [4002669](#)
- [5] D. Chelkak, A. Glazman, and S. Smirnov, Discrete stress-energy tensor in the loop $O(n)$ model. 2017, arXiv:[1604.06339](#)
- [6] N. H. Christ, R. Friedberg, and T. D. Lee, [Random lattice field theory: general formulation](#). *Nuclear Phys. B* **202** (1982), no. 1, 89–125 MR [668986](#)
- [7] F. David and B. Eynard, [Planar maps, circle patterns and 2D gravity](#). *Ann. Inst. Henri Poincaré D* **1** (2014), no. 2, 139–183 Zbl [1297.52007](#) MR [3229942](#)
- [8] M. de Berg, O. Cheong, M. van Kreveld, and M. Overmars, *Computational geometry. Algorithms and applications*. 3rd edn., Springer, Berlin, 2008 Zbl [1140.68069](#) MR [2723879](#)
- [9] P. Deligne, P. Etingof, D. S. Freed, L. C. Jeffrey, D. Kazhdan, J. W. Morgan, D. R. Morrison, and E. Witten (eds.), *Quantum fields and strings: a course for mathematicians. Vol. 1, 2*. American Mathematical Society, Providence, RI, 1999 Zbl [0984.00503](#) MR [1701618](#)
- [10] P. Di Francesco, P. Mathieu, and D. Sénéchal, *Conformal field theory*. Grad. Texts Phys., Springer, New York, 1997 Zbl [0869.53052](#) MR [1424041](#)
- [11] E. Domany, D. Mukamel, B. Nienhuis, and A. Schwimmer, [Duality relations and equivalences for models with \$O\(N\)\$ and cubic symmetry](#). *Nuclear Phys. B* **190** (1981), no. 2, 279–287
- [12] D. Friedan, Introduction to Polyakov’s string theory. In *Recent advances in field theory and statistical mechanics (Les Houches, 1982)*, pp. 839–867, North-Holland, Amsterdam, 1984 MR [782514](#)
- [13] J. Gallier, Notes on convex sets, polytopes, polyhedra, combinatorial topology, Voronoi diagrams and Delaunay triangulations. 2008, arXiv:[0805.0292](#)
- [14] B. Gärtner and M. Hoffmann, Computational geometry. Lecture notes, HS 2012. 2013, <https://ti.inf.ethz.ch/ew/lehre/CG12/lecture/CGlecturenotes.pdf>, visited on 6 March 2024
- [15] C. Hongler, K. Kytölä, and F. Viklund, [Conformal field theory at the lattice level: discrete complex analysis and Virasoro structure](#). *Comm. Math. Phys.* **395** (2022), no. 1, 1–58 Zbl [1504.82009](#) MR [4483015](#)
- [16] A. Kassel and R. Kenyon, [Random curves on surfaces induced from the Laplacian determinant](#). *Ann. Probab.* **45** (2017), no. 2, 932–964 Zbl [1377.82037](#) MR [3630290](#)
- [17] R. Kenyon, [The Laplacian and Dirac operators on critical planar graphs](#). *Invent. Math.* **150** (2002), no. 2, 409–439 Zbl [1038.58037](#) MR [1933589](#)

- [18] R. Kenyon and J.-M. Schlenker, [Rhombic embeddings of planar quad-graphs](#). *Trans. Amer. Math. Soc.* **357** (2005), no. 9, 3443–3458 Zbl [1062.05045](#) MR [2146632](#)
- [19] I. K. Kostov, [O\(n\) vector model on a planar random lattice: spectrum of anomalous dimensions](#). *Modern Phys. Lett. A* **4** (1989), no. 3, 217–226 MR [1016518](#)
- [20] C. L. Lawson, Software for \mathcal{C}^1 surface interpolation. In *Mathematical software. III, Proceedings of a Symposium conducted by the Mathematics Research Center, the University of Wisconsin, Madison, Wis.*, pp. 161–194, Publication of the Mathematics Research Center, University of Wisconsin 39, Academic Press, Inc., New York, 1977 Zbl [0407.68033](#)
- [21] C. Mercat, [Discrete Riemann surfaces and the Ising model](#). *Comm. Math. Phys.* **218** (2001), no. 1, 177–216 Zbl [1043.82005](#) MR [1824204](#)
- [22] B. Nienhuis, Coulomb gas formulation of two-dimensional phase transitions. In *Phase transitions and critical phenomena, Vol. 11*, pp. 1–53, Academic Press, London, 1987 MR [942673](#)
- [23] A. M. Polyakov, [Quantum geometry of bosonic strings](#). *Phys. Lett. B* **103** (1981), no. 3, 207–210 MR [623209](#)
- [24] I. Rivin, [Euclidean structures on simplicial surfaces and hyperbolic volume](#). *Ann. of Math. (2)* **139** (1994), no. 3, 553–580 Zbl [0823.52009](#) MR [1283870](#)

Communicated by Adrian Tanasă

Received 5 January 2022.

François David

Université Paris-Saclay, CNRS, CEA, Institut de Physique Théorique, 91191 Gif-sur-Yvette, France; francois.david@ipht.fr

Jeanne Scott

Department of Mathematics, Brandeis University, 415 South Street, Waltham, MA 02453, USA; jeanne@imsc.res.in